WORLD ACADEMY OF SCIENCE, ENGINEERING, AND TECHNOLOGY
INTERNATIONAL SCIENTIFIC COMMITTEES AND EDITORIAL REVIEW BOARDS

Mission

The World Academy of Science, Engineering, and Technology supports, promotes, preserves, expands, and disseminates scholarly research knowledge in the sciences, technology, arts, and humanities while embracing the philosophical principle of the universality, freedom, and responsibility of science. The Academy is dedicated to excellence in scholarly research and innovation, creative endeavors, and fosters free inquiry while embracing diversity.

Vision

The World Academy of Science, Engineering and Technology strives to be one of the world's premier organizations in scholarly research and innovation for global sustainable development. The Academy is devoted to transforming the lives of scholarly researchers and shaping the future of our global society by offering scholarly researchers in diverse disciplines a climate of inquiry, engagement, collegiality, achievement, and global distinction.

Committees

The World Academy of Science, Engineering and Technology's International Scientific Committees and Editorial Review Boards are comprised of distinguished and competent scholars, scientists & researchers from around the world. The full list of the International Scientific Committees and Editorial Review Boards is online accessible at www.waset.org/Committees

- Aerospace and Mechanical Engineering
- Agricultural and Biosystems Engineering
- Animal and Veterinary Sciences
- Architectural and Environmental Engineering
- Bioengineering and Life Sciences
- Biomedical and Biological Engineering
- Biotechnology and Bioengineering
- Business and Economics Engineering
- Chemical and Molecular Engineering
- Civil and Environmental Engineering
- Cognitive and Language Sciences
- Computer and Information Engineering
- Computer and Systems Engineering
- Control and Information Engineering
- Defense and Security Engineering
- Economics and Management Engineering
- Educational and Pedagogical Sciences
- Electrical and Computer Engineering
- Electronics and Communication Engineering
- Energy and Power Engineering
- Environmental and Ecological Engineering
- Fashion and Textile Engineering
- Forestry and Wildlife Sciences
- Geological and Environmental Engineering
- Geomatics and Civil Engineering
- Geotechnical and Geological Engineering
- Health and Medical Engineering
- Hospitality and Tourism Sciences
- Humanities and Social Sciences
- Industrial and Manufacturing Engineering
- Information and Communication Engineering
- Law and Political Sciences
- Management and Industrial Engineering
- Marine and Atmospheric Sciences
- Materials and Metallurgical Engineering
- Mathematical and Computational Sciences
- Mechanical and Mechatronics Engineering
- Medical and Health Sciences
- Nuclear and Quantum Engineering
- Nursing and Health Sciences
- Nutrition and Food Engineering
- Pharmacological and Pharmaceutical Sciences
- Physical and Mathematical Sciences
- Psychological and Behavioral Sciences
- Robotics and Mechatronics Engineering
- Software and Systems Engineering
- Sport and Exercise Sciences
- Structural and Construction Engineering
- Transport and Vehicle Engineering
- Urban and Civil Engineering

The Political Economy of the Global Climate Change Adaptation Initiatives: A Case Study on the Global Environmental Facility

Anar Koli

Abstract**—**After the Paris agreement in 2015, a comprehensive initiative both from the developed and developing countries towards the adaptation to climate change is emerging. The Global Environmental Facility (GEF), which is financing a global portfolio of adaptation projects and programs in over 124 countries is playing a significant role to a new financing framework that included the concept of "climate-resilient development". However, both the adaptation and sustainable development paradigms remain continuously contested, especially the role of the multilateral institutions with their technical and financial assistance to the developing world.

Focusing on the adaptation initiatives of the GEF, this study aims to understand to what extent the global multilateral institutions, particularly the GEF is contributing to the climate-resilient development?

From the political ecology perspective, the argument of this study is that the global financial framework is highly politicized, and understanding the contribution of the global institutions of the global climate change needs to be related both from the response and causal perspectives. A holistic perspective, which includes the contribution of the GEF as a response to the climate change and as well the cause of global climate change, are needed to understand the broader environment- political economic relation. The study intends to make a critical analysis of the way in which the political economy structure and the environment are related along with the social and ecological implications. It does not provide a narrow description of institutional responses to climate change, rather it looks at how the global institutions are influencing the relationship of the global ecologies and economies.

This study thus developed a framework combining the global governance and the political economy perspective. This framework includes environment-society relation, environment-political economy linkage, global institutions as the orchestra, and division between the North and the South. Through the analysis of the GEF as the orchestra of the global governance, this study helps to understand how GEF is coordinating the interactions between the North and the South and responding the global climate resilient development. Through the other components of the framework, the study explains how the role of the global institutions is related to the cause of the human induced global climate change.

The study employs a case study based on both the quantitative and qualitative data. Along with the GEF reports and data sets, this study it draws from an eclectic range of literatures from a range of disciplines to explain the broader relation of the environment and political economy. Based on a case study on GEF, the study found that the GEF has positive contributions in bringing developing countries' capacity in terms of sustainable development goal, local institutional development. However, through a critical holistic analysis, this study found that this contribution to the resilient development helps the developing countries to conform the fossil fuel based capitalist political economy. The global governance institution contributing both to the pro market based environment society relation and, to the consequences of this relation.

Keywords**—**Climate change adaptation, Environment-society relation, Global institution such as Global Environmental Facility (GEF), Political economy.

Anar Koli, PhD is a lecturer at Soka University, Tokyo, Japan (phone: 81-8035767446; e-mail: koli@ soka.ac.jp).

Understanding Innovation by Analyzing the Pillars of the Global Competitiveness Index

Ujjwala Bhand, Mridula Goel

***Abstract*—**Global Competitiveness Index (GCI) prepared by World Economic Forum has become a benchmark in studying the competitiveness of countries and for understanding the factors that enable competitiveness. Innovation is a key pillar in competitiveness and has the unique property of enabling exponential economic growth. This paper attempts to analyze how the pillars comprising the Global Competitiveness Index affect innovation and whether GDP growth can directly affect innovation outcomes for a country. The key objective of the study is to identify areas on which governments of developing countries can focus policies and programs to improve their country's innovativeness. We have compiled a panel data set for top innovating countries and large emerging economies called BRICS from 2007-08 to 2014-15 in order to find the significant factors that affect innovation. The results of the regression analysis suggest that government should make policies to improve labor market efficiency, establish sophisticated business networks, provide basic health and primary education to its people and strengthen the quality of higher education and training services in the economy. The achievements of smaller economies on innovation suggest that concerted efforts by governments can counter any size related disadvantage, and in fact can provide greater flexibility and speed in encouraging innovation.

***Keywords*—**Innovation, Global Competitiveness Index, BRICS, Economic growth

I. Introduction

GLOBALIZATION has compelled firms and countries to explore different ways to cut down the competition. As a result, countries have realized the pressing need to innovate. Innovation is the only way for the countries to stay apart and be unique in the global competitive market. It has been found globally that science, technology and innovation are the major drivers for national development [1].The combination of science, technology and innovation leads to new value creation. Scientific research utilizes substantial quantity of funds for the creation of knowledge.

Innovation provides solution and thereby helps to convert scientific knowledge into wealth. Innovation thus implies Science and Technology based solutions that are successfully deployed in the economy. Innovation is being assumed to be the critical factor in the developmental goals of a country. In order to sustain in the global market, countries need to formulate their competitiveness strategies that are more focused towards science, technology and innovation. Innovation gives a country competitive edge over others and enhances its competitive position relative to other countries. Thus, realizing the importance of innovation to growth of economy and to achieve global competitiveness, both high growth countries as well as developing economies are trying to adopt policies and mechanisms focused on innovation and innovation led growth.

The current study focuses on studying the innovativeness of BRICS economies with respect to the top innovating countries in the world. An effort has been made to identify the critical enablers of innovation in these countries, so as to propose policy responses that can help to enhance innovation and in turn lead to greater competitiveness. Such policy prescriptions are especially important for a developing country like India, which has resource constraints but is keen to step up innovation and earn a position for its products in the global market place. The current policy focus on manufacturing led growth in India strengthens the need for pushing innovation in the country. We hope that our findings can throw up some policy prescriptions in this context for India and similarly positioned economies.

During the past decade the World Economic Forum (WEF) has been publishing the Global Competitiveness Reports (GCRs) annually which rank countries on their competitiveness. The reports contain large and relevant datasets that can be helpful for countries to understand their competitive position with respect to other countries. These reports are used by policy makers as a benchmark to assess their relative performance in achieving competitiveness and in understanding its various components so that they can overcome existing limitations. Competitiveness of any country is viewed as a relative position of the country in the international market, specially comparing at similar economic development levels [2].

The World Economic Forum has based its competitiveness analysis on the Global Competitiveness Index (GCI), which is a comprehensive tool that measures the microeconomic and macroeconomic foundations of national competitiveness. The components which measure the different determinants of competitiveness are grouped into 12 pillars namely: Institutions, Infrastructure, Macroeconomic environment, Health and primary education, Higher education and training, Goods market efficiency, Labor market efficiency, Financial market development, Technology readiness, Market size, Business Sophistication and Innovation [2]. For our study, we have taken data from the Global Competitiveness Reports from 2007-08 to 2014-15 for the 10 top performing countries on the index, along with the emerging economies called BRICS. These top performing countries have been selected as per their competitiveness in the year 2014-15. The GDP annual Growth rate is also taken as an explanatory factor in our study [3].

Ujjwala Bhand is a Doctoral Scholar in the Department of Economics, BITS, Pilani K.K. Birla Goa Campus, Goa 403726 India (phone: +91 9604466702, e-mail: ujjwalabhand@gmail.com).

Dr. Mridula Goel is Associate Professor in the Department of Economics, BITS, Pilani K.K. Birla Goa Campus, Goa 403726 India (corresponding author, e-mail: mridula@goa.bits-pilani.ac.in).

In the current era of globalization, competitiveness has become a key factor in the growth of both advanced and developing countries. Due to globalization there is an increase in competition among firms and among countries. To succeed in the globalized world firms and countries need to gain a competitive edge over others. The world has moved towards the knowledge economy and gaining a competitive edge in this scenario can be done by generating knowledge and through innovation. To withstand the competition countries need to innovate. Innovation acts as an important factor to acquire a competitive edge [4]. It has been observed in the Global Competitiveness Reports, that innovation plays a very important role in enhancing the competitiveness of a country [2].

As per the Global Competitiveness Index rankings for the last several years, the competitiveness rank of India showed a decline. India falls far behind the top innovation performing countries as can be seen from TABLE I .The data clearly suggest that efforts are needed to work on improving the country's competitiveness. We attempt to find the factors which can contribute to increasing the overall competitiveness of the country. The present work is an attempt to understand the key factors that can help India and other emerging economies to improve their competitiveness, especially through a focus on innovation led growth.

TABLE I
INDIA'S RANK IN THE GLOBAL COMPETITIVENESS INDEX (2007-15)

Year	Rank	Year	Rank
2007-08	48	2011-12	56
2008-09	50	2012-13	59
2009-10	49	2013-14	60
2010-11	51	2014-15	71

Data Source: Global Competitiveness Reports, 2007-08 to 2014-15.

Innovation is found to be a key driver of competitiveness for both businesses and countries. The scores for Global Competitiveness Index (GCI) and Innovation from 2007-08 to 2014-15 for the 15 selected countries are found to have a correlation of 0.93 [2], [5]-[11]. It suggests that if a country is able to step up its innovation outcomes it will also, be more competitive in the global market place.

In order to study the influencers of innovation, we attempt to understand the role of each of the pillars of Global Competitiveness Index and how they affect innovation at a level.

II. LITERATURE REVIEW

Globalization has brought a lot of change in the global economic scenario. In the past, when the markets were closed, firms were bound to carry out business within their own countries. There existed less competition among firms as there were few players in the market. Customers did not have a lot of product choices; there existed a monopoly of certain companies in producing specific goods. For example there was a kind of monopoly of 'Fiat' and 'Ambassador' cars in the Indian automobile industry or of Indian Airlines in domestic aviation industry.

Due to globalization in the latter part of the 20th century, specifically in post-World War II era, many multinational companies entered the global market and people started getting better quality products at a lower price. Customers could get better value for their money. This led to increased competition among the companies. Companies started finding new ways to attract customers, here the concept of value added service also came into the picture. Companies not only started providing better quality products but also started providing good service to the customer to enhance customer satisfaction. Today consumers drive markets. Globalization has also, led to an increase in the quality of the products, it has made it possible to have quality products available at an affordable price as a virtue of increased competition among firms [12].

Globalization has helped to remove the trade barriers among the countries and resulted in formation of global markets for the firms [13]. The increase in cross border trade has resulted in more competition not only amongst firms but also among the countries. Globalization has not only resulted in the global expansion of multinational companies but has also, brought about the exchange and interplay of new developments in science, technology and products throughout the world. Globalization has enabled most nations of the world to have access to similar information, technology and markets. It depends on the ability of a country to make use of those available resources and innovative ways to gain an edge over others [14], [15].

Competition plays a very important role in economic growth of a country because it necessitates the need for innovation. Competition can be at various levels: competition among individuals, among the organizations, between different regions and between countries [15]. In order to succeed in the global economy a country needs to be highly competitive at all levels. As a result of globalization, competitiveness is critical to the growth of both advanced and developing countries. Countries continuously strive to gain competitive advantage over others. Globalization has created a need for countries to have a framework for analyzing the competitive position of the country in the international market rather than simply focusing on measures to improve internal productivity [16]. The improvement in the competitiveness of business firms and countries is a prior requirement for successful business development in the global market [15].

Need for innovation

In the traditional economy framework competitive edge was gained through access to cheap labor, abundant natural resources, etc. However, today the world has moved towards a Knowledge economy. In knowledge based systems, the growth of the economy is based on the production and use of knowledge [17].

In today's knowledge era and innovation driven global economy, scientific and technological knowledge are the key drivers of production and growth [18]. In order to succeed in the knowledge economy countries need to generate knowledge and thereby innovate different ways to cut down the competition. Countries which work towards knowledge production, its usage and adopt innovative ways by making use of science and technology to cut down the competition grow their economy well and have more

likelihood to become a global leader. For long term economic growth and sustainable competitiveness, countries need to develop global competitiveness strategies which are focused towards Science, Technology and Innovation [19]. Many researchers have found that technological change and innovation are the major drivers of economic growth and act as the important factors for achieving competitiveness [20]. Technology plays a vital role in enhancing national economy and international competitiveness; it is also a key source in increasing profitability and growth of the companies [21].

It has been found in many studies that technological developments help the firms of a country to improve their profitability, give them competitive edge over others and thus, contribute to the growth of the firms. This in turn helps to boost the economy and competitiveness of a country. On the basis of technological development; companies, industries and countries can foster their competitive capabilities and increase their competitive advantage [16]. It has been found that the firms that innovate have better productivity levels and economic growth as compared to the non- innovating firms [20].

According to a Boston Consulting Group (BCG) study (2015), innovative companies excel in the market and innovation remains as a top agenda for these companies. In this study, maximum respondents ranked innovation as the top-most priority for their company. The results of the study reveal that the top officials of the companies around the world believe that innovation plays an important role for the organizations to acquire competitive advantage and profitability. Science and Technology act as an important basis for innovation. The leading companies at the top of the list of innovation like: Apple, Google, Tesla Motors, Microsoft Corp., Samsung Group, Toyota, BMW and such are making use of science and technology and innovative methods such as: emphasis on speed, well run (very often lean) research and development processes, use of technological platforms and the systemic exploration of adjacent markets. [22]. The BCG study also specifies that out of the top 50 performing list of companies, 29 of these belong to United States of America, 11 of them belong to Europe and 10 belong to Asia. While most of the companies are from developed countries, companies from the emerging markets have also found a place in this list. In the case of the emerging markets 3 companies are from China and 1 is from India; companies from developing countries also use innovative ideas and techniques to compete in the global market. Thus, it can be concluded that by making use of science, technology and innovation companies can outperform in the market [22].

The Global Competitiveness Report 2013-14 also shows that the top performing countries like Switzerland, Singapore, Finland, Germany, United States of America, Sweden, Hong Kong SAR etc. are putting a lot of efforts into development of high quality education, research and development and making use of highly sophisticated advanced technology. It appears that the use of innovative technologies by their companies helps to make them the top productive and competitive economies. [2]. A country can attain economic growth and prosperity by its competitive technologies and innovation [23]. Therefore, countries need to increasingly invest in generating scientific knowledge and try to be technologically advanced which will lead to innovation and thereby add to the competitiveness of their country.

According to the Global Competitiveness Report of 2013-14, due to the financial crisis of 2008-09, emerging economies have gained importance because of which a notable shift in the global economy has taken place. As a result of the financial crisis, growth across many economies had slowed down. To overcome the crisis countries tried to identify the critical areas that need investment and to develop a prosperous environment in the country. Countries have to identify and strengthen the forces that will make a marked change in driving their economic growth. It was recommended that countries should develop the ability to create value added products, processes and business models through innovation. Accordingly, instead of distinguishing countries as being developed or developing, countries will be distinguished on whether they are "innovation rich" or "innovation poor". Thus, the report specifies the need for collaboration among business, government and civil society to create the enabling environment that will promote innovation.

The Global Innovative Index (GII) is an annual ranking of countries with respect to capacity for innovation and success in innovation. It is published by Cornell University, INSEAD and the World Intellectual Property Organization in partnership with other organizations and institutions. The focus of Global Innovation Index (GII) is to improve the ways to measure innovation and to understand it. It also focuses on identifying targeted policies and various practices to increase innovation in a country. In Global innovation index four measures are calculated namely: 1. Over all Global Innovation Index, 2. Innovation Input Sub-Index, 3. Innovation Output Sub-Index and 4. Innovation Efficiency Ratio. The overall Global Innovation score is calculated by taking the simple average of Input and Output Sub- Index scores. Innovation Input Sub-Index comprises five input pillars that calculate the elements of the national economy that enable innovation activities: 1. Institutions, 2. Human Capital and Research 3. Infrastructure 4. Market Sophistication and 5. Business Sophistication .Whereas, the Innovation Output Sub-Index gives the information about the outputs that are the results of innovative activities within the economy. There are two output pillars 6. Knowledge and Technology outputs and 7. Creative outputs. Innovation Efficiency Ratio is the ratio of the Output Sub-Index score to Input-Sub Index score [24].

As per The 'Global Innovation Index- 2015: Effective Innovation Policies for Development', innovation is being considered as an important factor of all economic activities around the world. Both advanced as well as developing economies have understood the importance of innovation and also, that it plays a key role in driving the economic growth of a country. So, the countries are trying to formulate policies that support innovation led growth. The developing countries are also, no longer falling behind the high-income-countries in formulating the policies that will increase their innovation capacity. The main findings of Global Innovation Index 2015 reports show that: Among the Top performers or High income groups the quality of

innovation plays a crucial role. Due to the world – class universities, countries like USA and United Kingdom stay ahead in their economic group. The middle-income-countries such as China and Malaysia are the champions among their peers and are fast rising in innovation ranking and even have performed at par with the lower tier of high income countries. The Institution pillar is found to be the most important and a crucial factor to increase the innovation performance of a country. To have a good innovation policy there is a need to have good supporting institutions in the country. Among the poor economies business sophistication pillar is found to be the important factor that enhances the level of innovation in these countries. Among the top 10 middle-income-economies, BRICS economies are at the top in terms of innovation quality. Within BRICS countries, China has shown a lot of progress in terms of innovation quality and has left other countries in the group far behind [24].

An Australian study also supports the fact that innovation acts as a basic driver for sustainable productive growth and social wellbeing [25]. The increase in the level of competition in the global economy has become a driving force for businesses to become more innovative. In turn the capacity for innovation has become an important factor for the success of the individual firm and also for improving the competitiveness of the country in the current global economy. [15]. Capacity to innovate plays a very important role for countries to survive in the global market place. Also, countries can gain prosperity and growth by making use of their innovative capacity [26] , [24].

To be recognized in the global market place, countries need to identify and understand their competitive position among other countries and to strengthen their competitiveness by becoming more innovative.

Competitiveness

According to the Global Competitiveness Report (2014-15) the competitiveness of a nation is defined as, "The set of institutions, policies and factors that determine the level of productivity of the country" or as per the OECD definition "the degree to which it can under free and fair market conditions, produce goods and services that meet the national standards of international markets while simultaneously expanding the real income of the citizens, thus improving their quality of life" [27]. The level of productivity sets the level of prosperity that can be reached by an economy. A more competitive economy tends to grow faster over time.

Every year the World Economic Forum (WEF) publishes Global Competitiveness Reports which help the countries to understand their competitive position with respect to other countries in the world. These reports serve as benchmarks for national policymakers to assess the relative performance of each country in achieving competitiveness as represented by the accepted indices, so that countries can overcome the barriers to improve the competitiveness. The competitiveness of a country can be viewed as the position of the country in the international market as compared to the other countries especially in similar states of economic development. According to the Global Competitiveness reports there are many determinants that drive productivity and competitiveness like education and training, technological progress, macroeconomic stability, good governance, firm sophistication, market efficiency, etc. which are often mutually supportive.

Description of the 12 pillars of Global Competitiveness Index

The twelve pillars are combined as a weighted average to calculate the Global Competitiveness Index. Innovation is a key pillar and as per review of existing studies a positive relationship is expected between innovation and the other eleven pillars of the Global Competitiveness Index.

1. *Institutions:*

According to the Global Competitiveness Report 2014-15, the institutional environment is determined by the legal and administrative framework in a country, within which institutions, firms and government interact to generate wealth. The report specifies that it is important for the countries to have a sound and fair institutional environment. The quality of institutions is supposed to have a strong impact on competitiveness and the growth of a country [28], [29]. The quality of institutions not only influence the investment decision and organization of production but also play an important role in the manner in which societies distribute benefits and bear the cost of development strategies and policies. It also, includes government attitude towards markets and market efficiency. Stringent rules and regulations, corruption, lack of transparency, inability to provide appropriate services to the business sector, act as barriers and slow down innovation and the economic growth of a country. [11].

2. *Infrastructure:*

Well-developed transport and communications network including effective modes of transportation like: good roads, railway tracks, port and air transport, adequate electricity supply and an efficient telecommunication system. These are useful for efficient conduct of business [11]. A developed infrastructure network has a significant effect on economic growth of a country; it also helps in reducing the inequality in income and poverty in several ways [30], [31].

3. *Macroeconomic environment:*

A stable macroeconomic environment in the country is important for harboring business development [32]. While productivity cannot be increased by macroeconomic stability alone but instability can prove detrimental to business performance and economic growth [11]

4. Health and primary education:

A country having a strong and healthy work force is essential for achieving labor productivity and competitiveness. A less educated work force in a country will be a constraint for it to use more advanced and innovative technologies. Therefore, it is imperative for a country to take measures to impart quality basic education to its citizens [11].

5. *Higher education and training:*

In today's era of globalization it has become extremely important for countries to nurture a pool of well educated workers who can do complex jobs and are capable of adapting to the changing environment and needs of the production system. As per research, quality of higher education and training is most essential for the countries whose aim is to excel in innovations and complex technological process and products [33], [34]. Higher education and training includes secondary and tertiary enrolment rates of education. These along with extent of vocational and continuous-on-job training are important to ensure constant upgrading of the skills of the workers [11].

6. *Goods Market Efficiency:*

A healthy competition in the market is important to drive the market efficiency and business productivity. Minimum government intervention in the processes that affects the business activities is required for an efficient environment of exchange of goods. Countries which have efficient goods market are well positioned in the market. These companies produce the right mix of products and services as per the supply and demand of goods in the market. Market efficiency also depends on demand condition like customer orientation and buyer sophistication [11].

7. *Labor market efficiency:*

The efficiency and flexibility of the labor market is considered as an important factor in innovation and competitiveness. It should be ensured that workers are allocated to jobs where they can perform their best. There should be flexibility in the labor market so that workers can easily be shifted from one economic activity to another and the flexibility in wages can minimize the disruption in production process and systems. In an efficient labor market, clear and strong incentives must be provided to the workers, workers should be promoted on the basis of their meritorious performance, the business environment should be fair and non-discriminatory [11].

8. *Financial market development*:

A sound and well-functioning financial sector is very important for carrying out the economic activities efficiently. An efficient financial sector allocates the resources saved by the citizens and those received from other countries to their most productive use, the financial resources are provided to the entrepreneurial and investment projects that have highest expected rate of return. A thorough assessment of risk is an essential and important part of sound financial markets .Since business investments are critical for enhancing productivity, economies need to have sophisticated financial markets that can make capital available for investment by the private sector. The financial markets need to have appropriate rules and regulations to protect the interest of investors and others players in an economy [11].

9. *Technology readiness:*

The technology readiness factors measure how fast an economy adopts the existing technologies to enhance the productivity of its firms. It also has a strong emphasis on the capacity of the economy to take full advantage of information and communication technology (ICT) in its day to day activity and in production processes in order to increase efficiency and enable innovations [35], [11].

10. *Market size:*

The size of the market affects the productivity of a firm. If the size of the market is large, firms will produce and sell more quantity of goods that will result in reduced production cost; i.e. firms will be benefited due to economies of scale [11]. Globalization has made it possible for the firms to carry out their business operations not only within the geographical boundaries of their own nation but throughout the world. Studies have shown that the openness of trade has a positive relationship with the growth of an economy. It has also, been observed that trade has a positive relation with growth especially for the countries having small domestic markets [36] – [39]. For the countries having small size of domestic market, they can export the products in order to gain better market access.

11. Business sophistication:

Business sophistication is thought to be mainly dependent on: quality of a country's overall business networks, quality of individual firm operations and strategies and interplay between all these. The quality of business network is measured by the quality and quantity of local suppliers and the extent of interaction between business networks and local suppliers. Efficient networks enhance business performance and result in more opportunity for innovation of processes and products. They help in reducing the barriers to the entry of new firms. [11]. By increasing competition, business sophistication encourages firms to produce unique products and be innovative.

12. *Innovation:*

This factor in GCI focuses on technological innovations. Non technological innovations which arise from know-how, skills and working conditions and are embedded in the organization are largely covered under the factor of business sophistication. The Global Competitiveness Report, 2014-15 discussed that although a large amount of progress can be made by a country through carrying out improvements in: institutions, infrastructure, macroeconomic stability etc. but these gains keep on diminishing over time. This is also true for gains from efficiency of labor, financial markets and goods market. It is technological innovation alone that leads to enhanced standard of living in the long run and does not exhibit diminishing gains. Innovation plays a very important role in the economic growth of a country. Countries must provide an environment that facilitates innovative activities carried out by companies so that their companies design and develop cutting edge products and processes to gain a global advantage. This requires the private and public sector to make sufficient investment in research and development (R&D) [11].

III. METHODOLOGY

In the present paper we have compiled the data on all the 12 pillars, influencing factors, of Global Competitiveness

Index (GCI) as mentioned in the Global Competitiveness Report 2014-15 for the top 10 countries on the basis of their competitiveness for the period of 8 years i.e. (2007-08 to 2014-15). These 10 top performing countries have been selected as per their rank in the 2014-15 competitiveness index. In order to identify the key factors that influence innovation the empirical analysis also, considers data from the big emerging economies called BRICS. The BRICS countries are not high on innovation performance but they have high GDP growth rate. We have included these 5 nations as they are large, emerging economies and can help us to study if high income growth rates have an important effect on innovativeness. The value of GDP annual Growth rate for all countries for the period 2008 to 2015 is taken from the World Bank data [3]. The data is arranged in panel form and then analyzed to identify the significant variables that determine a country's innovativeness.

TABLE II provides variable and variable abbreviations used in the study for purpose of data analysis.

TABLE II
VARIABLE ABBREVIATIONS USED IN THE REGRESSION

Variable	Variable Abbreviation
Innovation	INNOV
Business Sophistication	BUS SOP
Market Size	MKTSIZE
Technology Readiness	TECRED
Financial Market Development	FINMKTDEV
Labor Market Efficiency	LABMKTEFF
Goods Market Efficiency	GODMKTEFF
Health and Primary Education	HEA/PRIEDU
Higher Education and Training	HIGEDU/TRA
Macroeconomic environment	MACECOENV
Infrastructure	INFR
Institutions	INSTI
GDP growth rate	GDPGRWRT

A regression model was fitted to the data in order to understand the determinants of innovation. Along with the twelve GCI pillars of competitiveness and GDP growth rate for the countries is being taken from World Data Bank [3]. GDP is an important explanatory factor of innovation [40].

Model and Findings:

INNOV= f (BUS SOP, MKTSIZE, TECRED, FINMKTDEV, LABMKTEFF, GODMKTEFF, HEA/PRIEDU, HIGEDU/TRA, MACECOENV, INFR, INSTI, GDPGRWRT)

TABLE III
REGRESSION RESULTS

Variables	Coefficient	T-Statistic	Significance (P>|t|)
BUS SOP	0.46	2.92	0.004***
MKTSIZE	- 0.263	- 2.68	0.009***
TECRED	0.027	0.5	0.619
FINMKTDEV	- 0.0009	- 0.02	0.986
LABMKTEFF	0.386	3.87	0.00***
GODMKTEFF	0.043	0.27	0.791
HEA/PRIEDU	0.184	1.77	0.08*
HIGEDU/TRA	0.263	2.6	0.011**
MACECOENV	- 0.043	- 0.98	0.332
INFR	0.014	0.23	0.821
INSTI	- 0.149	- 1.21	0.229
GDPGRWRT	0.003	- 0.66	0.511
CONSTANT	0.005	0.01	0.996

R^2 = 0.7826; ***Significant at 0.01 level, **Significant at 0.05 level, *Significant at 0.1 level

The fitted regression model was a good fit and yielded the following results: of all the 12 explanatory variables considered in the model, only five variables were found to be significant. Out of these five variables; four variables have a direct effect on improving the innovative ability of the country viz. BUS SOP, LABMKTEFF, HIGEDU/TRA, HEA/PRIEDU. Among them two variables, namely: BUS SOP i.e. Business Sophistication (coefficient= 0.46) which is a measure of Business Sophistication in a country and LABMKTEFF i.e. Labor market efficiency (coefficient= 0.386) which is a measure of efficiency and flexibility of Labor Market of a country were found to be significant at 1% level of significance and were directly related to innovation. HIGEDU/TRA i.e. Higher Education and Training which is a measure of the secondary and tertiary enrolment rate of students for higher education, the quality of education and extent of training in a country was significant at 5% level (coefficient 0.263) and HEA/PRIEDU (coefficient 0.184) i.e. Health and Primary Education which is a measure of Health facilities provided to the workforce and the quality and quantity of basic education received by the population of a country was found to be significant at 10% level of significance. Both these variables exercised a positive influence on innovation.

The variable MKTSIZE i.e. Market Size (coefficient= - 0.263) which is a measure of the size of both domestic and international markets available to the firms of a country was significant at 1% level of significance. However, market size is inversely related to innovation in our model. This suggests that increases in the size of the market reduce the innovation by a country.

IV. INTERPRETATION OF RESULTS

Based on the results of the regression analysis, it can be concluded that the innovation ability of a country is significantly affected by the quality of the 5 significant explanatory variables:

1. The quality of a country's business networks,

supporting industries and quality of individual firm operations and strategies determine the level of Business Sophistication. In order to enhance the quality of business networks, a country needs to focus on enhancing the quality and quantity of local suppliers and increasing the interaction between suppliers and business entities. Companies need to have more than one local supplier, to obtain quality raw material which will lead to the production of quality products. The local suppliers should be located close to the production unit of the company to have timely supply of the raw material with low transportation costs. This will help in producing better quality products at lesser price and in less time. The geographical proximity between companies and local suppliers will help to increase the mutual interaction between both the parties that will result in increased operational efficiency. It will also help to create a greater opportunity for producing innovative products and processes and increase the level of innovation in the country. It will also reduce the barrier for the entry of new firms in the market. Thus, increasing the level of business sophistication in the country will enhance the innovative ability of the country.

2. The efficiency and flexibility of labor market (Labor Market Efficiency): To enhance the labor market efficiency in the country, workers should be provided incentives in order to motivate them to perform their best. This will help to retain quality workers in the company and result in enhanced total factor productivity for the company. Workers should be skilled to perform more than one job so that the company will have a pool of skilled workers that will enhance the possibility of making innovative products and will support any changes required to innovate. This can also, be enabled through job rotation. In some cases job rotation helps the company to shift the workers easily in less time and in less cost and makes it easy for a company to address the labor requirements of products or process innovation. Labor Market Efficiency has positive relation with innovation i.e. by increasing the level of labor market efficiency in a country the innovation ability of the country will also increase.

3. Quality of higher education and training in a country (Higher education and training): Increasing the level of higher education and training in a country will help the labor force to come up with new ideas, develop innovative products and advance technologies. More emphasis can be given for vocational and on-the-job training to enhance the skills of the work force. This will help a country to have a pool of workers who will be able to carry out complex jobs and who can adapt easily to the changing environment and upcoming needs of the production system, thereby contributing to the overall growth of the economy.

4. Adequate health facilities to the workforce and the quality and quantity of basic education received by the population of the country (Health and primary education): In order to increase the level of Health and Primary Education in the country, efforts need to be made to provide better health services to the citizens that will help to enhance the productivity and competitiveness of the country. Unhealthy workers cannot perform well and will be less productive, that will lead to loss of income and output for business and the economy. Better health services will decrease the rate of absenteeism and improve productivity and performance.

5. Market size: The negative correlation observed between market size and innovation is significant. As a pillar in the Global Competitiveness Index market size offer advantages of economies of scale and resultant efficiency gains help to make products competitive. The inverse relation of market size and innovation in our study can be attributed in part to the nature of the data. The 5 BRICS economies are big markets but not high on innovation. However, the importance of downstream innovation, not just basic research; openness to the world, its ideas and opportunities; a sense of national mission; a government whose wider policies support innovation and technology; and strong but flexible institutions to back this up can enable small economies to innovate effectively [41].

V. Conclusion and Recommendations

The paper attempts to study the factors that are important influencers of innovation at the macro level. Innovation appears to be a key driver of competitiveness and growth, with the unique feature that it can contribute to exponential growth of a country.

Our findings suggest that government policies should focus on improving labor market efficiency and flexibility. In case of India inefficient and rigid labor markets have for long been attributed as a cause for poor productivity and business performance. They have been an impediment in attracting Foreign Direct Investment (FDI), curbing the advantages from being an emerging, fast growing market. In the current government budget for India (2017-18) mention is made that legislative reforms will be undertaken to simplify, rationalize and amalgamate the existing labor laws into four codes – wages, industrial relations, social security and welfare and working conditions. Such efforts in this regard would help to improve innovativeness for India [42].

Market needs and profit considerations guide the development of both firm and industry level operation and strategies. Businesses establish linkages, associations and networks that help to promote their business. However, governments can provide support by putting in place regulations and institutions that reduce the risk of creating business networks and enable grounds for interaction and discussion between businesses across industries and regions.

Promotion of higher education has now become an important objective for all developing countries. Efforts to provide both quality and quantity in this regard are being implemented so as to create a 'global workforce'. In India the present government's Skill India Initiative is a step in this direction. This policy also, focuses on developing vocational skills which can directly contribute to supporting innovation in products and processes at the micro level. Benchmarking with international standards is also, a feature of the Skill India policy.

In fact, while higher education is generally available at lower costs in developing countries relative to the developed west, quality concerns have been a serious issue for long. Thus, adopting quality standards in this area would be essential to create a work force that is more productive and is able to benefit from global job opportunities. An added

advantage would accrue when members of a country's work force gain experience globally and return to share and adopt 'best practices' at home.

Basic needs of primary education and health have to be promoted as a necessary condition for a productive labor force. There are huge resource challenges in this context for economies like India and China, with the largest populations in the world, as also for other BRICS nations like Brazil. Nevertheless these are essential areas of focus to enable the other influencers to work on improving innovation in the country. Perhaps innovations in health products and service provision and progress in using technology to reach basic education to the masses can support government efforts to bring about more visible and quick outcomes.

Large markets provide an opportunity to reach markets for innovations but we find that often the advantage to innovate rests with smaller economies. Recent examples of high innovations from Israel and Scandinavian countries suggests that concerted efforts towards R&D investment, flexibility to adopt new ideas and scope for quick commercialization can offset the advantages of market size.

REFERENCES

[1] Science, Technology and Innovation Policy 2013. Government of India, Ministry of Science and Technology, New Delhi, India, Printed at: Paras Offset Pvt. Ltd., dst.gov.in/st-system-india/science-and-technology-policy-2013.

[2] Klaus Schwab (Ed.), Xavier Sala-i-Martin, Borge Brende, Global Competitiveness Report 2013-14. World Economic Forum, 2013. Geneva, Switzerland.

[3] World Databank, World Development Indicators, http://databank.worldbank.org/data/reports.

[4] Ramadani, V., & Gerguri, S. (2011). 'Theoretical Framework of Innovation and Competitiveness and Innovation Program in Macedonia'. European Journal of Social Sciences, 23(2), pp.268-276.

[5] Lopez-Claros, Augusto, Michael Porter, Xavier Sala-i-Martin, and Klaus Schwab. Global Competitiveness Report 2007-2008. World Economic Forum, 2007. Geneva, Switzerland.

[6] Michael Porter, Klaus Schwab (Co- Directors) Global Competitiveness Report 2008-09. World Economic Forum, 2008. Geneva, Switzerland.

[7] Klaus Schwab (Ed.), Xavier Sala-i-Martin, Global Competitiveness Report 2009-10. World Economic Forum, 2009. Geneva, Switzerland

[8] Klaus Schwab (Ed.), Xavier Sala-i-Martin, Robert Greenhill, Global Competitiveness Report 2010-11. World Economic Forum, 2010. Geneva, Switzerland.

[9] Klaus Schwab (Ed.), Xavier Sala-i-Martin, Robert Greenhill, Global Competitiveness Report 2011-12. World Economic Forum, 2011. Geneva, Switzerland.

[10] Klaus Schwab (Ed.), Xavier Sala-i-Martin, Robert Greenhill, Global Competitiveness Report 2012-13. World Economic Forum, 2012. Geneva, Switzerland.

[11] Klaus Schwab (Ed.), Xavier Sala-i-Martin, Global Competitiveness Report 2014-15. World Economic Forum, 2014. Geneva, Switzerland.

[12] Sedere, U. M., 2000. Globalization and the Low Income Economies: Reforming Education, the Crisis of Vision, Universal Publisher. ISBN-10:1581127456

[13] Muhammad A. C., Mohammad, A.F., Mohammad, K.B. and Iqra, A. (2011). 'Globalization and its impacts on the world Economic development', International Journal of Business and social science, 2(23), pp.291-297.

[14] Friedman, T.L. (2000). The Lexus and the Olive Tree: Understanding Globalization. Anchor Books, New York. ISBN: 0-385-49934.

[15] Jatuliaviciene, G. and Kucinskiene, M. (2010). 'Competitiveness and Innovation Synthesis in the Integrated Global Economy', EKONOMIKA, 89 (2), pp. 76-94.

[16] Mehregan,M.R., Hashemi,S. and Neshanl.,M., (2015). 'Analysing the Bilateral Relationship between Technological Readiness and Innovation of Countries by considering the Mediating Effect of GDP by Considering the Mediating Effect of GDP', Iranian Journal of Management Studies (IJMS), 8 (1), pp: 27-45.

[17] Neef, D., Siesfeld, G.A., Cefola, J. (1998). The Economic Impact of Knowledge. Butterworth-Heinemann, United States of America. ISBN: 0-7506-7009-6.

[18] Arumugam, V. and Jain, K., (2012). 'Technological Transfer from Higher Technological Institutions to the industry in India- A case study of IIT Bombay', Journal of Intellectual Property Rights, 17, pp 141-151.

[19] Sefer, S. and Ercan, S., (2011). 'The effects of Science-Technology-Innovation on competitiveness and economic growth', Procedia Social and Behavioural Sciences, Elsevier, 24, pp. 815-828.

[20] Cainelli,G., Evangelista,R.and Savona,M., (2004). 'The impact of Innovation on the Economic performance in services', The Service Industries Journal, Routledge Taylor & Francis group, 24 (1), pp. 116-130.

[21] Chandra Shekhar, L. and Balasubramanian, S., (2010). 'Initiatives for strengthening Technology Commercialization and the Technology commercialization and the Intellectual property rights systems in South East Asia and India', International Journal of Intellectual Property rights (IJIPR), 1(1), pp. 25-47.

[22] Ringel, M., Taylor, A., Zablit, H., (2015). 'The most innovative companies 2015 Four Factors that Differentiate Leaders', The Boston Consulting Group, USA.

[23] Jackson F.H., Sara T, Kahai S.K., (2014). 'Determinants of Innovative Capabilities of a country and its role in Economic Growth' International Business & Economic Research, 13(5), pp. 1141 to 1148, The Clue Institute.

[24] Soumitra Dutta, Bruno Lanvin, and Sacha Wunsch- Vincent (2015): The Global Innovation Index 2015: Effective Innovation Policies for Development, Cornell University, INSEAD and WIPO Fontainebleau, Ithaca, and Geneva.

[25] Australian Innovation System Report 2010: Australian Government, Department of Innovation Industry Science and Research, Canberra, Australia. www.innovation .gov.au

[26] Belitz, H., Clemens,M.,Schmidt-Ehmcke,J., Schneider, S.,Werwatz,A. (2008). 'Deficits in Education Endanger Germany's Innovative Capacity', DIW Berlin Weekly Report No. 14 /2008, Volume (4), pp. 86-93., www.diw.de/english/produkte/publikationen/weeklyreport.

[27] OECD, (1992).Technology and the economy: the key relationships, Organization for Economic Co-operation and Development, Volume 42, pp.237.

[28] Schumpter, J. (1942). Capitalism, Socialism and Democracy. Harper & Row, New York, 3rd Edition,1950

[29] Solow,R., (1956). 'A Contribution to the Theory of Economic Growth', Quarterly Journal of Economics ,70 pp.65-94.

[30] Aschauer, D. A., (1989). 'Is Public Expenditure Productive? , Journal of Monetary Economics, 23 (2), pp. 117-200.

[31] Easterly, W., (2002). The Elusive Quest for Growth. Cambridge, MA, MIT Press.

[32] Fisher, S., (1993). 'The Role of Macroeconomic Factors in Growth', Journal of Monetary Economics ,32 (3), pp. 485-512.

[33] Schultz, T. W., (1961). 'Investment in Human Capital', American Economic Review, 51 (1): 1-17.

[34] Kremer, M. (1993). 'The O-Ring Theory of Economic Development', Quarterly Journal of Economics, 108 (3) pp. 551-75

[35] Aghion P. and Howitt P. (1992). 'A Model of Growth through Creative Destruction', Econometrica, 60(2), pp. 323-51.

[36] Sachs, J. and Warner. A., (1995). 'Economic Reform and the Process of Economic Integration', Brookings Papers on Economic Activity, 1, pp. 1-118.

[37] Frenkel, J. and Romer, D., (1999). 'Does Trade Cause Growth?' American Economic Review, 89 (3), pp. 379-99.

[38] Rodrik, D. and Rodriguez, D., (1999). 'Trade Policy and growth: A Skeptics' Guide to Cross National Evidence.' NBER Working Paper No. 7081, pp. 261-325, Cambridge, MA: National Bureau of economic Research.

[39] Feyrer, J., (2009). 'Trade and Income: Exploiting Time Series in Geography', NERB Working Paper No. 14910, pp. 1-37, Cambridge, MA, National Bureau of Economic Research.

[40] Wong, P.K., Ho,Y.P. and Autio,E. (2005). 'Entrepreneurship, Innovation and Economic Growth: Evidence from GEM Data', Small Business Economics, 24 (3), pp.335-350, Springer, DOI 10.1007/s11187-005-2000-1.

[41] Rae, J. and Westlake, S.(June 2014) When small is beautiful lessons from highly–innovative smaller countries.www.nesta.org.uk

[42] http://indiabudget.nic.in, Accessed 15 February, 2017

Ujjwala Bhand obtained her B.Sc. (microbiology) in 1998 and M.B.A. (Systems) from Institute of Management Studies Devi Ahilya University Indore India in 2002. Currently she is a doctoral student at Department of Economics, BITS Pilani K.K. Birla Goa Campus, India.

Mridula Goel is an Associate professor, Department of Economics, Birla Institute of Technology and Science, Pilani, K K Birla Goa Campus, Goa, India. She is also in charge of the Center for Innovation, Incubation and Entrepreneurship. She actively manages incubators in the area of ICT and Healthcare in the institute campus. She has been teaching at university level for 35 years and her teaching and research interests span across development economics, international economic order to entrepreneurship. She has mentored several startups in areas of education and finance.

Sport Mega-Events and Media: A Case of the 2014 FIFA World Cup in Selected Key Markets

Gift Muresherwa, Tracy Daniels, Kamilla Swart

***Abstract*—**The hosting of 2014 FIFA World Cup was an ideal opportunity for Brazil to enhance its international image. The aim of this study is to investigate the impact on Brazil and on Rio de Janeiro (as a host city and major tourist destination) of mainstream media reporting on the hosting of the 2014 FIFA World Cup. It provides a picture of how Brazil and Rio de Janeiro were reported in selected newspapers at different stages of the event: pre-, lead-up, during, and post- the 2014 World Cup. The study also seeks to ascertain whether the major objectives of the Brazil World Cup bid were met in the hosting of this mega-event. A media content analysis was conducted in four key tourism markets: Argentina, USA, Germany and Portugal. These countries were chosen because they represent Brazil's main tourism markets and reported significant numbers of ticket sales for the event. The methodology used was qualitative analysis, including content sourcing, content identification and the use of Leximancer, an analytic tool for large amounts of textual data. The study examined online newspapers with the largest readership and circulation numbers in the selected markets. In total, 1961 online newspaper articles relevant to Brazil's hosting of the 2014 FIFA World Cup were analysed. The findings revealed both positive and negative sentiments associated with Brazil's hosting of the event. A key finding from the analysis was that for all markets, there was a shift from relatively positive sentiment in the pre-World Cup period, to more negative sentiment in the lead-up, followed by a return to positive sentiment during and after the World Cup. Having shifted to a more negative view leading up to and during the event, the USA market was dominated by media attention to social unrest and corruption. The period immediately prior to the tournament recorded an increase in both positive and negative media coverage in the US, German and Portuguese markets, but became more positive in the Argentinian market. Thus the lead-up period was particularly significant in all markets. Safety and security concerns expressed in the lead-up period decreased significantly during the hosting and post- periods, and a positive image of the country was noticeable in the international media. Therefore, while the positive sentiments emerging during the event should be capitalised on, Brazil should also address the lurking concerns and negative perceptions that continue despite its successful hosting of the mega-event. By doing this, the nation can consolidate its brand's position in a sustained and positive way. As different reporting tones were noticed in the different markets across the time periods, it becomes important to consider these changes in the future event marketing and positioning of Rio de Janeiro as the leading tourism destination and events capital for Brazil, especially in relation to Rio's hosting of future events.

***Keywords*—**Content analysis; FIFA World Cup; mega-event; sport tourism.

Gift Muresherwa is with Cape Peninsula University of Technology (CPUT), South Africa (corresponding author, e-mail: giftmuresherwa@gmail.com).

Tracy Daniels is with Cape Peninsula University of Technology (CPUT), South Africa.

Kamilla Swart is with American University in Dubai (AUD).

Barriers Facing the Implementation of Lean Manufacturing in Libyan Manufacturing Companies

Mohamed Abduelmula, Martin Birkett, Chris Connor

Abstract**—**Lean manufacturing has developed from being a set of tools and methods to becoming a management philosophy which can be used to remove or reduce waste in manufacturing processes and so enhance the operational productivity of an enterprise. Several enterprises around the world have applied the lean manufacturing system and gained great improvements. This paper investigates the barriers and obstacles that face Libyan manufacturing companies to implement lean manufacturing. A mixed-method approach is suggested, starting with conducting a questionnaire to get quantitative data then using this to develop semi-structured interviews to collect qualitative data. The findings of the questionnaire results and how these can be used further develop the semi-structured interviews are then discussed. The survey was distributed to 65 manufacturing companies in Libya and a response rate of 64.6% was obtained. The results showed that these are five main barriers to implementing lean in Libya, namely organizational culture, skills and expertise and training program, financial capability, top management and communication. These barriers were also identified from the literature as being significant obstacles to implementing Lean in other countries industries. Having an understanding of the difficulties that face the implementation of lean manufacturing systems, as a new and modern system and using this to develop a suitable framework will help to improve the manufacturing sector in Libya.

Keywords**—**Lean manufacturing, barriers, questionnaires, Libyan manufacturing companies.

Mohamed Abduelmula is with Department of Mechanical and Construction Engineering, Northumbria University Newcastle, UK (e-mail: m.abduelmula@Nourthumbria.ac.uk)

Martin Birkett is with Department of Mechanical and Construction Engineering, Northumbria University Newcastle, UK (e-mail: M.birkett@Northumbria.ac.uk)

Chris Connor is with Department of Mechanical and Construction Engineering, Northumbria University Newcastle, UK (e-mail: chris.connor@Northumbria.ac.uk).

Geo-Spatial Methods to Better Understand Urban Food Deserts

Brian Ceh, Alison Jackson-Holland

***Abstract*—**Food deserts are a reality in some cities. These deserts can be described as a shortage of healthy food options within close proximity of consumers. The shortage in this case is typically facilitated by a lack of stores in an urban area that provide adequate fruit and vegetable choices. This study explores new avenues to better understand food deserts by examining modes of transportation that are available to shoppers or consumers, e.g. walking, automobile, or public transit. Further, this study is unique in that it not only explores the location of large grocery stores, but small grocery and convenience stores too. In this study, the relationship between some socio-economic indicators, such as personal income, are also explored to determine any possible association with food deserts. In addition, to help facilitate our understanding of food deserts, complex network spatial models that are built on adequate algorithms are used to investigate the possibility of food deserts in the city of Hamilton, Canada. It is found that Hamilton, Canada is adequate serviced by retailers who provide healthy food choices and that the food desert phenomena is almost absent.

***Keywords*—**Canada, desert, food, Hamilton, stores.

I. Introduction

FOOD deserts are defined as areas of low food retail access and economic deprivation characterized by poor accessibility to healthy, affordable food [2]-[4], [10], [12], [21], [35], [55], [56]. Since the mid-1990's, the term has become more widely used. In the policy debate, food deserts have been associated with a complexity of inter-linkages between increasing health inequalities, social marginalization, disparities in food retail accessibility, compromised nutrition and poor health outcomes [41], [43], [45], [54].

The lack of access to affordable healthy food has been suggested to be a contributing factor to poor diet [25], [33]. Consequently, the concept of food deserts has been gaining attention, particularly in North America and Britain, where there has been the mass suburbanization of food retailers and residents [3], [4], [27], [54]. Large grocery stores and supermarkets have moved away from the city centres in preference for suburban and exurban locations leaving some residents of older inner-city neighbourhoods with few grocery shopping options.

Food deserts are localized phenomena that are found throughout many cities, yet their existence and classification remains contested. Some researchers, government agencies and social agencies claim that food deserts are the result of misguided social policy and local government. In actuality, food deserts can be linked to the historical shift of economic activity from centralized to more dispersed locations. Also, increasing automobile ownership facilitated the rapid expansion of urban areas and has allowed more distant grocery stores to be accessible. Automobile mobility became the primary determinant in network planning over public transportation or walking. Municipal planning focused on the automobile as the predominant mode of transportation and it has enabled growth of urban areas to develop at a much faster pace and larger scale. And it is this car-centric urban development that supports the theory that a lack of grocery store access for the socio-economically disadvantaged is the consequence of the government's failure to consider the mobility constraints of disadvantaged individuals. In reality, the prevailing economic pressures of retailers and a growing suburban population necessitates supermarkets and grocery stores to locate in areas accessible by car to reach a large customer base and facilitate the distribution of goods. The oversight of these market pressures has led some to suggest that retailers and government are purposefully marginalizing segments of consumers. The distribution of stores may result in some neighbourhoods having lower accessibility to healthy foods than others. However, retailers and governments do not actively seek to marginalize any area.

The exact cause of food deserts is difficult to identify. Several studies have concluded that the issue is multifaceted. The existence of food deserts can be attributed to market pressures and mass suburbanization that, in combination, effectively worsens the situation for the disadvantaged. A lack of supermarkets and grocery stores impacts food availability and overall health outcomes, particularly for economically-deprived individuals, as good health is dependent on adequate nutrition [13], [14], [51]. Yet other less measurable factors may also be at play [11], [33], [40]. The failure of many people in the developed world to consume a healthy diet has, in part, been linked to the contested existence of food deserts [40]. Furthermore, the fact that the definition of what constitutes a food desert remains largely dependent on the focus of the research makes them difficult to understand.

Much of the retail-related research has been focused on the demand-side. This study incorporates a supply-side approach by examining the spatial distribution of food stores and accessibility for local residents of the Hamilton CMA. Few food study papers explore the difference in distance between large chain grocery stores and smaller food stores. The Hamilton CMA was chosen as the area of study for this research as it is a mid-sized city with socioeconomically

Brian Ceh is an Associate Professor at Ryerson University, Toronto, Canada (e-mail: bceh@ryeson.ca).

Allison Jackson-Holland is a graduate of the Masters of Spatial Analysis Program at Ryerson University, Toronto, Canada (e-mail: alison.jackson@ryerson.ca).

contrasting areas, and as suggested by [44].

II. Research Statement

The research conducted in this paper will focus on examining if disparities in access to food stores exist for individuals residing in different neighbourhoods (dissemination blocks) across the Hamilton CMA. This study uses the dimension of proximity (distance) to assess accessibility. First, by following the research by [24] to assess the distance that individuals living within different neighbourhoods of the Hamilton CMA must travel to access their closest grocery store. And second, by following the research by [7] to determine the level of accessibility for three modes of transportation: private automobile, walking and public transit (bus). Four tiers of food stores will be examined:

1) Tier One – high end supermarket chains (e.g. Loblaws);
2) Tier Two – discount supermarket chains (e.g. No Frills);
3) Tier Three –small local independent food stores;
4) Tier Four – neighbourhood convenience stores.

The purpose of this major research paper is to detect spatial variation in food retail accessibility, establish the statistical relationship between locations of potential food deserts and low-income areas, and determine if potential food deserts exist at any of the four tiers of food stores. The focus of this paper is to explore the concept of food deserts and food store accessibility. For this reason, several accessibility measures will be used to identify areas of concern where potential food retail gaps may exist. The objectives of this study are:

1) Calculate the distance to the closest grocery store by tier for each neighbourhood (Dissemination Block) in the Hamilton CMA.
2) Assess change in grocery store accessibility between 2006 and 2011.
3) Define the relationship between the locations of potential food deserts and the locations of low-income areas.
4) Calculate the service areas of food stores for each Tier for different modes of transportation and identify any potential food deserts.

The service areas will be examined for three modes of transportation. To delineate service areas for **private automobile** a 5 km service area that represents an average travel time of 10-12 minutes will be created, and for **walking** a 1 km service area will be used that reflects a 15 minute walk. To analyze accessibility to food stores using **public transportation** an economic analysis of the population living within a 500 m walking distance of Hamilton Street Railway (HSR) bus routes will be performed. This method was chosen because most of the supermarkets and local food stores are located in the areas accessible by this mode of transportation. This will help determine the characteristics of the population that are within the accessible distance and beyond the accessible distance of food stores. As the cost of a good includes the effort it takes to get to a store, consumers weigh the perceived costs versus benefits. They are only willing to travel so far to purchase a particular product. This concept of distance decay refers to the consumers' willingness to purchase a given product whereby fewer customers purchase a good as the cost (in time and distance) increases

III. Defining Food Deserts

Food deserts, grocery gaps, and food poverty are terms all used to refer to the notion of food inaccessibility or unavailability related to the underservice of grocery retailing within certain places [15], [30], [36], [40], [55]. In the most literal sense, food deserts can refer to a lack of food retailers in a defined area - typically a neighbourhood or greater. More commonly, the concept links to the importance of quality, varied and affordable food offered by food stores. In neighbourhoods where food deserts have been found, for many residents, particularly those with low-income or limited mobility, the lack of nearby stores creates a significant barrier to proper nutrition and a healthy diet [49]. Food deserts are commonly identified in neighbourhoods of relative social deprivation, particularly low income. Consequently, access to food retail is examined in relation to local socioeconomic characteristics [3], [4], [27], [36], [55].

The definition of food deserts has remained fluid and largely conceptual. The lack of consensus amongst researchers as to which measures are relevant to identifying geographical areas of food deserts has contributed to the debate over their actual existence (particularly in the UK) [3], [11], [40]. Part of the difficulty is attributed to the numerous ways in which people access food; access to food is largely understood to be more than a function of geography or individual lifestyle factors alone [3], [36].

Studies have been found to be based largely on measures to nearby supermarkets without the inclusion of small independent grocers and convenience stores [27], [31], [56]. Chain supermarkets are commonly understood to offer better quality foods, availability and selection in number and type of goods available at lower prices [6], [8], [26], [27], [56].

Chain supermarkets have the advantage of economies of scale, greater bargaining power with distributors and can negotiate lower rent that allow them to sell food products for cheaper prices on average than in small grocery and convenience stores [8], [22], [31], [36]. Discount chain grocery stores rely heavily on economies of scale and run larger stores to operate profitably; the physical need for more space makes them unsuitable for inner-city neighbourhoods [8]. In socially distressed areas, the absence of supermarkets in socially distressed areas means that residents without access to a car have few shopping choices; fresh fruits and vegetables have been found to be less available and more difficult to acquire [26], [27], [54].

Though much of the research on food deserts focuses on accessibility to supermarkets, partly because data can be easily attained on large food retailers, the role and location of the independent or small chain food provider often goes unseen. A study on food availability in Francisco [41] found that in areas without large chain supermarkets smaller retail chains and independent grocers offer residents healthy foods at affordable prices. Yet others have found that while small food and convenience stores offer opportunities for support of local economies, residents living in food deserts must pay more for

groceries [26], [27] and that healthy foods are more expensive in low-income areas compared to more affluent ones [37].

IV. Health Risks Associated with Food Deserts/Food Insecurity

It is well recognized that a healthy diet leads to better health and reduced healthcare costs, whereas an unhealthy diet leads to poor health [18], [28], [56]. In particular, a diet that includes fresh fruits and vegetables is linked to the reduced risk of obesity, diabetes, and cardiovascular disease [19], [56]. It has been found that individuals living in low-income areas do not consume the recommended amount of fruits and vegetables. Furthermore, the absence of these foods may be associated with a higher prevalence of morbidity and mortality rates observed in low-income populations [23]. Residents of some low-income areas must rely on convenience stores and gas stations that offer foods of lower quality, but are more filling [27], [29], [42].

Residents of food deserts who experience food insecurity are at risk of important physical, psychological, physiological and socio-familial consequences. Household food insecurity has been linked to high cholesterol, heart disease, diabetes and developmental deficiencies in children [17], [19], [48]. A study of elementary school children in US metropolitan areas showed a strong correlation between the cost of fruits and vegetables and gains in body mass index (BMI), and observed greater impact on those children living in poverty [46].

Among socioeconomic determinants of health, low-income and relative deprivation is consistently linked to poor health outcomes [14], [19], [52]. In the examination of food deserts, a range of socioeconomic factors are used to measure neighbourhood deprivation including: income, home value, population density, level of education, family status, mobility (car ownership), age, social assistance and low-income cut-off [27], [31], [56]. Consequently, how neighbourhood status is defined is subjective, and to a certain degree, determined by the focus of research [7]. Nevertheless, where potential food deserts have been identified, low-income prevalence has been a common characteristic. In the UK, poor food retail provision has been found in areas with low-income and poor mobility [16], [36]. Whereas in the U.S., food deserts are more commonly related to poverty and race (African Americans and Hispanics) in inner-city neighbourhoods [38], [56]. Canada's poorest neighbourhoods tend to have large concentrations of recent immigrants and visible minorities experiencing declining incomes [29], [49].

Not everyone living in a food desert experience physical constraints, as those with access to a vehicle can drive to the closest grocery store. Yet for individuals who must leave their neighbourhood or travel further to shop for groceries, the lack of vehicle access further compounds the problem and thereby makes routine tasks task much more difficult; it is often inconvenient and time-consuming [9], [14]. Households with limited transportation, of which low-income individuals and the elderly are the most likely, must plan ahead and be flexible in their transportation options. Mobility strategies include lengthy bus commutes, expensive cab fares, the dependence on a family member, partner or friend for transportation, and walking [9], [34], [44].

V. Where Food Deserts Have Been Found

Food deserts are a phenomenon of the industrialized world found in both rural and urban areas. A current review of the research by [4] summarizes the findings of studies that have identified food deserts in the US, UK, Canada, Australia and New Zealand. This review suggests that the degree of food desertification is worse in the US, where localized deprivation exacerbates individual disadvantage.

In the US, studies regarding geographic accessibility have found that areas of low-income and a high proportion of African Americans had fewer supermarkets and chain grocery retailers per capita than socioeconomically advantaged areas [31], [39], [56]. In terms of distance, residents of low-income neighbourhoods [53], [56] and a high proportion of African Americans [20] and [56] had to travel greater distances to shop for groceries at supermarkets. And in rural America, [32] found that of all US counties, 418 were food deserts, nearly 98% of which were located in counties with less than 10,000 people. Counties where food deserts are commonplace are concentrated in North Dakota and Montana, and stretch along a band to the western portion of Texas.

Spatial variations in urban and suburban neighbourhood (by census tracts) access to supermarkets in London, Ontario, as well as the changing levels of supermarket accessibility over time (1961-2005) were analyzed [27]. Similar to the methods used by [3], this study examined distance to the closest supermarket and number of supermarkets within 1 km, but unlike the Montreal study, measured accessibility in relation to walking and public transit. Furthermore, areas with the poorest access by walking were located in neighbourhoods with the greatest socioeconomic distress. Those supermarkets that had the best access by means of walking were typically located in less distressed neighbourhoods. And over time, access to supermarkets was found to have diminished with the average proportion of census tract population with easy access dropping from 45% in 1961 to 18% in 2005.

VI. Policy Implications

Early accessibility research conducted in the 1990's that identified some areas of Britain as food deserts. Consequently, the results influenced policy recommendations to promote adequate retail provision [1]. It has been argued that a lack of empirical evidence that food deserts exist and that policy responses aimed at retailers are misguided [11]. Studies suggest that it is the interplay of factors including income, access, transportation, availability, price, cooking skills and confidence that contribute to the formation of food and shopping behaviour [25]. A study conducted by [33] in an economically-deprived urban area in South Yorkshire, England found that neither the lack of supermarket access or food price influenced fruit and vegetable consumption, but that socio-cultural values towards diet held by individuals discouraged healthy food consumption. It has been found that

in Montreal, Canada, some of the most affluent residents had the poorest availability of fruits and vegetables [5]. These studies indicate that poor nutritional intake is not always a consequence of measurable factors such distance to food stores, healthy food availability, affordability or mode of transportation. They suggest that an individual's socio-cultural values and attitudinal beliefs strongly influence dietary lifestyles.

VII. Data and Methods

This study examines the differences in accessibility that residents of different areas have to purchase groceries in the Hamilton CMA. The metropolitan area, located approximately 70 km west of the City of Toronto, includes the Cities of Hamilton, Burlington and Grimsby. The City of Hamilton was amalgamated in 2001 from previously separate administrative areas of the City of Hamilton, towns of Dundas, Ancaster, Flamborough, township of Glanbrook and Stoney Creek (Fig. 1). The CMA's total population in 2011 is $721,053, a 4% increase from 2006, and had a Median Total Income (all economic families) of $71,600 in 2006 [47].

To determine if potential food deserts exist in the Hamilton CMA at any of the four tiers of food stores, four analyses were conducted. The first was a minimum distance analysis utilizing ArcGIS Network Analyst to examine the spatial variation in grocery store accessibility based on distance to closest store, the results of which were used in a correlation analysis. These findings allowed for the identification of areas of relative economic disadvantage that may need to be monitored. The second was a service area analysis using Network Analyst that allowed the demarcation of the estimated extent of travel in distance to a grocery store by driving and walking for each tier of food stores and for the tiers combined. The third was a service area analysis of all food stores using the Hamilton Street Railway bus routes. The fourth was a hot-spot analysis of large chain supermarkets (tiers one and two combined) and smaller independent and convenience stores (tiers three and four combined). These findings identified areas where store clusters may be present.

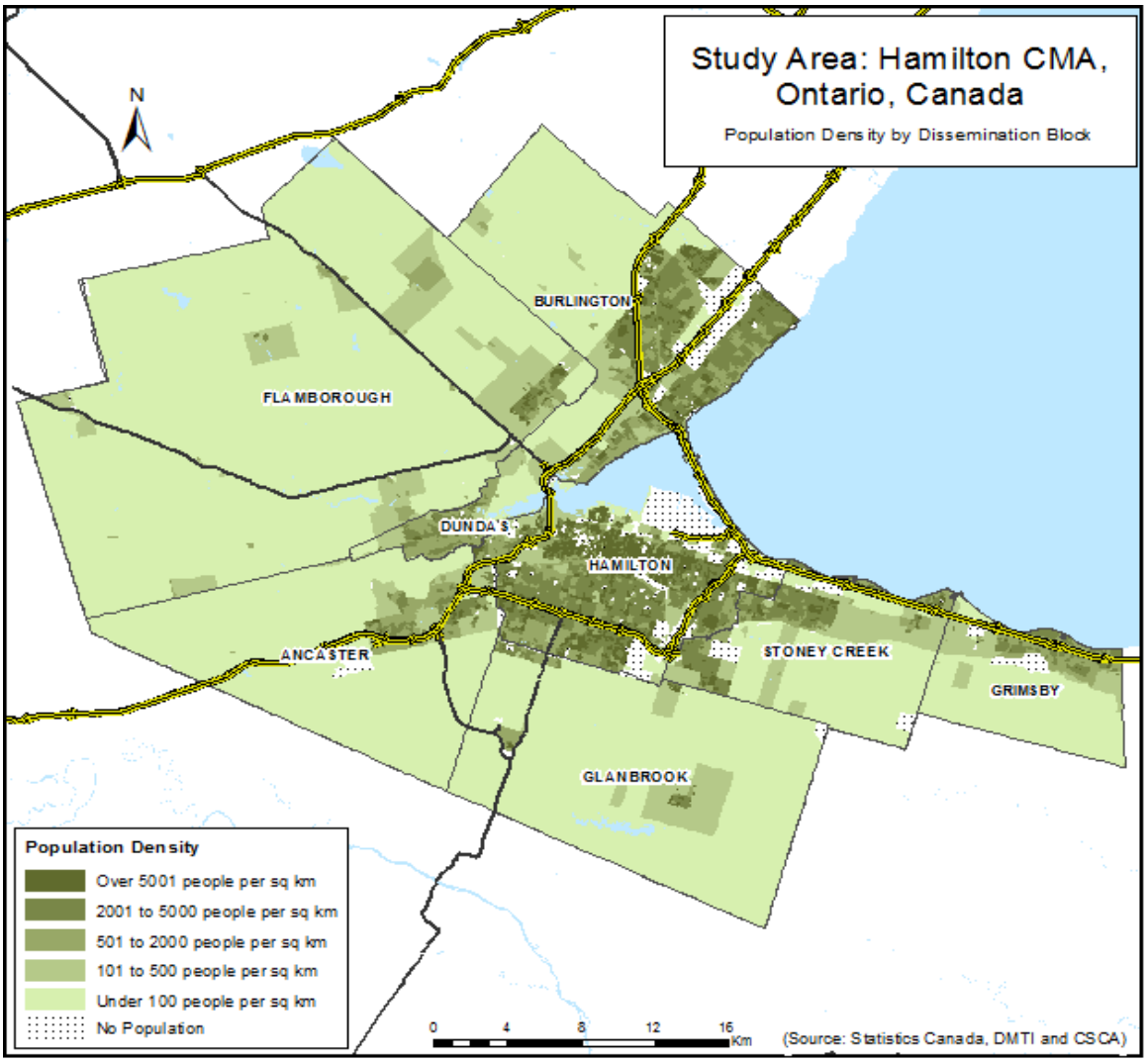

Fig. 1 The study Area: The Hamilton CMA [47], [56]

Although this study uses the finest geographic level at which census data are available (dissemination blocks), some units span a larger distance than others. Depending on the spatial distribution of the population within a given dissemination block, the distance measured from the block's centroid to the closest grocery store are estimates of the true distance residents must to travel for groceries, and the extent of the population serviced by the food providers are only estimates of the true service coverage for the different modes of transportation.

The dataset containing all of the food stores that were open in the Hamilton CMA in 2007 and 2011 was provided by the CSCA at Ryerson University [57]. The stores have been selected based on the NAICS classification code, first three digits 445, relating to the category of food and beverage stores. This includes food stores (supermarkets, other grocery stores, and convenience stores), specialty food stores (meat markets, fish and seafood markets, fruit and vegetable markets, other specialty food stores, baked goods stores, confectionery and nut stores, and other specialty food stores), as well as beer, wine, and liquor stores [50]. Store data from 2007 was used rather than 2006 because it was a more complete dataset (data collection of strip malls and power centres began in 2007). A minor difference (gap) exists between the time of collection of store data and census data. For the sake of simplicity, all discussion based on store data and results based on 2007 stores will be referred to as 2006 to correspond with the matching year of the census.

TABLE I
HAMILTON CMA TIER ONE AND TIER TWO CLASSIFICATIONS

Tier	Food Store Name
Tier One	A&P
	Ultra Mart & Drugs
	Ultra Mart & Drugs
	Sobeys
Tier Two	Fortinos
	Food Basics
	Price Chopper
	No Frills
	Foodland
Tier Three	The Barn Fruit Markets
	Longo's Fruit Markets
	Ernie's Meat Market
	Vallentino's Bakery
	Fenworth Food Market
Tier Four	Hasty Market/Farah's Foods
	Fresh Variety Convenience
	M&M Meat Shops

VIII. DIVISION OF TIERS

The food stores that were open in 2007 and 2011 have been separated into four tiers based on the average cost of goods they sell. It is also important to distinguish full-line supermarkets from smaller food stores as the former have been found to carry more healthy food items at lower prices. Supermarkets are defined as large corporate 'chain' grocers and are further classified based on pricing strategy. This classification was chosen to simulate consumer choice in store selection through product pricing. Tier One consists of high-end large chain grocery stores whose target market includes customers of higher income households or individuals that have no choice but to shop there due to accessibility constraints (Table I). Tier Two consists of large chain discount grocery stores that use everyday low pricing. They offer value-brand products with generic labels and cater to consumers that are more conscious of price and less discriminate about brand and service (Table I). Tier Three includes small independent food stores, specialty food stores such as bakeries, fruit and vegetable markets and other stores that offer healthy food items that do not fit into Tier One or Two divisions. Tier Four consists of convenience and franchise stores.

IX. SPATIAL AND TEMPORAL CONCORDANCE BETWEEN 2006 AND 2011 DISSEMINATION BLOCKS

The lowest level of geography that income data is available from Statistics Canada is at the dissemination area. To help calculate 2011 median household income values of residents living inside and outside of service areas, it was necessary to match the 2006 dissemination block polygons to those present in 2011. This was done by first applying the 2006 median household income information at the dissemination area to the dissemination block level, and then to the corresponding 2011 dissemination blocks. This is possible because dissemination blocks are 'nested' within dissemination areas and boundary files include an attribute field with a unique identifier that describes which dissemination area each block belongs to.

X. NETWORK ANALYSIS: SERVICE AREA DELINEATION

The service areas for each of the tiers of food stores were delineated based on travel distances to estimate accessibility by multiple modes of transportation. These analyses were conducted in ArcGIS Network Analyst using the Service Area function and the same road network dataset as used in the minimum distance analysis. The service area for private transportation was defined based on 5 km travel distance that followed vehicle road restrictions (i.e. one-ways, turn restrictions), whereas the walking service area was based on a 1 km travel distance without any restrictions. These values assume that it will take an individual approximately 10-12 minutes to drive at 50 km/h, whereas a 1 km distance will take approximately 15 minutes to walk at a speed of 4 km/h. Each service area for the four tiers of stores were mapped separately and collapsed to identify potential food retail gaps by store type. The third service area analysis examined accessibility to all food stores for residents living within a 6-8 minute walk or 500 m of bus routes in the City of Hamilton. Public transportation accessibility was not defined by network distance to stores as it was found that the majority of stores were located in close proximity to bus routes. The population residing within the defined service area was considered to have access to all stores.

XI. Findings

Between 2006 and 2011, the total number of food stores at all tiers increased only very slightly (Table II). Over this five-year period the Hamilton CMA gained seven Tier One high-end chain grocery stores and eight Tier Three independently-owned food stores accounting for a positive change of 33% and 18%, respectively. At the same time, there was a loss of eight Tier Two discount chain grocery stores as well as five Tier Four convenience and franchise stores, representing respectively a negative 23.5% and 2.6% change. While such a loss in the proportion of discount supermarkets may be cause for concern regarding affordability of healthy food for certain individuals living in affected neighbourhoods, the overall change in the number of large chain grocery stores (Tier One and Tier Two) together was insignificant with a loss of only 1 or a 1.8% decrease. With relatively little change in the total number of large chain grocery stores, few food deserts are likely to be found, particularly once the independent grocery and convenience-type food stores are taken into consideration. It is likely that from 2006 to 2011, individuals will have a shorter distance to travel to the nearest grocery store (Figs. 2 and 3). The minimum distance to the nearest grocery store was calculated from the centroids of 4,956 and 5,237 centroids of 2006 and 2011 dissemination blocks, respectively. As Table III shows, between 2006 and 2011, the weighted average distance to the closest Tier One chain grocery store and Tier Three independent grocery store *decreased* respectively by approximately 10% and 4%, and *increased* for Tier Two chain grocery store and Tier Four food store by 23% and 21%, respectively. The most drastic change was the increase in distance to Tier Two discount chain stores, whereas the least change was found in the distance to Tier Three independent food stores. Another interesting observation that can be made is that the greatest average distance to travel to any tier of food retailer is for Tier Four convenience and franchise stores for both years (Figs. 2 and 3).

TABLE II
Number of Stores by Tier Category and Year

Tier	2006	% of TOTAL	2011	% of TOTAL
Tier One (high-end chain)	21	7.1%	28	9.4%
Tier Two (discount chain)	34	11.5%	26	8.7%
Tier Three (independents)	44	14.9%	52	17.4%
Tier Four (convenience)	197	66.5%	192	64.5%
TOTAL STORES	296	100%	298	100%

TABLE III
Weighted Average Distance to the Closest Grocery Store by Store Tiers (in Meters)

Tier	2006	2011	% Change
Tier One (high-end chain)	3,166	2,839	-10.3%
Tier Two (discount chain)	2,867	3,533	23.2%
Tier Three (independents)	1,807	1,739	-3.8%
Tier Four (convenience)	3,334	4,038	21%

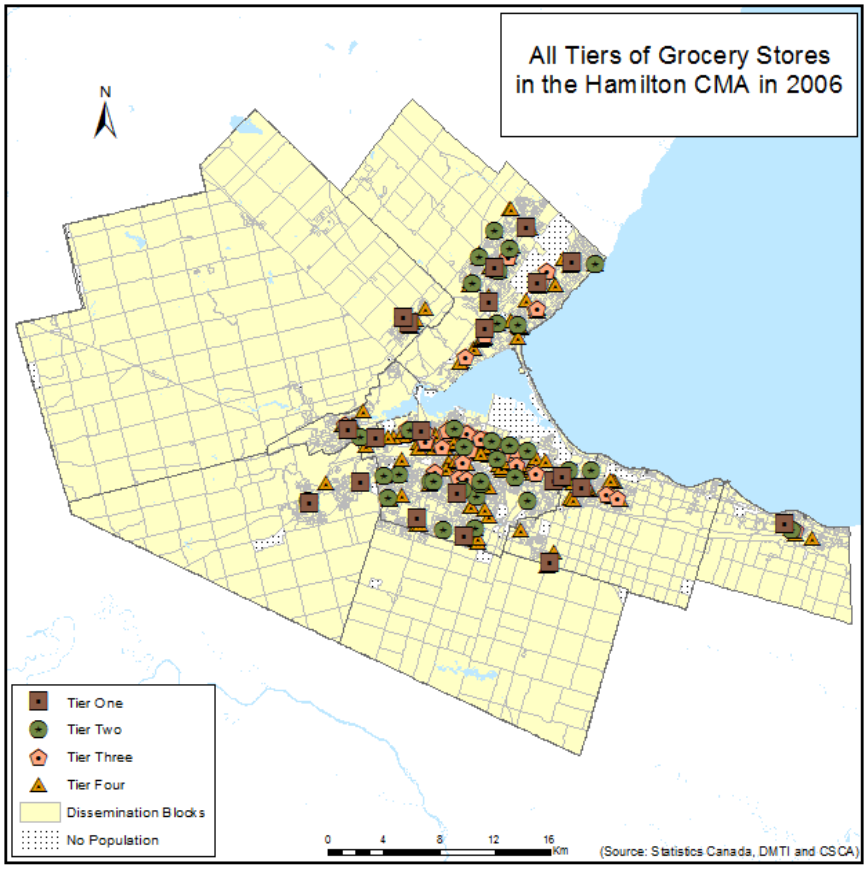

Fig. 2 Food stores by Tier in 2006 [47], [57]

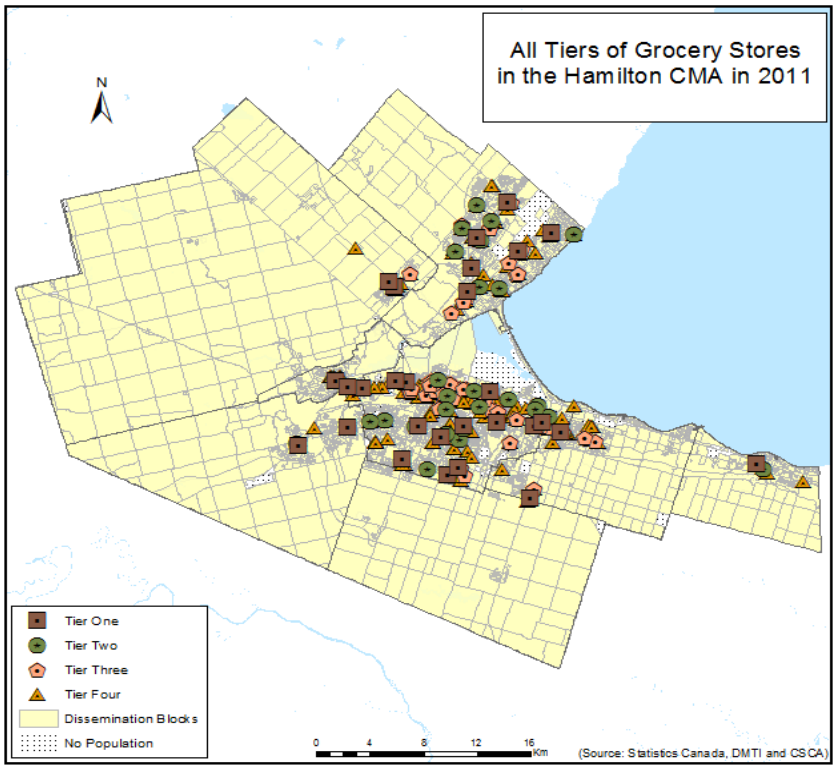

Fig. 3 Food stores by Tier in 2011 [47], [57]

Figs. 4-7 show the changes in distance to the closest grocery store for individuals living in different areas of the Hamilton CMA in 2011. In general, the average distance is greater for individuals residing in the rural areas than for those living in suburban and urban neighbourhoods. The following observations relating to each of the tiers can be made:

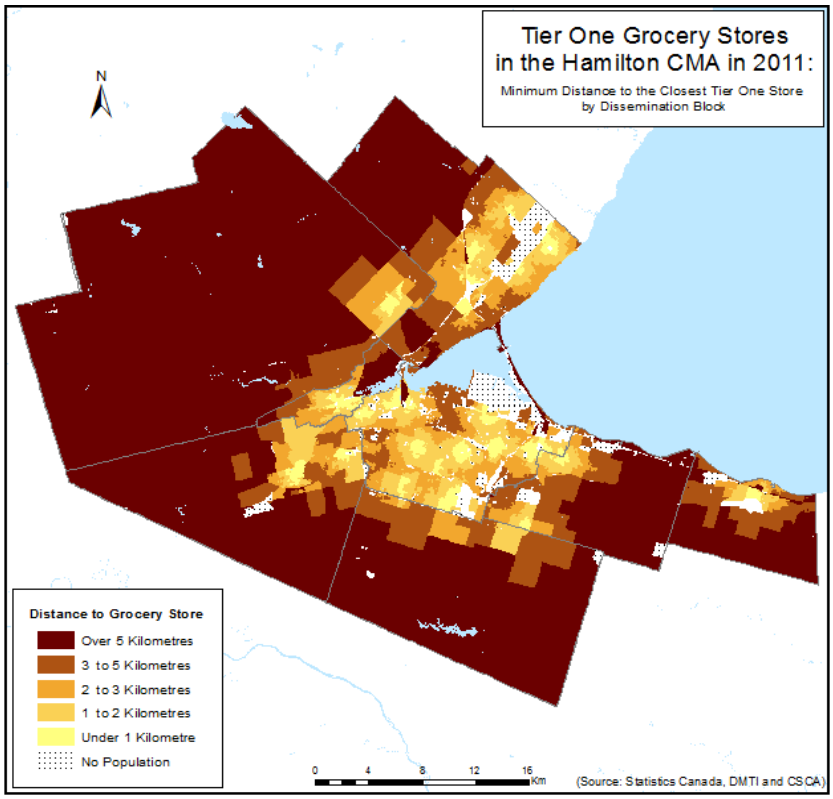

Fig. 4 Minimum Distance to the Closest Tier One Grocery Store in 2011 [47], [57]

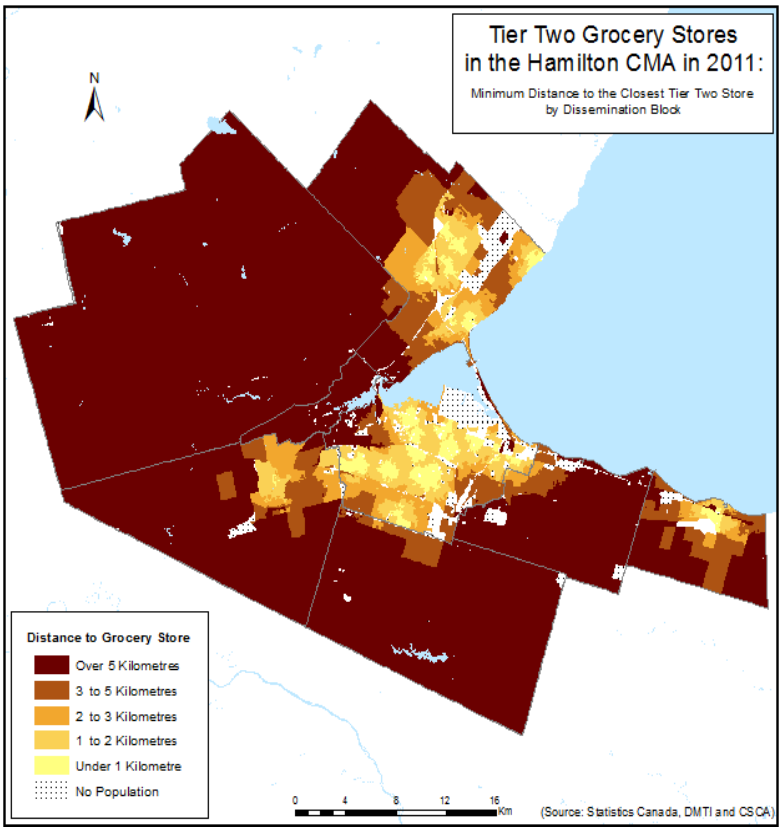

Fig. 5 Minimum Distance to the Closest Tier Two Grocery Store in 2011 [47], [57]

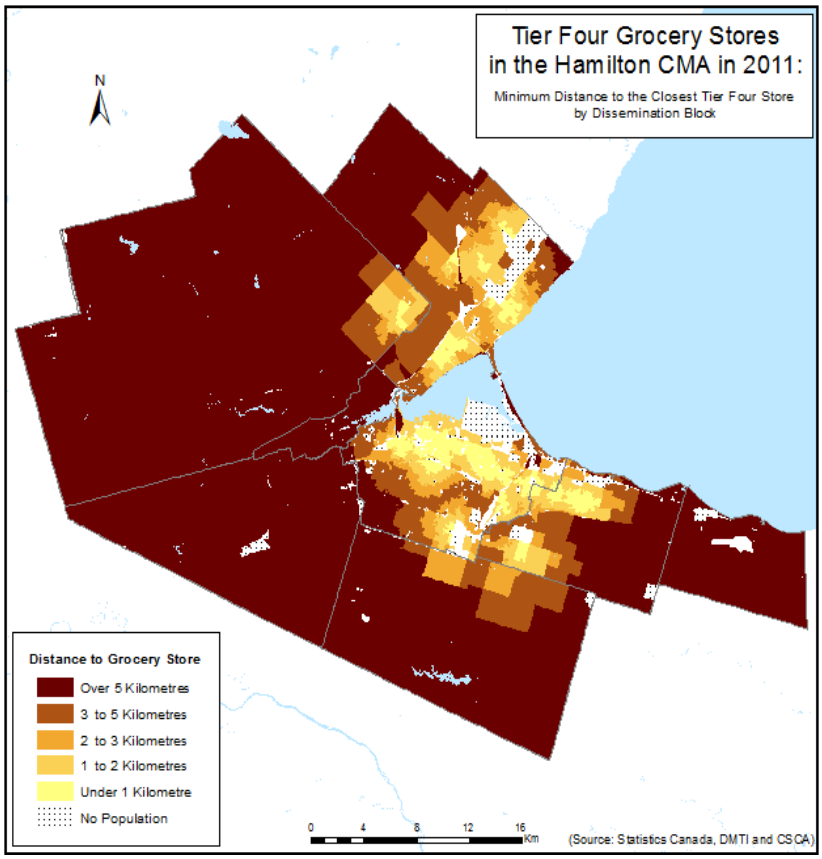

Fig. 6 Minimum Distance to the Closest Tier Three Store [47], [57]

Tier One: Some Hamilton residents had shorter distances to travel in 2011, as the City of Hamilton gained 2 Tier One supermarkets downtown and three on the Hamilton Mountain. Similarly, residents of Dundas and nearby Ancaster gained a Tier One grocery store located in Dundas.

Tier Two: Certain individuals living in Hamilton and Dundas had farther distances to shop to access a Tier Two supermarket. In West Hamilton and Downtown Hamilton as well as in Dundas, Tier Two discount chain stores have been replaced by Tier One high-end supermarkets. Overall, East Hamilton lost two Tier Two stores as did Downtown Hamilton and the Hamilton Mountain area which lost four.

Tier Three: Although the overall number of Tier Three stores increased, particularly in the more densely populated areas, certain regions experienced an overall loss. Dundas lost 1 and Grimsby lost both of its only independent food stores. The Hamilton Mountain showed an overall gain of 1 Tier Three store. Several new Tier Three stores located in the areas of Downtown and East Hamilton as well as in Burlington.

Tier Four: In general, the distribution of Tier Four convenience and franchise stores are well dispersed. Little change occurred in the overall number of Tier Four stores in the City of Hamilton and Stoney Creek. The City of Burlington lost five and town of Dundas lost one; the towns of Flamborough and Ancaster both gained one Tier Four store each.

XII. Correlation between Minimum Distance to a Grocery Store and Income

Median family income by dissemination block for the year 2006 has been mapped to determine if the pattern shows any similarities to that of the minimum distance for 2006 across each of the four tiers (Fig. 8). The incidence of low income after tax (all age groups) as defined by Statistics Canada is 12.1% (11% male and 12.1% female) of the Hamilton CMA population. The map clearly illustrates the difference in household earnings between the various regions. No similarities between the spatial pattern of median household income and the minimum distance to the closest grocery store are identifiable for any of the tiers (Fig. 8). Although a positive relationship was expected between minimum distance and income, all correlation values showed a much weaker relationship than anticipated (Table IV). The strongest relationship was found between Tier Four convenience stores and minimum distance with an r-value of 0.188 that is statistically significant at the 0.01 confidence level. The correlation value of a single variable that explains 18% of the variation in a bivariate correlation is moderately notable. However, in an attempt to improve upon these results, correlation was performed using other variables related to household size. These variables have been chosen to represent the city-suburban differences identified in the patterns of minimum distance. Similar to the resulting correlation values between distance and income, the strongest correlation is that between the minimum distance to Tier Four stores and 6+ person households with an r-value of 0.371. All correlation values show a moderate-weak positive relationship between minimum distance and large household size (6+ persons) and are statistically significant at the 0.01 confidence level (Table V).

TABLE IV
Correlations between Minimum Distance and Median Household Income in 2006

Tier	Sig. (P-value)	Pearson Coefficient
Tier One (high-end chain)	0.193	0.180
Tier Two (discount chain)	0.000	0.142**
Tier Three (independents)	0.000	0.118**
Tier Four (convenience)	0.000	0.188**

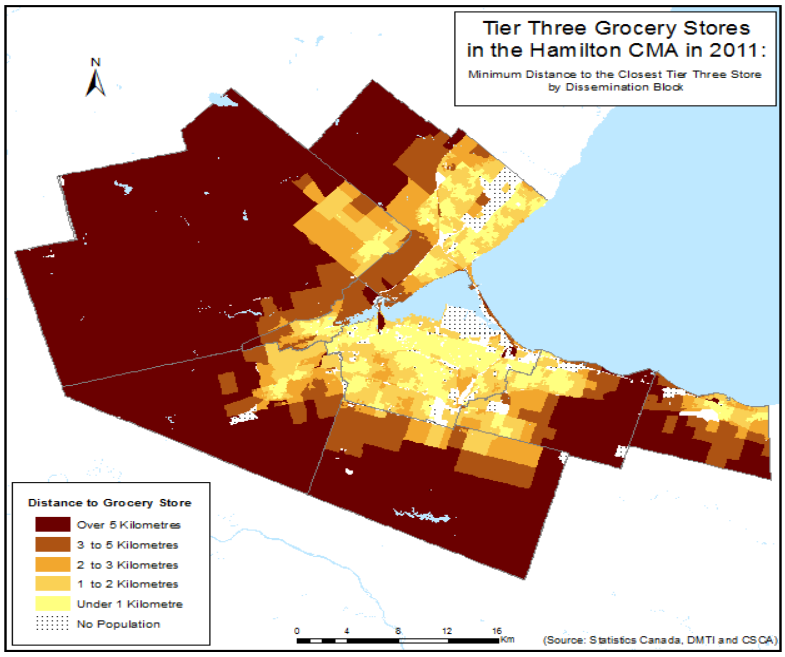

Fig. 7 Minimum Distance to the Closest Tier Four Grocery Store in 2011 [47], [57]

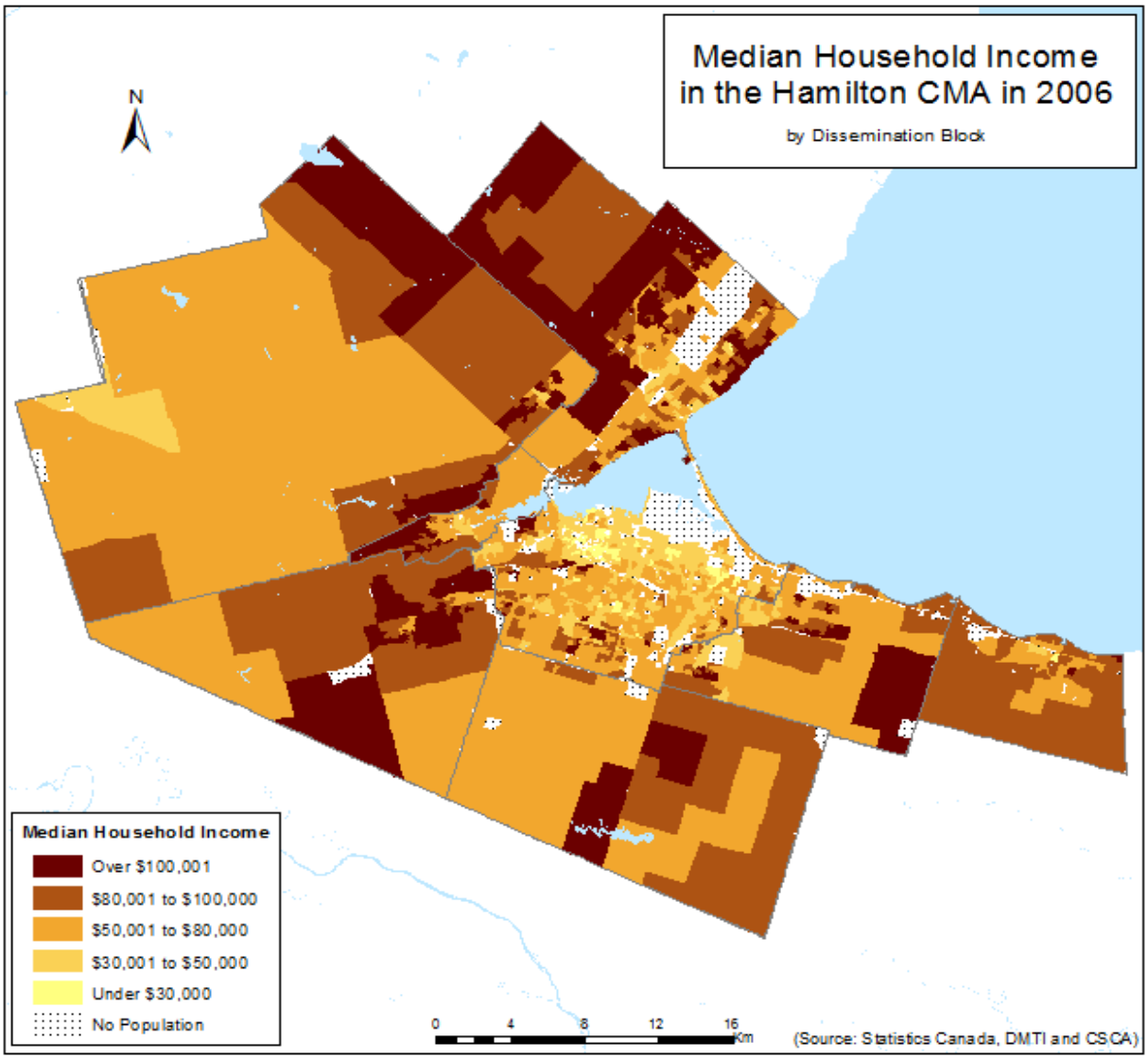

Fig. 8 Median Household Income in 2006 [47], [57]

TABLE V
CORRELATIONS BETWEEN MINIMUM DISTANCE AND 6+ PERSON HOUSEHOLDS IN 2006

Tier	Sig. (P-value)	Pearson Coefficient
Tier One (high-end chain)	0.000	0.292**
Tier Two (discount chain)	0.000	0.338**
Tier Three (independents)	0.000	0.353**
Tier Four (convenience)	0.000	0.371**

** Denotes values significant at the 0.01 Confidence Level

TABLE VI
DRIVE DISTANCE SERVICE AREA ANALYSIS

Grocery Store Type	Service Area Coverage (%)	Area (km²)
Tier One	22.59%	303
Tier Two	16.85%	226
Tier Three	17.67%	237
Tier Four	28.70%	385
All Tiers	28.93%	388

XIII. PRIVATE TRANSPORTATION SERVICE AREA ANALYSIS

The extent of the service areas for each of the four tiers of food stores using the proxy of private transportation (Figs. 12-16) indicated that approximately 23% of the Hamilton CMA was serviced by Tier One stores, 17% and 18% by Tier Two and Tier Three stores, respectively, and 29% was serviced by Tier Four stores (Table VI). Nearly one third of the study area is serviced by food providers when all of the food retail stores are accounted for.

Across all of the tiers, the greatest proportion (89%) of the population using private transportation is serviced by Tier Four convenience and franchise stores, while Tier Three independent food stores service the smallest proportion (72%). For Tier One, the population characteristics indicate that approximately 89% of the population residing in the Hamilton CMA is adequately serviced by high-end chain grocery stores (Table VII). Despite this, there are two densely populated areas where service area coverage was lacking and are classified as potential food gaps: (1) downtown Hamilton (2)

the western Hamilton 'mountain' (Fig. 9). The Tier Two findings show that approximately 78% of the population was serviced by discount chain grocery stores. Five smaller gaps in service coverage are classified as potential food deserts: (1) west Stoney Creek (2) west downtown Hamilton (3) Ancaster (near the Hamilton mountain) (4) Dundas (5) central Burlington (Fig. 10). The Tier Three independent grocery service areas cover approximately 72% of the population. Five small areas lack service and have been identified as potential food deserts: (1) Grimsby (2) central Hamilton 'mountain' (3) Ancaster (4) Dundas (5) central Burlington (Fig. 11). One finding of particular significance is that despite the loss of Tier Two stores from the downtown and east Hamilton neighbourhoods identified earlier, these areas did not reveal any potential food deserts and appear to be adequately serviced. For Tier Four, approximately 91% of the Hamilton CMA residents are serviced by convenience and franchise stores. No potential food deserts are identified as the Tier Four stores are well distributed and the only areas lacking coverage are located in sparsely populated areas (Fig. 12).

When all fields/tiers are collapsed the notion of a food desert virtually disappears from analysis (Fig. 13).

One interesting finding is that the level of income was higher for those individuals living outside of the service areas reflecting the typical city-suburban pattern of wealth, whereby the suburban and rural areas tend to have higher proportions of high income households compared to the central city (Tables VII and VIII).

TABLE VII
POPULATION CHARACTERISTICS OF RESIDENTS WITHIN THE PRIVATE TRANSPORTATION SERVICE AREA

Walk Distance	Total Pop.	Pop. (%)	Median Income ($)	Density (persons per km²)
Tier One	88,109	12.21%	69,420	3,879
Tier Two	120,243	16.66%	62,661	4,860
Tier Three	161,144	22.33%	59,588	6,119
Tier Four	355,721	49.29%	68,722	4,881

TABLE VIII
POPULATION CHARACTERISTICS OF RESIDENTS OUTSIDE THE PRIVATE TRANSPORTATION SERVICE AREA

Drive Distance	Total Pop.	Pop. (%)	Median Household Income ($)	Density (persons per km²)
Tier One	643,050	89.11	77,457	4,468
Tier Two	564,788	78.26	76,095	4,647
Tier Three	522,355	72.38	74,712	4,761
Tier Four	659,789	91.43	77,860	4,391

XIV. WALKING SERVICE AREA ANALYSIS

The walking service area analysis for each tier of stores (Figs. 14-19) shows a much more distinct pattern concentrated around each store. Also, compared to private transportation the walking service areas have many more smaller gaps where service is lacking. Consequently, a much greater proportion of the population is underserviced by each of the store tiers. For example, approximately only 12% of residents of the Hamilton CMA are within a 1 km walking distance of Tier One supermarkets, 17% by Tier Two discount supermarkets, 22% by Tier Three food stores and 49% by Tier Four convenience stores (Table IX). Given the spatial distribution of food stores and extent of underservice at each tier, it is not surprising that several areas are classified as potential food deserts at Tier One, Tier Two and Tier Three and one at Tier Four (Figs. 14-17). Interestingly, the areas that lost several Tier Two stores that correspond with lower income neighbourhoods did not reveal any potential food gaps (Fig. 8).

Tier Three stores had the highest population density of residents whereas Tier One stores had the lowest (Table IX). This reflects locational differences with Tier Three smaller food stores being located closer to city centres, whereas Tier One and Tier Two chain stores are located in more suburban areas (Figs. 14–17).

Examination of the 500 m buffer created around the City of Hamilton's public transportation bus routes indicates that the majority of individuals reside within close proximity to bus service (Table XI).

TABLE IX
POPULATION CHARACTERISTICS OF RESIDENTS WITHIN THE WALKING SERVICE AREA

Drive Distance	Total Pop.	Pop. (%)	Median Household Income	Density (persons per km²)
Tier One	78,620	10.80	90,936	1,481
Tier Two	156,882	21.72	89,045	2,170
Tier Three	199,315	27.62	89,820	2,336
Tier Four	61,881	8.57	90,045	1,175

TABLE X
POPULATION CHARACTERISTICS OF RESIDENTS OUTSIDE THE WALKING SERVICE AREA

Walk Distance	**Total Pop.**	**Pop (%)**	**Median Income ($)**	**Density (persons per km²)**
Tier One	633,560	87.79%	80,112	4,131
Tier Two	601,427	83.34%	81,811	3,982
Tier Three	560,526	77.67%	84,330	3,446
Tier Four	365,949	50.71%	90,594	3,114

This accounts for approximately 62% of residents within the Hamilton CMA with an average density of 4,723 people per km². These findings are of significance because the majority of food stores within all four tiers are located along major roads and bus routes (Fig. 20).

TABLE XI
CHARACTERISTICS OF RESIDENTS WITHIN AND OUTSIDE PUBLIC TRANSPORTATION SERVICE AREA

Bus Routes	**Total Pop**	**Pop (%)**	**Median Household Income ($)**	**Density (persons per km²)**
Inside 500m Buffer	446,194	61.83%	67,939	4,723
Outside 500m Buffer	275,476	38.17%	97,562	2,956

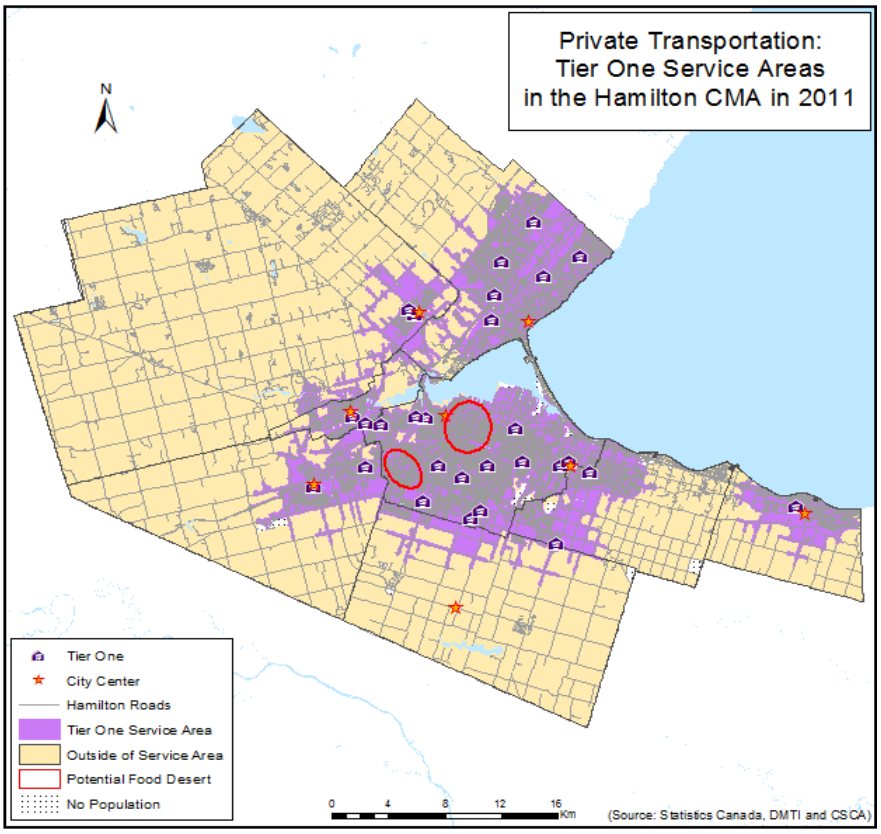

Fig. 9 Tier One Service Areas with Potential Food Deserts for Private Transportation [47], [57]

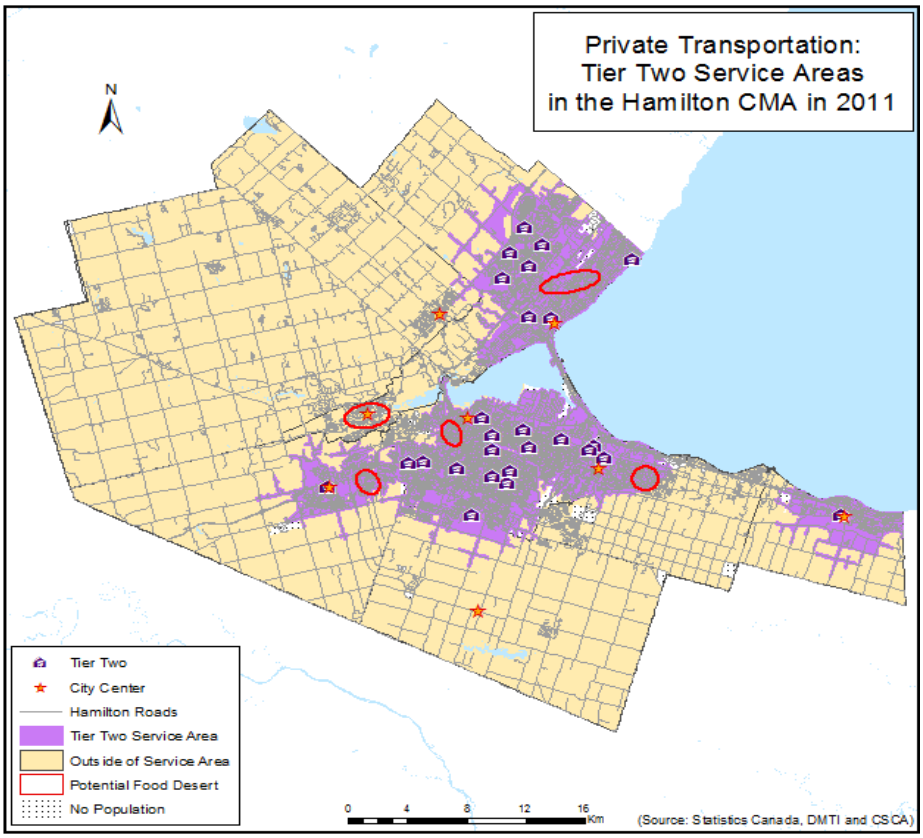

Fig. 10 Tier Two Service Areas with Potential Food Deserts for Private Transportation [47], [57]

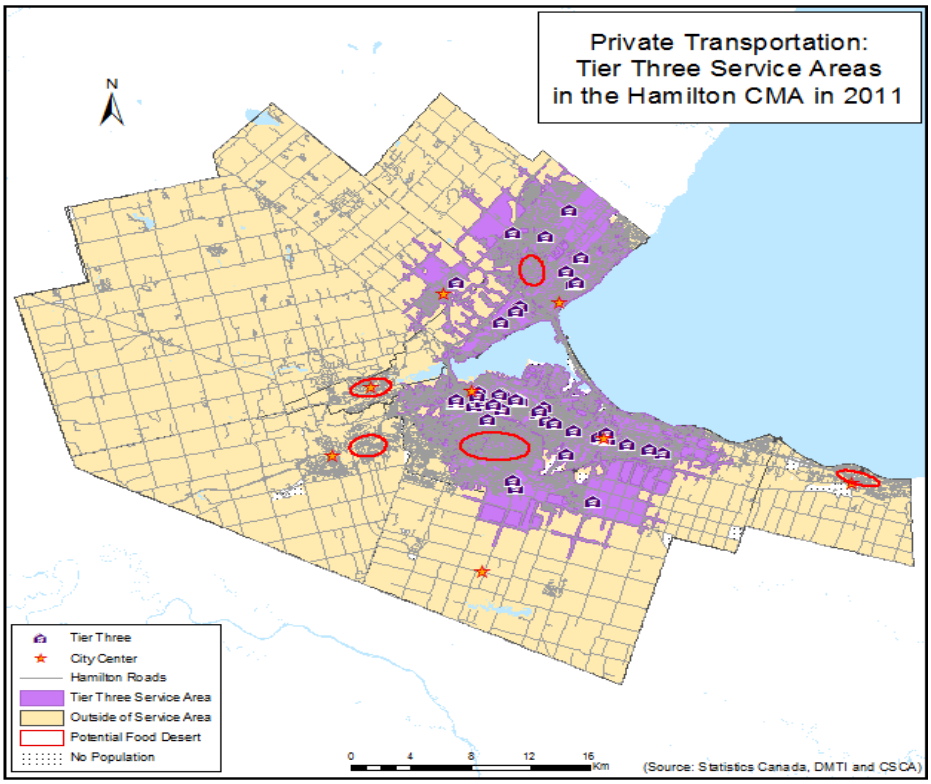

Fig. 11 Tier Three Service Areas with Potential Food Deserts for Private Transportation [47], [57]

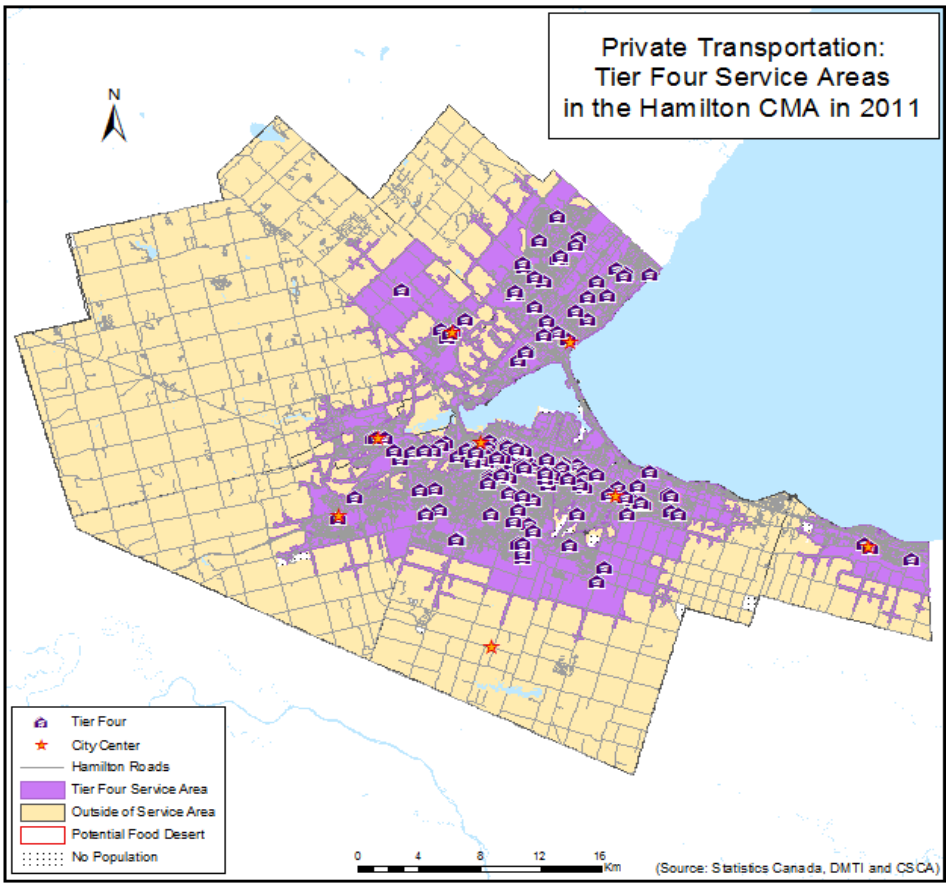

Fig. 12 Tier Four Service Areas with Potential Food Deserts for Private Transportation [47], [57]

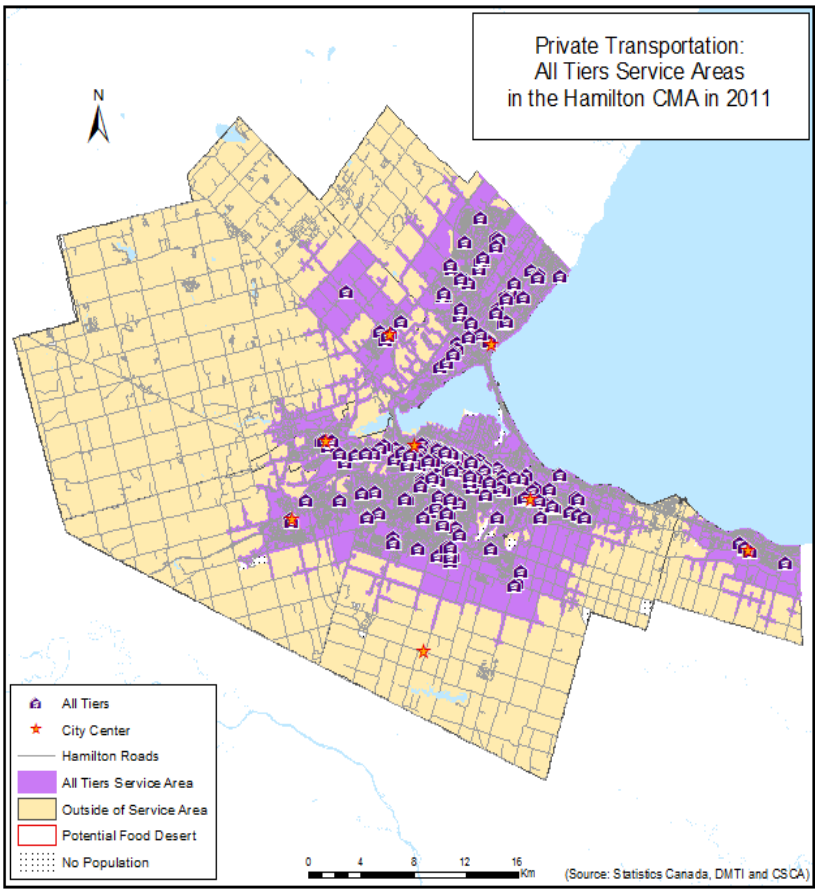

Fig. 13 All Tiers Collapsed Service Areas with Potential Food Deserts for Private Transportation [47], [57]

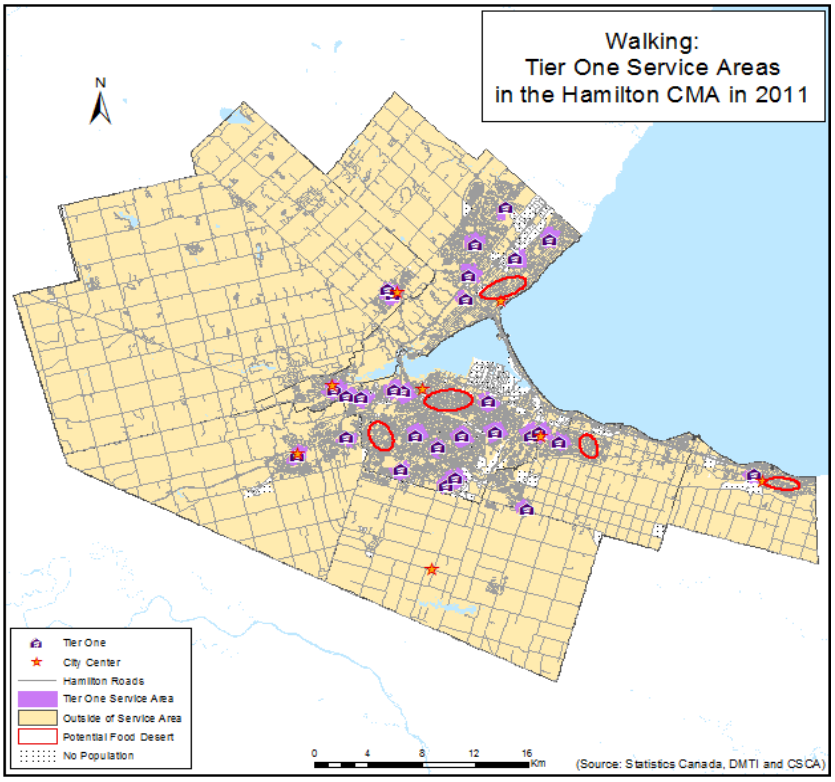

Fig. 14 Tier One Service Areas with Potential Food Deserts for Walking [47], [57]

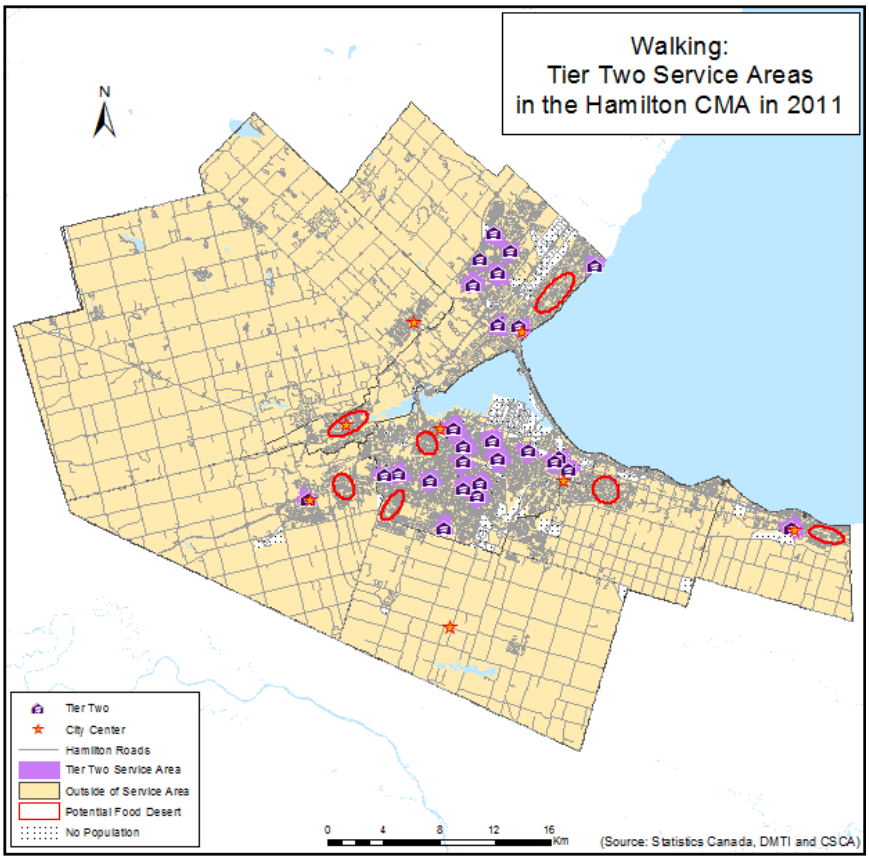

Fig. 15 Tier Two Service Areas with Potential Food Deserts for Walking [47], [57]

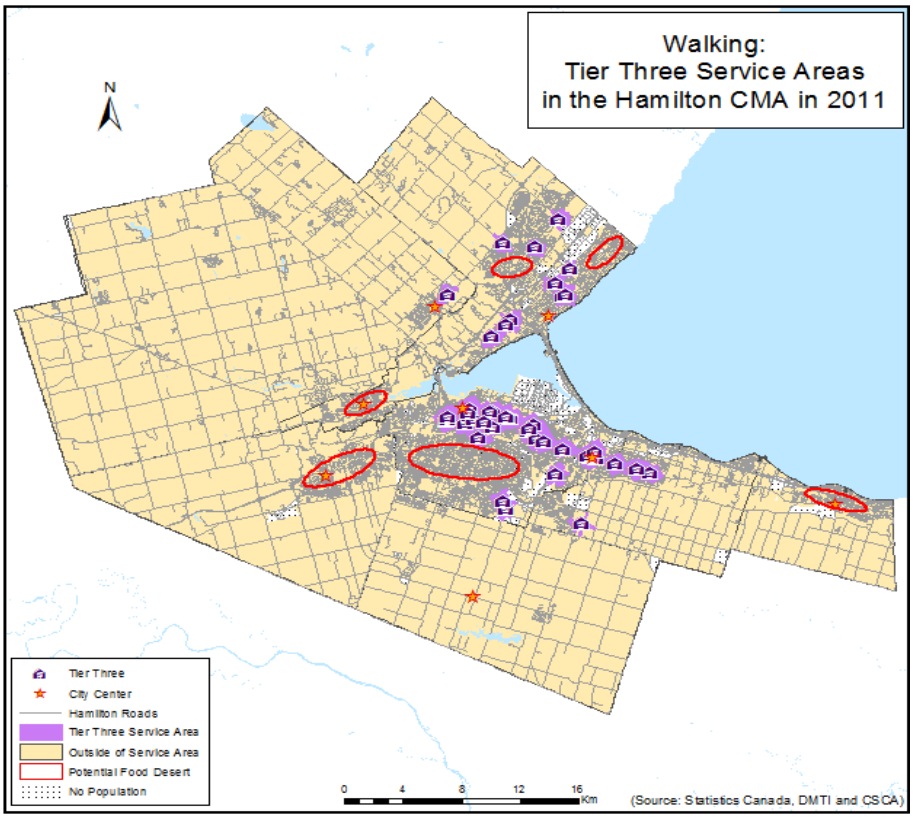

Fig. 16 Tier Three Service Areas with Potential Food Deserts for Walking [47], [57]

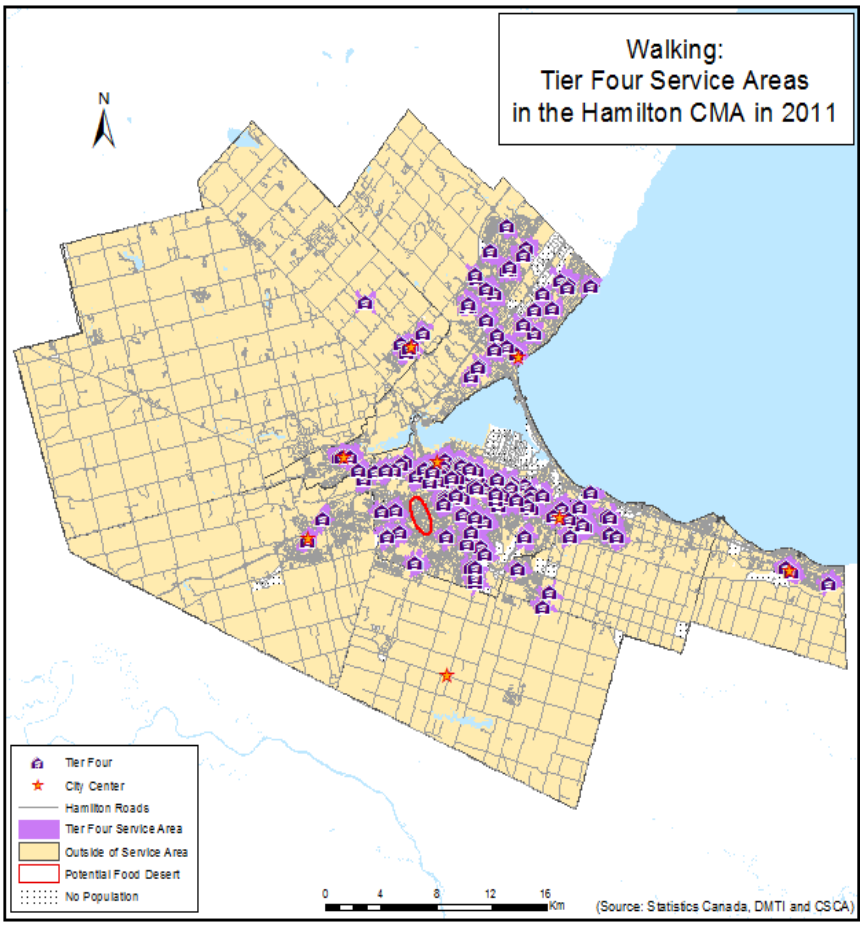

Fig. 17 Tier Four Service Areas with Potential Food Deserts for Walking [47], [57]

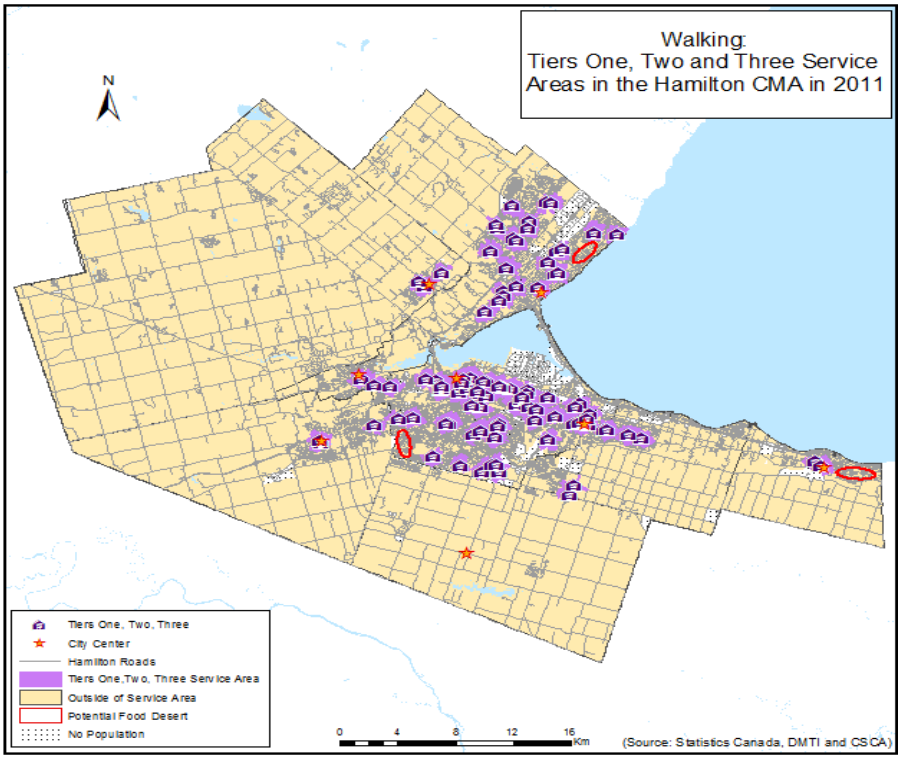

Fig. 18 Tiers One, Two and Three Collapsed Service Areas with Potential Food Deserts for Walking [47], [57]

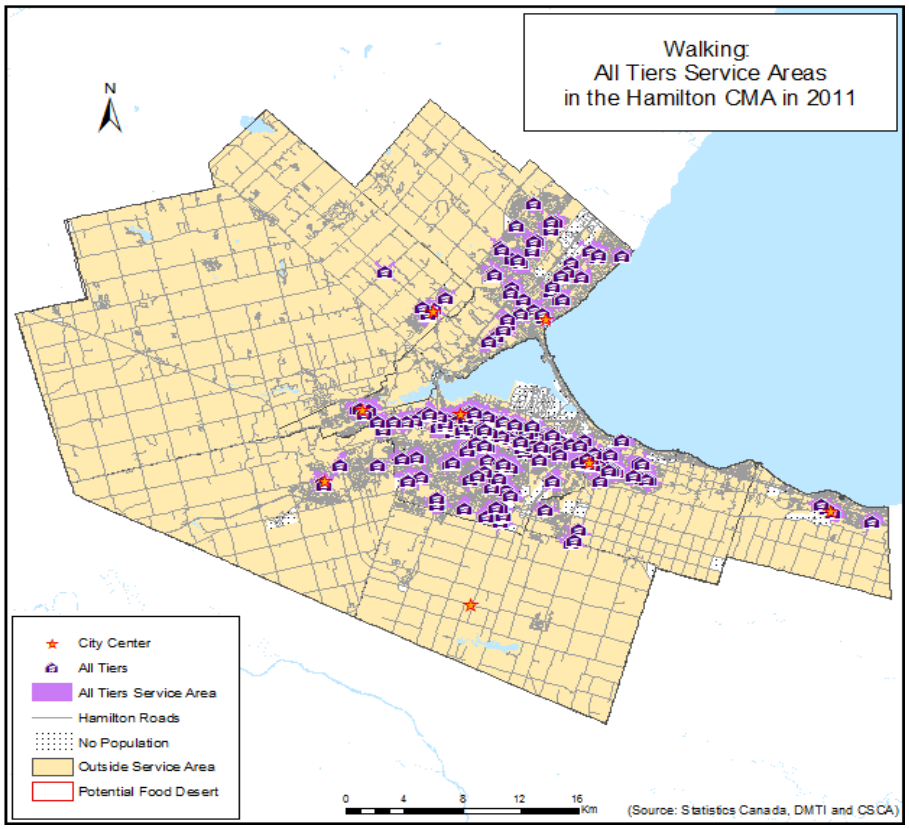

Fig. 19 All Tiers Collapsed Service Areas with Potential Food Deserts for Walking [47], [57]

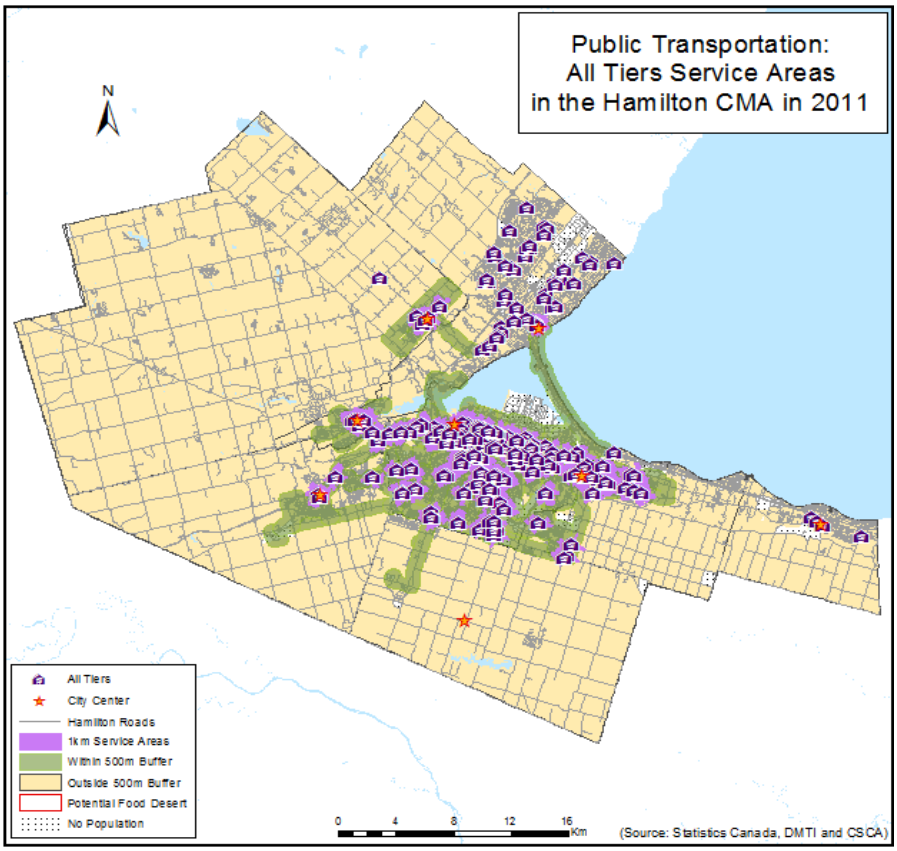

Fig. 20 All Tiers Service Areas with Potential Food Deserts for Public Transportation [47], [57]

XV. Conclusion

The findings of this study have revealed three important conclusions: 1) that more food stores are found to be present in the Hamilton CMA than expected, 2) that the residents of the Hamilton CMA have adequate access to affordable, healthy food by multiple modes of transportation, and 3) very few potential food gaps are found at each of the tiers with no areas qualifying as food deserts when all four tiers of food stores are included. Other important findings of this paper can be summarized as follows:

The Hamilton CMA experienced a negligible change in the total number of food stores between the years 2006 and 2011 (Table II). Across the categories, the study area gained 33% of Tier One high-end chain grocery stores and 18% of Tier Three independent food stores and lost 2.6% of Tier Four convenience and franchise food stores. The most significant loss was 23.5% of Tier Two discount grocery stores, the majority of which are located in the lower income areas of Downtown and East Hamilton;

The average distance that residents needed to travel to the closest grocery store decreased by 10% for Tier One stores and 4% for Tier Three stores over the five year period, while it increased 23% to reach Tier Two stores and 21% for Tier Four stores (Table III). The distance to the nearest grocery store showed very little correlation with the median household income, however a moderately-low positive relationship was found with large households of 6-plus persons. All of the tiers of food stores are accessible by at least one mode of affordable transportation.

It was expected that the total number of food stores in the Hamilton CMA would be lower than what is present since, as discussed earlier, grocery retailers have become increasingly consolidated and many have a preference towards larger store formats. Moreover, fewer Tier Three independent food stores were expected. Contrary to expectations, it was found that the Hamilton CMA had essentially the same total number of food stores in 2011 as it did five years previous. And in actuality, the number of Tier Three and Tier One stores increased. The reason for this could be that less profitable Tier Two stores were closed and new Tier One stores opened operating under the same conglomerate. As well, the loss of Tier Two stores likely provided greater need and market opportunities for small independent grocery start-ups. For example, several independent grocers, deli's, meat, and ethnic specialty food stores located in the areas of Downtown and East Hamilton where Tier Two stores had closed since 2006. To better understand the overall changes in grocery retail in the Hamilton CMA, future studies should include an analysis of floor space and average food basket cost as proxies for food availability and affordability.

As expected, rural areas had a much greater distance to travel to reach a grocery store than urban and suburban neighbourhoods. This makes sense since stores require a certain population living within close proximity in order to be profitable. In order to better understand differences in accessibility related to distance, future research of the Hamilton CMA should divide the study area. However, the general trends of this study are still valid. The distance to the closest store was expected to be greater for large chain grocery stores (Tiers One and Two) than for independent (Tier Three) and convenience stores (Tier Four). The average distance to reach a Tier One or Tier Two supermarket was further than for Tier Three stores; however, it was shorter than the closest Tier Four store in both 2006 and 2011. This may be contrary to that which would be expected but is attributable to differences in urban form. The majority of Tier Four stores are located in the urban areas making it necessary for individuals living in suburban and rural areas to travel much further.

While a positive relationship between income and distance was expected, no substantial relationship was found. The likely reason is that stores are locating in areas with sufficient population density. The linear distribution of stores that parallels the waterfront shows a clear relationship between store location and urban form. Since the correlation results for the median household income variable were not as strong as hoped, an attempt to rectify this shortcoming was made by using a variable representing household size. The variable of households with six or more people was found to be positively correlated with distance, but was moderately-weak. Once again, dividing the study area between urban/suburban and rural would likely provide a more accurate understanding of the relationship between income and distance that may exist.

The service areas for private transportation indicated that over 91% of individuals residing in the Hamilton CMA have access to all tiers of food stores by automobile. Theoretically, assuming that all individuals have access to a vehicle, over 91% of the population had adequate service when all four tiers of food stores combined. This finding is of significance because it indicates that the networks of transportation and grocery retail have been well-planned and food stores have been made accessible by the most predominant mode of transportation. The income levels of individuals living within the 5 km service areas across all Tiers are relatively similar to those residing outside. The findings also suggest that food stores locate based on population density rather than income. As expected, food stores are accessible to much fewer people for residents walking than for driving to shop for groceries since the distance a person is willing to walk to shop and carry groceries is quite short. More distinct differences in income and density are found in the walking distance service areas.

The findings suggest that certain economic and population criteria may drive grocery store locational choices. As mentioned earlier, Tier One high-end chain grocery stores target individuals that will typically spend more for higher quality foods and service, whereas Tier Two discount chain grocery stores cater to more price conscious consumers. The findings are significant as they indicate that individuals living in areas of economic deprivation have access to all tiers of food stores by bus. Consequently, 62% is an underestimate of the actual proportion of individuals with access to public transit

This study has shown that food deserts seem to be absent in the Hamilton CMA. A suggestion for further research would be to focus in on the areas identified as potential food deserts

to determine the demographic characteristics of the population. Furthermore, with the available data there was no way to determine if in actuality residents are making healthy food choices when purchasing groceries. One way to improve this analysis would be to conduct a qualitative ground-truthing analysis that surveys customers at food stores and the items purchased. This would help to better understand the non-spatial dimensions of access to grocery retail and whether greater public education is needed to ensure healthy dietary lifestyles.

Given that most of the areas in the Hamilton CMA have a relatively high level of accessibility to food stores by private automobile and public transportation no areas can be defined as food deserts. For any disadvantaged individuals that do not have access or cannot afford a vehicle, other feasible options for longer distance shopping trips include taking the bus, bicycling, carpooling, making larger shopping trips less frequently, taxicabs and short-term car rentals. The high level of accessibility can be attributed to Tier Three and Tier Four stores filling in the gaps where Tier One and Tier Two stores are lacking. If poor dietary choices are being made by individuals living in the Hamilton CMA, it is not attributable to accessibility. This study revealed the importance of local, independent neighbourhood stores as vital players in the grocery retail landscape of cities. If poor diet is a public policy concern, it may be that people are either choosing to shop at Tier One and Tier Two stores but not purchase healthy foods or they are choosing to purchase the majority of their food from convenience stores where few healthy food options are available. Therefore, more government action is necessary to better educate the public on the importance of healthy diet and lifestyle choices. Furthermore, cities should foster economic policies that encourage and support local independent providers of grocery retail.

REFERENCES

[1] Acheson, D. *Independent Inquiry into inequalities in health*. London: Stationary Office, 1998.

[2] Agriculture and Agri-food Canada. *Food retailing in Canada: Trends, dynamics and consequences.* http://www.pecc.org/food/papers/2005-2006/Canada/foodretailing-in-canada.pdf, 2005.

[3] Apparicio, P., Cloutier, M.S., Shearmur, R. "The case of Montreal's missing food deserts: Evaluation of accessibility to food supermarkets", *International Journal of Health Geographics,* 6 (4), 4-16, 2007.

[4] Beaulac, J., Kristjansson, E., Cummins, S. "A systematic review of food deserts, 1966-2007". *Preventing Chronic Disease, Public Health Research, Practice, and Policy,* 6 (3), 1-10, 2009.

[5] Bertrand, L., Therien, F. & Cloutier, M. "Measuring and mapping disparities in access to fresh fruits and vegetables in Montreal", *Canadian Journal of Public Health*, 1 (99), 6-11, 2008.

[6] Bodor J., Rose D., Farley T., Swalm C., Scott S. "Neighborhood fruit and vegetable availability and consumption: the role of small food stores in an urban environment", *Public Health Nutrition*, 11 (4), 413–20, 2008.

[7] Boyko, D. *Food Deserts: Hype, Myth or Reality. A Case Study of the City of Toronto*. Toronto: MSA thesis, Ryerson University, Toronto, Canada. 2010.

[8] Chung, C. & Myers, S. "Do the poor pay more for food? An analysis of grocery store availability and food price disparities", *Journal of Consumer Affairs*, 33, 276-296, 1999.

[9] Clifton, K. "Mobility strategies and food shopping for low-income families- a case study". *Journal of Planning Education and Research*, 23 (4), 402-413, 2004.

[10] Cohen, M. *Minorities mostly hunger in 'food deserts'*. The *Toronto Observer Magazine*. http://www.torontoobserver.ca/2009/04/14/minorities-mostly-hunger-in-food-deserts-study/. April 14, 2014.

[11] Cummins, S. & Macintyre, S. "Food deserts-evidence and assumption in health policy". *British Medical Journal*. 325(7361, 436-438, 2002.

[12] Daniel, C., Aversa, J. & Hernandez, T. *Emerging Trends in Grocery Retailing*. Toronto, Centre for the Study of Commercial Activity, Ryerson University, 2010.

[13] Eckert, J. & Shetty, S. "Food systems, planning and quantifying access: Using GIS to plan for food retail", *Applied Geography*, 31 (4), 1216-1223, 2011.

[14] Eisenhauer, E. "In poor health: Supermarket redlining and urban nutrition". *GeoJournal* 53(2), 125-133, 2001.

[15] Gentile, A. "Agencies move to close grocery gaps". *The American City & County*, 123 (3), 22-24, 2008.

[16] Guy, C., Clarke, G., & Eyre, H. "Food retail change and the growth of food deserts: A case study of Cardiff". *International Journal of Retail & Distribution Management*, 32(2/3), 72-88, 2004.

[17] Hamelin, A-M., Habicht, J-P & Beaudry, M. Food Insecurity: Consequences for the Household and Broader Social Implications. The Journal of Nutrition, Feb. 129, (2S), 525S-528 (2000).

[18] Health Canada, *It's Your Health - Healthy Eating.* http://www.hc-sc.gc.ca/hl-vs/iyh-vsv/food-aliment/healthy-eating-saine-alimentation-eng.php, 2008

[19] Health Canada, Statistics Canada, and the Canadian Institute for Health Information. *Statistical report on the health of Canadians.* http://www.phac-aspc.gc.ca/ph-sp/report-rapport/stat/pdf/all_english.pdf, 1999.

[20] Helling A. & Sawicki, DS. Race and residential accessibility to shopping and services, *Housing Policy Debate,* 14 (1-2), 69-101, 2003.

[21] Hubbard, R. A review of selected factors conditioning consumer travel behaviour, *Journal of Consumer Research,* 5 (1), 1-21, 1978.

[22] Jones, K., & Simmons, J. *Location, Location, Location: Analyzing the Retail Environment* (2nd ed.). Scarborough: International Thomson Publishing, 1993.

[23] Kratt, P., Reynolds, K., Sewchuk, R. "The role of availability as a moderator of family fruit and vegetable consumption", *Health Education & Behavior*, 27 (4), 471-482, 2000.

[24] Kogan, A. *Food Deserts and Income in the Greater Toronto Area: A Spatial Correlation Analysis.* Toronto, Ryerson University, Master's Thesis, 2010.

[25] Lang, T. & Caraher, M. "Access to healthy foods: Part II. Food poverty and shopping deserts: what are the implications for health promotion policy and practice?" *Health Education Journal*, 57 (3), 202-211, 1998.

[26] Lathom, J. & Moffat, T. "Determinants of variation in food cost and availability in two socioeconomically contrasting neighbourhoods of Hamilton, Ontario, Canada". *Health & Place*, 13(1), 273-287, 2007.

[27] Larson, K. & Gilliland, J. "Mapping the evolution of 'food deserts' in a Canadian city: Supermarket accessibility in London, Ontario, 1961-2005", *International Journal of Health Geographics*, 7(16), 1-16, 2008.

[28] Malla, S., Hobbs, J. E., & Perger, O. "Valuing the health benefits of a novel functional food", *Canadian Journal of Agricultural Economics*, 55 (1), 115-136, 2007.

[29] Martin Prosperity Institute, *Food deserts and priority neighbourhoods in Toronto.* http://martinprosperity.org/2010/06/15/food-deserts-and-priority-neighbourhoods-in-toronto, 2010.

[30] Mishkovsky, N. "Support the farm stand to feed" locavores" and the economy", *Public Management*, 91 (2): 24-28, 2009.

[31] Morland, K., Wing, S., Diez-Roux, A., Poole, C. "Neighborhood characteristics associated with the location of food stores and food service places". *American Journal of Preventative Medicine*, 22(1), 23-29, 2002.

[32] Morton LW, Blanchard TC. "Starved for access: life in rural America's food deserts", *Rural Realities*, 1(4), 1–10, 2007.

[33] Pearson, T., Russell, J., Campbell, M., & Barker, M. "Do 'food deserts' influence fruit and vegetable consumption? – a cross sectional study", *Appetite*, 45 (2), 195-197, 2005.

[34] Piacentini, M., Hibbert, S. & Al-Dajani, H. "Diversity in deprivation: exploring the grocery shopping behaviour of disadvantaged consumers", *Int. Rev. of Retail, Distribution and Consumer Research*, 11 (2), 141–158, 2001.

[35] Pothukuchi, K. "Attracting supermarkets to inner-city neighborhoods: economic development outside the box", *Economic Development Quarterly*, 19 (3), 232-244, 2005.

[36] Reisig, VMT., & Hobbiss, A. “Food deserts and how to tackle them: a study of one city’s approach”, *Health Education Journal,* 59 (2), 137-149, 2002.
[37] Rose, D. & Richards, R. “Food store access and household fruit and vegetable use among participants in the US Food Stamp Program”, *Public Health Nutrition*, 7 (8), 1081–1088, 2004.
[38] Russell, S. & Heidkamp, P. “Food desertification: The loss of a major supermarket in New Haven, Conneticut”, Applied Geography, 31 (4), 1197-1209, 2011.
[39] Shaffer A. *The Persistence Of La’s Grocery Gap: The Need For A New Food Policy And Approach To Market Development.* Center for Food and Justice, LA; http://departments.oxy.edu/uepi/cfj/publications/Supermarket%20Report%20November%202002.pdf, 2002.
[40] Shaw, H. “Food deserts: towards the development of a classification”. *Geografiska Annaler: Series B, Human Geography,* 88 B (2): 231–247, 2006.
[41] Short, A., Guthman, J. & Raskin, S. “Food deserts, oases, or mirages?: small markets and community food security in the San Francisco Bay area”, *Journal of Planning Education and Research,* 26(3), 352-364, 2007.
[42] Silver, L., & Bassett, M. T. “Food safety for the 21st century”, *Jama,* 300(8), 957-959, 2008.
[43] Smoyer-Tomic, K., Hewko, J., Hodgson, M. “Spatial accessibility and equity of playgrounds in Edmonton, Canada”, *Canadian Geographer*, 48(3), 287-302, 2004.
[44] Smoyer-Tomic, K., Spence, J. & Amrhein C. “Food deserts in the prairies? Supermarket accessibility and neighbourhood need in Edmonton, Canada”. *Professional Geographer*, 58(3), 307-326, 2006.
[45] Spencer, A. H. “Deriving measures of attractiveness for shopping centres”, *Regional Studies*, 12(6), 713-726, 1978.
[46] Sturm, R. & Datar, A. “Body mass index in elementary school children, metropolitan area food prices and food outlet density”, *Public Health*, 119(12), 1059-1068, 2005.
[47] Statistics Canada, *Census Data*, Ottawa: Ministry of Supply, 2016.
[48] Tarasuk, V. & Vogt, J. “Household food insecurity in Ontario”, *Quantitative Research*, 100(3), 184-188, 2009.
[49] Toronto Public Health, *Food Connections: Toward a Healthy and Sustainable Food System for Toronto* http://www.toronto.ca/health/food_connections_report.pdf, 2010.
[50] US Census Bureau. *2002 NAICS Codes and Titles*. http://www.census.gov/epcd/naics02/naicod02.htm, 2002.
[51] Van Duyn, M. A. & Pivonka, E. “Overview of the health benefits of fruit and vegetable consumption for the dietetics professional selected literature”, *Journal of the American Dietetic Association*, 100, 1511–1521, 2000.
[52] Wilkinson, R. & Marmot M. (eds), *Social Determinants Of Health: The Solid Facts.* 2nd ed. Copenhagen: World Health Organization. http://www.euro.who.int/__data/assets/pdf_file/0005/98438/e81384.pdf, 2003.
[53] Witten, K., Exeter, D. & Field, A. “The quality of urban environments: mapping variation in access to community resources”, *Urban Studies*, 40 (1), 161–177, 2003.
[54] Wrigley, N. “’Food deserts’ in British cities: policy context and research priorities”, *Urban Studies*, 39(11), 2029-2040, 2002.
[55] Wrigley, N., Warm, D., Margetts, B., Whelan, A. “Assessing the impact of improved retail access on diet in a food desert”, *Urban Studies*, 39(11): 2061-2082, 2002.
[56] Zenk, S., Schultz, A., Israel, B., Sherman, James, S., Bao, S., Wilson, M. “Neighborhood Racial composition, neighborhood poverty, and the spatial accessibility of supermarkets in metropolitan Detroit”, A*merican Journal of Public Health*, 95(4): 660-667, 2005.
[57] Z. Center for the Study of Commercial Activity. *Data Library*. Toronto, Ryerson University, 2015.

A Stochastic Vehicle Routing Problem with Ordered Customers and Collection of Two Similar Products

Epaminondas G. Kyriakidis, Theodosis D. Dimitrakos, Constantinos C. Karamatsoukis

Abstract**—**The vehicle routing problem (VRP) is a well-known problem in Operations Research and has been widely studied during the last fifty-five years. The context of the VRP is that of delivering or collecting products to or from customers who are scattered in a geographical area and have placed orders for these products. A vehicle or a fleet of vehicles start their routes from a depot and visit the customers in order to satisfy their demands. Special attention has been given to the capacitated VRP in which the vehicles have limited carrying capacity for the goods that are delivered or collected. In the present work we present a specific capacitated stochastic vehicle routing problem which has many realistic applications.

We develop and analyze a mathematical model for a specific vehicle routing problem in which a vehicle starts its route from a depot and visits N customers according to a particular sequence in order to collect from them two similar but not identical products. We name these products, product 1 and product 2. Each customer possesses items either of product 1 or product 2 with known probabilities. The number of the items of product 1 or product 2 that each customer possesses is a discrete random variable with known distribution. The actual quantity and the actual type of product that each customer possesses are revealed only when the vehicle arrives at the customer's site. It is assumed that the vehicle has two compartments. We name these compartments, compartment 1 and compartment 2. It is assumed that compartment 1 is suitable for loading product 1 and compartment 2 is suitable for loading product 2. However it is permitted to load items of product 1 into compartment 2 and items of product 2 into compartment 1. These actions cause costs that are due to extra labor. The vehicle is allowed during its route to return to the depot to unload the items of both products. The travel costs between consecutive customers and the travel costs between the customers and the depot are known. The objective is to find the optimal routing strategy, i.e. the routing strategy that minimizes the total expected cost among all possible strategies for servicing all customers.

It is possible to develop a suitable dynamic programming algorithm for the determination of the optimal routing strategy. It is also possible to prove that the optimal routing strategy has a specific threshold-type strategy. Specifically, it is shown that for each customer the optimal actions are characterized by some critical integers. This structural result enables us to design a special-purpose dynamic programming algorithm that operates only over these strategies having this structural property. Extensive numerical results provide strong evidence that the special-purpose dynamic programming algorithm is considerably more efficient than the initial dynamic programming algorithm. Furthermore, if we consider the same problem without the assumption that the customers are ordered, numerical experiments indicate that the optimal routing strategy can be computed if N is smaller or equal to eight.

Keywords**—**Collection of similar products, dynamic programming, stochastic demands, stochastic preferences, vehicle routing problem.

Epaminondas G. Kyriakidis is with Department of Statistics, Athens University of Economics and Business, Patission 76, 10434, Athens, Greece (e-mail: ekyriak@aueb.gr).

Theodosis D. Dimitrakos is with Department of Mathematics, University of the Aegean, Karlovassi 83200, Samos, Greece (e-mail: dimitheo@aegean.gr).

Constantinos C. Karamatsoukis is with Department of Military Sciences, Hellenic Military Academy, Vari 16673, Attica, Greece (e-mail: ckaramatsoukis@sse.gr).

The Existence of a Sciatic Artery in Congenital Limb Deformities

Waseem Al-Talalwah[1], Shorok Al- Dorazi[2], Roger Soames[3]

[1] Dr. King Saud bin Abdulaziz University for Health Sciences, College of Medicine, P.O. Box 3660, Riyadh 11481, Mail Code: 3127

[2] Dr. Directorate of Prevention and Control of Healthcare Associated Infection, Eastern Province, MOH, KSA, P.O.Box 411, Saihat 31972, Kingdom of Saudi Arabia, Telephone number: 00966505888967, e-mail:drazi2@hotmail.com

[3] Prof. Centre for Anatomy and Human Identification, College of Art, Science and Engineering, University of Dundee, Dundee, DD1 5EH, UK

Corresponding author

Dr. Waseem Al Talalwah (BSc, MSc, MD, PhD)
Assistant Professor
King Saud bin Abdulaziz University for Health Sciences
college of medicine
Department of Basic Medical Sciences
Anatomy division
PO Box 3660, Riyadh 11481, Mail Code: 3127
e-mail: altalalwahw@ksau-hs.edu.sa

Abstract

Persistent sciatic artery is a rare anatomical vascular variation resulting from a lack of regression of the embryonic dorsal axial artery. The axial artery is the main artery supplying the lower limb during development in the first trimester. The current research includes 206 sciatic artery cases in 171 patients between 1864 and 2012. It aims to identify the risk factor of sciatic artery aneurysm in congenital limb anomalies. Sciatic artery aneurysm was diagnosed incidentally in amniotic band syndrome (ABS) existing with no congenital anomaly in 0.7% or with double knee in 0.7%, with the tibia in 0.7% and with hemihypertrophy or soft tissue hypertrophy in 1.4%. Therefore, the current study indicates a relationship the same gene responsible for the congenital limb deformities may be responsible for non-regression of the sciatic artery. Furthermore, pediatricians should refer cases of congenital limb anomalies for vascular evaluation prior to interventional corrective surgery.

Keywords: Amniotic band syndrome, Congenital limb deformities, Double knee, Sciatic artery, Sciatic artery aneurysm, Soft tissue hypertrophy**.**

Introduction

The sciatic artery a very rare congenital anomaly resulting in lack of regression of the embryonic dorsal axial artery ranging from 0.04 to 0.06% (Ikezawa et al 1994). As the sciatic artery regresses, the femoral system develops (Sidway 2005). The variability of femoral systems is due to sciatic artery persistency modifying the surgical intervention of lower extremities. (Al Talalwah W 2015). Further, the coexistence of sciatic artery modifies the pelvic arteries origins which also need radiologic studies previous to surgery (Al Talalwah and Soames 2014) such as obturator artery arising from external iliac artery instead of internal iliac artery result in corona mortis as a source of bleeding in case of hernia repair (Al Talalwah 2015)

Based on Senior series (1919-1925), the sciatic artery development to involution process occurred in almost 6 mm to 22 mm embryonic stage. Further, it is also controlled by stimulating factors which is a decrease of stretch

result in vascular injury leading to involution and disappearance partially or completely at the end of embryonic life e.g. umbilical ligament.

Amniotic band syndrome a teratogenic syndrome may occur in between 6mm to 22mm embryonic length stages (Kennedy and Persaud 1977, Daya and Makakole 2009) is characterized by Bone abnormalities and nerve compression (Daya and Makakole 2009) and is associated with several vascular anomalies with incidence of 2% (Robertson et al 1990) or 60% (Daya and Makakole 2009) in population. The sciatic artery is associated with such as Hemi-hypertrophy leg in 1.3% (2 cases) (Ikezawa et al 1994).

Method and objectives

The presenting study is a revising study of 206 sciatic cases of 171 patients between 1864 and 2012. The search is based on electronic databases Pubmed, EMBASE, Scopus, ScienceDirect, Web of Science, SciELO, BIOSIS, and CNKI were performed to identify all articles reporting data on the sciatic artery cases. Moreover, a wide search of sciatic artery cases, article and their references without any language restriction. The Statistical Package for the Social Sciences (SPSS) Program has been used to analysis data and its interpretation. The present research study aim is to identify the risk factor of congenital lower limb associated with sciatic artery aneurysm to alert genetic scientist to clarify the responsible gene.

Result

The sciatic artery aneurysm diagnosed incidentally in Amniotic band syndrome with no coexisting of congenital anomaly. However, the sciatic artery aneurysm also found in case of lower limb deformities such as double knee and Tibia as well as Hemihypertrophy or Soft tissue hypertrophy (Table 1).

Discussion

Green (1832) was the first person described PSA on post-mortem. Sciatic artery has carried several names as the axial, ischiatic or persistent sciatic and axial artery or ischiopopliteal arterial trunk (Bardsley 1970, Papon et al 1999) which has been first described Green (1832). Sciatic artery has been observed in various congenital syndromes as amniotic band syndrome (Daya 2008), Pelvic infantile haemangioma (Kircher et al 2010), Mullerian agenesis (Madson et al 1995 , Hooft et al 2009), Renal agenesis (Madson et al 1995), Solitary pelvic kidney (Muller et al 1967; Hooft et al 2009), haemangioma (Kurtoglu & Haluk 2001). In addition, it is also have seen in group congenital disorders associated with vascular anomlies of the lower limb (Madson et al 1995; van Hooft et al 2009), bone or soft tissue hypertrophy/hypotroph leg deformities (van Hooft et al 2009) such as shortening (Mayschak and Flye1984; Williams et al 1983; Batchelor and Vowden 2000) and Hemihypertrophy (Mayschak and Flye1984; Williams et al 1983; Batchelor and Vowden 2000; Kurtoglu & Haluk 2001) of the leg (Mayschak and Flye1984; Williams et al 1983; Batchelor and Vowden 2000). A process of vascular development during embryo life referred as vasculogenesis is a process of vascular development during embryo life regulating by positive factors. The regulator factor has been identified in mammals such as Vascular Endothelial Growth Factor (VEGF), Angiopoietin-1, Transforming Growth Factor-b (TGF-b), Platelet-derived Growth Factor B (PDGF-B), Heparin-binding Epidermal Growth Factor (HB-EGF) and negative factors such as

angiopoietin-2 and Angiostatin (Funke and Kuhn 1988). The lung Kruppel-like factor is transcription factor (LKLF) is required for normal tunica media formation and blood vessel stabilization during murine embryogenesis (Kuo et al 1977). Therefore, the failure of regression result in persistent of sciatic artery is due of gene. The sciatic artery a rare congenital anomaly resulting from failure of regression of the dorsal axial artery during the 6 mm to 22 mm embryonic length stage: it has been observed in a number of congenital syndromes. Amniotic band syndrome, a teratogenic syndrome, may occur during the same embryonic stages (Kennedy and Persaud 1977; Daya and Makakole 2009) being characterized by bone abnormalities and nerve compression (Daya and Makakole 2009): it is associated with several vascular anomalies. A previous review (Ikezawa et al 1994) of 159 sciatic artery cases in 122 patients between 1864 and 2007 estimated the incidence of the sciatic artery associated with hemihypertrophy leg in 1.3% (2 cases) and with amniotic band syndrome in 3.5%. A sciatic artery exists with amniotic band syndrome in 3.5%, suggesting that this vascular anomaly is linked with limb deformities. In present study, the coexistence of the sciatic artery aneurysm is less than one percent. Further, the sciatic artery aneurysm coexists in 4.2% in current study indicating the vascular anomaly links with limb deformities.

Conclusion

Based on current study findings, the sciatic artery may links with limb deformities. The sciatic artery associated with congenital limb deformities group disorders leading to Genetic scientists have to start to investigate the gene most responsible for sciatic artery. Furthermore, Pediatricians has to report any congenital anomalies case to radiologist for further vascular evaluation previous to any surgery should be aware. Orthopedics has to be careful and well prepared for any surgical correction in lower limb of amniotic band syndrome.

References

1. Al Talalwah W. (2015) The Medial Circumflex Femoral Artery Origin variability and its radiological and surgical intervention significance. Springerplus 2015. 4:149. doi:10.1186/s40064-015-0881-2
2. Al Talalwah W.(2016) A new concept and classification of corona mortis and its clinical significance, Chinese Journal of Traumatology 19(5):251-254.
3. Al Talalwah, W. & Soames, R. (2014) Internal iliac artery classification and its clinical significance. Rev. Argent. Anat. Clin. 62:63-71.
4. Bardsley JL. Variations in branching of the popliteal artery. Radiology 1970 94:581-87.
5. Batchelor TJP, Vowden P. (2000) A persistent sciatic artery aneurysm with an associated internal iliac artery aneurysm. Eur J Vasc Endovasc Surg 20:400-2.
6. Daya M. (2008) Amniotic band syndrome with persistent sciatic artery: a case report. Ann Plast Surg. 61(5):549-51.
7. Daya M., Makakole M. (2011) Congenital vascular anomalies in amniotic band syndromeof the limbs. Journal of Pediatric Surgery 46: 507–5.
8. Funke C, Kuhn HJ. (1988) The morphogenesis of the arteries of the pelvic extremity. A comparative study of mammals with special reference to the tree shrew Tupaia belangeri Tupaiidae, Scandentia, Mammalia. Adv Anat Embryol Cell Biol 144:1–97.
9. Green (1832) was the first person described PSA on post-mortem.
10. Ikezawa T, Naiki K, Moriura S, Ikeda S, Hirai M. (1994) Aneurysm of bilateral persistent sciatic arteries with ischemic complications: case report and review of the world literature. J Vasc Surg 20:96–103.
11. Kennedy LA, Persaud TVN. (1977) Pathogenesis of developmental defects induced in the rat by amniotic sac puncture. Acta Anat;97:23-35.
12. Kircher MF, Lee EY, Alomari AI. (2010) Case Report: MRI findings of persistent sciatic artery associated with pelvic infantile hemangioma. Clinical Radiology 65: 172–175.
13. Kuo CT, Veselits ML, Barton KP, Lu MM, Clendenin C, Leiden MM. The LKLF transcription factor is required for normal tunica media formation and blood vessel stabilization during murine embryogenesis. Genes Dev 1997 11:2996–3006.
14. Kurtoglu z, Uluutku H. (2001) Persistent sciatic vessels associated with an arteriovenous malformation. J Anat 199:349-51.
15. Madson DI, Wilkerson DK, Ciocca RG, Graham AM. (1995) Persistent sciatic artery in association with varicosities and limb length discrepancy: An unrecognized entity? Am Surg 61:387-92.
16. Mayschak DT, Flye MW. (1984) Treatment of the persistent sciatic artery. Ann Surg 199:69-74.
17. Muller P, Dellenbach P, Gillet JY. (1967) Apropos of a triple abnormal combination: solitary pelvic kidney, uterovaginal agenesis and absence of the umbilical artery. Gynecol Prat 18:201-10
18. Papon X, Picquet J, Fournier HD, Enon B, Mercier P. (1999) Persistent sciatic artery: report of an original aneurysm-associated case. Surg Radiol Anat 21:151–3.
19. Robertson GS, Ristic CD, Bullen BR. (1990) The incidence of congenitally absent foot pulses. Ann R Coll Surg Engl 72:99-100.

20. Senior HD. (1919) The development of the arteries of the human lower extremity. Am J Anat 25:55–95.
21. Senior HD. (1919-1920) The development of the human femoral artery, a correction. Anat Res 17:271-9.
22. Senior HD. (1925) An interpretation of the recorded arterial anomalies of the human pelvis and thigh. Am J Anat 36:1–46.
23. Sidway AN. (2005) Embryology of the vascular system. In: Rutherford RB, editor. Vascular surgery. 6th ed. Philadelphia: Elsevier:53-63.
24. van Hooft IM, Zeebregts CJ, van Sterkenburg SM, de Vries WR, Reijnen MM. (2009) The persistent sciatic artery. Eur J Vasc Endovasc Surg 37(5):585-91.
25. Williams LR, Flanigan DP, O'Connor RJ. Schuler JJ. (1983) Persistent sciatic artery. Clinical aspects and operative management. Am J Surg 145:687–93.

Figure legend

Figure 1: the regular sciatic artery arising from the posterior trunk of the internal iliac artery inside the pelvic cavity. IIA. Internal iliac artery, AT. Anterior trunk. PT. Posterior trunk, UMA. Umbilical artery, OA. Obturator artery, ON. Obturator nerve, IPA. Internal pudendal artery, SA. Sciatic artery, LSA. Lateral sacral artery, ILA. Iliolumbar artery.

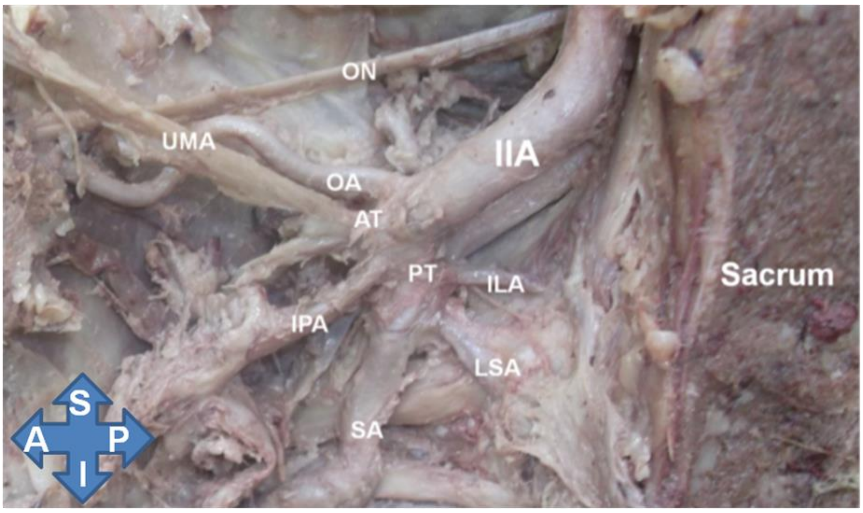

Table 1: The coexistence of sciatic artery in different congenital limb deformities

Congenital deformities	Frequency	Rate %
Overlap syndrome	1	.7
Double knee	1	.7
Double tibia	1	.7
Ameniotic band syndrome	1	.7
Hemihypertrophy	1	.7
Soft tissue hypertrophy	1	.7

Association of Body Composition Parameters with Lower Limb Strength and Upper Limb Functional Capacity in Quilombola Remnants

L. C. Pereira, F. S. Santana, M. Kanikowski, L. S. S. Neto, A. O. Gomes, M. P. Safons, M. G. O. Kanikowski

***Abstract*—**In Brazil, projections of population aging follow all world projections, the birth rate tends to be surpassed by the mortality rate around the year 2045 Historically, the population of Brazilian blacks suffered for several centuries from the oppression of dominant classes. A group especially of blacks stands out in relation to territorial, historical and social aspects, and for centuries they have isolated themselves in small communities, in order to maintain their freedom and culture. The isolation of the Quilombola communities generated socioeconomic effects as well as the health of these blacks. Thus, the objective of the present study is to verify the association of body composition parameters with lower and upper limb strength and functional capacity in Quilombola remnants. The research was approved by ethics committee (1,771,159). Anthropometric evaluations of hip and waist circumference, body mass and height were performed. In order to verify the body composition, the relationship between stature and body mass (BM) was performed, generating the body mass index (BMI), as well as the dual energy X-ray absorptiometry (DEXA) test. The Time Up and Go (TUG) test was used to evaluate the functional capacity, and a maximum repetition test (1MR) for knee extension and handgrip (HG) was applied for strength magnitude analysis. Statistical analysis was performed using the statistical package SPSS 22.0. Shapiro Wilk's normality test was performed. For the possible correlations, the suggestions of the Pearson or Spearman tests were adopted. The results obtained after the interpretation identified that the sample (n = 18) was composed of 66.7% of female individuals with mean age of 66.07 ± 8.95 years. The sample's body fat percentage (%BF) (35.65 ± 10.73) exceeds the recommendations for age group, as well as the anthropometric parameters of hip (90.91 ± 8.44cm) and waist circumference (80.37 ± 17.5cm). The relationship between height (1.55 ± 0.1m) and body mass (63.44 ± 11.25Kg) generated a BMI of 24.16 ± 7.09Kg/m^2, that was considered normal. The TUG performance was 10.71 ± 1.85s. In the 1MR test, 46.67 ± 13.06Kg and in the HG 23.93±7.96Kgf were obtained, respectivetily. Correlation analyzes were characterized by the high frequency of significant correlations for height, dominant arm mass (DAM), %BF, 1MR and HG variables. In addition, correlations between HG and BM (r = 0.67, p = 0.005), height (r = 0.51, p = 0.004) and DAM (r = 0.55, p = 0.026) were also observed. The strength of the lower limbs correlates with BM (r = 0.69, p = 0.003), height (r = 0.62, p = 0.01) and DAM (r = 0.772, p = 0.001). In this way, we can conclude that not only the simple spatial relationship of mass and height can influence in predictive parameters of strength or functionality, being important the verification of the conditions of the corporal composition. For this population, height seems to be a good predictor of strength and body composition.

***Keywords*—**African Continental Ancestry Group, Body Composition, Functional Capacity, Strength.

L. C. Pereira was with Centro Universitário Euro Americano, Brasília and University of Brasilia, DF 72120-00 Brazil (phone: +55 61 9 8166 8753; e-mail:leonardo.pcllcp@gmail.com).

F. S. Santana was with Centro Universitário Euro Americano, Brasília and University of Brasilia, DF 72120-00 Brazil (phone: +55 61 9 8138 9485; e-mail: frederico.santana@unieuro.com.br).

Influence of Periodized Resistance Training on Muscle Mass Gain in Sedentary Elderly

D. A. Neves, L. C. Pereira, G. Pucci, M. G. O. Kanikowski, M. P. Safons, R. G. Alagia, H. A. Pinheiro, F. S. Santana

***Abstract*—**With the aging of the populatio, researchers have delved deeper into the effects of strength training (ST) on gaining muscle mass for the elderly in order to reduce sarcopenia [1], [2]. However, due to a large combinatorial variation among the various components that are attributable to training, little is discussed about the influence of the systematized prescription of ST frequency on the gain of muscle mass in the elderly. Thus, the objective of the study was to verify the influence of strength training with linear progressive periodization on the increase of the muscular thickness of the elderly. A total of 34 elderly subjects were randomly divided into two groups: control (CG) with body mass of 69.3 ± 15.03 kg and height of 1.57 ± 0.078 m (n = 17, 15 women and two men) and ST with body mass of 71.73 ± 9.14 kg and height 1.53 ± 0.065 m. The results presented indicate significant improvements in post-intervention muscle mass for the ST group (20,84%), and in the comparison between groups (4,53%) with significance of $p < 0.05$. Based on the results found in the present study, it was concluded that a training program with linear load control seems to optimize the hypertrophic responses of sedentary elders.

***Keywords*—**Elderly, Muscle Mass Gain**,** Resistance Training, Periodization.

REFERENCES

[1] Funghetto, S.S., et al., Interleukin-6− 174G/C gene polymorphism affects muscle damage response to acute eccentric resistance exercise in elderly obese women. Experimental gerontology, 2013. 48(11): p. 1255-1259.

[2] Pereira, L.C., et al., The influence of body composition in the strength of elderly Brazilian men. Revista Brasileira de Medicina do Esporte, 2015. 21(3): p. 196-199.

D. A. Neves is with the Centro Universitário Euro Americano, Brasília, DF 72120-00 Brazil (phone: +55 61 9 9193 7845; e-mail: dhianeyneves@hotmail.com).

L. C. Pereira was with Centro Universitário Euro Americano, Brasília and University of Brasilia, DF 72120-00 Brazil (phone: +55 61 9 8166 8753; e-mail:leonardo.pcllcp@gmail.com).

F. S. Santana was with Centro Universitário Euro Americano, Brasília and University of Brasilia, DF 72120-00 Brazil (phone: +55 61 9 8138 9485; e-mail: frederico.santana@unieuro.com.br).

Profile of the Elderly Users of Alcohol and Other Drugs Attended at the Psychosocial Care Centers in the Federal District

J. S. P. Barbosa, L. C. Pereira, K. R. Garcia, P. C. P. Bouchardet, S. C. T. Vieira, A. O. Gomes, S. S. Funghetto, M. G. O. Kanikowski

Abstract**—**For this population, height seems to be a good predictor of strength and body composition. Abstract - This increase in life expectancy of the Brazilian's population is associated with sociodemographic variables, but also to more access to health services in the prevention and better living conditions. With the growth of elderly population, a problem that has been a concern to health's professionals and public health at all is the use of psychoactive substances. The purpose of this study was identify the sociodemographic profile of the elderly people who was attended at the Center of Psychosocial Care of alcohol and other drugs in the Federal District of Brazil. 408 medical records of people aged 60 years or over were evaluated, and it is possible to know that most of them were males (85.3%), with a mean age of 64 years (DP ± 4.16), 60 and 84 years and a mean age of 64 years (DP ± 4.42); 88.2% have some family ties, are married and have children, with relatives living in masonry housing. The educational level of drug users was considered low with more emphasis on those who had elementary education being the majority retired or unemployed. Regarding the street situation, there was no significance (p = 0.084) and the women (OR = 2.98) had few chances of street situations compared to men (OR = 0.89). As for substance consumption, the highest quantity of drug consumption bids in relation to the number of illicit. It did not present significant statistical value and there is a greater probability of consumption / abuse of legal and / or illicit drugs for both sexes (OR = 0.96) for men and (OR = 1.32) for women. In relation to the use of multiple drugs, there was no significant difference between the sexes, (OR = 1.1) male sex and (OR = 0.74) female sex. Based on the results found in the present study, it was concluded that alcohol consumption is the main agent that causes vulnerability in the elderly and predisposes the latter to the consumption of other associated drugs.

Keywords**—**Centers of Attention Psychosocial alcohol and drugs, Elderly, Mental disorder due to drug use, street situations.

J. S. P. Barbosa is with the Brasília and University of Brasilia, DF 72120-00 Brazil (phone: +55 61 9 8463 7900; e-mail: jspb06@gmail.com).

L. C.Pereira was with Centro Universitário Euro Americano, Brasília and University of Brasilia, DF 72120-00 Brazil (phone: +55 61 9 8166 8753; e-mail:leonardo.pcllcp@gmail.com).

M. G. O. Kanikowski was with with the Brasília and University of Brasilia, DF 72120-00 Brazil (phone: +55 61 9 9821 1336; e-mail: margounb@gmail.com).

Relationship between Prolonged Timed up and Go Test and Worse Cardiometabolic Diseases Risk Factors Profile in a Population Aged 60-65 Years

Bartłomiej K. Sołtysik, Agnieszka Guligowska, Łukasz Kroc, Małgorzata Pigłowska, Elizavetta Fife, Tomasz Kostka

***Abstract*—**Introduction: Functional capacity is one of the basic determinants of health in older age. Functional capacity may be influenced by multiple disorders, including cardiovascular and metabolic diseases. Nevertheless, there is relatively little evidence regarding the association of functional status and cardiometabolic risk factors. Aim: The aim of this research is to check possible association between functional capacity and cardiovascular risk factor in a group of younger seniors. Materials and Methods: The study group consisted of 300 participants aged 60-65 years (50% were women). Total cholesterol (TC), triglycerides (TG), high density lipoprotein cholesterol (HDL-C), low density lipoprotein cholesterol (LDL-C), glucose, uric acid, body mass index (BMI), waist-to-height ratio (WHtR) and blood pressure were measured. Smoking status and physical activity level (by Seven Day Physical Activity Recall Questionnaire) were analysed. Functional status was assessed with the Timed Up and Go (TUG) Test. The data were compared according to gender, and then separately for both sexes regarding prolonged TUG score (>7 s). The limit of significance was set at $p \leq 0.05$ for all analyses. Results: Women presented with higher serum lipids and longer TUG. Men had higher blood pressure, glucose, uric acid, prevalence of hypertension and history of heart infarct. In women group, those with prolonged TUG displayed significantly higher obesity rate (BMI, WHTR), uric acid, hypertension and ischemic heart disease (IHD), but lower physical activity level, TC or LDL-C. Men with prolonged TUG were heavier smokers, had higher TG, lower HDL and presented with higher prevalence of diabetes and IHD. Discussion: This study shows association between functional status and risk profile of cardiometabolic disorders. In women, the relationship of lower functional status to cardiometabolic diseases may be mediated by overweight/obesity. In men, locomotor problems may be related to smoking. Higher education level may be considered as a protective factor regardless of gender.

***Keywords*—**Seniors, functional capacity, TUG test, cardiovascular risk factors.

Bartomiej K. Sołtysik is with Department of Geriatrics Medical University of Lodz Żeromskiego 113 st. 90-549 Lodz Poland (Tel (Fax). (48)(42) 6393590, e-mail: bartlomiej.soltysik@umed.lodz.pl).

Tomasz Kostka is with Department of Geriatrics Medical University of Lodz Żeromskiego 113 st. 90-549 Lodz Poland (Tel (Fax). (48)(42) 6393609, e-mail: tomasz.kostka@umed.lodz.pl).

The Effects of the Light Therapy on Activities of Daily Living and Sleep on Patients with Alzheimer's Disease: A University Project

Guler Balcı Alparslan, Ayse Ozkaraman, Demet Ozbabalık, Ertugrul Colak

Abstract**—**Alzheimer is chronic disease which causes many symptoms such as sleep disorders and poor sleep quality. The light therapy is a non pharmacologic treatment and it may help to cope with symptoms like sleep problems. It should be used to cope sleep problems by health professionals.

The aim of study is to analysis the effects of the light therapy on activities of daily living and sleep in patients with Alzheimer's disease.

In this study, the actiwatches (light, sleep and daily activites recorder) sleep and light therapy forms, mini mental test forms, Cornell Demans Depresion Index forms and Barthel Daily Life Activities forms were used. This randomized clinical trial was carried out on patients with Alzheimer in a Alzheimer Care Center in Eskisehir, Turkey. The ethical approval and the necessary other permissions were obtained from care center and the patients. The data will be evaluated by using a statical program. The patients adhered to criterions, were observed for four weeks. This study was carried as follows:

*At the first time, all forms were filled and the patients wore the actiwacties. Before light therapy, for first one week, the patients with actiwatches were watched.

*During second weeks, the light therapy was applied to patients with actiwatches and the patients with actiwatches were watched. The sleep and light therapy forms were filled.

*After than, during third and fourth weeks the patients with actiwatches were watched. The study has been conducted. The results will be disscused in session.

Keywords**—**Alzheimer's disease, non pharmacologic therapy, nursing, sleep disorders.

G. B. Alparslan is in Eskisehir Osmangazi University Faculty of Health Science Eskisehir Turkey (phone: 00905358627069; e-mail: gbalci80@hotmail.com).

A. Ozkaraman is in Eskisehir Osmangazi University Faculty of Health Science Eskisehir Turkey (e-mail: aozaydin26@hotmail.com).

D. Ozbabalik is in Acibadem Hospital Eskisehir Turkey (e-mail: demetozbabalik@gmail.com).

E. Colak is in Eskisehir Osmangazi University Faculty of Medical Eskisehir Turkey (e-mail: ecolak@ogu.edu.tr).

Prognostic Factors for Mortality and Duration of Admission in Malnourished Hospitalized, Elderly Patients: A Cross-Sectional Study

Christos E. Lampropoulos, Maria Konsta, Vicky Dradaki, Irini Dri, Tamta Sirbilatze, Ifigenia Apostolou, Christina Kordali, Konstantina Panouria, Kostas Argyros, Georgios Mavras

Abstract**—**Objectives: Malnutrition in hospitalized patients is related to increased morbidity and mortality. Purpose of our study was to assess nutritional status of hospitalized, elderly patients with various nutritional scores and to detect unfavorable prognostic factors, related to increased mortality and extended duration of admission. Methods: 150 patients (78 men, 72 women, mean age 80±8.2) were included in this cross-sectional study. Nutritional status was assessed by Mini Nutritional Assessment (MNA full, short-form), Malnutrition Universal Screening Tool (MUST) and short Nutritional Appetite Questionnaire (sNAQ). The following data were incorporated in analysis: Anthropometric and laboratory data, physical activity (International Physical Activity Questionnaires, IPAQ), smoking status, dietary habits and mediterranean diet (assessed by MedDiet score), cause and duration of current admission, medical history (co-morbidities, previous admissions). Primary endpoints were the mortality (from admission until 6 months afterwards) and duration of admission, compared to national guidelines for closed consolidated medical expenses. Mann-Whitney two-sample statistics or t-test was used for group comparisons and Spearman or Pearson coefficients for testing correlation between variables. Results: Normal nutrition was assessed in 54/150 (36%), 92/150 (61.3%) and in 106/150 (70.7%) of patients, according to full MNA, MUST and sNAQ questionnaires respectively. Mortality rate was 20.7% (31/150 patients). The patients who died until 6 months after admission had lower BMI (24±4.4 vs 26±4.8, p=0.04) and albumin levels (2.9±0.7 vs 3.4±0.7, p=0.002), significantly lower full MNA (14.5±7.3 vs 20.7±6, p<0.0001) and short-form MNA scores (7.3±4.2 vs 10.5±3.4, p=0.0002) compared to non-dead one. In contrast, the aforementioned patients had higher MUST (2.5±1.8 vs 0.5±1.02, p=<0.0001) and sNAQ scores (2.9±2.4 vs 1.1±1.3, p<0.0001). Additionally, they showed significantly lower MedDiet (23.5±4.3 vs 31.1±5.6, p<0.0001) and IPAQ scores (37.2±156.2 vs 516.5±1241.7, p<0.0001) compared to remaining one. These patients had extended hospitalization [5 (0-13) days vs 0 (-1-3) days, p=0.001]. Patients who admitted due to cancer depicted higher mortality rate (10/13, 77%), compared to those who admitted due to infections (12/73, 18%), stroke (4/15, 27%) or other causes (4/49, 8%) (p<0.0001). Extension of hospitalization was negatively correlated to both full (Spearman r=-0.35, p<0.0001) and short-form MNA (Spearman r=-0.33, p<0.0001) and positively correlated to MUST (Spearman r=0.34, p<0.0001) and sNAQ (Spearman r=0.3, p=0.0002). Additionally, the extension was inversely related to MedDiet score (Spearman r=-0.35, p<0.0001), IPAQ score (Spearman r=-0.34, p<0.0001), albumin levels (Pearson r=-0.36, p<0.0001), Ht (Pearson r=-0.2, p=0.02) and Hb (Pearson r=-0.18, p=0.02). Conclusion: A great proportion of elderly, hospitalized patients are malnourished or at risk of malnutrition. All nutritional scores, physical activity and albumin are significantly related to mortality and increased hospitalization.

Keywords**—**Dietary habits, duration of admission, malnutrition, prognostic factors for mortality.

Christos Lampropoulos is with Department of Internal Medicine, Argolidos General Hospital, Argos, Greece (e-mail: christosnina@hotmail.com).

Full Mini Nutritional Assessment Questionnaire and the Risk of Malnutrition and Mortality in Elderly, Hospitalized Patients: A Cross-Sectional Study

Christos E. Lampropoulos, Maria Konsta, Tamta Sirbilatze, Ifigenia Apostolou, Vicky Dradaki, Konstantina Panouria, Irini Dri, Christina Kordali, Vaggelis Lambas, Georgios Mavras

***Abstract*—**Objectives: Full Mini Nutritional Assessment (MNA) questionnaire is one of the most useful tools in diagnosis of malnutrition in hospitalized patients, which is related to increased morbidity and mortality. The purpose of our study was to assess the nutritional status of elderly, hospitalized patients and examine the hypothesis that MNA may predict mortality and extension of hospitalization.

Methods: One hundred fifty patients (78 men, 72 women, mean age 80±8.2) were included in this cross-sectional study. The following data were taken into account in analysis: anthropometric and laboratory data, physical activity (International Physical Activity Questionnaires, IPAQ), smoking status, dietary habits, cause and duration of current admission, medical history (co-morbidities, previous admissions). Primary endpoints were mortality (from admission until 6 months afterwards) and duration of admission. The latter was compared to national guidelines for closed consolidated medical expenses. Logistic regression and linear regression analysis were performed in order to identify independent predictors for mortality and extended hospitalization respectively.

Results: According to MNA, nutrition was normal in 54/150 (36%) of patients, 46/150 (30.7%) of them were at risk of malnutrition and the rest 50/150 (33.3%) were malnourished.

After performing multivariate logistic regression analysis we found that the odds of death decreased 20% per each unit increase of full MNA score (OR=0.8, 95% CI 0.74-0.89, p<0.0001). Patients who admitted due to cancer were 23 times more likely to die, compared to those with infection (OR=23, 95% CI 3.8-141.6, p=0.001). Similarly, patients who admitted due to stroke were 7 times more likely to die (OR=7, 95% CI 1.4-34.5, p=0.02), while these with all other causes of admission were less likely (OR=0.2, 95% CI 0.06-0.8, p=0.03), compared to patients with infection.

According to multivariate linear regression analysis, each increase of unit of full MNA, decreased the admission duration on average 0.3 days (b:-0.3, 95% CI -0.45 - -0.15, p<0.0001). Patients admitted due to cancer had on average 6.8 days higher extension of hospitalization, compared to those admitted for infection (b:6.8, 95% CI 3.2-10.3, p<0.0001).

Conclusion: Mortality and extension of hospitalization is significantly increased in elderly, malnourished patients. Full MNA score is a useful diagnostic tool of malnutrition.

***Keywords*—**Duration of admission, malnutrition, mini nutritional assessment score, prognostic factors for mortality.

Christos Lampropoulos is with Department of Internal Medicine, Argolidos General Hospital, Argos, Greece (e-mail: christosnina@hotmail.com).

Validation of Nutritional Assessment Scores in Prediction of Mortality and Duration of Admission in Elderly, Hospitalized Patients: A Cross-Sectional Study

Christos E. Lampropoulos, Maria Konsta, Vicky Dradaki, Irini Dri, Konstantina Panouria, Tamta Sirbilatze, Ifigenia Apostolou, Vaggelis Lambas, Christina Kordali, Georgios Mavras

Abstract**—**Objectives: Malnutrition in hospitalized patients is related to increased morbidity and mortality. Purpose of our study was to compare various nutritional scores in order to detect the most suitable one for assessing the nutritional status of elderly, hospitalized patients and correlate them with mortality and extension of admission duration, due to patients' critical condition.

Methods: Sample population included 150 patients (78 men, 72 women, mean age 80±8.2). Nutritional status was assessed by Mini Nutritional Assessment (MNA full, short-form), Malnutrition Universal Screening Tool (MUST) and short Nutritional Appetite Questionnaire (sNAQ). Sensitivity, specificity, positive and negative predictive values and ROC curves were assessed after adjustment for the cause of current admission, a known prognostic factor according to previously applied multivariate models. Primary endpoints were mortality (from admission until 6 months afterwards) and duration of hospitalization, compared to national guidelines for closed consolidated medical expenses.

Results: Concerning mortality, MNA (short-form and full) and SNAQ had similar, low sensitivity (25.8%, 25.8% and 35.5% respectively) while MUST had higher sensitivity (48.4%). In contrast, all the questionnaires had high specificity (94%-97.5%). Short-form MNA and sNAQ had the best positive predictive value (72.7% and 78.6% respectively) whereas all the questionnaires had similar negative predictive value (83.2%-87.5%). MUST had the highest ROC curve (0.83) in contrast to the rest questionnaires (0.73-0.77).

With regard to extension of admission duration, all four scores had relatively low sensitivity (48.7%-56.7%), specificity (68.4%-77.6%), positive predictive value (63.1%-69.6%), negative predictive value (61%-63%) and ROC curve (0.67-0.69).

Conclusion: MUST questionnaire is more advantageous in predicting mortality due to its higher sensitivity and ROC curve. None of the nutritional scores is suitable for prediction of extended hospitalization.

Keywords**—**Duration of admission, malnutrition, nutritional assessment scores, prognostic factors for mortality.

Christos Lampropoulos is with Department of Internal Medicine, Argolidos General Hospital, Argos, Greece (e-mail: christosnina@hotmail.com).

Mediterranean Diet, Duration of Admission and Mortality in Elderly, Hospitalized Patients: A Cross-Sectional Study

Christos E. Lampropoulos, Maria Konsta, Ifigenia Apostolou, Vicky Dradaki, Tamta Sirbilatze, Irini Dri, Christina Kordali, Vaggelis Lambas, Kostas Argyros, Georgios Mavras

***Abstract*—**Objectives: Mediterranean diet has been associated with lower incidence of cardiovascular disease and cancer. Purpose of our study was to examine the hypothesis that mediterranean diet may protect against mortality and reduce admission duration in elderly, hospitalized patients. Methods: Sample population included 150 patients (78 men, 72 women, mean age 80±8.2). The following data were taken into account in analysis: anthropometric and laboratory data, dietary habits (MedDiet score), patients' nutritional status [Mini Nutritional Assessment (MNA) score], physical activity (International Physical Activity Questionnaires, IPAQ), smoking status, cause and duration of current admission, medical history (co-morbidities, previous admissions). Primary endpoints were mortality (from admission until 6 months afterwards) and duration of admission, compared to national guidelines for closed consolidated medical expenses. Logistic regression and linear regression analysis were performed in order to identify independent predictors for mortality and admission duration difference respectively. Results: According to MNA, nutrition was normal in 54/150 (36%) of patients, 46/150 (30.7%) of them were at risk of malnutrition and the rest 50/150 (33.3%) were malnourished. After performing multivariate logistic regression analysis we found that the odds of death decreased 30% per each unit increase of MedDiet score (OR=0.7, 95% CI:0.6-0.8, p<0.0001). Patients with cancer-related admission were 37.7 times more likely to die, compared to those with infection (OR=37.7, 95% CI:4.4-325, p=0.001). According to multivariate linear regression analysis, admission duration was inversely related to mediterranean diet, since it is decreased 0.18 days on average for each unit increase of MedDiet score (b:-0.18, 95% CI:-0.33 - -0.035, p=0.02). Additionally, the duration of current admission increased on average 0.83 days for each previous hospital admission (b:0.83, 95% CI:0.5-1.16, p<0.0001). The admission duration of patients with cancer was on average 4.5 days higher than the patients who admitted due to infection (b:4.5, 95% CI:0.9-8, p=0.015). Conclusion: Mediterranean diet adequately protects elderly, hospitalized patients against mortality and reduces the duration of hospitalization.

***Keywords*—**Mediterranean diet, malnutrition, nutritional status, prognostic factors for mortality.

Christos Lampropoulos is with Department of Internal Medicine, Argolidos General Hospital, Argos, Greece (e-mail: christosnina@hotmail.com).

The Mediating Role of Orthorexia Nervosa over the Explanation of Relationship between Obsessive Compulsive Symptoms and Eating Attitudes

Duygu Kuzu, Omer Faruk Simsek

Abstract**—**Orthorexia Nervosa is newly defined term that characterized with obsessions about healthy foods and dietary restrictions. Even though it is not defined in DSM 5, similarity with obsessive compulsive disorder is investigated. From this perspective mediation role of orthorexia nervosa between OCD and eating attitudes was tested with structural equation modeling. Although previous researches founded the relationship between OCD and eating disorders there is not any research about mediating role of orthorexia nervosa for this relationship. Present research is composed of non-clinical sample of 100 students which are from nutrition and dietetics program. Maudsley OCD scale, Eating Attitude Inventory and Ortho-15 scales were used to test the model. According to results the full mediation role of orthorexia nervosa was found over the relationship between OCD and eating disorder. Results will be expected to contribute to clinical area by understanding the possible mediation effects of orthorexia nervosa and future researchers may focus of the other possible mediators.

Keywords**—**Eating disorders, orthorexia nervosa, OCD, Structural Equation Modeling.

Duygu Kuzu and Omer Faruk Simsek are with Psychology Department, Istanbul Arel University, Istanbul, Turkey (e-mail: duygukuzu@arel.edu.tr, omersimsek@arel.edu.tr).

The Relationship of the Gap between Experience and Language with Depression in Hearing-Impaired People: Aggression as a Mediator Variable

Gizem Hüroğlu, Aylin Ipek Timur, Omer Faruk Şimşek

Abstract**—**Research Objectives: Hearing impaired individuals are more prone to experience psychopathology like depression, agression, post travmatic stress disorder because of language and communication problems. This study tested a structural equation model in which agression mediated the relationship between perception of gap between experience and language and depression in a hearing impaired sample. Although previous research gave clear evidence that language is closely related to depression, the resarch on intervening variables in the relationship has been limited. Methodology: The main aim of the present study was to provide additional knowledge about the mediatory processes through which language relates to depression. Two-hundred hearing impaired individual (99 female, 100 male, 1 other) participated in the study. The Beliefs about the Functions of Language Scale was used to measure personal perception of the gap between experience and language; Buss Perry Agression Questionnaire was used to measure aggression level and Beck Depression Inventory was used to measure depression levels of the participants. The model proposed by the current investigation was tested using structural equation modeling using LISREL 8.80. Findings: The results supported the model and showed that perception of the gap between language and experience predicted aggression, which in turn predicted the participants' depression in hearing impaired sample. Research Outcomes: Under the light of previous research and current findings, suggestions for prevention and treatment strategies for depression will be provided, especially for the hearing impaired people. Future Scope: Future research should also focus on other potential mediator variables.

Keywords**—**Language, depression, aggresion, hearing impairment.

Gizem Hüroğlu is with Istanbul Arel University, Turkey (e-mail: gizemhuroglu@arel.edu.tr).

Omer Faruk Şimşek is with Istanbul Arel University, Turkey (e-mail: omersimsek@arel.edu.tr).

A Clinical Audit on Screening Women with Subfertility Using Transvaginal Scan and Hysterosalpingo Contrast Sonography

Aarti M. Shetty, Estela Davoodi, Subrata Gangooly, Anita Rao-Coppisetty

Abstract**—**Background: Testing Patency of Fallopian Tubes is among one of the several protocols for investigating Subfertile Couples. Both, Hysterosalpingogram (HSG) and Laparoscopy and dye test have been used as Tubal patency test for several years, with well-known limitation. Hysterosalpingo Contrast Sonography (HyCoSy) can be used as an alternative tool to HSG, to screen patency of Fallopian tubes, with an advantage of being non-ionising, and also, use of transvaginal scan to diagnose pelvic pathology.

Aim: To determine the indication and analyse the performance of Trasnvaginal scan and HyCoSy in Broomfield Hospital.

Methods: We retrospectively analysed fertility workup of 282 women, who attended HyCoSy clinic at our institution from January 2015 to June 2016.

An Audit proforma was designed, to aid data collection. Data was collected from patient notes and electronic records, which included patient demographics; age, parity, type of subfertility (primary or secondary), duration of subfertility, past medical history and base line investigation (hormone profile and semen analysis). Findings of trasnvaginal scan, HyCoSy and Laparoscopy were also noted.

Results: The most common indication for referral were as a part of primary fertility workup on couples who had failure to conceive despite intercourse for a year, other indication for referral were recurrent miscarriage, history of ectopic pregnancy, post reversal of sterilization(vasectomy and tuboplasty), Post Gynaecology surgery(Loop excision, cone biopsy) and amenorrhea. Basic Fertility workup showed 34% men had abnormal semen analysis. HyCoSy was successfully completed in 270 (95%) women using ExEm foam and Trasnvaginal Scan. Of the 270 patients, 535 tubes were examined in total. 495/535 (93%) tubes were reported as patent, 40/535 (7.5%) tubes were reported as blocked. A total of 17 (6.3%) patients required laparoscopy and dye test after HyCoSy. In these 17 patients, 32 tubes were examined under laparoscopy, and 21 tubes had finding similar to HyCoSy, with a concordance rate of 65%. In addition to this, 41 patients had some form of pelvic pathology (endometrial polyp, fibroid, cervical polyp, fibroid, bicornuate uterus) detected during transvaginal scan, who referred to corrective surgeries after attending HyCoSy Clinic.

Conclusion: Our audit shows that HyCoSy and Transvaginal scan can be a reliable screening test for low risk women. Furthermore, it has competitive diagnostic accuracy to HSG in identifying tubal patency, with an additional advantage of screening for pelvic pathology. With addition of 3D Scan, pulse Doppler and other non-invasive imaging modality, HyCoSy may potentially replace Laparoscopy and chromopertubation in near future.

Keywords**—**HyCoSy, Transvaginal Scan, tubal infertility, tubal patency test.

Aarti.M.Shetty is with Mid Esses NHS Hospital Trust, Broomfield Hospital, CM1 7ET, U.K (phone: 0044-0-7456414580; e-mail: Aarti.shetty@meht.nhs.uk).

Estela Davoodi, is with Mid Esses NHS Hospital Trust, Broomfield Hospital, CM1 7ET, U.K (e-mail: Estela.Davoodi@meht.nhs.uk).

Subarata Gangooly is with Mid Esses NHS Hospital Trust, Broomfield Hospital, CM1 7ET, U.K (e-mail: Subrata.Gangooly@meht.nhs.uk).

Anita Rao-Coppisetty is with Mid Esses NHS Hospital Trust, Broomfield Hospital, CM1 7ET, U.K (e-mail: CoppisettyAnita.Rao@meht.nhs.uk).

Mitochondrial Contribution in Egg Rejuvenation and Pre-Implantation of Embryo

Sana Abbas, Shahzad Bhatti, Muhammad Aslamkhan, Magali Segundo Trinidad, Hikmet Hakan Aydin, Gerardo Rodriguez Gonzalez

***Abstract*—**Background: Mitochondria are integral part of a cell known as "*power house*" of the cell, manifested by highly multifaceted and entirely organized intricate biological processes. Traditionally, it portrayed two essential physiological liabilities: periodic release of energy during the cell cycle and activation of specific integral proteins. Several studies predicted its manifold functions by producing heterogeneous proteins that are unequivocally involved in a plethora of phosphorylation pathways, calcium signaling, cellular respiration, embryonic development and sequential programmed cell death. However, in early oogenesis and embryogenesis mitochondria has a nexus of developmental regulations and overwhelming role in infertility treatments. The oocyte quality is directly related with ovarian aging and devastating mitochondrial function which is important for infertility and age related ovarian dysfunction.

Objective: Nearly 23% patients visiting the infertility centers consulting for infertility depicted signs of premature ovarian senescence (POS) and quality compromise oocyte. This study emphasize on the role of mitochondria in ovarian aging and on the expected effects in the next generation.

Subjects and Methods: PubMed was employed to search the MEDLINE database for peer-reviewed original research papers and reviews about mitochondria and ovarian ageing, in human species from 2002 to 2017.

The patients are divided into two groups, premature ovarian senescence (POS) group and normal ovarian senescence group (NOPS). Statistically, we apply orthogonal partial least squares discriminant analysis (OPLS-DA). In order to compute the value of oocyte mtDNA content we used OPLS model.

Results: Our data showed a correlative capability (Q2 = 0.769) when OPLS-DA has employed among two groups. The POS group showed three important variables by using projection matric i.e. oocyte mtDNA content (0.82), the cumulus cell mtDNA content (0.85) and peroxisome active receptor γ co activator factor (1.02) all are lower in POS group than NOPS groups of patients. While OPLS model predict oocyte mtDNA content only in the NOPS group (Q2 = 0.634). Moreover, we found four new positively correlated variables that are directly linked with mitochondrial inner mass of quality compromised oocytes (0.56), the cumulus cell mtDNA contents (1.032), expression of polymerase gamma (1.85) and mitochondrial DNA transcription factor (1.50).

***Keywords*—**Mitochondrial DNA, infertility, in vitro Fertilization (IVF), egg rejuvenation.

Sana Abbas is with Hameed Latif Hospital, Lahore Institute of Fertility and Endocrinology, Pakistan (e-mail: christosnina@hotmail.com).

Common Used Non-Medical Practice and Perceived Benefits in Couples with Fertility Problems in Turkey

S. Fata, M. A. Tokat, N. Bagardi, B. Yilmaz

Abstract**—**Nowadays, various traditional practices are used throughout the world with aim to improve fertility. Various traditional remedies, acupuncture, religious practices such as sacrifice are frequently used. Studies often evaluate the traditional practices used by the women. But the use of this non-medical practice by couples and specific application reasons of this methods has been less investigated. The aim of this study was to evaluate the common used non-medical practices and determine perceived benefits by couples with fertility problems in Turkey.

This is a descriptive study. Research data were collected between May-July 2016, in Izmir Ege Birth Education and Research Hospital Assisted Reproduction Clinic, from 151 couples with fertility problem. Personal Information Form and Non-Medical Practices Used for Fertility Evaluation Form was used. Number "GOA 2649" permission letter from Dokuz Eylul University Non-Invasive Research Ethics Board, permission letter from the institution and the written consent from participants has been received to carry out the study. In the evaluation of the data, frequencies and proportions analysis were used.

The average age of women participating in the study was 32.87, the 35.8% were high school graduates, 60.3% were housewife and the 58.9% lived in city. The 30.5% of husbands were high school graduates, the 96.7% were employed and the 60.9% lived in city. The 78.1% of couples lived as a nuclear family, the average marriage year was 7.58, in 33.8% the fertility problem stems from women, 42.4% of them received a diagnosis for 1-2 years, 35.1% were being treated for 1-2 years.

The 35.8% of women reported use of non-medical applications. The 24.4% of women used figs, onion cure, hacemat, locust, bee-pollen milk, the 18.2% used herbs, the 13.1% vowed, the 12.1% went to the tomb, the 10.1% did not bath a few days after the embryo transfer, the 9.1% used thermal water baths, the 5.0% manually corrected the womb, the 5.0% printed amulets by hodja, the 3.0% went to the hodja/pilgrims.

Among the perceived benefits for using non-medical practices; facilitate pregnancy and implantation, improve oocyte quality were the most recently expressed. Women said that they often used herbs to develop follicles, did not bath after embryo transfer with aim to provide implantation, and used thermal waters to get rid of the infection.

Compared to women, only the 25.8% of men used the non-medical practice. The 52.1% reported that they used peanuts, hacemat, locust, bee-pollen milk, the 14.9% used herbs, the 12.8% vowed, the 10.1% went to the tomb, the 10.1% used thermal water baths.

Improve sperm number, motility and quality were the most expected benefits. Men said that they often used herbs to improve sperm number, used peanuts, hacemat, locust, bee-pollen milk to improve sperm motility and quality.

Couples in Turkey often use non-medical practices to deal with fertility problems. Some of the practices considered as useful can adversely affect health. Healthcare providers should evaluate the use of non-medical practices and should inform if the application is known adverse effects on health.

Keywords**—**Couples, fertility, non-medical practice, perceived benefit.

Sevcan Fata is with the Dokuz Eylul University Nursing Faculty, Research Assistant, Turkey (phone: +90 232 412 69 75; e-mail: sevcan_fata@hotmail.com).

Merlinda Alus Tokat is with Dokuz Eylul University Nursing Faculty, Assistant Professor, Turkey (e-mail: merlinda_alus@yahoo.com).

Nese Bagardi is with the Tepecik Training and Research Hospital Assisted Reproductive Clinic, Nurse, Turkey (e-mail: nesebagardi@hotmail.com).

Bülent Yilmaz is with the Tepecik Training and Research Hospital Assisted Reproductive Clinic, Doctor, Turkey (e-mail: bulent.yilmaz@ikc.edu.tr).

Gestational Diabetes Mellitus (GDM) Knowledge Levels of Pregnant Women with GDM and Affecting Factors

Nuran Nur Aypar, Merlinda Alus Tokat

***Abstract*—**The aim of the study is to determine the knowledge level of pregnant women with Gestational Diabetes Mellitus (GDM) about the disease and affecting factors. The data of this descriptive study were collected from 184 pregnant women who were followed up in Dokuz Eylul University Hospital (n=34), Izmir Ege Maternity Hospital, Gynecology Training and Research Hospital (n=133), and Egepol Private Hospital (n=17). Data collection forms were prepared by the researcher according to the literature. ANOVA test, Kruskal Wallis test, Mann Whitney U test, Student's t-test, and Pearson correlation test were used for statistical analyses. Average GDM knowledge score of pregnant women was 40.10±19.56. The GDM knowledge scores were affected by factors such as age, educational level, working status, income status, educational level of the spouse, and the GDM background. It has been shown in our study that the GDM knowledge scores were negatively affected by factors such as young age, low educational level, low income level, unemployment, having a spouse with low educational level, absence of the GDM story. It has been identified that 86.4% of the pregnant women were trained about GDM. The education provided in the antenatal period significantly increased GDM knowledge scores of pregnant women (p=0.000, U=515.0). It has been determined that GDM knowledge of the pregnant women with GDM is affected by various factors. These factors must be considered in order to determine new strategies.

***Keywords*—**Affecting factors, Gestational Diabetes Mellitus (GDM), knowledge level, nursing, pregnancy.

Nuran Nur Aypar is with the Dokuz Eylül University Nursing Faculty Gynecology and Obstetrics Department, 35340, Izmir, Turkey (phone: +90 232 412 69 70; e-mail: nuraypar@gmail.com).

Merlinda Alus Tokat is with Dokuz Eylül University Nursing Faculty Gynecology and Obstetrics Department, 35340, Izmir, Turkey (e-mail: merlinda_alus@yahoo.com).

Effects of Some Characteristics of Gynecological Cancer Diagnosis and Treatment on Women's Sexual Life Quality

Buse Bahıtlı, Samiye Mete

Abstract**—**The aim of study was to evaluate the quality of sexual life of women with diagnosed gynecological cancer and receive treatment. The study was a descriptive and cross-sectional type, and it was carried out with 276 women. Information Form and Sexual Quality of Life Scale-Female (SQOL) form was used in study. The data was evaluated using Mann Whitney U and Kruskal-Wallis test. In study, Sexual Quality of Life Scale-Female average score was 68.83 ± 21.17. The %43.1 of women was endometrial cancer, %30.8 was cervical cancer, %24.6 was ovarian cancer and %1.4 was vulvar cancer. The average time to diagnosis of patients is 41.80 ± 47.64 months. There was no significant difference mean SQOL according to individual/sociodemographic characteristics like age, education. Gynecological cancer related characteristics like gynaecological cancer type, treatment type, surgery type were found not to affect the mean score of SQOL. However, it was found that the difference was due to the higher SQOL score in the group with a diagnosis time of 25 months and over ($X^2KW= 6.356$, $p= 0.046$). The reason of significant difference mean SQOL according to diagnosis over time might be that women adaptate to cancer diagnosis. While women with gynaecologic cancer are evaluating their sexual lives, it is necessary to evaluate them with good evaluation tools.

Keywords**—**Gynecological cancers, sexuality, quality of sexual life, SQOL.

Buse Bahitli is with Dokuz Eylul University Nursing Faculty, İzmir, Turkey (phone: +902324124773; e-mail: busebahitli@gmail.com).

Samiye Mete was with Dokuz Eylul University Nursing Faculty, İzmir, Turkey (phone: +902324124751; e-mail: samiye.mete@deu.edu.tr).

Pregnancy Outcomes in Women of Advanced Age

Mehrnaz Valadan, Fatemeh Davari, Azam Sepahi, Pouya Bandegi

Abstract—Objective: The aim of this study was to investigate prenatal and obstetrical outcome in mothers aged 40 years or older. Materials and methods: A prospective comparative study was conducted for the women aged 40 years and over who delivered at 20 week's gestation or beyond from January 2004 to December 2005 at four Hospitals of Tehran University of Medical Sciences. For comparison, a control group of patients who were 20-29 years of age was considered. Results: There were statistically significant increases in the rates of gestational diabetes, preeclampsia, caesarean section, breech presentation and stillbirth in women 40 years of age or older. Conclusion: There is a need to offer older women special counseling both before and after conception so that they become informed of the increased risks involved.

Keywords—advanced maternal age, high risk, outcomes, pregnancy

Corresponding Author
Mehrnaz Valadan from Tehran University of Medical Sciences, Iran, Islamic Republic Of
e-mail: mehrnaz_valadan@yahoo.com

Preoperative Gabapentin to Prevent Postoperative Shoulder Pain after Laparoscopic Ovarian Cystectomy: A Randomized Clinical Trial

Mehrnaz Valadan, Sakineh Banifatemi, Fardin Yousefshahi, Pouya Bandegi

Abstract—Background: Patients undergoing gynecology laparoscopy frequently experience shoulder pain as a common postoperative complication. Considering diaphragm stimulation in its pathophysiology, there are some advice to prevent or control this special form of referral pain. Objectives: The current study aimed to assess the prophylactic effect of preoperative administration of oral gabapentin to prevent Post Laparoscopic Shoulder Pain (PLSP) after laparoscopic ovarian cystectomy. Patients and Methods: In a randomized, double blind, placebo controlled trial 40 female patients who were candidates to have elective laparoscopic ovarian cystectomy, received uniformed capsules containing gabapentin 600 mg or placebo 30 minutes before anesthesia induction. All patients had the American Society of Anesthesiologists (ASA) Physical Status of I-II and none had pervious abdominal surgery. Thereafter, the presence of side effects and PLSP and its severity was assessed by Visual Analog Scale (VAS) in the beginning of surgery and 2, 6, 12 hours after the surgery. Results: Comparing the gabapentin (n = 20) and placebo (n = 20) groups, basic characteristics including age (P = 0.446), Body Mass Index (BMI) (P = 0.876), pregnancy history (P = 0.660), and surgery time (P = 0.232) were statistically similar. PLSP occurrence was less frequent in the gabapentin group (45%) compared with the placebo group (75%) (P = 0.053), while In gabapentin group the VAS scores were lower in 2(P = 0.004), 6 (P = 0.132), and 12 (P = 0.036) hours, post operatively. Conclusions: Prophylactic gabapentin administration could be considered as an effective and safe intervention to reduce occurrence and severity of PLSP after gynecologic laparoscopic cystectomy.

Keywords—gabapentin, shoulder pain, visual analog scale, laparoscopy

Corresponding Author
Mehrnaz Valadan from Tehran University of Medical Sciences, Iran, Islamic Republic Of
e-mail: mehrnaz_valadan@yahoo.com

Sickle Cell Disease: Review of Managements in Pregnancy and the Outcome in Ampang Hospital, Selangor

Z. Nurzaireena, K. Azalea, T. Azirawaty, S. Jameela, G. Muralitharan

Abstract**—**The aim of this study is the review of the management practices of sickle cell disease patients during pregnancy, as well as the maternal and neonatal outcome at Ampang Hospital, Selangor. The study consisted of a review of pregnant patients with sickle cell disease under follow up at the Hematology Clinic, Ampang Hospital over the last seven years to assess their management and maternal-fetal outcome. The results of the review show that Ampang Hospital is considered the public hematology centre for sickle cell disease and had successfully managed three pregnancies throughout the last seven years. Patients' presentations, managements and maternal-fetal outcome were compared and reviewed for academic improvements. All three patients were seen very early in their pregnancy and had been given a regime of folic acid, antibiotics and thrombo-prophylactic drugs. Close monitoring of maternal and fetal well being was done by the hematologists and obstetricians. Among the patients, there were multiple admissions during the pregnancy for either a painful sickle cell bone crisis, haemolysis following an infection and anemia requiring phenotype- matched blood and exchange transfusions. Broad spectrum antibiotics coverage during and infection, hydration, pain management and venous-thrombolism prophylaxis were mandatory. The pregnancies managed to reach near term in the third trimester but all required emergency caesarean section for obstetric indications. All pregnancies resulted in live births with good fetal outcome. During post partum all were nursed closely in the high dependency units for further complications and were discharged well. Post partum follow up and contraception counseling was comprehensively given for future pregnancies. Sickle cell disease is uncommonly seen in the East, especially in the South East Asian region, yet more cases are seen in the current decade due to improved medical expertise and advance medical laboratory technologies. Pregnancy itself is a risk factor for sickle cell patients as increased thrombosis event and risk of infections can lead to multiple crisis, haemolysis, anemia and vaso-occlusive complications including eclampsia, cerebrovasular accidents and acute bone pain. Patients mostly require multiple blood product transfusions thus phenotype-matched blood is required to reduce the risk of alloimmunozation. Emphasizing the risks and complications in preconception counseling and establishing an ultimate pregnancy plan would probably reduce the risk of morbidity and mortality to the mother and unborn child. Early management for risk of infection, thromboembolic events and adequate hydration is mandatory. A holistic approach involving multidisciplinary team care between the hematologist, obstetricians, anesthetist, neonatologist and close nursing care for both mother and baby would ensure the best outcome. In conclusion, sickle cell disease by itself is a high risk medical condition and pregnancy would further amplify the risk. Thus, close monitoring with combine multidisciplinary care, counseling and educating the patients are crucial in achieving the safe outcome.

Keywords**—**Anemia, haemoglobinopathies, pregnancy, sickle cell disease.

I. Introduction

SICKLE cell disease (SCD) is initially found in the Sub-Saharan African continent and the Middle East region. Yet, over the past decades with wide trading and slavery, the disease can be found among those of African descent, in the Caribbean and Middle East regions, India, Mediterranean, including South and Central America [1]. Nowadays, with easily accessible transportation worldwide, intercontinental migration and marriage, it is not uncommon for cases to exist around the globe in other regions with wide phenotypic variations which still need further observation and studies to improve the health care among these patients [2].

SCD is single gene autosomal recessive inheritance disorders where sickled hemoglobin (Hb S) under low oxygen tension and certain stress conditions such as high altitude and ongoing infection, cause the Hb S intracellular molecules to polymerize, reducing its solubility and thus becomes stiff and rigid. The hemoglobin structure changes from disc-like to sickle shaped which exposes its surface membrane to molecules adhesion and adherence to vascular endothelium. This sickling conditions leads to vaso-occlusive events in micro vessels and premature disruption of hemoglobin which leads to chronic anemia. Further complications following vaso-occlusion in various organs especially if it involves vital organs includes acute chest syndrome, cerebrovascular accident, avascular necrosis of the bones, hemolytic anemia, sickle cell crisis, recurrent infection and pain which further contribute to higher morbidity and mortality [3].

SCD is a general term referring to the sickle hemoglobin disorders. There are classifications depending on the genotypes of the patients and usually resemble the severity of clinical presentation. *Sickle cell anemia (HbSS disease)* is homozygote for beta S globin which commonly presents with a severe or moderate severe phenotype. While *HbS/beta0 thalassaemia* is a severe double heterozygote for HbS and

Nurzaireena Z is the Senior Medical lecturer; Obstetric & gynaecology Specialist in Medical & Health Science Faculty, Universiti Sains Islam, Malaysia; 55100, Kuala Lumpur; Malaysia (phone +603-4289 2400; fax:+603-4289 2477; e-mail: nurzaireena@gmail.com).

Azalea K is the medical officer in O&G Department in Ampang Hospital, Malaysia (e-mail azalea.khairuddin@gmail.com). Azirawaty T is trainee Medical officer O&G DepartmentUniversiti Sains Islam Malaysia (e-mail: gy_aaa@yahoo.com).

Jameela S is the consultant hematologist & Muralitharan G, consultant of Obstetric & gynaecology Department; both in Ampang Hospital, Malaysia (e-mail: jsathar@hotmail.com; drgmurali@yahoo.com)

beta0 thalassaemia, yet the clinical presentation is almost interchangeable from sickle cell anemia itself. Double heterozygote for HbS and HbC are known as HbSC disease where the clinical presentation may be intermediate in severity. *HbS/beta+ thalassaemia* is known to have between mild to moderate severity, but studies have shown that it varies between ethnic groups. The are other genotypes with very mild or subtle presentation include *HbS/hereditary persistence of fetal Hb (S/HPHP), HbS/HbE syndrome* and other rare combinations of HbS genotypes including HbD Los Angeles (Hb SD- Punjab), HbO Arab and G-Philadelphia [4]. Few case reviews reported wide variation among the major SCD due to the genotypic presentation and suggest looking at the detail phenotype presentation, while many focused on the adverse outcomes especially those pregnancy related [3]. Due to its uncommon presentation, most reports were retrospective over a period of years in which the management would differ from one case to another.

The evolving medical technology and advancement in current decades allows early diagnosis, prophylactic treatment and prevention of further complications. Multidisciplinary approach and combined care of these patients' results in better quality of life among SCD patients and longer life expectancy to the mid-50s [5]. Thus, allowing female patients to accomplish their obstetric carrier. Unfortunately, pregnancy itself is a risk factor for SCD patients due to its hypercoagulable state [4]. Physiological changes in pregnancy predisposes SCD patients to multiple maternal complication including recurrent miscarriages, preeclampsia, acute chest syndrome, deep vein thrombosis, recurrent pain crisis, recurrent infection and anemia with risk of blood transfusion [2]. The fetus is at risk of intrauterine growth restriction, intrauterine death, and prematurity which contributes to higher maternal and perinatal morbidity and mortality [1]-[3]. Thus, comprehensive care with multidisciplinary approach throughout gestation is required for reducing the risk to both mother and fetus.

II. Objective

The aim of this paper is to review the management practices of SCD patient during pregnancy and the maternal and neonatal outcome in Ampang Hospital, Malaysia over the last seven years. The discussion from this review is meant to improve the care between disciplines managing the patient throughout the gestation and post partum period.

III. Methods

All Sickle cell patients' records at the Hematology Clinic Ampang Hospital were reviewed retrospectively with their confidentiality preserved. Only pregnant patients with SCD under follow up over the last seven years (2009-2016) were reviewed for antenatal and post partum management practice. The maternal and fetal outcomes were compared and recorded.

IV. Reviewed Results

A. Case Reviews

Ampang Hospital situated in the state of Selangor, which is just a few blocks away from the capital city of Malaysia, Kuala Lumpur. The distribution of sickle cell patients in Malaysia were sparse and only found in a certain state. Throughout the seven years under review, seven sickle patients were under follow up of the Hematology Clinic, Hospital Ampang with three male and four female patients between the reproductive ages. Only three of the patients were pregnant under our care for the last seven years. Their pregnancies were monitored closely and outcomes were recorded with combine care between hematologist and obstetricians.

B. Genotype and Diagnosis

The first two patients, Indian ethnic in origin, had sickle cell anemia (HbSS disease) which was homozygous. Their diagnoses were made when they were young as they were closely related. The third patient was a young Malay ethnic with compound heterozygous for sickle Beta (β) thalassaemia with heterozygous Constant Spring. All their spouses were screened for haemoglobinopathies and were negative.

C. Antenatal Care

The first two patients were both in their third pregnancy and the third patient was a primigravidae. All three of them were seen early in the first trimester. The first and third patient were on oral hydroxyurea due to a recurrent bone crisis prior to the pregnancy, and the medication was stopped once the pregnancy was confirmed. All patients were given folic acid, penicillin V as prophylactic antibiotic, low dose aspirin and low molecular weight heparin for thromboprophylaxis. The third patient only received low dose aspirin, and they were counseled for adequate hydration and possible worsening pain crisis, risk of infections and worsening anemia throughout the pregnancy. All three of them were noted to be moderately anemic at antenatal booking visit yet clinically asymptomatic. The patients were referred early to the obstetric unit and they were seen frequently between 2 to 4 weekly alternating between obstetricians and hematologist. The maternal and fetal conditions were monitored closely for any possible complications.

The pregnancy in the second trimester for the second and third patients, seem to have progressed well. All of them managed to keep hemoglobin level above 8mg/dL. However, the first patient had a few episodes of painful bone crisis requiring regular opioids during the second trimester and was managed as an outpatient. While only the second patient managed to benefit detail fetal morphological scan as part of a prenatal screening. Otherwise all fetal growth was satisfactory during this gestation without evidence of growth restriction.

A stormier episode for these patients was recorded during the last trimester. The first patient was admitted for community acquired pneumonia with left parotitis at 31 weeks of gestation, followed with worsening haemolysis anemia. She recovered well with broad spectrum antibiotics and

phenotype-matched blood transfusion. Unfortunately, she was readmitted again at 37 weeks of gestation with another episode of worsening hemolytic anemia complicated with symptoms of obstructive jaundice. She was treated with exchange transfusion and subsequently went into labor. An emergency caesarean section was performed in view of two previous caesarean scars in labor and tubal ligation was performed as she completed her family.

The second patient presented with severe bone crisis at 35 weeks of gestation, whereby she was admitted, required an escalating dose of opioid drugs and managed by the anesthetic team. She was planned for exchange transfusion, yet there was no phenotypicly compatible blood available. Her thromboprophylaxis was continued together with good hydration. During this admission, fetal well-being was monitored and evidence of distress noted; thus, an emergency caesarean delivery was performed due to fetal compromise. The third patient was admitted at 33 weeks of gestation with a painful sickling bone crisis. During this admission, the patient was given opioid as analgesia, covered with low molecular weight heparin as thromboprophylaxis and broad spectrum antibiotics; she recovered well a few days later and her medications were continued. She presented again at completion of 37 weeks gestation with pre-labor rupture of the membrane, and was subsequently induced with prostaglandins. Unfortunately she did not progress, and therefore, caesarean section for obstetric indication was done. All surgeries were uncomplicated and there was no post partum hemorrhage.

D.Post Partum Care and Outcome

In view of the crisis events preceding the delivery, the first two patients were nursed closely in a high dependency unit for any possible worsening complication with combined care between the obstetricians, hematologist and anesthetic team. The hemoglobin was optimized with phenotype matched blood transfusion. Broad spectrum antibiotics and thromboprophylaxis were given. Adequate pain controls were ensured with opioids together with good hydration. The third patient recovered well post delivery and was discharged with antibiotics, thromboprophylaxis and adequate analgesia. Upon discharge, all patients were extensively counseled regarding contraception and planning for their future pregnancies and associated complications.

All the babies had good weight upon delivery between 2.8 kg to 3.3 kg and their APGAR scores in one minute were 9. The babies were nursed in the neonatal intensive care unit (NICU) as protocol for observation and discharged well. Subsequent hemoglobin screening of the babies revealed both HbSS disease patients had an HbS trait child, while the third patient with compound heterozygous for sickle Beta (β) thalassaemia with heterozygous Constant Spring child showed Beta (β) thalassaemia trait.

V.DISCUSSION

Despite SCD being commonly seen in some parts of the globe, it is still less common in South East Asian region. Yet more cases were reported and managed with growing expertise and advancement in medical technologies. Although there were few reported cases from Malaysia on sickle cell patients, growing expertise with interest and medical technologies has made the diagnosis possible, made it easily accessible and the management were up to date. Malaysia is unique in a way that it has large diversities and mixture of ethnical origin which may have different sets of inherited haemoglobinopathies [6]. A study by Lie-Injo LE et al. in 1986 revealed that a small population of Indian estate workers in Negeri Sembilan, Malaysia, which originates from Orissa, India had a higher frequency of HbS yet with milder symptoms and had longer life span up to 60 years of age. Among the 12 sickle cell anemia patients screened, all had alpha-thalassemia2 (alpha-thal2), either in the homozygous or heterozygous condition [7].

Pregnancy itself is a risk factor for sickle cell patients as increased thrombosis event and risk of infections due to the immunosuppressive state can lead to increased incidence of crisis, haemolysis, anemia and vaso-occlusive complications including eclampsia, cerebrovasular accidents, renal complications and acute bone pain [8]. The unborn fetus is at risk of recurrent miscarriages, second trimester loss, intrauterine growth restriction and even death due to severe placenta hypoxia following insufficient placenta blood flow. It is a vicious cycle where poor placental blood flow increases the risk of hypertensive disease in pregnancy and preeclampsia. Studies shows that on top of the above mentioned complication, there were increased risk of admission up to 60%, premature delivery, blood transfusions and operative delivery [3], [9].

Good preconception counseling is required for couples, with emphasis on the increased risk of morbidity and mortality to the patient and unborn child. This will ensure good compliance to medication as well as to frequent hospital visits, where medications will be reviewed. Unintended pregnancies among these patients result in increased risks both to the mother and fetus. This is because the maternal health was not optimized and they were unable to benefit the preconception counseling and optimizing their health prior to embarking on a new pregnancy. This is the case for two of the patients in this review, who were having unplanned pregnancies. They only found that they were in early pregnancy while on hydroxyurea and medication, which was subsequently stopped. It is recommended that hydroxyurea treatment be stopped three months prior to conception, due to the teratogenicity found in animal studies, and that the patient be started on folic acid at the same time. A level 3 ultrasonography is recommended to rule out fetal abnormality if exposed, yet termination is not recommended [1], [10], [11]. These patients were subsequently started with a low dose aspirin by 12 weeks gestation as they were considered as in the high risk group for developing preeclampsia in view of the disease pathophysiology; although there was no specific evidence [1], [12].

Yet, there were known increased risk associated with thromboembolic events which increases the risk of maternal

morbidity and mortality [3], [13]. Thus, adequate hydration, the use of appropriate graduated compression stockings and low molecular weight heparin, especially during admission are highly recommended [1], [14]. Pregnancy itself is an immunosuppressive condition and patients are more susceptible to infection then normal populations. Although infections were not the main cause of morbidity among pregnant SCD patients, evidence has shown that sepsis was among the cause of death of young children with SCD in Brazil [15]. For pregnant SCD women the risk of infection is higher and can easily deteriorate; consequently, further worsening the hemolytic anemia, as in our case review. Thus early and prompt management for risk of infection are crucial in reducing morbidity.

All the patients reviewed were anemic from the outset of the pregnancy and required multiple blood product transfusions at the later trimester. Although iron supplementation is generally recommended during pregnancy to reduce the incidence of anemia, it is only recommended for pregnant SCD patients if there is evidence of iron deficiency [1]. SCD patients were usually anemic but the severity and clinical presentation varies depending on their genotypes. Up to 50% of sickle cell anemia patients have received blood transfusions at some stage in their life [16]. Thus, blood transfusion is common and at times requires exchange transfusion due to the severe haemolysis. SCD patients are exposed to various antigens due to multiple blood transfusions. This is the main reason that the use of phenotype-matched blood is mandatory to reduce the risk of alloimmunozation and hemolytic transfusion reaction which can increase morbidity and mortality. Studies have shown that a patient who has received more than 10 transfusions throughout their life-time has a higher risk of developing alloimmunozation ($p=0.005$) [16]. Although previous studies show a decrease in maternal and perinatal morbidity with prophylactic blood transfusion, but it is now debatable as evidence of alloimmunization, delayed transfusion reactions, and possible transmission of infection and the risk of iron overload were higher [3], [17]. It is recommended to assess the patient clinically together with their hemoglobin levels as a guide, phenotype matched blood for transfusions and cytomegalovirus free infection [1].

A painful crisis is one of the major causes for admission of all SCD patients, similarly with the patients of this study. Studies have revealed that some 27% to 50% of SCD present with a painful crisis [18], [19]. However, it is very important to assess and determine the cause of pain as it could be due to more serious complications such as acute chest syndrome, sign of sepsis or another sickling event. The use of milder analgesia such as paracetamol and weak opioids between 12 weeks and 28 weeks of gestation is recommended on top of rest and adequate hydration [1]. However, in cases of more severe pain, the use morphines as stronger opioids are recommended with monitoring and combined care between the obstetrician, hematologist and anesthetist. The use of pethidine was strongly discouraged as evidence showed an increased risk of seizures [20].

All three patients delivered via emergency caesarean section due to the obstetric indications with combined care between multidisciplinary team management. Although the findings seem to agree with those of other studies that show increased risk of operative delivery among SCD patients, all the subjects of this study had uncomplicated outcomes. The babies had good birth weight upon delivery and a good APGAR score. Considering the observation number of this study was small, larger multicentered observation is recommended to be conducted. Post partum care is very crucial as patient should be closely monitored for further complications including risk of thromboembolism. Furthermore, these patients underwent a caesarean delivery and were already at risk prior to the delivery itself, and therefore, the use of low molecular weight heparin should be continued till six weeks post partum. Good post natal counseling on adequate hydration, contraception and family planning, compliance to subsequent follow up and medications should be emphasized. Screening for the risk of inheritance of the newborn child should be counseled and conducted between the hematologist and pediatric team. Close monitoring of the maternal and fetal well being with hematologists, obstetricians, anesthetist and neonatologist throughout the antenatal period and continuing to post partum care, and including the patients' family, should be conducted to ensure the best outcome for both mother and baby.

VI. Conclusion

Pregnancy with SCD is a high risk medical condition with increased risk of maternal and perinatal morbidity and mortality. However with growing expertise of the disease, good medical technology updates and healthcare services, SCD patients are able to reach live birth pregnancies. Yet, preconception counseling is very important, emphasizing on the increased risk of complications, the need of more frequent hospital visits and medications should be revised. Management throughout the gestation period includes adequate hydration, prompt treatment of infections with antibiotics, thromboprophylaxis coverage, adequate pain control, and phenotype-matched blood to reduce the risk of alloimmunization with combined multidisciplinary care between the hematologist, obstetricians, anesthetist, pediatricians and nursing staff is very crucial in achieving the best outcome. It is hoped that this multicenter review of SCD cases, the current management practices and maternal fetal outcomes will reflect a better picture of the management of this disease, which is uncommon in the region.

Acknowledgment

We thank staff in Hematology Unit, Obstetric & Gynecology Department, Ampang Hospital; Malaysia who indirectly help in reviewing the documents.

References

[1] Management of Sickle Cell Disease in Pregnancy. London: RCOG Green-top Guideline no. 61, July 2011, pp. 2-20.
[2] Resende Cardoso P. S, Lopes Pessoade Aguiar R. A, Viana M. B,

"Clinical complications in pregnant women with sickle cell disease: Prospective study of factors predicting maternal death or near miss," Revista Brasileira de Hematologia e Hemoterapia, vol.36, no.4, pp. 256-263, 2014.

[3] Silva-Pinto A. C, Ladeira S. O. D, Brunetta D. M., De Santis G. C, Angulo I. L, Covas DT," Sickle cell disease and pregnancy: Analysis of 34 patients followed at the Regional Blood Center of RibeirãoPreto, Brazil,"Revista Brasileira de Hematologia e Hemoterapia, vol. 36, no.5, pp. 329-333, 2014.

[4] Rees DC, Williams TN, Gladwin MT," Sickle-cell disease," Lancet, vol.376, no.9757, pp. 2018-2031, December 2010.

[5] Rogers DT, Molokie R, "Sickle cell disease in pregnancy,"Obstet Gynecol Clin North Am, vol.37, pp. 223-237, 2010.

[6] Rahimah A, Syahira LO, SitiHida, et al, "Haemoglobin Sickle D Punjab," Med J Malaysia, vol. 69, pp. 42-43, Feb 2014.

[7] Lie-Injo LE, Hassan K, Joishy SK, et al., "Sickle cell anemia associated with alpha-thalassemia in Malaysian Indians," Am J Hematol, vol.22, no.3, pp. 265-274, July 1986.

[8] Oteng-Ntim E, Meeks D, Seed PT, et al, "Adverse maternal and perinatal outcomes in pregnant women with sickle cell disease: systematic review and meta-analysis," Blood, vol.125, no.21, pp. 3316-3325, 2015.

[9] Leborgne-Samuel Y1, Janky E, Venditelli F, "Sickle cell anemia and pregnancy: review of 68 cases in Guadeloupe," J Gynecol Obstet Biol Reprod (Paris), vol.34, no.8, pp. 830, Dec 2005.

[10] Gye HW, Kei-ichi K, Eun JB, et al," Effects of prenatal hydroxyurea: treatment on mouse offspring," Experimental and Toxicologic Pathology, vol. 56, no. 1–2, pp. 1-7, Oct 2004.

[11] Diav-Citrin O, Hunnisett L, Sher GD, Koren G,"Hydroxyurea use during pregnancy: a case report in sickle cell disease and review of the literature," Am J Hematol, vol.60, no.2, pp. 148-150, 1999.

[12] National Institute for Health and Clinical Excellence. Hypertension in pregnancy. The management of hypertensive disorders during pregnancy. NICE clinical guideline 107. London: NICE; 2010

[13] Villers MS, Jamison MG, De Castro LM, James AH," Morbidity associated with sickle cell disease in pregnancy," Am J Obstet Gynaecol,vol.199, no.2 , pp.125, 2008.

[14] Royal College of Obstetricians and Gynaecologists, Reducing the risk of thrombosis and embolism during pregnancy and the puerperium. London, United Kingdom: Green-top Guideline, No. 379(a) , 2009

[15] Giovanna Abadia Oliveira Arduini, Letícia Pinto Rodrigues, "Mortality by sickle cell disease in Brazil," Rev Bras de Hematol Hemoter In Press, 2016.

[16] Patricia Costa,Alves Pinto et al, "Risk factors for alloimmunozation in patients with sickle cell anemia," Revista da Associação Médica Brasileira (English Edition), vol. 57, no. 6, pp. 654-659, Nov-Dec 2011.

[17] Howard RJ, Tuck SM, Pearson TC. Br," Pregnancy in sickle cell disease in the UK: results of a multicentre survey of the effect of prophylactic blood transfusion on maternal and fetal outcome," J Obstet Gynaecol, vol.102, pp. 947–51, 1995.

[18] Rajab KE, Issa AA, Mohammed AM, Ajami AA," Sickle cell disease and pregnancy in Bahrain," Int J GynaecolObstet, vol. 93, pp.171–175, 2006.

[19] Al Jama FE, Gasem T, Burshaid S, Rahman J, Al Suleiman SA, Rahman MS," Pregnancy outcome in patients with homozygous sickle cell disease in a university hospital," Arch GynecolObstet, vol. 280, pp. 793–797, 2009.

[20] Rees DC, Olujohungbe AD, Parker NE, Stephens AD, Telfer P, Wright J, " Guidelines for the management of acute painful crisis in sickle cell disease," Br J Haematol, vol. 120, pp.744–752, 2003.

Correlation between Fetal Umbilical Cord pH and the Day, the Time and the Team Hand over Times: An Analysis of 6929 Deliveries of the Ulm University Hospital

S. Pau, S. Volz, E. Bauer, A. De Gregorio, F. Reister, W. Janni, F. Ebner

Abstract**—**Purpose: The umbilical cord pH is a well evaluated contributor for prediction of neonatal outcome.

This study correlates nenonatal umbilical cord pH with the weekday of delivery, the time of birth as well as the staff hand over times (midwifes and doctors).

Material and methods: This retrospective study included all deliveries of a 20 year period (1994-2014) at our primary obstetric center. All deliveries with a newborn cord pH under 7,20 were included in this analysis (6929 of 48974 deliveries (14,4%)). Further subgroups were formed according to the pH (< 7,05; 7,05 – 7,09; 7,10 – 7,14; 7,15 – 7,19). The data were then separated in day- and night time (8am-8pm/8pm-8am) for a first analysis. Finally handover times were defined at 6am – 6.30 am, 2 pm -2.30 pm, 10 pm- 10.30 pm (midwives) and for the doctors 8-8.30 am, 4 – 4.30 pm (Monday- Thursday); 2pm -2.30 pm (Friday) and 9am – 9.30 am (weekend). Routinely a shift consists of at least three doctors as well as three midwives.

Results: During the last 20 years, 6929 neonates were born with an umbilical cord ph < 7,20 (< 7,05 : 7,1%; 7,05 – 7,09 : 10,9%; 7,10 – 7,14 : 30,2%; 7,15 – 7,19:51,8%). There was no significant difference between either night/day delivery (p = 0.408), delivery on different weekdays (p = 0.253), delivery between Monday to Thursday, Friday and the weekend (p = 0.496) or delivery during the handover times of the doctors as well as the midwives (p = 0.221). Even the standard deviation showed no differences between the groups.

Conclusion: Despite an increased workload over the last 20 years the standard of care remains high even during the hand over times and night shifts. This applies for midwives and doctors. As the neonatal outcome depends on various factors, further studies are necessary to take more factors influencing the fetal outcome into consideration. In order to maintain this high standard of care, an adaption of work-load and changing conditions is necessary.

Keywords**—**Delivery, fetal umbilical cord pH, day time, hand over times.

S. Pau is with University Ulm, Germany (e-mail: sabine.pau@uniklinik-ulm.de).

Efficacy of Preimplantation Genetic Screening in Women with a Spontaneous Abortion History with Eukaryotic or Aneuploidy Abortus

Jayeon Kim, Eunjung Yu, Taeki Yoon

***Abstract*—**Most spontaneous miscarriage is believed to be a consequence of embryo aneuploidies. Transferring eukaryotic embryos selected by PGS is expected to decrease the miscarriage rate. Current PGS indications include advanced maternal age, recurrent pregnancy loss, repeated implantation failure. Recently, use of PGS for healthy women without above indications for the purpose of improving in vitro fertilization (IVF) outcomes is on the rise. However, it is still controversial about the beneficial effect of PGS in this population, especially, in women with a history of no more than 2 miscarriages or miscarriage of eukaryotic abortus. This study aimed to investigate if karyotyping result of abortus is a good indicator of preimplantation genetic screening (PGS) in subsequent IVF cycle in women with a history of spontaneous abortion. A single-center retrospective cohort study was performed. Women who had spontaneous abortion(s) (less than 3) and dilatation and evacuation, and subsequent IVF from January 2016 to November 2016 were included. Their medical information was extracted from the charts. Clinical pregnancy was defined as presence of a gestational sac with fetal heart beat detected on ultrasound on week 7. Statistical analysis was performed using SPSS software. Total 234 women were included. 121 out of 234 (51.7%) underwent karyotyping of the abortus and 113 did not have the abortus karyotyped. Embryo biopsy was performed on 3 or 5 days after oocyte retrieval, followed by embryo transfer (ET) on a fresh or frozen cycle. The biopsied materials were subjected to microarray comparative genomic hybridization. Clinical pregnancy rate per ET was compared between PGS and non-PGS group in each study group. Patients were grouped by two criteria: karyotype of the abortus from previous miscarriage (unknown fetal karyotype (n=89, Group 1), eukaryotic abortus (n=36, Group 2) or aneuploidy abortus (n=67, Group 3)), and pursuing PGS in subsequent IVF cycle (pursuing PGS (PGS group, n=105) or not pursuing PGS (non-PGS group, n=87)). The PGS group was significantly older and had higher number of retrieved oocytes and prior miscarriages compared to non-PGS group. There were no differences in BMI and AMH level between those two groups. In PGS group, the mean number of transferrable embryos (eukaryotic embryo) was 1.3 □□0.7, 1.5 □□0.5 and 1.4 □□ 0.5, respectively (p = 0.049). In 42 cases, ET was cancelled because all embryos biopsied turned out to be abnormal. □In all three groups (group 1, 2, and 3), clinical pregnancy rates were not statistically different between PGS and non-PGS group (Group 1: 48.8 % vs. 52.2% (p=0.858), Group 2: 70% vs. 73.1% (p=0.730), Group 3: 42.3% vs. 46.7% (p=0.640), in PGS and non-PGS group, respectively). In both group who had miscarriage with eukaryotic and aneuploidy abortus, the clinical pregnancy rate between IVF cycles with and without PGS was not different. When we compare miscarriage and ongoing pregnancy rate, there were no significant differences between PGS and non-PGS group in all three groups. Our results show that the routine application of PGS in women who had less than 3 miscarriages would not be beneficial, even in cases that previous miscarriage had been caused by fetal aneuploidy.

Jayeon Kim is with the department of Obstetrics and Gynecology, Fertility Center of CHA Seoul Fertility Center, CHA University, Seoul, Korea (phone: 82-2-200-0300; fax: 82-2200-0427; e-mail: jayeon_kim@chamc.co.kr).

Eunjung Yu and Taeki Yoon are with the department of Obstetrics and Gynecology, Fertility Center of CHA Seoul Fertility Center, CHA University, Seoul, Korea.

***Keywords*—**Preimplantation genetic diagnosis, miscarriage, karyotyping, in vitro fertilization.

Primary Fallopian Tube Carcinoma: A Case Report

Mary Abigail T. Ty, Mary Jocelyn Yu-Laygo, Jocelyn Z. Mariano

***Abstract*—**This is a case of L.S.T., a 61 year old, G6P4 (3124) who presented with a one month history of intermittent, brownish, watery, non foul smelling vaginal discharge. There were no other accompanying symptoms. On rectovaginal examination, a palpable adnexal mass on the left was appreciated, with the lower border measuring 3 cm. The mass was non-tender, had irregular borders and solid areas. On transvaginal sonography, it revealed a left pelvic mass measuring 3 x 4 x 2 cm, with a Sassone score of 9. It had vascularization. The primary consideration was Ovarian Newgrowth, probably malignant in nature. CA-125 results were slightly elevated at 43.2 u/ml (NV: 0-35 u/ml). After intraoperative evaluation, the left fallopian tube was converted into a 9 x 4.5 x 3 cm bulbous cystic mass with solid areas. On cut section, the ampullary portion of the fallopian tube contained necrotic and friable looking tissues. Specimen was sent for frozen section and results revealed adenocarcinoma of the left fallopian tube. Patient subsequently underwent complete surgical staging with unremarkable post-operative course. The surgicopathologic diagnosis was G6P4 (3124) Fallopian tube serous cystadenocarcinoma stage 1.

The mean incidence of PFTC is 3.6 per million women yearly. This is associated with a generally low survival rate. The primary diagnosis is very difficult to establish because only 0–10% of patients suffering from PFTC are diagnosed pre-operatively. Symptoms play a very important role in the discovery of this disease, because there will be no presentation to the hospital without symptoms. The most common of which may be vaginal bleeding, abdominal pain, a palpable mass and ascites. A conglomerate of manifestations may be encountered, but not at all times. This is termed hydrops tubae profluens where there is presence of colicky pain with relief from intermittent passage of serosanguinous vaginal discharge. The significance of this report is to emphasize the rarity of the case and how the dilemma in the diagnosis is almost always present despite ancillary procedures.

***Keywords*—**Fallopian tube carcinoma, prognosis, rare, risk factors.

Dr. Mary Abigail T. Ty is currently a resident physician at the University of Santo Tomas Hospital under the Department of Obstetrics and Gynecology, Sampaloc, Manila, 1008, Philippines (phone: +639175200426; e-mail: m.abigailty@yahoo.com).

Dr. Mary Jocelyn Yu-Laygo is a practicing Obstetrician-Gynecologist at the University of Santo Tomas Hospital under the Department of Obstetrics and Gynecology, Sampaloc, Manila, 1008, Philippines (e-mail: mjyulaygo@yahoo.com).

Dr. Jocelyn Z. Mariano is a practicing Gynecologic Oncologist at the same institution. University of Santo Tomas Hospital, Sampaloc, Manila, 1008, Philippines (e-mail: jzmariano_325@yahoo.com).

Association of Maternal Age, Ethnicity and BMI with Gestational Diabetes Prevalence in Multi-Racial Singapore

Nur Atiqah Adam, Mor Jack Ng, Bernard Chern, Kok Hian Tan

Abstract**—**Introduction: Gestational diabetes (GDM) is a common pregnancy complication with short and long-term health consequences for both mother and fetus. Factors such as family history of diabetes mellitus, maternal obesity, maternal age, ethnicity and parity have been reported to influence the risk of GDM. In a multi-racial country like Singapore, it is worthwhile to study the GDM prevalences of different ethnicities. We aim to investigate the influence of ethnicity on the racial prevalences of GDM in Singapore. This is important as it may help us to improve guidelines on GDM healthcare services according to significant risk factors unique to Singapore.

Materials and Methods: Obstetric cohort data of 926 singleton deliveries in KK Women's and Children's Hospital (KKH) from 2011 to 2013 was obtained. Only patients aged 18 and above and without complicated pregnancies or chronic illnesses were targeted. Factors such as ethnicity, maternal age, parity and maternal body mass index (BMI) at booking visit were studied. A multivariable logistic regression model, adjusted for confounders, was used to determine which of these factors are significantly associated with an increased risk of GDM.

Results: The overall GDM prevalence rate based on WHO 1999 criteria & at risk screening (race alone not a risk factor) was 8.86%. GDM rates were higher among women above 35 years old (15.96%), obese (15.15%) and multiparous women (10.12%). Indians had a higher GDM rate (13.0 %) compared to the Chinese (9.57%) and Malays (5.20%). However, using multiple logistic regression model, variables that are significantly related to GDM rates were maternal age ($p < 0.001$) and maternal BMI at booking visit (p=0.006).

Conclusion: Maternal age ($p < 0.001$) and maternal booking BMI (p=0.006) are the strongest risk factors for GDM. Ethnicity per se does not seem to have a significant influence on the prevalence of GDM in Singapore (p=0.064). Hence we should tailor guidelines on GDM healthcare services according to maternal age and booking BMI rather than ethnicity.

Keywords**—**Ethnicity, gestational diabetes, healthcare, pregnancy.

Nur Atiqah Adam is with Duke-NUS Medical School, Singapore (e-mail: atiqahadam@u.duke.nus.edu).

Mor Jack Ng is with KK Women's and Children's Hospital, Singapore (e-mail: ng.mor.jack@kkh.com.sg).

Bernard Chern is with KK Women's and Children's Hospital, Singapore (e-mail: bernard.chern.s.m@singhealth.com.sg).

Kok Hian Tan is with KK Women's and Children's Hospital, Singapore (e-mail: tan.kok.hian@singhealth.com.sg).

Novel Hafnium and Samarium Hydroxyapatite Composites and Their Characterization

Meltem Nur Erdöl, Feyzanur Bayrak, Elif Emanetçi, Faik Nüzhet Oktar, Cevriye Kalkandelen, Oğuzhan Gündüz

Abstract**—**Nowadays, the bioceramic graft applications are very important due to the fact that especially European population is getting much older. Recent researches say that half of the population in Europe will be over 50-65 ages till the year 2050. Consequently, healing approaches for some health problems become more important in the near future. For instance, osteoporosis is one of the reasons for serious hip fractures. Beside these, the traffic accidents playing role increasing of various hip fractures and other bone fractures. Naturally all these are leading the importance developing new bioceramic graft materials. Hydroxyapatite (HA) is one of the leading bioceramics on the market. Beside the high biocompatibility HA bioceramics unfortunately are weak materials for loaded areas. For improvement mechanical properties of HA material, some oxides and metallic powders can be added. In the past studies, rare earth oxides like lanthanum oxide (La_2O_3) and cerium oxide (CeO_2) are added as reinforcement material in the matrix of the bioceramics. In this study, some rare earth oxides like hafnium (IV) oxide (HfO_2) and samarium (III) oxide (Sm_2O_3) are added to HA for improvement of their material characteristics. Thus, compression, microhardness and theoretical density tests are performed. X-ray diffraction patterns are also investigated corresponding x-ray diffraction equipment. At the end, studies of scanning electron microscope (SEM) and energy-dispersive x-ray spectroscopy (EDX) are completed. All values were compared with past BHA and various composites.

Keywords**—**Biocomposite, hafnium oxide, hydroxyapatite, nanotechnology, samarium oxide.

M. N. Erdol is with Bioengineering Department, Faculty of Engineering, University of Marmara, Goztepe Campus, 34722, Istanbul, Turkey (phone: +905378194927; e-mail: mnerdol@yahoo.com.tr).

F. Bayrak is with Bioengineering Department, Faculty of Engineering, University of Marmara, Goztepe Campus, 34722, Istanbul, Turkey.

E. Emanetci is with Bioengineering Department, Faculty of Engineering, University of Marmara, Goztepe Campus, 34722, Istanbul, Turkey.

F. N. Oktar is with Bioengineering Department, Faculty of Engineering, University of Marmara, Goztepe Campus, 34722, Istanbul, Turkey (e-mail: foktar@marmara.edu.tr).

C. Kalkandelen is with Biomedical Equipment Technology, Vocational School of Technical Sciences, İstanbul University, Avcilar Campus, 34320, Istanbul, Turkey.

O. Gunduz is with Metallurgical and Materials Engineering Department, Faculty of Technology, University of Marmara, Goztepe Campus, 34722, Istanbul, Turkey.

Process Optimization of Electrospun Fish Sarcoplasmic Protein Based Nanofibers

Sena Su, Burak Ozbek, Yesim M. Sahin, Sevil Yucel, Dilek Kazan, Faik N. Oktar, Nazmi Ekren, Oguzhan Gunduz

***Abstract*—**In recent years, protein, lipid or polysaccharide-based polymers have been used in order to develop biodegradable materials and their chemical nature determines the physical properties of the resulting films. Among these polymers, proteins from different sources have been extensively employed because of their relative abundance, film forming ability and nutritional qualities. In this study, the biodegradable composite nanofiber films based on fish sarcoplasmic protein (FSP) were prepared via electrospinning technique. Biodegradable polycaprolactone (PCL) was blended with the FSP to obtain hybrid FSP/PCL nanofiber mats with desirable physical properties. Mixture solutions of FSP and PCL were produced at different concentrations and their density, viscosity, electrical conductivity and surface tension were measured. Mechanical properties of electrospun nanofibers were evaluated. Morphology of composite nanofibers were observed using scanning electron microscopy (SEM). Moreover, fourier transform infrared spectrometer (FTIR) studies were used for analysis chemical composition of composite nanofibers. This study revealed that the FSP based nanofibers have the potential to be used for different applications such as biodegradable packaging, drug delivery and wound dressing, etc

***Keywords*—**Biodegradable packaging, electrospinning, fish sarcoplasmic protein, nanofibers.

S. Su is with the Metallurgical and Materials Engineering Department, University of Marmara, Goztepe Campus, 34722, Istanbul, Turkey(phone: +905413360550; e-mail: senasu@marun.edu.tr).

B. Ozbek is with the Metallurgical and Materials Engineering Department, University of Marmara, Goztepe Campus, 34722, Istanbul, Turkey (e-mail:ozbekbrk@gmail.com).

Y. M. Sahin is with Biomedical Engineering Department, University ofArel, Tepekent Campus, 34537, Istanbul, Turkey (e-mail: ymugesahin@arel.edu.tr).

S. Yucel is with Bioengineering Department, University of Yildiz Technical, Davutpasa Campus, 34220, Istanbul, Turkey (e-mail: syucel@yildiz.edu.tr).

D. Kazan is Bioengineering Department, Faculty of Engineering, University of Marmara, Goztepe Campus, 34722, Istanbul, Turkey (e-mail: dkazan@marmara.edu.tr).

F. N. Oktar is Bioengineering Department, Faculty of Engineering, University of Marmara, Goztepe Campus, 34722, Istanbul, Turkey (e-mail: foktar@marmara.edu.tr).

N. Ekren is Electric-Electronic Engineering Department, Faculty of Technology, University of Marmara, Goztepe Campus, 34722, Istanbul, Turkey (e-mail: nazmiekren@marmara.edu.tr).

O. Gunduz is with the Metallurgical and Materials Engineering Department, Faculty of Technology, University of Marmara, Goztepe Campus, 34722, Istanbul, Turkey (e-mail: oguzhan@marmara.edu.tr).

Different Types of Bismuth Selenide Nanostructures for Targeted Applications: Synthesis and Properties

Jana Andzane, Gunta Kunakova, Margarita Baitimirova, Mikelis Marnauza, Floriana Lombardi, Donats Erts

Abstract**—**Bismuth selenide (Bi_2Se_3) is known as a narrow band gap semiconductor with pronounced thermoelectric (TE) and topological insulator (TI) properties. Unique TI properties offer exciting possibilities for fundamental research as observing the exciton condensate and Majorana fermions, as well as practical application in spintronic and quantum information. In turn, TE properties of this material can be applied for wide range of thermoelectric applications, as well as for broadband photodetectors and near-infrared sensors. Nanostructuring of this material results in improvement of TI properties due to suppression of the bulk conductivity, and enhancement of TE properties because of increased phonon scattering at the nanoscale grains and interfaces. Regarding TE properties, crystallographic growth direction as well as orientation of the nanostructures relative to the growth substrate play significant role in improvement of TE performance of nanostructured material. For instance, Bi_2Se_3 layers consisting of randomly oriented nanostructures and/or of combination of them with planar nanostructures show significantly enhanced in comparison with bulk and only planar Bi_2Se_3 nanostructures TE properties.

In this work, a catalyst-free vapour-solid deposition technique was applied for controlled obtaining of different types of Bi_2Se_3 nanostructures and continuous nanostructured layers for targeted applications. For example, separated Bi_2Se_3 nanoplates, nanobelts and nanowires can be used for investigations of TI properties; consisting from merged planar and/or randomly oriented nanostructures Bi_2Se_3 layers are useful for applications in heat-to-power conversion devices and infrared detectors.

The vapour-solid deposition was carried out using quartz tube furnace (MTI Corp), equipped with an inert gas supply and pressure/temperature control system. Bi_2Se_3 nanostructures/nanostructured layers of desired type were obtained by adjustment of synthesis parameters (process temperature, deposition time, pressure, carrier gas flow) and selection of deposition substrate (glass, quartz, mica, indiumtin-oxide, graphene and carbon nanotubes).

Morphology, structure and composition of obtained Bi_2Se_3 nanostructures and nanostructured layers were inspected using SEM, AFM, EDX and HRTEM techniques, as well as homebuild experimental setup for thermoelectric measurements.

It was found that introducing of temporary carrier gas flow into the process tube during the synthesis and deposition substrate choice significantly influence nanostructures formation mechanism.

Electrical, thermoelectric and topological insulator properties of different types of deposited Bi_2Se_3 nanostructures and nanostructured coatings are characterized as function of thickness and discussed.

J. Andzane, G, Kunakova, M. Baitimirova, M. Marnauza, D. Erts are with the Institute of Chemical Physics, University of Latvia, LV-1586, Riga, Latvia (e-mail: jana.andzane@lu.lv, donats.erts@lu.lv).

F. Lombardi is with Department of Microtechnology and Nanoscience, Chalmers University of Technology, SE-41296, Göteborg,, Sweden (e-mail: floriana.lombardi@chalmers.se).

Keywords**—**Bismuth selenide, nanostructures, topological insulator, vapour-solid deposition.

An Introductory Study on Optimization Algorithm for Movable Sensor Network-Based Odor Source Localization

Yossiri Ariyakul, Piyakiat Insom, Poonyawat Sangiamkulthavorn, Takamichi Nakamoto

***Abstract*—** In this paper, the method of optimization algorithm for sensor network comprised of movable sensor nodes which can be used for odor source localization was proposed. A sensor node is composed of an odor sensor, an anemometer and a wireless communication module. The odor intensity measured from the sensor nodes are sent to the processor to perform the localization based on optimization algorithm by which the odor source localization map is obtained as a result. The map can represent the exact position of the odor source or show the direction toward it remotely. The proposed method was experimentally validated by creating the odor source localization map using three, four, and five sensor nodes in which the accuracy to predict the position of the odor source can be observed.

***Keywords*—** odor sensor, odor source localization, optimization, sensor network

I. Introduction

Olfaction is one of the important means for creatures by which they live and experience the world. For example, animals use olfactory cues to find food and identify its freshness, recognize individuals or conspecifics, avoid danger, and trigger mating behavior for sexual reproduction [1], [2]. Those successful examples have encouraged the development of odor sensors which can be used to detect the presence of odors and measure their intensities.

Due to the widespread of the study on odor sensing, the amount of researches in the field of odor source localization has also grown substantially [3]–[5]. The latter topic attracts research attention as it can be used for similar purposes to the examples in nature, for example, by realizing the accurate and reliable odor source localization system, it is possible to identify the position of the sources of fire [6], toxic gases leak [7], and pollutant gas emission [8]. It is also expected to be used for finding survivals under wreckages [9], explosive substances [10], and chemical weapons [11].

Existing method of odor source localization can be categorized into two main approaches: approach with mobile sensors which is also called active olfaction [12]–[14] and approach with stationary sensors [15].

The former utilizes one or more mobile robots equipped with odor and wind sensors to track down the odor plume with the moving direction based on the information of odor intensity gradient and wind direction obtained from the sensors until the robots reach the odor source. Due to the robot movement, this approach is robust against turbulence and complex odor intensity distribution. However, the result excessively relies on the movement of robot and environment. Moreover, it is particularly difficult to track down the instantaneous odor source [16].

The latter approach utilizes a network of the spatially distributed stationary sensors. Information of the odor intensities and wind direction obtained from each sensor are processed concurrently to identify the position the odor source. This approach can locate an instantaneous source remotely without the requirement to move the sensors. However, the drawback of this approach is that the emission rate of the odor source should be assumed to be unchanged and the result is strongly affected by the turbulence [16].

To overcome the limitations of the two main approaches, in this study, an optimization algorithm for the sensor network comprised of movable sensor nodes for odor source localization was proposed. While two and three sensor nodes were used in our previous work [17], three, four, and five sensor nodes were used in the experiment in this study. The localization results obtained from different arrangements of the sensor nodes were evaluated to investigate the validity of the proposed concept.

II. Methodology

A. Movable Sensor Network

The concept of using a movable sensor network proposed in this study is shown in Fig. 1. Each sensor node is comprised of an odor sensor, an anemometer, and a wireless communication module. The measurement data obtained from each sensor node are sent to the central processor via wireless communication by which the optimization algorithm is performed to determine the possibility to be the odor source position of each position throughout the area. After the processing, the sensor nodes will move into the direction toward the area with a lot of positions with high possibilities to be the emission source in an appropriate alignment. The movement, measurement, data sending, and processing are performed repetitively until the

Yossiri Ariyakul is with the Faculty of Engineering, King Mongkut's Institute of Technology Ladkrabang, Bangkok, Thailand (corresponding author, phone: +6699-219-6007; e-mail: yossiri.ar@ kmitl.ac.th).

Piyakiat Insom was with Faculty of Engineering, King Mongkut's Institute of Technology Ladkrabang, Bangkok, Thailand.

Poonyawat Sangiamkulthavorn was with Faculty of Engineering, King Mongkut's Institute of Technology Ladkrabang, Bangkok, Thailand.

Takamichi Nakamoto is with the Laboratory for Future Interdisciplinary Research of Science and Technology, Tokyo Institute of Technology, Kanagawa, Japan (e-mail: nakamoto@nt.pi.titech.ac.jp).

sensor nodes can localize the exact position of the odor source.

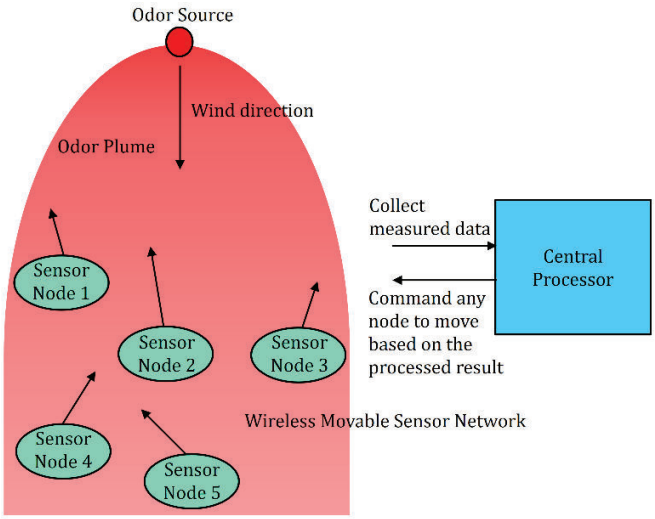

Fig. 1 Concept of odor source localization using movable sensor network

B. Odor Intensity Distribution Model

In the processing stage, the obtained measurement data from the sensor nodes are then compared with the gas distribution model to form the odor plume structure. The gas distribution in the real environment is complicated as the gas concentration and wind speed and direction at each position largely fluctuates due to air turbulence. However, in this introductory study, the air flow was assumed to be unidirectional, the time-averaged wind speed was assumed to be constant, and the wind turbulence was assumed to be isotropic and homogeneous for simplicity. Under these conditions, the gas concentration at each position can be calculated by using a relatively simple turbulent diffusion equation. If the gas source is located on the floor, the time-averaged gas intensity in two dimensions, C_0, at the point (x, y) is given by (1) [18]:

$$C_0(x,y)=\frac{2q}{4\pi K d_s}e^{-\frac{U}{2K}(d_s-\Delta x)} \tag{1}$$

where

$$d_s=\sqrt{(x_s-x)^2+(y_s-y)^2} \tag{2}$$

and

$$\Delta x=(x_s-x)\cos\theta+(y_s-y)\sin\theta \tag{3}$$

where q is the gas emission rate, K is the turbulent diffusion coefficient, U is the wind speed, θ is the angle from the x–axis to the upwind direction.

C. Odor Source Localization Technique Using Optimization

The optimization approach proposed in this study can be expected to identify the position of the odor source remotely based on the information obtained from sensor nodes. In this approach, an unconstrained nonlinear optimization technique [19] was used to adopt (1) so that the calculated result of the odor source position $(\hat{x}_s, \hat{y}_s)$, at which sum of the absolute value of intensity error between C_0 and C_i shown in (4) is minimum, when the sensor nodes were placed at (x_i, y_i), can be identified.

$$(\hat{x}_s,\hat{y}_s)=\arg\min_{x_{sa},y_{sa}}\sum_{i=1}^{N}\left|C_0(x_i,y_i:x_s,y_s)-C_i(x_i,y_i:x_{sa},y_{sa})\right| \tag{4}$$

where N is the number of sensor nodes, C_0 is the odor intensity at point (x_i, y_i) as a consequent of the actual odor source located at point (x_s, y_s), and C_i is the odor intensity at point (x_i, y_i) as a consequent of the assumed odor source located at point (x_{sa}, y_{sa}).

III. Experiments and Results

A. Odor Intensity Distribution Measurement

Even though robots were used to move the sensors [20] as the proposed concept is expected to be used for online measurement, the sensor nodes were moved manually in this study so that the alignment of the sensor nodes and its corresponding result can be focused. The sensor node used in this study comprises of a PID detector (ppbRAE3000, RAE System) and a thermal anemometer (ISA-12, Sibata). Even though the sensor nodes should work cooperatively via wireless communication, in this experiment the measured data was stored into a memory and they were sent to the processor manually. All processing in this study was performed using MATLAB 2015b on windows 10 platform.

In the experiment, an odor intensity and wind speed and direction at 41 specific positions in a closed room were measured by a PID detector and an anemometer. The dimension and actual appearance of the experimental area are shown in Fig. 2(a) and 2(b), respectively. The measurement points were demonstrated by the blue crosses. The odor source used in the experiment was situated on the floor. It was composed of a bubbler filled with 99.5% ethanol connected with an air pump and a flow meter. The flow rate was set to 9 L/min. A fan was used to create wind. The odor had been emitted for 2 minutes before the measurement started. The intensity measurement at each position was performed for 10 s. The time-averaged measured intensities from all 41 positions were then used to plot an odor intensity distribution. The plot was then processed by using linear interpolation to increase the data resolution from 71 cm to 1 cm. The obtained result is shown in Fig. 3.

As various parameters in the odor distribution model used in this study were assumed for simplicity, the evaluation of the validity of the simplified distribution model is required. The actual parameters in the experiment were substituted into (1) - (3) to form a plume model. The result of the calculation is shown in Fig. 4. Since the conformity of the measurement and calculation results can be observed, the validity of the simplified odor distribution model was confirmed.

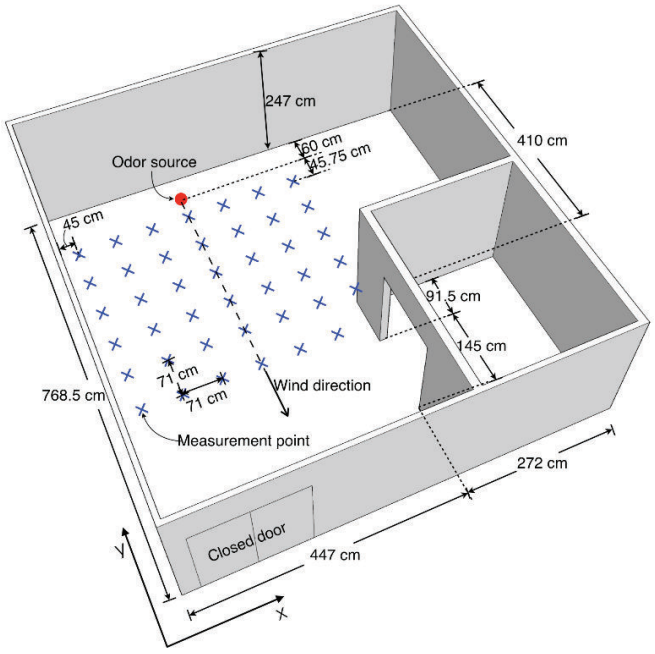

(a)

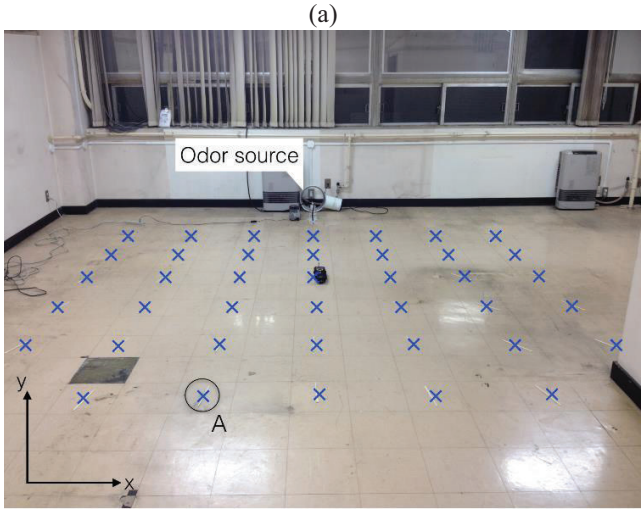

(b)

Fig. 2 (a) Dimension of the experimental area and (b) actual appearance of the experimental area

B. Odor Source Localization

Since the validity of the simplified odor distribution model used in this study was confirmed in the previous section, from this step, the spatial odor intensity distribution obtained from (1) was used as a raw data in the localization process. In this step, two sensor nodes were used and the odor source was placed at position (x_s, y_s) indicated by the red sphere in Fig. 2(a). A sensor node was fixed at position $A(x_1 = 142, y_1 = 0)$ indicated in Fig. 2(b) while another node was moved through all other position.

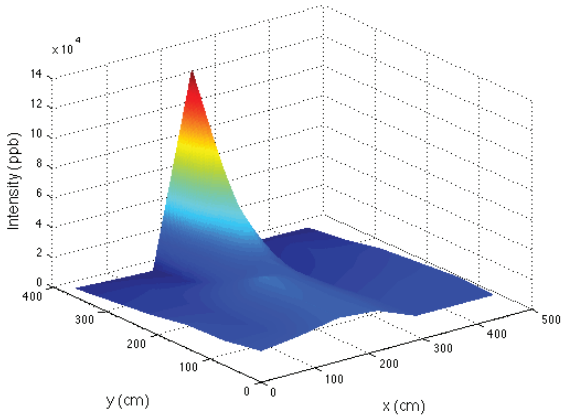

Fig. 3 Time-averaged spatial odor intensity distribution obtained from the measurement

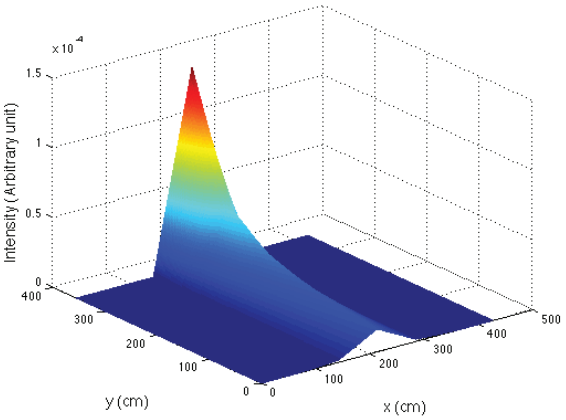

Fig. 4 Spatial odor intensity distribution obtained from (1)–(3)

Euclidean distance between the position of the actual odor source (x_s, y_s) and the calculated result of the odor source position $(\hat{x}_s, \hat{y}_s)$ in when the position of the second sensor node is varied was calculated. The summarized result is shown in Table I. Each row and column in the table corresponds with all positions indicated by blue spheres in Fig. 2.

According to the result, when the second sensor node was moved to some position, the zero Euclidean distance of the error can be observed. Therefore, it can be concluded that the proposed optimization technique can localize the position of the odor source accurately and remotely before reaching it if the sensor nodes in the network are situated at the proper positions.

TABLE I
EUCLIDEAN DISTANCE BETWEEN POSITION OF ACTUAL ODOR SOURCE AND CALCULATED RESULT OF ODOR SOURCE POSITION AT EACH POSITION OF SECOND SENSOR NODE WHEN FIRST SENSOR NODE IS FIXED AT POINT A (UNIT : %)

				X_2			
Y_2	17.556	17.556	17.556	15.720	17.556	17.556	17.556
	17.556	17.556	0	7.408	0	17.556	17.556
	17.556	17.556	0	0.001	0	17.556	17.556
	17.556	17.556	0	0	0	17.556	17.556
	17.556	17.556	0	0	0.01	17.509	17.556
	17.556	16.980	A	0	0	16.714	-

C. Investigation of Sensor Node Alignment

The previous section shows that the proposed optimization technique can be used to localize the position of the odor source accurately and remotely if the sensor nodes are situated at the proper positions. Therefore, suitable alignment of the sensor nodes was investigated in this section.

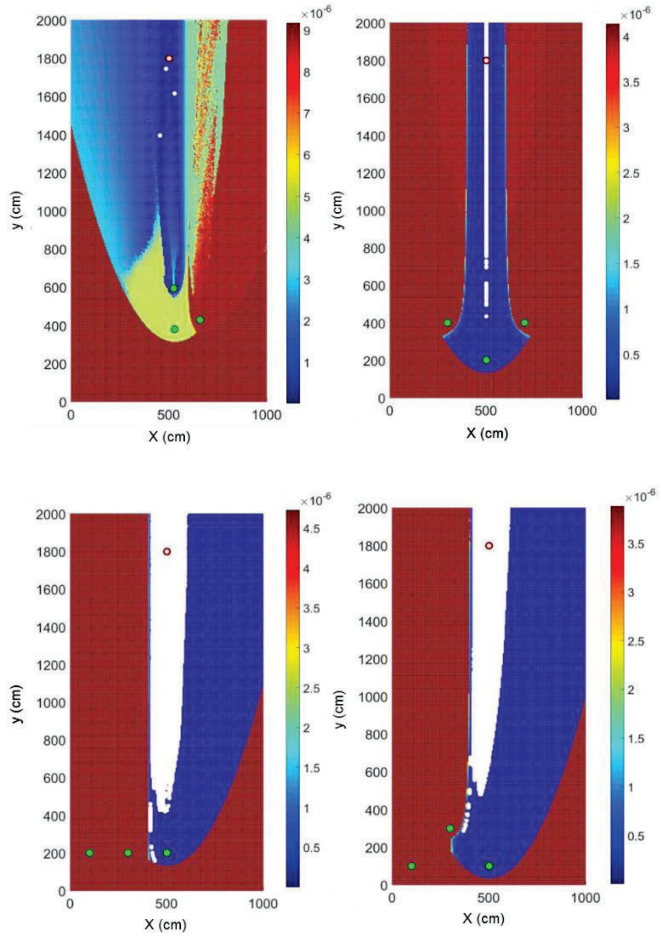

Fig. 5 The odor source localization maps obtained from optimization technique using three sensors with various alignments

In the experiment, (1) was used to calculate a spatial odor intensity distribution at 80,000 positions in the 10 x 20 m area. The calculated intensity distribution was used as a raw data in this step. The data resolution was 5 cm. The odor source was located at position $(x_s = 209, y_s = 520)$. Data obtained from the sensor nodes were then fitted into the equation using an unconstrained nonlinear optimization technique to reach for optimal K and q.

Sum of the absolute value of intensity error between the intensity at the sensor node position as a consequent of the actual odor source located at point and the intensity at the sensor node position as a consequent of the calculated result of the odor source position while the position of was varied through all 80,000 positions in the area were calculated as in (5)–(6) to create an odor source localization map which shows the possibility to be the odor source of any positions in the whole area.

$$\left(\hat{q},\hat{K}\right) = \arg\min_{q_a,K_a} \sum_{i=1}^{N} \left| C_0(x_i, y_i : x_s, y_s : q, K) - C_i(x_i, y_i : \hat{x}_s, \hat{y}_s : q_a, K_a) \right| \quad (5)$$

$$\Delta C = \sum_{i=1}^{N} \left| C_0(x_i, y_i : x_s, y_s : q, K) - C_i(x_i, y_i : \hat{x}_s, \hat{y}_s : q_a, K_a) \right| \quad (6)$$

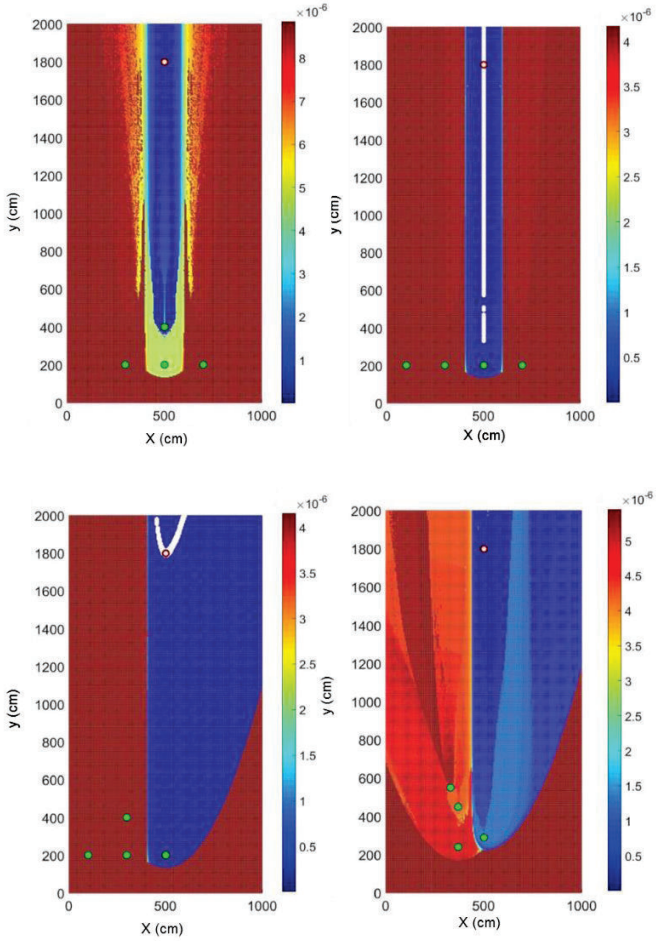

Fig. 6 The odor source localization maps obtained from optimization technique using four sensors with various alignments

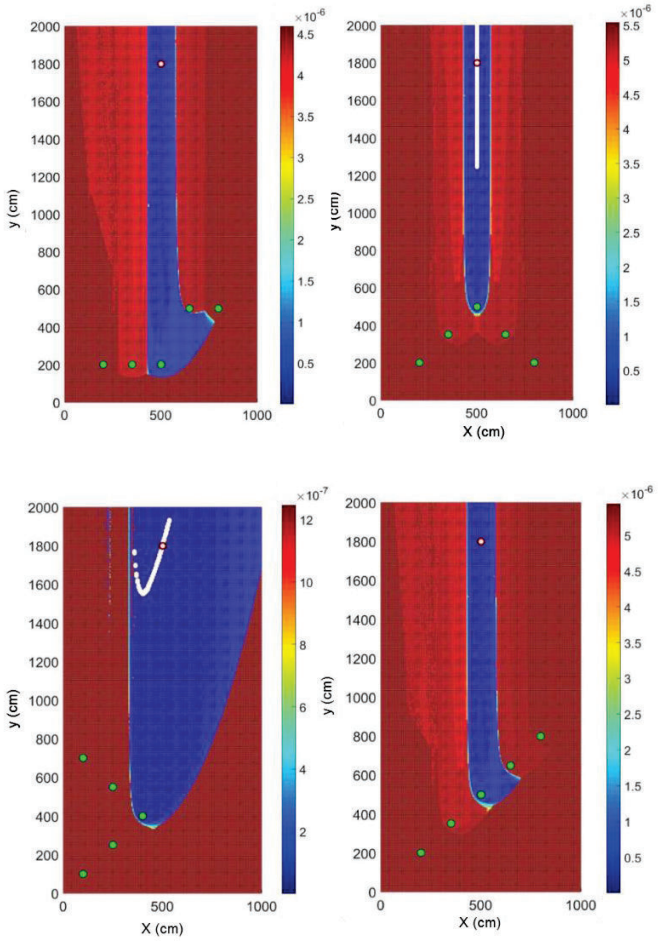

Fig. 7 The odor source localization maps obtained from optimization technique using five sensors with various alignments

In the experiment, three, four, and five sensor nodes were used and their placement were varied. The result of odor source localization maps in various alignment are shown in Fig. 5–7 in which the wind travels in opposite direction with y–axis, the position of the actual odor source is demonstrated by the red sphere, and positions of the sensor nodes are demonstrated by the green spheres, respectively.

In the map, the positions with high possibility to be the odor source are colored dark blue. The positions with lower possibility to be the odor source are colored light blue, green, light green, yellow, orange, and red, respectively. The positions with highest possibility to be the odor source are colored white.

According to the result, the odor source localization map which shows the possibility to be the odor source of any positions in the whole area can be realized. The white area becomes smaller when the number of sensor node is increased. Thus, it can be concluded that using four sensor nodes can obtain more accurate result than using three nodes and the accuracy can be more slightly increased if the number of sensor nodes is increased to five. The accuracy of the obtained results was improved from our previous work [17] in which two and three sensor nodes were used two and three sensor nodes were used

Moreover, it can be observed that the more sensor nodes are in the exact downwind direction from the odor source, the more accurate result can be obtained**.** However, even though the sensor nodes are slipped from the exact downwind direction from the odor source, the odor source localization map still shows the roughly direction to which the sensor nodes should be moved. Thus, by repetitively perform the movement, measurement, data sending, and optimization process, the sensor nodes are expected to be able to eventually localize the exact position of the odor source.

IV. Conclusions

The approach of using optimization technique for sensor network composed of movable sensor nodes which can be used for remote odor source localization was proposed. The information of odor intensity obtained from the sensor nodes are processed by optimization algorithm to create the odor source localization map which shows the possibility to be the odor source of the position throughout the area so that the exact position of the odor source can be localized or the direction toward the odor source can be demonstrated. In the latter case, the process will be performed repetitively until the exact position of the odor source can be identified. The effectiveness of the proposed method in 10 x 20 m area was verified.

The experimental result shows that the accuracy of the proposed concept can be improved by increasing the number of sensor nodes. However, since the processing time also considerably increases in accordance with the added number of sensor nodes, the optimized number of the nodes is required to be investigated further for practical usage. Furthermore, even though an aim of this study is to overcome the drawbacks of the conventional methodologies, the emission rate of the odor source and wind related parameters in this study was still assumed to be unchanged as it is still in introductory stage.

In the next study, the odor source localization under plume fluctuation and the algorithm to determine the movement procedure based on the obtained odor source localization map will be investigated.

References

[1] J. Murlis, "Odor plumes and how insects use them," in *Annual Review of Entomology*, vol. 37, 1992, pp. 505–532.

[2] Gabrielle A. Nevitt, "Sensory ecology on the high seas: the odor world of the procellariiform seabirds," in *The Journal of Experimental Biology*, vol. 211, 2008, pp. 1706–1713.

[3] Jatmiko W, Jovan F, Dhiemas R.Y.S, T. Fukuda, and K. Sekiyama, "Robots implementation for odor source localization using PSO algorithm," in *WSEAS Transactions on Circuits and Systems*, vol. 10, no. 4, 2011, pp. 1706–1713.

[4] Chen Liwei and Yang Jianhua, "Experimental study on odor source localization system based on metal oxide gas sensors," in *Third International Conference on Measuring Technology and Mechatronics Automation*, 2011.

[5] Ahmet Kuzu, Metin Gokasan, and Seta Bogosyan, "Novel approach for detection and tracking of explosive carrying mobile humans with odor-sensor based multisensor networks," in *WSEAS Transactions on Systems and Control*, vol. 3, no. 2, 2008, pp. 63–70.

[6] Y. Takei, T. Fuma, H. Kawai, M. Uneda, H. Nanto and S. Koyama, "Odor source localization for early fire detection by using MOS-type gas sensor," in *ECS Transactions*, vol. 16, no. 11, 2008, pp. 325–329.

[7] Matthias Bartholmai and Patrick Neumann, "Micro-drone for gas measurement in hazardous scenarios via remote sensing," in *Proceedings of the 6th WSEAS International Conference on Remote Sensing*, 2010, pp. 149–152.
[8] X. Yang, J. Du, S. Liu, R. Li, and H. Liu, "Air pollution source estimation profiling via mobile sensor networks," in *International Conference on Computer, Information and Telecommunication Systems (CITS)*, 2016, pp. 1–5.
[9] B. Lorena Villarreal, Christian Hassard, and J. L. Gordillo, "Finding the direction of an odor source by using biologically inspired smell system," in *Advances in Artificial Intelligence – IBERAMIA*, 2012, pp. 511–560.
[10] V. N. Christopoulos and S. Roumeliotis, "Multi robot trajectory generation for single source explosion parameter estimation," in *Proceedings of the IEEE International Conference on Robotics and Automation*, 2005, pp. 2803–2809.
[11] Z. Liu and T. F. Lu, "Multiple robots plume-tracing in open space obstructed environments," in *IEEE International Conference on Robotics and Biomimetics (ROBIO)*, 2009, pp. 2433–2439.
[12] Ishida H., Nakamoto T., Moriizumi T., "Remote sensing and localization of gas/odor source and distribution using mobile sensing system," in *International Conference on Solid-state Sensors and Actuators*, 1997, pp. 559–562.
[13] Nakamoto T., Ishida H., Moriizumi T., "Active odor sensing system," in *Proceeding of the IEEE International Symposium on Industrial Electronics and Actuators*, 1997, pp. 128–133.
[14] Li Jigong and Cui Shigang, "Limitation of a mobile robot and methodology of tracing odor plume in airflow environments," in *Procedia Engineering*, 2011, pp. 1041–1045.
[15] Matthes J, Groll L, Hubert B K., "Optimal weighting of networked electronic noses for the source localization," in *Proceedings of the Systems Communications*, 2005.
[16] Lei Yang, Junbao Zheng, Jingbo Chen, and Yaming Wang, "Review of odor source localization robot based on bionic olfaction," in *Applied Mechanics and Materials*, vol. 462–463, 2014, pp. 750–754.
[17] Y. Ariyakul, T. Nakamoto, T. Onodera, and K. Toko, "Simulation of sensor network for odor source localization using numerical optimization technique," in *IEEJ Sensors and Micromachines (E)*, 2014.
[18] Hiroshi Ishida, Takamichi Nakamoto, and Toyosaka Moriizumi, "Remote sensing of gas/odor source location and concentration distribution using mobile system," in *Sensors and Actuators B: Chemical*, vol. 49, no. 1, 1998, 52–57.
[19] J. Kowalik and M.R. Osborne, *Methods for Unconstrained Optimization Problems*. Elsevier, 1968.
[20] Takamichi Nakamoto, Hiroshi Ishida, and Toyosaka Moriizumi, "A sensing system for odor plumes," in *Analytical Chemistry News and Features*, vol. 4, no. 7, 1999, 531A–537A.

Hand Controlled Mobile Robot Applied in Virtual Environment

Jozsef Katona, Attila Kovari, Tibor Ujbanyi, Gergely Sziladi

***Abstract*—**By the development of IT systems, human-computer interaction is also developing even faster and newer communication methods become available in human-machine interaction. In this article, the application of a hand gesture controlled human-computer interface is being introduced through the example of a mobile robot. The control of the mobile robot is implemented in a realistic virtual environment that is advantageous regarding the aspect of different tests, parallel examinations, so the purchase of expensive equipment is unnecessary. The usability of the implemented hand gesture control has been evaluated by test subjects. According to the opinion of the testing subjects, the system can be well used, and its application would be recommended on other application fields too.

***Keywords*—**Human-machine interface, hand control, mobile robot, virtual environment.

I. Introduction

HUMAN-machine relationships mean the interaction between users and different devices, most likely computers, where the tool of connection between human and computer is the User Interface (UI), which contain both the software and the hardware. The human-machine interaction examines the human and the computer together.

The usability of devices used nowadays is more important than features available in them, furthermore, the creation of such control panels, like human-computer interfaces (HCI) are getting more and more important, overshadowing features more emphasized in the past.

The proper design of human-machine interaction may still have its limits, even unwanted misunderstandings might occur, so interface designers need to create such multimodality computer systems and interfaces that help minimizing these misunderstandings, and that are easier-to-use, their usage can be learnt without professional knowledge, achieving the smooth handling of interfaces. As a summary, in the future, the design of such an interface would be important, such that can be integrated into devices and enable good handling; nowadays, we still do not have a universal solution.

In order to solve the problem, human-machine interface based solutions are at the centre of researches on such crucial areas like modernization of nuclear power plants and improvement of their security [1]-[3], supporting the everyday life of disabled people by the remote control of equipment [4]-[7], control of vehicles even in real-time by remote control [8]-[10], and solving simulation tasks [11]. Besides that, we can also meet that on such fields, like the Internet of Things [12], or virtual reality [13], [15].

The reason for the research is to create such a human-machine interface based test system, which is able to move a mobile robot by gesture control. For achieving the goals of the research, the so-called Leap Motion gesture controller unit, having been developed by Leap Motion Inc. since 2010, was applied, and an interactive 'native' graphic programming environment, the Robotino View, the Robotino Sim Demo simulation software, that realistically models the motion of a mobile robot in a virtual 3D environment [16], [17], a self-developed software that processes, evaluates and transforms data arriving from the gesture controller unit into the information required to move the mobile robot. The developed virtual test environment also has many opportunities for educational aspects [18], [19]. At the end of the article, the evaluation of the usability of the designed test environment, and conclusions made from the results are published.

The article presents an attempt to integrate independently implemented software artifacts into one system, using existing parts: Leap Motion controller and Festo Robotino mobile robot device. Data from Leap Motion is used to navigate the Festo Robotino mobile robot.

II. Applied Devices and Technologies

In order to comply with the requirements of the research, modern architecture devices and technologies have been applied and introduced in detail below.

A. Leap Motion

There are several working analogical motion sensing solutions such as the Kinect, and the Xtion Pro gesture recognition could be comfortable, but these devices focus more on body action.

The Leap Motion Inc. has been developing the so-called Leap Motion controller since 2010, whose goal is to reform human-computer interaction; moreover, the Leap Motion is small, and has low power dissipation and high precision [14].

The Leap Motion can serve as an excellent replacement of Kinect as a fast development opportunity for desktop applications of motion sensing technology.

B. System's Design

The control unit's design is a rounded aluminum cuboid, equipped with glossy black cover and rubber sole, its size is

Jozsef Katona is with the University of Dunaújváros, Dunaújváros, CO 2400 Hungary (corresponding author, phone: +3625-551-605, e-mail: katonaj@uniduna.hu).

Attila Kovari, Tibor Ujbanyi and Gergely Sziladi are with the University of Dunaújváros, Dunaújváros, CO 2400 Hungary (e-mail: kovari@uniduna.hu, ujbanyit@uniduna.hu, sziladig@uniduna.hu).

The project is sponsored by EFOP-3.6.1-16-2016-00003 founds, Consolidate long-term R and D and I processes at the University of Dunaujvaros.

smaller than an average computer mouse, it is approximately eight centimeters long. (Fig. 1) Thanks to the rubber sole, it sticks well on the table, and thus, there is no need to be concerned that the detector's own cable grabs it from its position.

Fig. 1 The 3-inch Leap Motion Controller with a glossy black face complimented by a smooth silver bezel

C. Communication from Leap Motion to Computer

The device connects to the computer via a USB 3.0 port, which provides its power supply and data exchange. The control unit's minimum system requirements contain AMD Phenom II or Nehalem architecture Intel processor and 2 gigabytes of RAM.

D. Operation Principle

The system applies three infrared LEDs and two monochrome infrared cameras to detect infrared light reflected from the hands, at 300 fps speed, they cover an approximately 1 meter diameter, almost semi-sphere shaped area, and the device can record not only the motion of our hand, but also the motion of each finger separately, so a computer can be controlled by smooth motoric motion.

The Leap Motion examines the environment on a much smaller area, but at a much higher resolution, thus enabling the separate tracking of fingers. If we perform hand and finger motions on the covered area, the system will recognize that as some kind of spatial position data, and execute the orders rendered to the gesture. The detector forwards the taken images to the computer, where the Leap Motion software processes the images of the two cameras by mathematical algorithms, so from the 2D sources, it can calculate 3D values regarding image position, this way managing the control. The program related to the device can be downloaded from the manufacturer's website, and following installation, Leap Motion can be used within minutes. Following the first switch on, the program guides through the basics of control, holding our hand above the detector, we can see its wireframe on the display, or we may draw by moving our fingers in the air (Fig. 2).

Fig. 2 Motion-controlled

E. Festo Robotino

Festo Robotino is a mobile robot system manufactured by Festo, which plays a major role in several researches. In Fig. 3, the Robotino itself is shown.

Fig. 3 Festo Robotino mobile robot

The completely functional mobile robot's central control unit is an embedded PC and a CompactFlash card, on which the Linux operation system specialized for the robot and the controller programs can be found. The control unit can be reached via Wireless LAN. The basics of controlling to all directions is enabled by the so-called omnidrive, which consists of three separate omni wheels placed into 120° angles, driven by a DC motor controlled by the omnidrive unit. Its advantage is that the robot is able to move from a specific starting point on any tracks, even rotating around itself. The omnidrive has got three inputs:

1) Vx [mm/s] (float) velocity;
2) Vy [mm/s] (float) velocity;
3) angle rotation velocity – omega [deg/s] (float), and three outputs, that define the velocity of each motor.

The block controlling the velocity of the motors controls the acceleration and brake of each motor using PID control.

The Robotino is equipped with several sensors, such as rubberized collision detector, infrared distance detector, encoder, VGA resolution camera, but it can be upgraded with any kind of sensors via the digital and analog I/O interface, or any other peripheries. The Robotino can be programmed in C++-ban, JAVA, .Net, MATLAB, but can be controlled in LabVIEW, or Robotino View programs. If properly programmed, it can autonomously perform the tasks.

F. Robotino View

The Robotino View (Fig. 5) is an interactive 'native' graphic programming environment, which is provided by Festo for the robot; it has got a user-friendly GUI and can be easily learnt through pre-defined examples.

The program can be downloaded for free from Festo's Didactic website. In the function block development environment control, image processing, logic, vector-algebra etc. objects are available, enabling complex control. In the Robotino View program, both blocks supporting image processing, oscilloscope and objects required for monitoring and controlling the change of detected signals in time are available. Instruction blocks may be executed sequentially (after each other) or iterated (repeatedly), and the execution of

the instruction depending on selection condition is also possible.

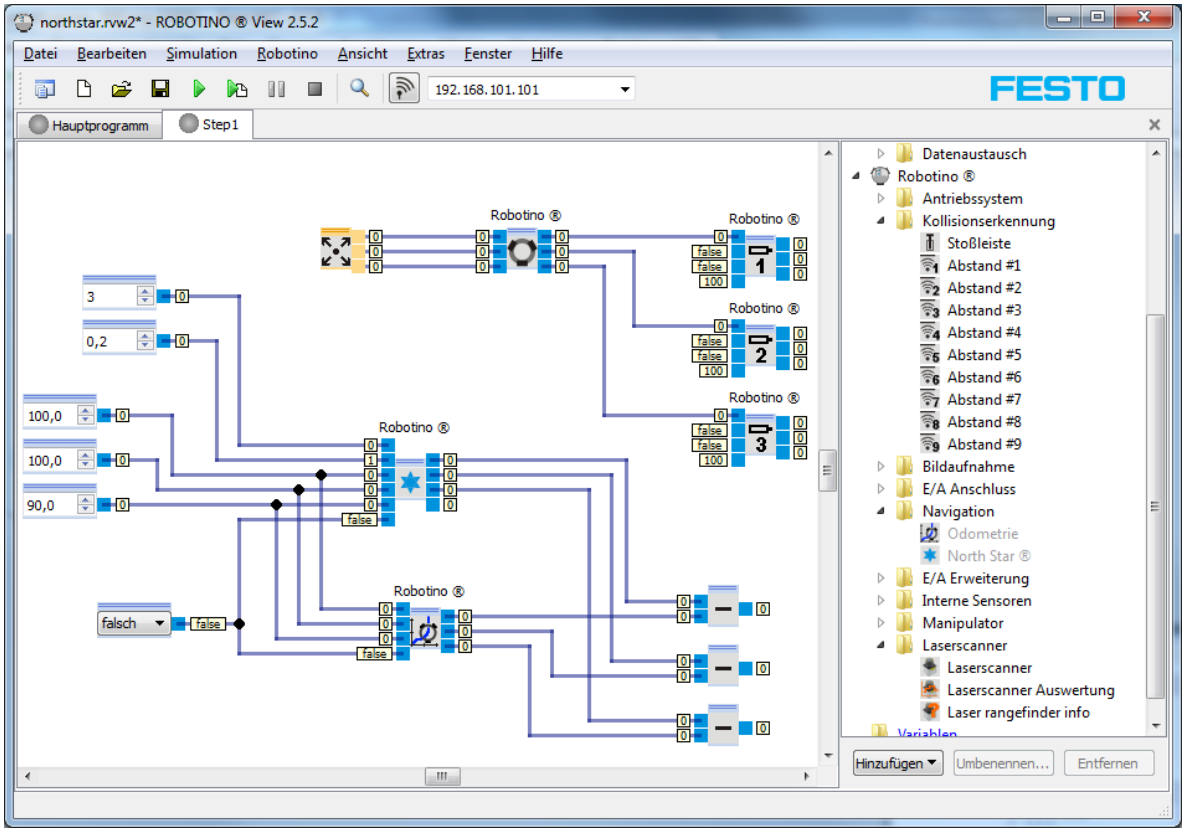

Fig. 4 Robotino View

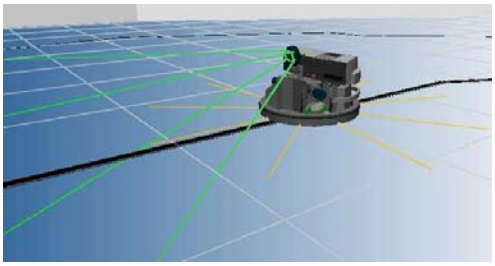

Fig. 5 Robotino Sim Demo

The program has two view options; the first one is the so-called “Subprogram view”. Here we have to work with such components that control each task of the robot (e.g. motion, reception of built-in detectors, camera image processing etc.). The second view is the so-called “Main program view”, where we can provide the quit conditions and execution sequences of different sub-programs. The development environment enables creating a data connection from external program via TCP/IP and UDP connection.

G.Robotino Sim Demo

The Robotino® Sim (Fig. 5) is a robot simulation software that realistically models the robot’s motion in virtual 3D environment, which can be very useful during several developments. The Robotino simulation model contains everything as the real robot. In order to properly use the software, we need a video card with at least 128 MB RAM, supporting OpenGL.

III. Implementation the Mobile Robot Control Software

Among the goals described in the introduction, development of such an application can be found that enables the navigation of the Festo Robotino mobile robot by Leap Motion based hand gesture control. The implementation of data processing application has been made by C# high-level program language, while the application enabling the motion of the mobile robot in virtual environment according to evaluated data has been implemented in the Robotino View development environment.

The Leap Motion SDK specifies how and under what conditions they have received the data coming from the Leap Motion control unit. Using the official SDK and the driver of Leap Motion we were able to specify how process data provided by device control unit. The device sends hand action information periodically while it is turned on. Packages information is called a frame. With sensor information ID for instance Frame::hand() and Frame:finger() functions can be used or override if necessary. UDP server was used to forward the data to Robotino View for further processing.

A. Design

Following requirement definition, we created the software structures, data structures and algorithm descriptions to be implemented. The planning was not performed sequentially, so step-by-step, but in an iterative way, several versions were developed, and we were making continuous backsteps to correct former plans. To design the logic plan, we chose an easy-to-read and follow flow chart, while the UML (Unified Modelling Language) supporting object-oriented paradigm was applied in planning static and dynamic components in time. As the end-result of the planning process, such algorithms and data structures to be implemented became available - whose application enabled the effective production of application code.

B. The Application's Logic Plan at a Glance

As the first step of the planning, the system's logic plan was made using flow chart, as shown in Fig. 6.

C. The Application's Static UML Class Chart (Detail)

To create the static model, we applied the most commonly used chart type in UML, the class chart, where we showed the system components static items, and thus, we could easily examine static items during running the application. The simplified class chart of the application can be read in Fig. 7.

D. Implementation

The application's implementation performed during implementation and integration according to formerly created plans, in C# program language, in the Microsoft Visual Studio software development environment. The application runs in the background, for its current functionality, no control panel is necessary.

Integration is one of the important phases of development, when independently implemented and tested program parts are assembled into a complete system.

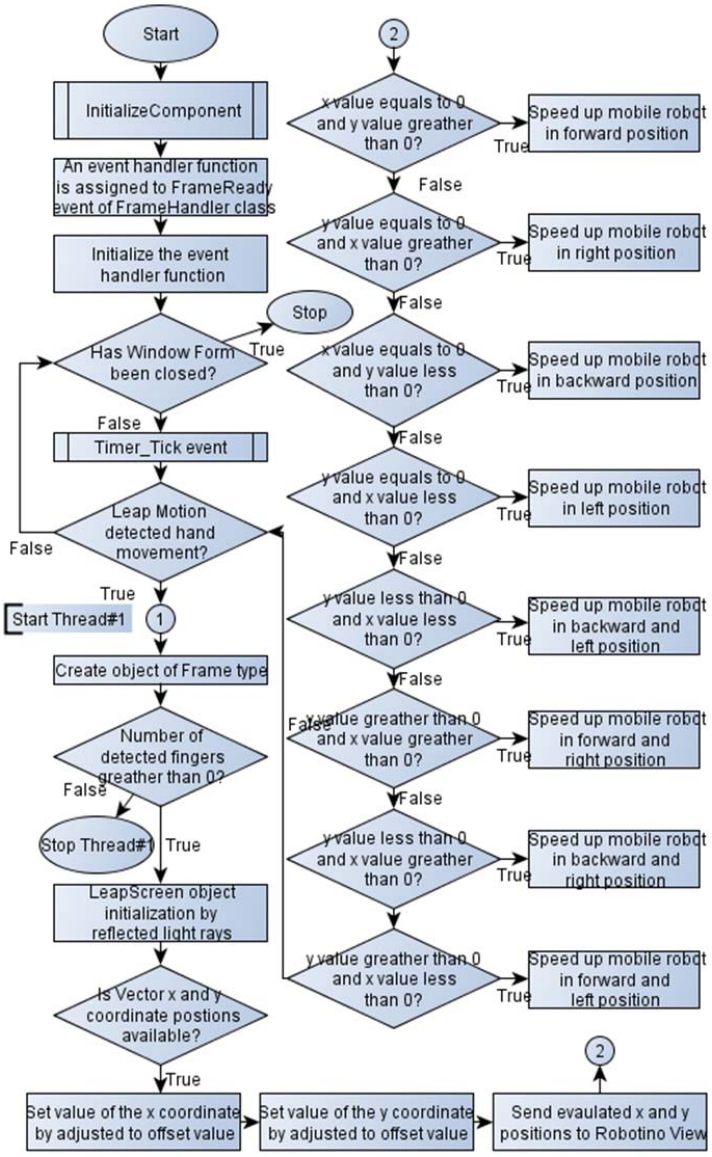

Fig. 6 The system's logic plan at glance

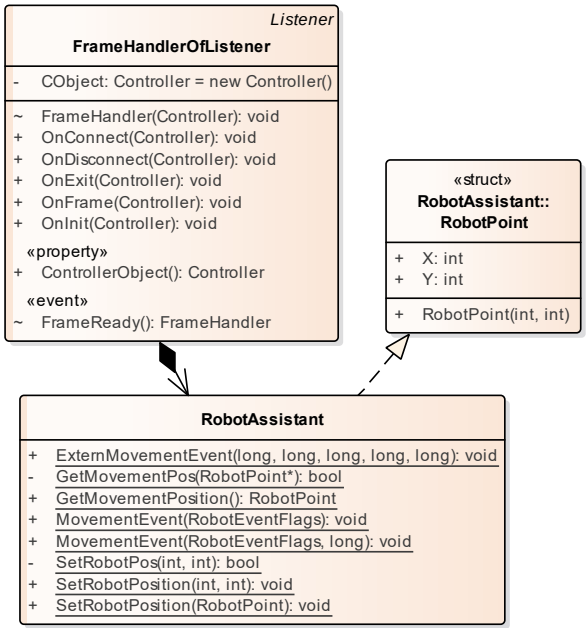

Fig. 7 The application's static UML class chart (part)

The now implemented application is built up from seven classes that are placed in one project. In the project, the addition of the so-called LeapCSharp.NET.3.5 DLL file as a reference was inevitable to manage data provided by the Leap Motion hardware. Furthermore, the DLL file embedded into the code base as a name space contains such class and function libraries already written by the manufacturer of the Leap Motion device that strongly support development. Following making the code base, the test environment was being tested.

IV. Results

The students were asked to fill in a questionnaire about the system. An eight-question survey was administered to students to elicit their opinion of the system, using a five-point Likert-type scale of "A": Strongly Agree; "B": Agree; "C": Unsure; "D": Disagree; and "E": Strongly Disagree).

In the examination of the implemented test environment, 14 test subjects participated, who were university students between the age of 18 years and 25 years.

Fig. 8 gives the mean of the results for each question, as asked of the university students. The students were asked about their experiences regarding the implemented system. Based on the answers given for the questions, it can be stated that the opinion of students about the implemented system and the gesture handle technology was very positive. In their opinion, the system was interesting, it helped them to use and learn the basics of Leap Motion to navigate a mobile robot. The system topic was interesting to 85% of the asked students and 100% strongly recommended that the grasping gesture should be adapted to different applications.

In the beginning of the testing, we asked the students to rate the system's usability on a scale ranging from 1 to 5, then repeat that after practicing for about 10-15 minutes. The result is shown on Table I.

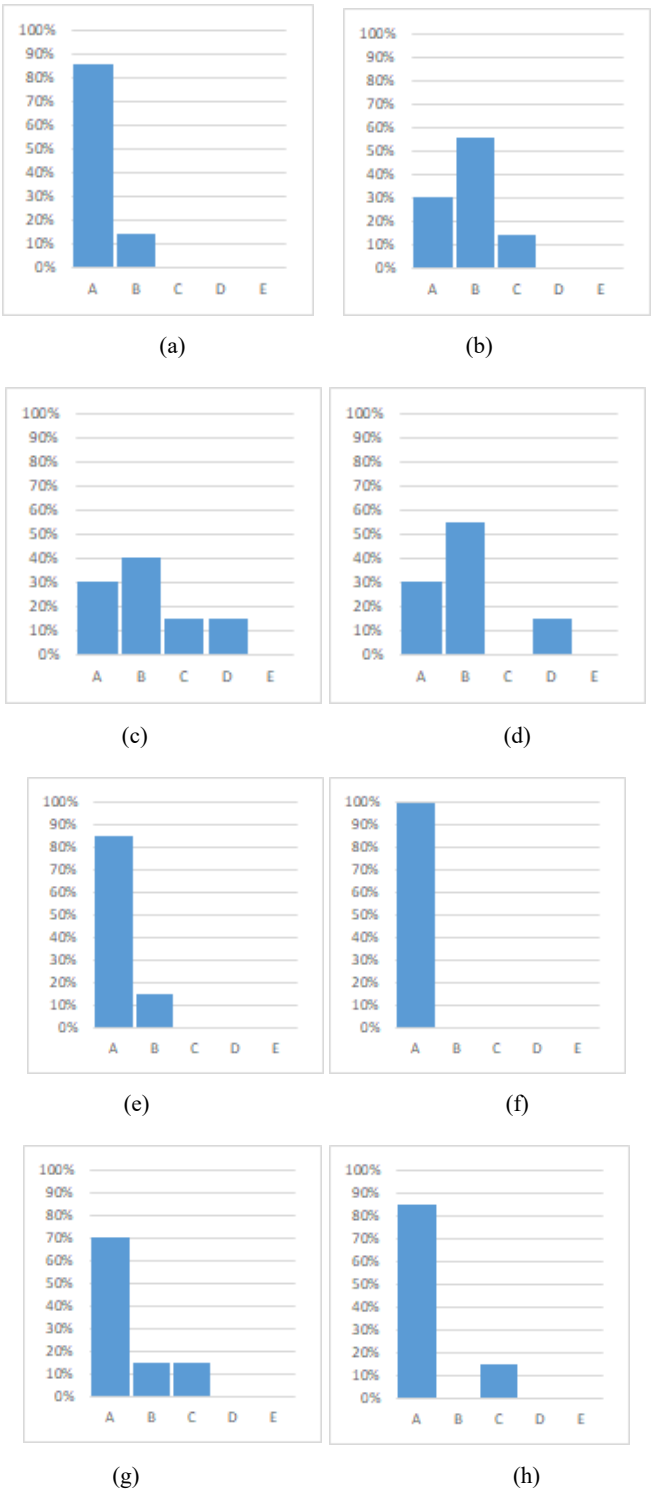

Fig. 8 Responses to the system questionnaire. (a) Q1: Did you find the implemented system interesting? (b) Q2: Was it difficult to learn the usage of Leap Motion? (c) Q3: Was mobile robot navigation system practical and efficient by using Leap Motion? (d) Q4: Is it possible to use Leap Motion instead of Kinetic to play games? (e) Q5: Can gesture handle adaptable in the daily life area? (f) Q6: Do you suggest that the grasping gesture should be adapted to different applications? (g) Q7: Were you satisfied with the system? (h) Q8: Do you think the gesture based control system can be more popular and attractive than traditional ways in the future?

TABLE I
MOBIL ROBOT MOVEMENT USABILITY TEST

Evaluation at the beginning		**Evaluation after practice**	
Test subjects	Usability[1]	Test subjects	Usability[1]
1.	4	1.	5
2.	3	2.	4
3.	3	3.	4
4.	2	4.	3
5.	5	5.	5
6.	3	6.	4
7.	4	7.	4
Average	**3.50**[2]	**Average**	**4.14**[2]

[1]The maximum mark was 5. 1 = unusable, 2 = hardly usable, 3 = usable, 4 = well-usable, 5 = excellent usable
[2]Average of the complete sample

We can get the conclusion from the results that according to the seven questioned test subjects, the test environment is usable, with a bit better result than average. There were such test subjects, who had difficulties in moving the mobile robot in the beginning, but others could easily move the mobile robot right at the beginning. Following 10-15 minutes of practice, according to the opinion of the test subjects, the system's usability improved by 0.72 points, so the 'usable' rating changed to 'well-usable'. Of course, the use of the system was not perfect though, the systems needs further fine tuning.

V. CONCLUSION

The application of a hand gesture controlled HCI was introduced in the article regarding the control of a mobile robot. The control of the mobile robot was implemented by the Leap Motion hand position detection system. The mobile robot's control was tested in realistic virtual environment. The implemented manual gesture control, as the usability of HCI based control, was examined by test subjects. According to the feedback given by the test subjects, the system can be handled well following a little practice. After performing the examination, according to the feedback given by the test subjects, the system's application also on other application fields would be useful. As a summary, by the development of IT systems, human-computer interaction is being developed to an even greater extent, and in the future, new communication methods will be available in human-computer interaction.

REFERENCES

[1] Y. Lin and W. Zhang, "A function-behavior-state approach to designing human-machine interface for nuclear power plant operators", IEEE Transactions on Nuclear Science, vol. 52, no. 1, pp. 430-439, 2005.

[2] Seong Soo Choi, Jin Kyun Park, Jin Hyuk Hong, Han Gon Kim, Soon Heung Chang and Ki Sig Kang, "Development strategies of an intelligent human-machine interface for next generation nuclear power plants", IEEE Transactions on Nuclear Science, vol. 43, no. 3, pp. 2096-2114, 1996.

[3] P. Lagari, A. Nasiakou and M. Alamaniotis, "Evaluation of Human Machine Interface (HMI) on a Digital and Analog Control Room in Nuclear Power Plants Using a Fuzzy Logic Approach", International Journal of Monitoring and Surveillance Technologies Research, vol. 4, no. 2, pp. 50-68, 2016.

[4] I. Rezazadeh, M. Firoozabadi, H. Hu and S. Golpayegani, "Co-Adaptive and Affective Human-Machine Interface for Improving Training Performances of Virtual Myoelectric Forearm Prosthesis", IEEE Transactions on Affective Computing, vol. 3, no. 3, pp. 285-297, 2012.

[5] M. Bosnak and I. Skrjanc, "Embedded Control System for Smart Walking Assistance Device", IEEE Transactions on Neural Systems and Rehabilitation Engineering, vol. 25, no. 3, pp. 205-214, 2017.

[6] C. Cipriani, J. Segil, J. Birdwell and R. Weir, "Dexterous Control of a Prosthetic Hand Using Fine-Wire Intramuscular Electrodes in Targeted Extrinsic Muscles", IEEE Transactions on Neural Systems and Rehabilitation Engineering, vol. 22, no. 4, pp. 828-836, 2014.

[7] B. Ravani, M. Gabibulayev and T. Lasky, "Improvement of a Human-Machine Interface (HMI) for Driver Assistance Using an Event-Driven Prompting Display", IEEE Transactions on Control Systems Technology, vol. 19, no. 3, pp. 622-627, 2011.

[8] P. Alvarado Mendoza, A. Lindgren and A. Angelelli, "Ecological interface design inspired human machine interface for advanced driver assistance systems", IET Intelligent Transport Systems, vol. 5, no. 1, pp. 53-59, 2011.

[9] C. Pickering, "The search for a safer driver interface: a review of gesture recognition human machine interface", Computing and Control Engineering, vol. 16, no. 1, pp. 34-40, 2005.

[10] S. Park and T. Sheridan, "Enhanced Human–Machine Interface in Braking", IEEE Transactions on Systems, Man, and Cybernetics - Part A: Systems and Humans, vol. 34, no. 5, pp. 615-629, 2004.

[11] D. Santana, C. da Silva Santos and H. Hernandez Figueroa, "Human-Computer Interface Techniques to Design and Evaluate an Electromagnetic Simulator", IEEE Latin America Transactions, vol. 12, no. 4, pp. 725-732, 2014.

[12] H. Saini and R. Daruwala, "Human Machine Interface in Internet Of Things system", 2016 International Conference on Computing Communication Control and automation (ICCUBEA), 2016.

[13] M. Gertz, D. Stewart and P. Khosla, "A human machine interface for distributed virtual laboratories", IEEE Robotics & Automation Magazine, vol. 1, no. 4, pp. 5-13, 1994.

[14] Jiang, Y. C., "Menacing motion-sensing technology, different leap motion." PC. Fan 11, pp. 32-33, 2013.

[15] Gy. Molnár and Z. Szűts, Visual Learning - Picture and Memory in Virtual Worlds, In: András Benedek, Kristóf Nyíri (ed.) Beyond Words: Pictures, Parables, Paradoxes. 260 p. Frankfurt: Peter Lang Verlag, 2015. pp. 153-161. (ISBN:978-3-631-66385-1)

[16] Gy. Molnár, Challenges and Opportunities in Virtual and Electronic Learning Environments, In: Szakál Anikó (ed.) SISY 2013: IEEE 11th International Symposium on Intelligent Systems and Informatics: proceedings. Budapest: IEEE Hungary Section, 2013. pp. 397-401. (ISBN:978-1-4799-0303-0)

[17] I. Horváth, Innovative engineering education in the cooperative VR environment, 7th IEEE Conference on Cognitive Infocommunications CogInfoCom 2016, 16-18 October 2016, Wroclaw, Poland, pp. 000359 - 000364, doi: 10.1109/CogInfoCom.2016.7804576

[18] I. Horváth, The education of disruptive technologies in the innovative engineering training, Australian Journal of Intelligent Information Processing System, Vol.14, No.4. 2016.

[19] Dr Molnár Gy., The role of electronic and virtual learning support systems in the learning process, In: Szakál Anikó (ed.) IEEE 8th International Symposium on Applied Computational Intelligence and Informatics: SACI 2013. (IEEE) New York: IEEE, 2013. pp. 51-54. (ISBN:978-1-4673-6397-6)

Dynamic Analysis of Composite Doubly Curved Panels with Variable Thickness

İ. Algul, G. Akgun, H. Kurtaran

Abstract**—**Dynamic analysis of composite doubly curved panels with variable thickness subjected to different pulse types using Differential Quadrature method (DQM) is presented in this study. Panels with variable thickness are used in the construction of aerospace and marine industry. Giving variable thickness to panels can allow the designer to get optimum structural efficiency. For this reason, estimating the response of variable thickness panels is very important to design more reliable structures under dynamic loads. Dynamic equations for composite panels with variable thickness are obtained using virtual work principle. Partial derivatives in the equation of motion are expressed with DQM and Newmark average acceleration scheme is used for temporal discretization. Several examples are used to highlight the effectiveness of the proposed method. Results are compared with finite element method. Effects of taper ratios, boundary conditions and loading type on the response of composite panel are investigated.

Keywords**—**Differential quadrature method, doubly curved panels, laminated composite materials, small displacement.

I. Introduction

THE usage of fiber reinforced composite shells is highly demanded for structural applications especially in the field of aircraft structures, space stations, automobiles, ships, submarines. Composite materials have attracted significant attentions due to their specific properties such as high strength-to-weight and stiffness-to-weight ratios, corrosion resistance, longer fatigue life, stealth characteristics and most importantly tailoring of these structures for desired usage area. The anisotropic behavior and bending-stretching coupling of composite structures create difficulties for the analysis of composite shells. Therefore, understanding the behavior of these structures under different type of loading is very important to enable safe and economical designs.

Most of the studies on the literature about tapered plate and panels have been limited to static, free vibration and buckling analysis. Ganesan and Rasul [1] studied buckling analysis of tapered laminated shells considering uniaxial compression using Ritz method based on different first order shell theories. A comprehensive parametric study including boundary conditions, stacking sequence, taper configurations, radius and geometric parameters of the shells has been done in this research. Ashaur [2] applied finite strip technique in conjunction with the transition matrix to examine the vibration of orthotropic tapered plates for different taper ratio, aspect ratio and different combinations of boundary conditions. Turvey [3] examined large deflection static analysis of thin tapered square plates with simply supported boundary conditions by using dynamic relaxation method. Javed et al. [4] carried out free vibration of anti-symmetric angle-ply composite plates with variable thickness using spline function approximation by taking parameter of material properties, ply orientation, number of lay ups, aspect ratio and coefficients of thickness variations. Bert and Malik [5] presented the free vibration analysis of rectangular tapered plates having simply supported conditions at two opposite edges and general boundary conditions at the other two edges by DQM which is firstly introduced by Bert as a tool for structural analysis. Babu et al. [6] investigated dynamic analysis of various configurations thickness tapered laminated composite plate by experimental study and validation of the developed finite element formulations. Kobayashi et al. [7] surveyed buckling problem of uniaxially compressed rectangular tapered plates by a power series method. The influences of thickness variation, plate aspect ratios, and boundary conditions on the buckling load have been taken as parameters in the survey. Civalek [8] solved free vibration problems of isotropic and orthotropic rectangular tapered plates by coupling discrete singular convolution (DSC). Torbabene et al. [9] studied natural frequencies of doubly curved shells with variable thickness taking into account various higher order Equivalent Single Layer theories using Generalized DQM.

As it can be seen from the literature survey, there are many studies about the static, free vibration and buckling analysis of moderately thick laminated composite plates. However, there is very limited study for the dynamic behavior of laminated composite panel with variable thickness in the literature. The purpose of this study is to examine the dynamic analysis of composite doubly curved panels with variable thickness subjected to different pulse types using DQM. Numerical results are presented to understand the behavior of the panels by changing taper ratios, boundary conditions and loading type and are compared with the commercial finite element program ANSYS. Virtual work principle is used to derive the governing differential equations. Partial derivatives in the equation of motion are expressed with Lagrange polynomials and time integration is carried out using Newmark average acceleration method for dynamic analysis. First-order shear deformation theory in association with an extension of linear strain-displacement relationships is used to consider the transverse shear effect through thickness direction.

İ. A. and G. A. are with the Department of Mechanical Engineering, Gebze Technical University, Gebze – Kocaeli, Turkey (phone: +90 262 605 27 88; e-mail: ilkees@gtu.edu.tr, agokce@gtu.edu.tr).

H. K. is with the Department of Mechanical Engineering, Gebze Technical University, Gebze – Kocaeli, Turkey (phone: +90 262 605 27 78; e-mail: hasan@gtu.edu.tr).

II. Statement of the Problem

A doubly curved composite panel composed of orthotropic layers with varying thickness h(x), length a and width b is given in Fig. 1. The x, y and z stated the orthogonal curvilinear coordinate system attached to the middle surface of the shell (z=0). R_x and R_y are denoted the principal radius of the middle surface of the panel curvature. h(x) indicates thickness function varying through the x direction and is linearly expressed as shown in (1):

$$h(x) = h_0.(1 + \beta\frac{x}{a}) \tag{1}$$

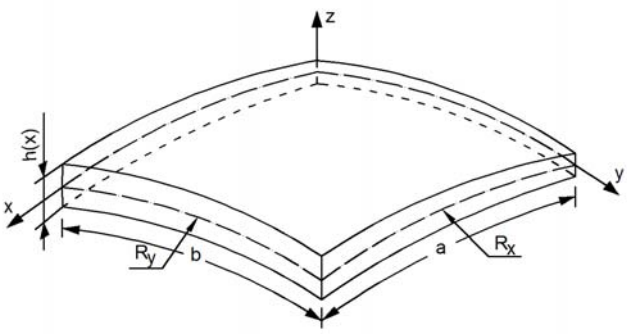

Fig. 1 Doubly curved panel with varying thickness

The displacement field at general point (x, y and z) of the panel at t time based on first-order shear deformation theory may be written as:

$$\begin{aligned} u(x,y,z,t) &= u_0(x,y,t) + z.\theta_x(x,y,t) \\ v(x,y,z,t) &= v_0(x,y,t) + z.\theta_y(x,y,t) \\ w(x,y,z,t) &= w_0(x,y,t) \end{aligned} \tag{2}$$

where u_0, v_0, w_0 are the displacement field of a point on the middle surface of the shell along the x, y and z axes, respectively. θx and θy are the rotations around the y and x axes, respectively and come from the rotations of the shell.

The strain-displacement relations for the doubly curved panels using the displacement fields in (2) from the theory of elasticity in curvilinear coordinates are given below [10]:

$$\begin{aligned} &\varepsilon_x = \frac{\partial u_0}{\partial x} + z\frac{\partial \theta_x}{\partial x} + \frac{w_0}{R_x}, \\ &\varepsilon_y = \frac{\partial v_0}{\partial y} + z\frac{\partial \theta_y}{\partial y} + \frac{w_0}{R_y}, \\ &\gamma_{xy} = \frac{\partial v_0}{\partial x} + \frac{\partial u_0}{\partial y} + z\frac{\partial \theta_x}{\partial y} + z\frac{\partial \theta_y}{\partial x} + \frac{1}{2}\left(\frac{1}{R_y} - \right. \\ &\left.\frac{1}{R_x}\right)\left(\frac{\partial v_0}{\partial x} - \frac{\partial u_0}{\partial y}\right), \\ &\gamma_{yz} = \theta_y + \frac{\partial w_0}{\partial y} - \frac{v_0}{R_y}, \\ &\gamma_{xz} = \theta_x + \frac{\partial w_0}{\partial x} - \frac{u_0}{R_x}. \end{aligned} \tag{3}$$

Virtual work principle to obtain the dynamic equilibrium equations of tapered panel in curvilinear coordinate system is written as:

$$\delta U + \delta T - \delta W = 0 \tag{4}$$

δU, δT and δW specify respectively the virtual potential work of internal forces caused by internal stress, the virtual work done by the inertia forces caused by accelerations and the work done by the distributed load. The governing equilibrium equations are obtained as:

$$\begin{aligned} &\frac{\partial N_x}{\partial x} + \frac{\partial N_{xy}}{\partial y} + \frac{Q_{xz}}{R_x} - \frac{\partial}{\partial y}\left(M_{xy}.\frac{1}{2}\left(\frac{1}{R_y} - \frac{1}{R_x}\right)\right) = \\ &I_0\frac{\partial u_0}{\partial t^2} + I_1\frac{\partial^2 \theta_x}{\partial t^2}, \\ &\frac{\partial N_y}{\partial y} + \frac{\partial N_{xy}}{\partial x} + \frac{Q_{yz}}{R_y} + \frac{\partial}{\partial x}\left(M_{xy}.\frac{1}{2}\left(\frac{1}{R_y} - \frac{1}{R_x}\right)\right) = \\ &I_0\frac{\partial^2 v_0}{\partial t^2} + I_1\frac{\partial^2 \theta y}{\partial t^2}, \\ &-\frac{N_x}{Rx} - \frac{N_y}{Ry} + \frac{\partial Q_{yz}}{\partial y} + \frac{\partial Q_{xz}}{\partial x} = I_0\frac{\partial^2 w_0}{\partial t^2} + q_w, \\ &\frac{\partial M_x}{\partial x} + \frac{\partial M_{xy}}{\partial y} - Q_{xz} = I_1\frac{\partial^2 u_0}{\partial t^2} + I_2\frac{\partial^2 \theta x}{\partial t^2}, \\ &\frac{\partial M_y}{\partial y} + \frac{\partial M_{xy}}{\partial x} - Q_{yz} = I_1\frac{\partial^2 v_0}{\partial t^2} + I_2\frac{\partial^2 \theta y}{\partial t^2}. \end{aligned} \tag{5}$$

Here, N_x, N_y, N_{xy} are the in-plane force resultants, M_x, M_y, M_{xy} are the in-plane moment resultants and Q_{xy}, Q_{yz} are the transverse shear resultants, I_0, I_1, I_2 are the mass moments of inertia and can be calculated as:

$$\begin{aligned} &\left(N_x, N_y, N_{xy}\right) = \sum_{k=1}^{n}\int_{z_{k-1}(x)}^{z_k(x)}\left(\sigma_x, \sigma_y, \sigma_{xy}\right)d_z \\ &\left(M_x, M_y, M_{xy}\right) = \sum_{k=1}^{n}\int_{z_{k-1}(x)}^{z_k(x)}\left(\sigma_x, \sigma_y, \sigma_{xy}\right)zd_z \\ &\left(Q_{yz}, Q_{xz}\right) = \sum_{k=1}^{n}\int_{z_{k-1}(x)}^{z_k(x)}k_s.\left(\tau_{yz}, \tau_{xz}\right)d_z \\ &\left(I_0, I_1, I_2\right) = \sum_{k=1}^{n}\int_{z_{k-1}}^{z_k}\rho^k.(1, z, z^2)\,d_z. \end{aligned} \tag{6}$$

The governing differential equations in (5) are written in terms of displacement and rotations. Equation of motion for doubly curved panel can be shortly written in matrix form as

$$M\ddot{U} + KU = F \tag{7}$$

where M and K denote mass and stiffness matrix respectively. $\ddot{U}$ and U denote the acceleration and displacement vectors, respectively. Transient response can be calculated by using implicit Newmark constant average acceleration time integration scheme.

$$\begin{aligned} \ddot{U}_{n+1} &= c_0(U_{n+1} - U_n) - c_1\dot{U}_n - \ddot{U}_n \\ \dot{U}_{n+1} &= \dot{U}_n + (1-\gamma)\Delta_t\ddot{U}_n + \gamma\Delta_t\ddot{U}_{n+1} \end{aligned} \tag{8}$$

Expressing (6) in terms of displacement, velocity and acceleration and substituting (8) into (6) leads to the following algebraic equation

$$[c_0M + K]U_{n+1} = F_{n+1} + M[c_0U_n + c_1\dot{U}_n + \ddot{U}_n] \tag{9}$$

where c_0=4/$\Delta_t{}^2$, c_1=4/Δ_t, γ=0.5 is chosen for constant average acceleration method. The entire number of unknown

coefficients in terms of displacements for each time step in (7) is 5(M+1)(N+1). The governing differential equations are written for internal grid points and gives us 5(M-1)(N-1) equations. The boundary conditions give 10(M+1)+10(N-1) equations. It can be seen that total number of equations is equal to the total number of unknown coefficients and can be easily solved. Equation (7) is solved successively to find displacements at other time steps until final time is reached.

III. Numerical Results and Discussions

Equilibrium equations of composite doubly curved panels (Rx = Ry = R) of square plan-form are obtained using virtual work principle. A MATLAB code is written to solve derived equations by using DQM. Firstly, the written code accuracy is validated with finite element and different transient numerical examples are studied to analyze the effect of boundary conditions, thickness variation ratios and loading type. For all the transient examples, each lamina has the same thickness and composite panel dimensions are: a=b=0.24, h_0=0.006 m, R/a=10. The stacking sequence is [0°/90°/0°]. Composite material properties are: E_1=204 GPa, E_2=18.5 GPa, G_{12}=G_{13}= G_{23}=5.59 GPa, ρ=2100 kg/m^3, ν12=0.23. Boundary condition types are prescribed as below:

a) For simply supported type:

x=0,a $u_0 = v_0 = w_0 = \theta_x = M_y$

y=0,b $u_0 = v_0 = w_0 = \theta_y = M_x$

b) For clamped type

x=0,a $u_0 = v_0 = w_0 = \theta_x = \theta_y = 0$

y=0,b $u_0 = v_0 = w_0 = \theta_x = \theta_y = 0$

The numerical results presented for dynamic response of composite panel subjected to following different dynamic loading:

a) Uniform step load: $q(t) = Q$

b) Sine pulse: $q(t) = \begin{cases} Qsin\left(\frac{2\pi t}{t_f}\right) \text{ for } t \le t_f \\ 0 \text{ for } t \ge t_f \end{cases}$

c) Blast pulse: $q(t) = \begin{cases} Q\left(1 - \frac{t}{t_f}\right) \text{ for } t \le t_f \\ 0 \text{ for } t \ge t_f \end{cases}$

In all cases, maximum pressure value Q=10^6 Pa, time duration t_f=0.004 s and time step Δt=0.0004 s are taken. For all the numerical results presented here, the displacement w, are computed at the middle of the panel and stress σ_x, are computed at the top of the composite panel (x=0, y=b/2). Nondimensional transverse displacement (w/h) and stress response of composite panel for thickness variation β=0, 0.7, 1.2 for both clamped and simply supported boundary conditions subjected to blast pulse are shown in Figs. 2-5. The results for simply supported boundary conditions under blast load with DQM are compared with the finite element results in Figs. 2 and 3 and similar results are achieved with the proposed method using 9x9 grid points. It is observed that amplitude of displacements in Figs. 2, 4 and stresses in Figs. 3, 5 decreases and frequency of motion increases with the increasing taper ratios for simply support and clamped boundary conditions. The displacement values of the composite panel are much higher for simply supported boundary conditions than those for clamped boundary conditions under blast load. However, stress values occurred in composite panel structures are much higher for clamped boundary conditions than those for simply supported boundary conditions under blast load due to the constraints of clamped edges. Nondimensional transverse displacements and stress responses of composite panel subjected to sinus pulse and step pulse are shown in Figs. 6-9 and Figs. 10-13, respectively for thickness variation β=0, 0.7, 1.2 with clamped and simply supported boundary conditions. It is observed that amplitude of displacements and stresses decreases and frequency of motion, as shown in Figs. 6-13, increases with the increasing taper ratios for simply support and clamped boundary conditions under sinus and step pulses. The displacement values of the composite panel are much higher for simply supported boundary conditions than those for clamped boundary conditions under sinus and step pulses like blast load. However, stress values occurred in composite panel structures are much higher for clamped boundary conditions than those for simply supported boundary conditions under sinus and step pulses due to the constraints of clamped edges as occurred under blast load.

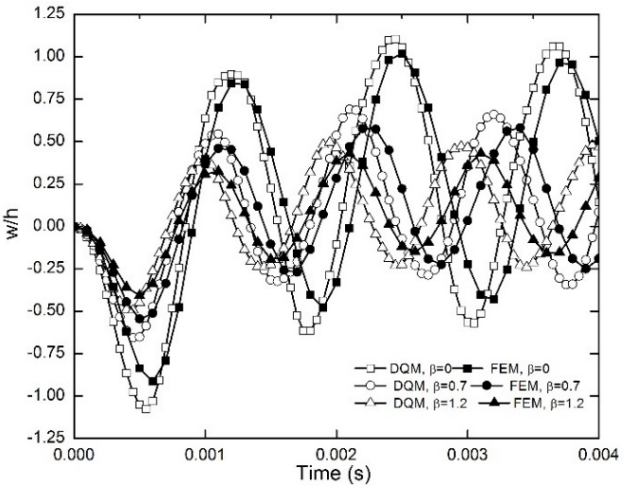

Fig. 2 Non-dimensional transverse displacement comparison of linear increasing taper ratios ($\beta = 0, 0.7, 1.2$) of simply supported composite panel under blast load with finite element method (a/h=40, R/a=10)

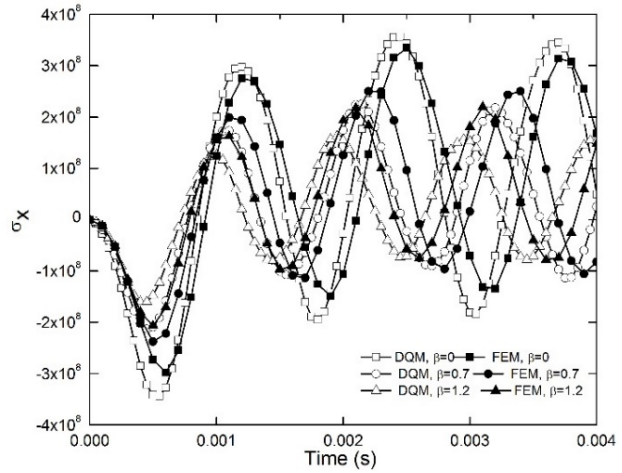

Fig. 3 Stress distribution comparison of linear increasing taper ratios ($\beta = 0, 0.7, 1.2$) of simply supported composite panel under blast load (a/h=40, R/a=10)

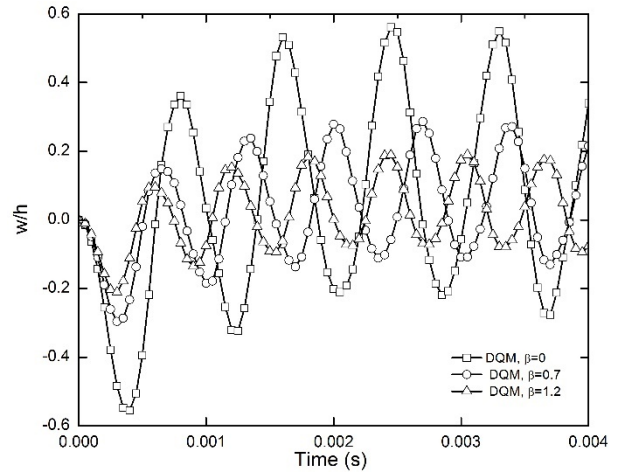

Fig. 4 Non-dimensional transverse displacement comparison of linear increasing taper ratios ($\beta = 0, 0.7, 1.2$) of clamped composite panel under blast load (a/h=40, R/a=10)

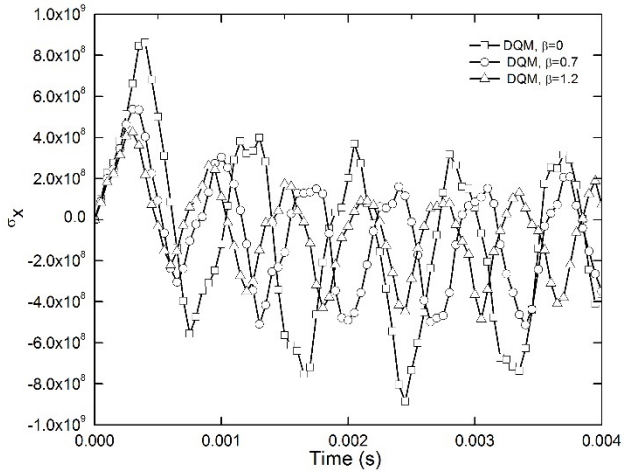

Fig. 5 Stress distribution comparison of linear increasing taper ratios ($\beta = 0, 0.7, 1.2$) of clamped composite panel under blast load (a/h=40, R/a=10)

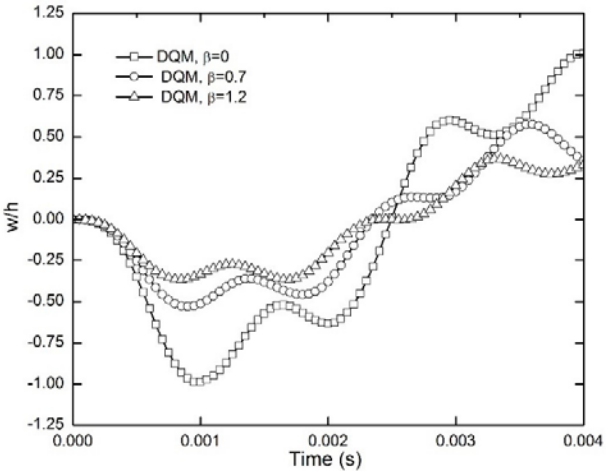

Fig. 6 Non-dimensional transverse displacement comparison of linear increasing taper ratios ($\beta = 0, 0.7, 1.2$) of simply supported composite panel under sinus load (a/h=40, R/a=10)

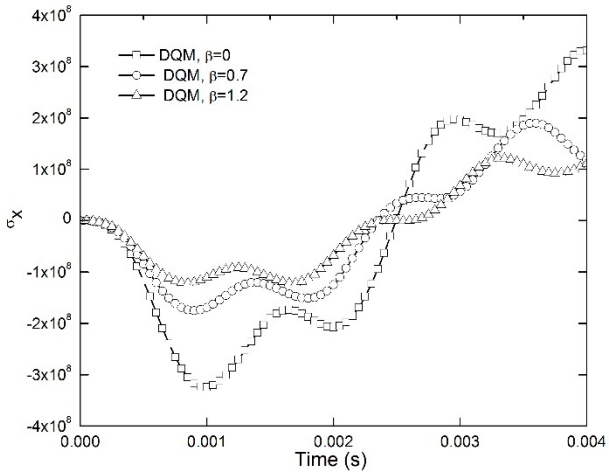

Fig. 7 Stress distribution comparison of linear increasing taper ratios ($\beta = 0, 0.7, 1.2$) of simply supported composite panel under sinus load (a/h=40, R/a=10)

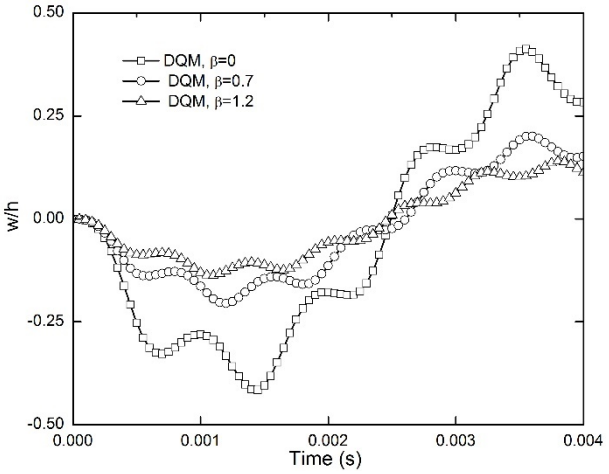

Fig. 8 Non-dimensional transverse displacement comparison of linear increasing taper ratios ($\beta = 0, 0.7, 1.2$) of clamped composite panel under sinus load (a/h=40, R/a=10)

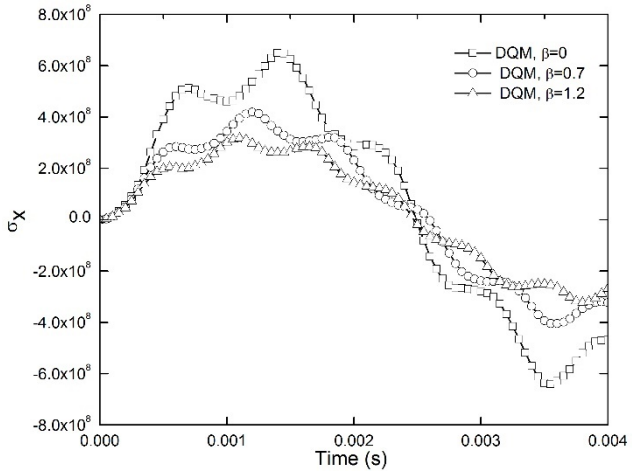

Fig. 9 Stress distribution comparison of linear increasing taper ratios ($\beta = 0, 0.7, 1.2$) of clamped composite panel under sinus load (a/h=40, R/a=10)

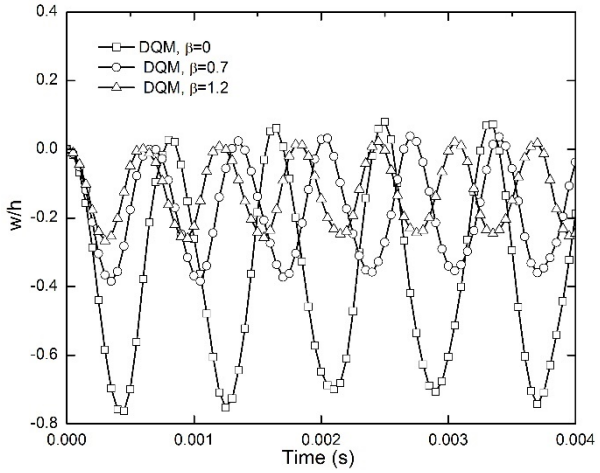

Fig. 12 Non-dimensional transverse displacement comparison of linear increasing taper ratios ($\beta = 0, 0.7, 1.2$) of clamped composite panel under step load (a/h=40, R/a=10)

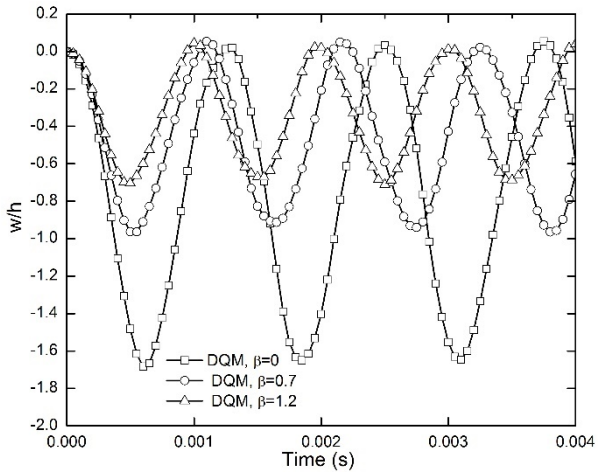

Fig. 10 Non-dimensional transverse displacement comparison of linear increasing taper ratios ($\beta = 0, 0.7, 1.2$) of simply supported composite panel under step load (a/h=40, R/a=10)

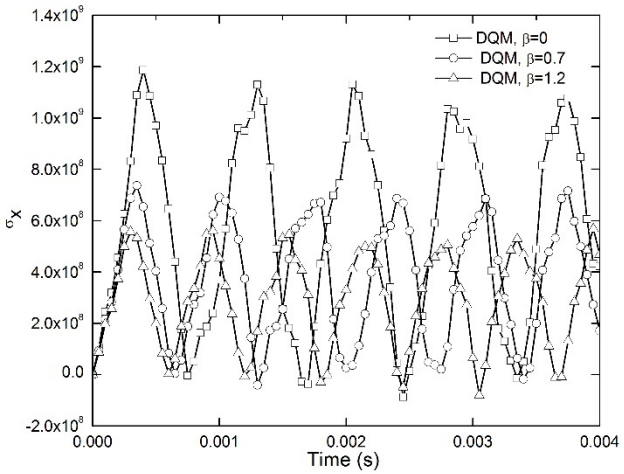

Fig. 13 Stress distribution comparison of linear increasing taper ratios ($\beta = 0, 0.7, 1.2$) of clamped composite panel under step load (a/h=40, R/a=10)

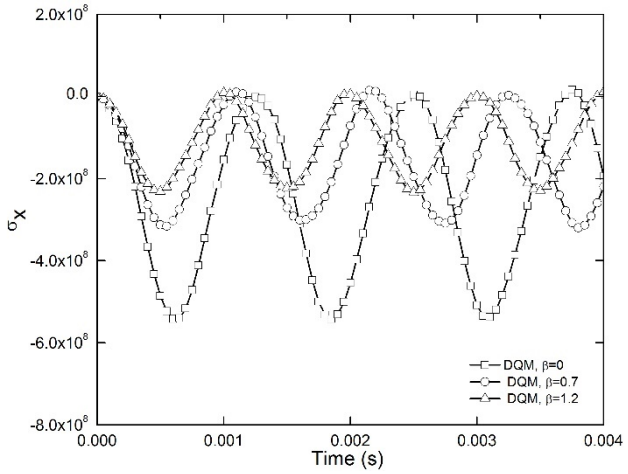

Fig. 11 Stress distribution comparison of linear increasing taper ratios ($\beta = 0, 0.7, 1.2$) of simply supported composite panel under step load (a/h=40, R/a=10)

IV. Conclusions

In this study, dynamic analysis of composite doubly curved panels with variable thickness subjected to different pulse types is investigated using DQM. The numerical results are obtained to understand the displacement and stress characters of the doubly curved panels for different boundary conditions, loading types and taper ratios and compared with ANSYS. It is seen that the numerical results with DQM are good agreement with ANSYS. Generally, 9x9 grid points give accurate results with proposed method. The method can be applied to the efficient solution of other engineering problems and can serve as a bench work for forthcoming surveys.

It is observed that amplitude of displacements and stresses decreases and frequency of motion increases with the increasing taper ratios for all boundary conditions and load types. The displacement values of the composite panel are much higher for simply supported boundary conditions than those for clamped boundary conditions under all type of load

pulses. However, stress values occurred in composite panel structures are much higher for clamped boundary conditions than those for simply supported boundary conditions under all type of load pulses.

REFERENCES

[1] R. Ganesan, "Compressive response of tapered composite shells," Composite Structures, vol. 93, pp. 2153-62, 2011.

[2] A. S. Ashour, "A Semi - Analytical Solution of the Flexural Vibration of Orthotropic Plates of Variable Thickness," Journal of Sound and Vibration, vol. 240, pp. 431-45, 2001.

[3] G. J. Turvey, "A Study of the Behavior of Square Plates at Large Deflections According to the Theories of Foeppl and Von Karman," Journal of Strain Analysis for Engineering Desig, vol. 13, pp. 11-16, 1978.

[4] S. Javed, K. K. Viswanahtan, Z. A. Aziz, K. Prabakar "Free vibration of anti-symmetric angle-ply plates with variable thickness," vol. 137, pp. 56-69, 2009.

[5] C. W. Bert, M. Malik "Free Vibration Analysis of Tapered Rectangular Plates By Differential Quadrature Method-A Semi-Analytical Approach," Journal of Sound and Vibration vol. 190, pp. 41-63, 1996.

[6] B. A. Ananda, S. P. Edwin, V. Rajamohan "Dynamic characterization of thickness tapered laminated composite plates," Journal of Vibration and Control pp. 1-21, 2015.

[7] H. Kobayashi, K. Sonoda "Buckling of Rectangular Plates with Tapered Thickness," Journal of Structural Engineering vol. 116, pp. 1278-89, 1990.

[8] Ö. Civalek "Fundamental frequency of isotropic and orthotropic rectangular plates with linearly varying thickness by discrete singular convolution method," Applied Mathematical Modelling vol. 33, pp. 3825-35, 2009.

[9] F. Tornabene, F. Nicholas, B. Michele "Local GDQ Method for the Natural Frequencies of Doubly-Curved Shells with Variable Thickness: A General Formulation," Composites Part B, vol. 92, pp. 265-289, 2016.

[10] J. N. Reddy "Mechanics of Laminated Composite Plates and Shells Theory and Analysis," 2nd Edition, CRC Press, 2004.

Large-Eddy Simulations for Aeronutical Systems

R. R. Mankbadi

Abstract**—**There are several technologically-important flow situations in which there is a need to control the outcome of the fluid flow. This could include flow separation, drag, noise, as well as particulate separations, to list only few. One possible approach is the passive control, in which the design geometry is changed. An alternative approach is the Active Flow Control (AFC) technology in which an actuator is embedded in the flow field to change the outcome. Examples of AFC are pulsed jets, synthetic jets, plasma actuators, heating and cooling, … etc. In this work will present an overview of the development of this field. Some examples will include: Airfoil Noise Suppression: Large-Eddy Simulations (LES) is used to simulate the effect of synthetic jet actuator on controlling the far field sound of a transitional airfoil. The results show considerable suppression of the noise if the synthetic jet is operated at frequencies. Mixing Enhancement and suppression: Results will be presented to show that imposing acoustic excitations at the nozzle exit can lead to enhancement or reduction of the jet plume mixing. In vertical takeoff of Aircrafts or in Space Launch, we will present results on the effects of water injection on reducing noise, and on protect the structure and payload from fatigue damage. Other applications will include airfoil-gust interaction and propulsion systems optimizations.

Keywords**—**Aeroacoustics, flow control, aerodynamics, large eddy simulations.

R. R. Mankbadi is with Embry-Riddle Aeronautical University. Daytona Beach, FL 32114 USA (e-mail: mankbadr@erau.edu).

The Prediction of Sound Absorbing Coefficient for Multi-Layer Non-Woven

Un-Hwan Park, Jun-Hyeok Heo, In-Sung Lee, Tae-Hyeon Oh, Dae-Gyu Park

***Abstract*—**Automotive interior material consisting of several material layers has the sound-absorbing function. It is difficult to predict sound absorbing coefficient because of several material layers. So, many experimental tunings are required to achieve the target of sound absorption. Therefore, while the car interior materials are developed, so much time and money is spent. In this study, we present a method to predict the sound absorbing performance of the material with multi-layer using physical properties of each material. The properties are predicted by Foam-X software using the sound absorption coefficient data measured by impedance tube. Then, we will compare and analyze the predicted sound absorption coefficient with the data measured by scaled reverberation chamber and impedance tubes for a prototype. If the method is used instead of experimental tuning in the development of car interior material, the time and money can be saved, and then, the development effort can be reduced because it can be optimized by simulation.

***Keywords*—**Multi-layer nonwoven, sound absorption coefficient, scaled reverberation chamber, impedance tubes.

I. Introduction

NONWOVEN fabric is widely used as industrial fibers in automotive interior part. It has usually multi-layer with various materials. For easy recycling, it is studied to develop a single material too. But, it is not easy to meet the required performance by single material because automotive interior has many targets. Specially, it must have a sound-absorbing performance to reduce the noise. Because automotive interior is composed of multi-layer material, it is difficult to meet the required performance. So, we have many experimental tunings to meet the required performance for sound absorption in the development. It is disadvantageous in terms of cost and time aspects.

In this paper, we will present the method to predict the sound absorption coefficient for nonwoven material with multi-layer using physical properties for each nonwoven.

First of all, the sound absorption coefficient is measured by using acoustic impedance tube. And we calculate the physical properties of the material with it [1]-[3]. We predicted it using Foam-X software with inverse algorithm. We predict the sound absorption coefficient of multi-layer using commercial analysis tool. Also, we verify the sound absorption coefficient calculated by commercial analysis tool with a prototype. And we do correlation analysis of the calculated and measured values. For measuring the physical properties, expensive measuring equipment is needed. So, we predict it by using a software. Fig. 1 shows the process of the analysis and test.

Un-Hwan Park is with the Smart Machine Research Department in KOTMI, #27 Sampung-Ro Gyeongsan-City Gyeongbuk, 38542, Korea (phone: +82-53-819-3141; fax: +82-53-819-3119; e-mail: uhpark@kotmi.re.kr).

Jun-Hyeok Heo is with the Acoustic and Vibration Team in KOTMI, #27 Sampung-Ro Gyeongsan-City Gyeongbuk, 38542, Korea (phone: +82-53-819-3124; fax: +82-53-819-3119; e-mail: jhheo@kotmi.re.kr).

Dae-Gyu Park is with the Korea Textile Machinery Research Institute, #27 Sampung-Ro Gyeongsan-City Gyeongbuk, 38542, Korea (phone: +82-53-819-3131; fax: +82-53-819-3119; e-mail: dkpark@kotmi.re.kr).

II. The Calculation of the Property for Acoustic Material

We measure the sound absorption coefficient with impedance tubes to predict the properties of nonwoven. The predicted properties are porosity, resistivity, tortuosity, viscous length, thermal length, and so on. It is calculated with the absorbed amount that is not reflected about the input sound in the tubes. The materials for the experiment are PET felt and mixed felt. Because the materials have high performance for sound absorption, those are widely used as automotive interior. The more experiments are conducted for prediction, the more it is accurate. First of all, the thickness of the materials for the experiment should be determined. It is 10 mm in thickness. The experiments for 1, 2, and 3-layer of the same material were conducted several times. Fig. 2 shows the result of the experiment for the sound absorbing coefficient. The physical properties are calculated with the measured sound absorbing coefficient. The used commercial software is Foam-X [2].

As shown in Fig. 3, the calculated properties are open porosity, resistivity, pore tortuosity, viscous length, thermal length, and so forth. For measuring the properties, expensive measurement system is required. But if it is calculated using the data of acoustic impedance, the cost and the time can be reduced.

III. The Calculation of the Sound Absorbing Coefficient for Multi-Layer

We predict the sound absorbing coefficient of compositing multi-layer using the commercial software NOVA as shown Fig. 4. The properties such as open porosity, resistivity, pore tortuosity, viscous length, thermal length and bulk density are required for the calculation [4], [5]. But, bulk density cannot be calculated using Foam-X. So, we measured it with Phi-X measurement system as shown Fig. 5. Table I shows the calculated and measured data for the prediction of the sound absorbing coefficient [6]. The data are the calculated value in the Foam-X software.

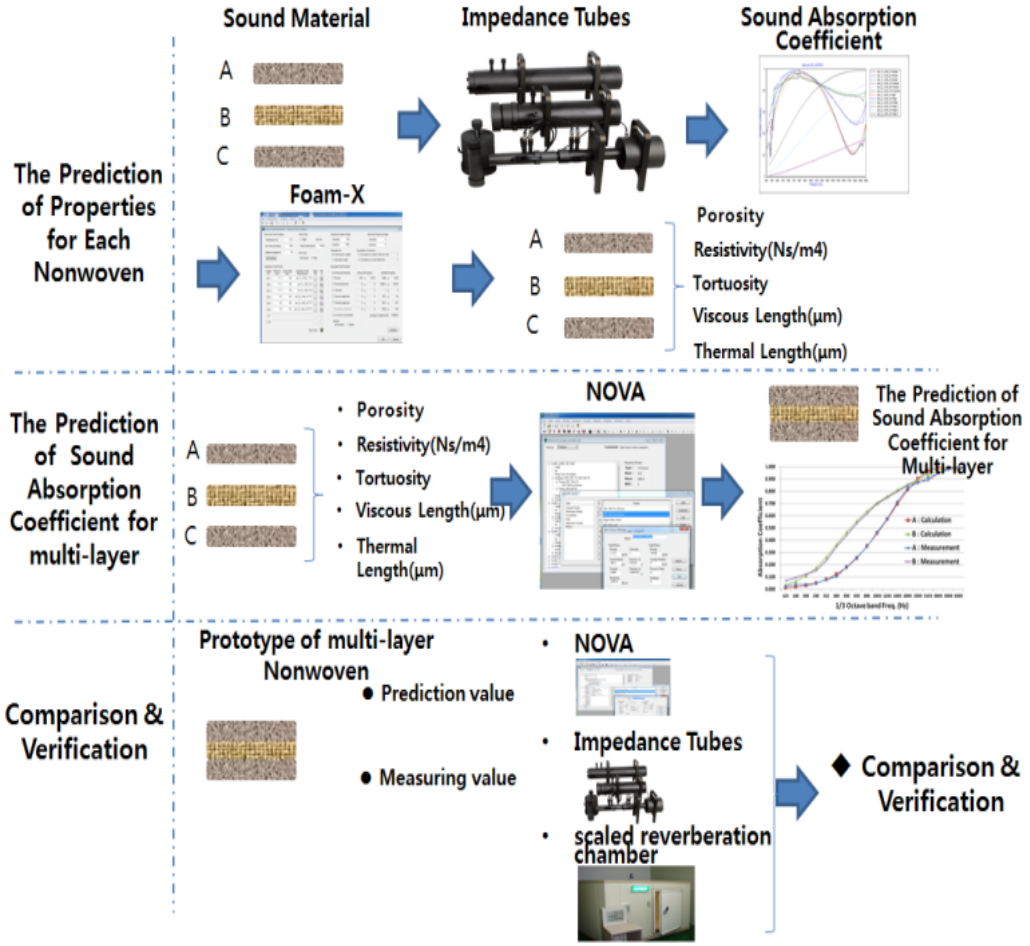

Fig. 1 The process for the prediction of sound absorption coefficient for automotive interior material with multi-layer

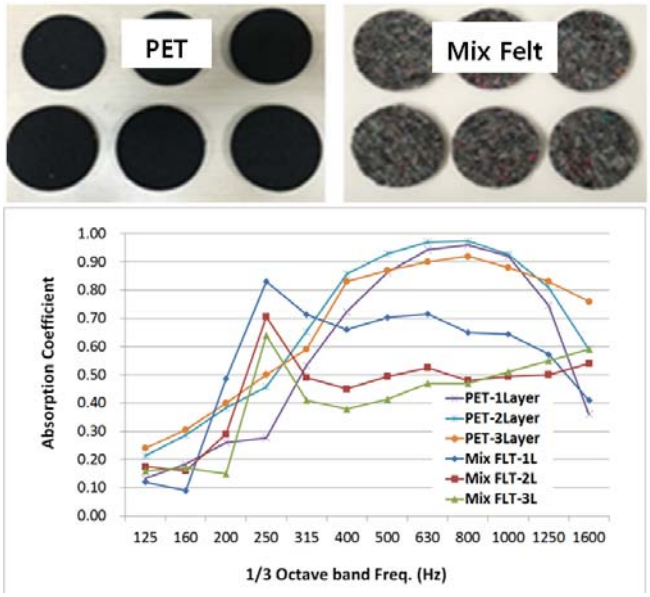

Fig. 2 The measured sound absorption coefficient by impedance tubes

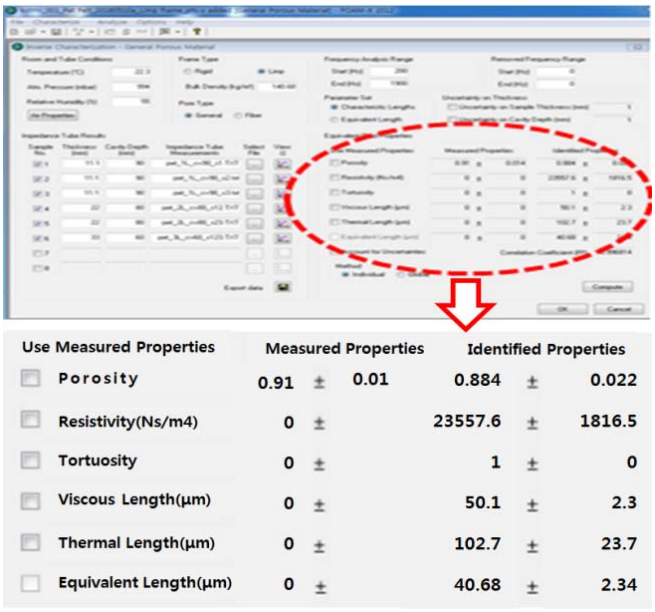

Fig. 3 The prediction by Foam-X with the measured sound coefficient

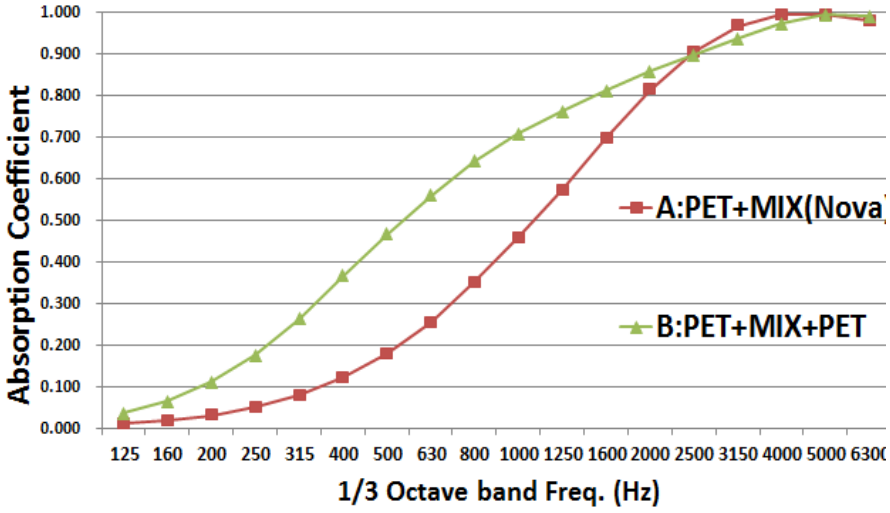

Fig. 4 The calculated sound absorbing coefficient

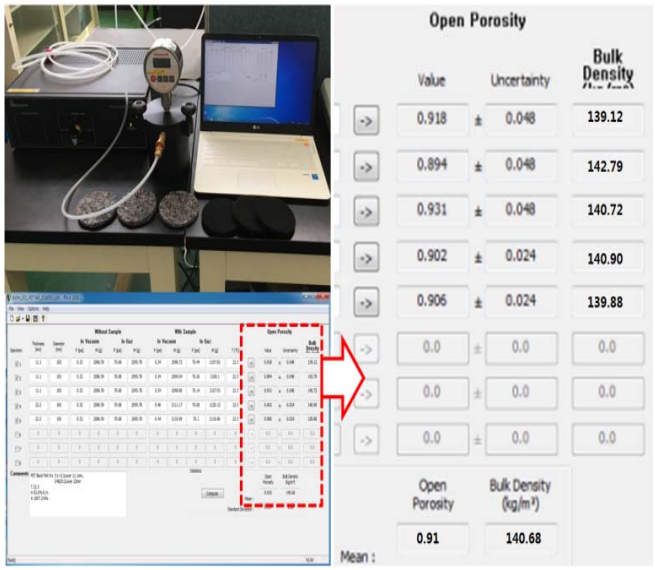

Fig. 5 The measurement of bulk density

TABLE I
MATERIAL PROPERTIES

material property	PET Felt	Mix Felt
open porosity	0.884	0.896
resistivity(Ns/m^4)	23557.6	138721.1
pore tortuosity	1	1
viscous length(μm)	50.1	70.2
thermal length(μm)	102.7	143.1
bulk density (kg/m^3)	140.68	135.21

Fig. 6 shows the test samples for scaled reverberation chamber and impedance tubes. The compositing multi-layer is 2-layer and 3-layer. The composition for 2-layer is PET felt and mixed felt. And the three layers are PET felt, mix felt, and PET felt. For the comparison and verification, we fabricated the prototypes for 2-layer and 3-layer. These are for the impedance tubes and the scaled reverberation chamber. We compared the data for two cases.

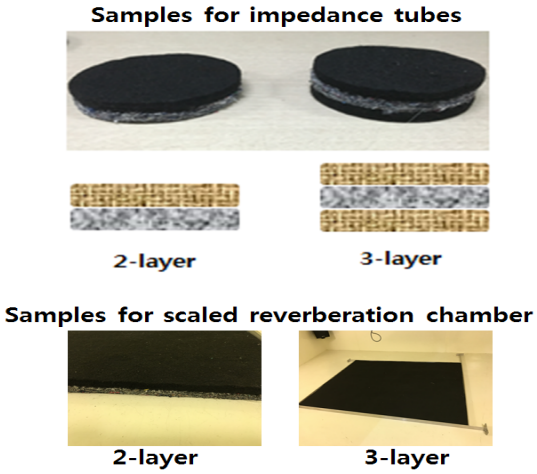

Fig. 6 The test sample with multi-layer

Fig. 7 shows the curves of the sound absorbing coefficient calculated by using NOVA and conducted by using impedance tubes. As shown in Fig. 7, the curves are similar because the error is in 10%. It shows that the sound absorbing coefficient for multi-layer with the calculated properties can be predicted. So, we can use the method for the sound absorption design of automotive interior with multi-layer for impedance tube. Fig. 8 shows the curves of the sound absorption coefficient calculated by using NOVA and conducted with the scaled reverberation chamber. As shown in Fig. 8, there is some error in the curves. For the impedance tubes, the direction of sound progress is perpendicular to the side of nonwoven. It is different from the scaled reverberation chamber. So, we need to identify it. Additionally, we will find correlation coefficient in the future.

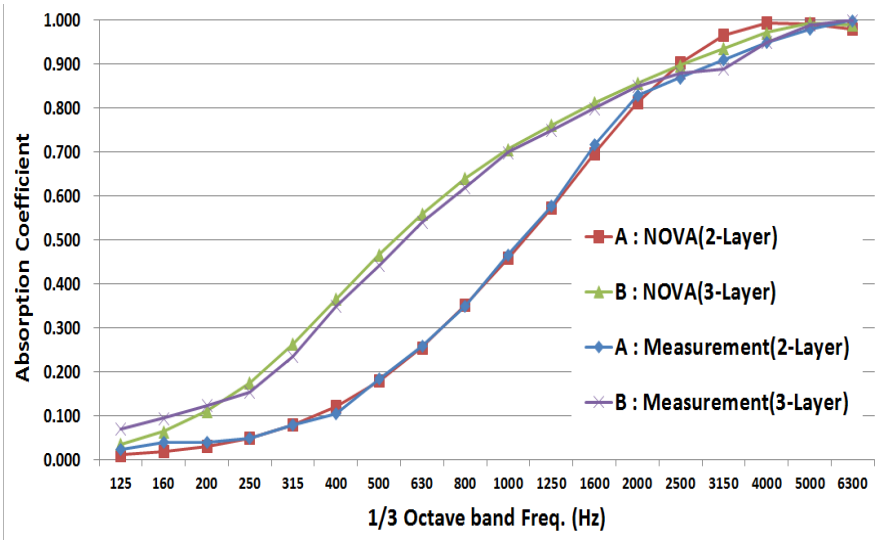

Fig. 7 The comparison of the calculated and measured data with impedance tubes

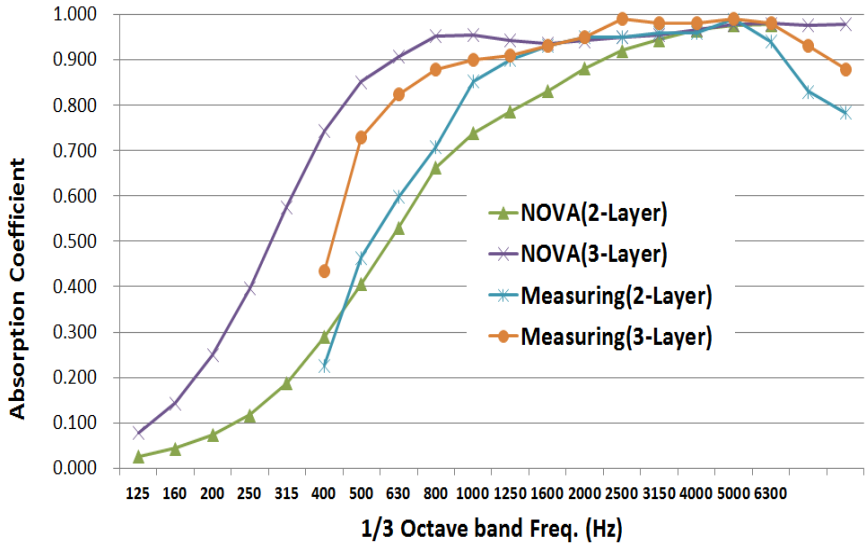

Fig. 8 The comparison of the calculated and measured data with scaled reverberation chamber

IV. Conclusion

We measured the sound absorption coefficient for several materials using impedance tube. With the data, we calculated the physical properties by using commercial software Foam-X. And using the data, we predicted the sound absorption coefficient for materials with multi-layer. And then it was compared with the measured value with the prototypes for the impedance tubes and the scaled reverberation chamber. The sound absorption coefficient curves predicted by software and measured by impedance tubes are nearly the same. But, for scaled reverberation chamber, it has some difference. We will investigate the reason and find the correlation coefficient for it in the future.

In this paper, it was verified that this method can be used for sound absorption design for automotive interior with multi-layer for impedance tubes. It is not easy to meet the target for the sound absorption since the material consists of multi-layer. While the automotive interior with multi-layer is developed, the tuning test is conducted so many times in practice. If sound absorption is predicted, it can be developed without many tuning tests. So, it can save money and time.

Acknowledgment

This research was supported by the Ministry of Trade, Industry & Energy (MOTIE), Korea Institute for Advancement of Technology (KIAT) through the Encouragement Program for The Industries of Economic Cooperation Region

References

[1] J. T. Kim, “Measurement of acoustic parameters and prediction of absorption coefficient of porous soundproofing materials,” Master’ Thesis, KAIST, 1997.

[2] Foam-X Instruction Manual, “Acoustic property identification for foam and fiber materials”, Mecanum, Canada.

[3] C.M. Lee, Y. S. Wang, “A Prediction method of the acoustic properties of multilayed noise control materials standing wave-duct systems,”

Belmont, Journal of Sound and Vibration, Vol. 298, No 1, pp.350~365, 2006

[4] T. Rostand, “On the holes interaction and heterogeneity distribution effects on the acoustic properties of air-cavity backed perforated plates,” Applied Acoustics, Vol. 74, pp. 1492~1498, 2013.

[5] H. J. Park, “A study on the effect of acoustic properties on the absorption characteristics of polyester fiber materials,” KSNVE, the Proceedings of KSNVE, pp.885~891, 2003

[6] M. E. Delany, E. N. Bazley, “Acoustical properties of fibrous materials,” Applied Acoustics, Vol 3, pp. 105~116, 1970.

Development and Sound Absorption and Insulation Performance Evaluation of Nonwoven Fabric Material including Paper Honeycomb Structure for Insulator Covering Shelf Trim

In-Sung Lee, Un-Hwan Park, Jun-Hyeok Heo, Dae-Gyu Park

***Abstract*—**Insulator Covering Shelf Trim is one of automotive interior parts located in the rear seat of a car. And it is a component that is the most strongly demanded for impact resistance, strength, and heat resistance. Such an Insulator Covering Shelf Trim is composed of a polyethyleneterephthalate(PET) nonwoven fabric which is a surface material appearing externally and a substrate layer which exerts shape and mechanical strength. In this paper, we develop a lightweight Insulator Covering Shelf Trim using the nonwoven fabric material with a high strength honeycomb structure and evaluate sound absorption and insulation performance by using acoustic impedance tubes .

***Keywords*—**Sound Absorption and Insulation, Insulator Covering Shelf Trim, Nonwoven fabric, Honeycomb.

I. INTRODUCTION

BY the time the driver remains in the car is increased, such as the material and upgrading quality of automobile interior materials are increasingly important.

In particular there is a growing demand for quiet due to noise blocking occurring inside and outside the vehicle.

We develop nonwoven fabric materials including honeycomb structure to develop high strength, lightweight Insulator Covering Shelf trim. And we will evaluate the physical properties and sound absorption performance of the developed nonwoven fabric material and compare the performance with the existing material.

In order to improve the shape maintenance and impact resistance of the nonwoven fabric material, it is necessary to increase the weight to increase the thickness.

However, if a honeycomb structure is used, it is possible to develop Insulator Covering Shelf trim which does not increase in weight even if it has a certain thickness, does not increase in weight, and has high strength and impact resistance[1].

In-Sung Lee and the others are with the Korea Textile Machinery Research Institute #27 Sampung-Ro Gyeongsan-City Gyeongbuk, 38542, Korea(phone: +82-53- 819-3145; fax: +82-53-819-3119; e-mail: islee@kotmi.re.kr)

Un-Hwan Park is with the Smart Machine Research Department in KOTMI, #27 Sampung-Ro Gyeongsan-City Gyeongbuk, 38542, Korea(phone: +82-53- 819-3141; fax: +82-53-819-3119; e-mail: uhpark@kotmi.re.kr).

Dae-Gyu Park is with the Korea Textile Machinery Research Institute, #27 Sampung-Ro Gyeongsan-City Gyeongbuk, 38542, Korea(phone: +82-53- 819-3131; fax: +82-53-819-3119; e-mail: dkpark@kotmi.re.kr).

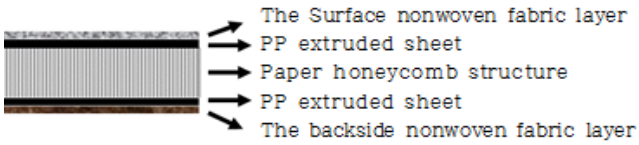

Fig. 1 Nonwoven material composition of integral type Covering Shelf Trim including honeycomb structure

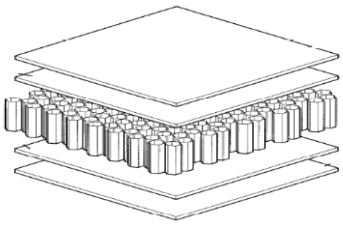

Fig. 2 Composite material composition of car interior material with honeycomb integral structure

Fig. 3 Paper honeycomb structure

Fig. 1 and Fig. 2 above show the composition of composite automotive interior material including honeycomb structure. And fig. 3 shows paper honeycomb structure.

II. LIGHTWEIGHT MATERIAL COMPOSITION

A. Material composition for lightweight

Table 1 Unit weight by material

Material of layer	Unit Weight	Material composition
Surface nonwoven fabric layer	250	PET 3d : 6d : 10D = 20% : 20% : 60%
PP extruded sheet	600	LDPE : PP = 20:80
Paper Honeycomb	100	paper 100%
PP extruded sheet	600	LDPE : PP = 20:80
Backside nonwoven fabric layer	150	PET 3d : 6d : 10D = 20% : 20% : 60%
Sum	**1,700**	

Table 1 shows the material composition and unit weight of each layer for light weight of the honeycomb integrated type nonwoven fabric material[2]. It indicates the weight of the material which achieved 30% or more weight reduction compared to the existing material.

III. EVALUATION OF SOUND ABSORPTION AND INSULATION PERFORMANCE OF NONWOVEN FABRIC MATERIAL

Sound absorption coefficient is measured with acoustic impedance tubes. It is calculated with the absorbed amount that is not reflected about the input sound[3].

Transmission loss uses the transmittance τ as a value indicating the sound insulation effect of the sound insulation material. And as for the transmission loss, TL is used as the symbol as the common logarithm of the reciprocal of τ multiplied by 10. It is displayed as TL = 10 log101 / τ [dB], and the higher the frequency, the higher the value the heavier the material[3]-[5].

Fig. 4 Experimental test sample

In the photograph of the test sample of Fig. 4, the two on the left are the samples for the sound absorption test and the two on the right are the samples for the sound insulation test.

The diameter of the sound absorption test sample is 100 mm (low frequency tube) and 30 mm (high frequency tube), the test sample of the sound insulation test has a diameter of 108 mm (low frequency tube) and 35 mm (high frequency tube).

1) Sound absorption coefficient (Vertical incidence, Low frequency tube)

Table 2 Sound absorption coefficient (Vertical incidence, Low frequency tube)

1/3 Octave Center Freq. [Hz]	S1
125	0.05
160	0.10
200	0.15
250	0.22
315	0.25
400	0.21
500	0.20
630	0.16
800	0.18
1000	0.28
1250	0.22
1600	0.17

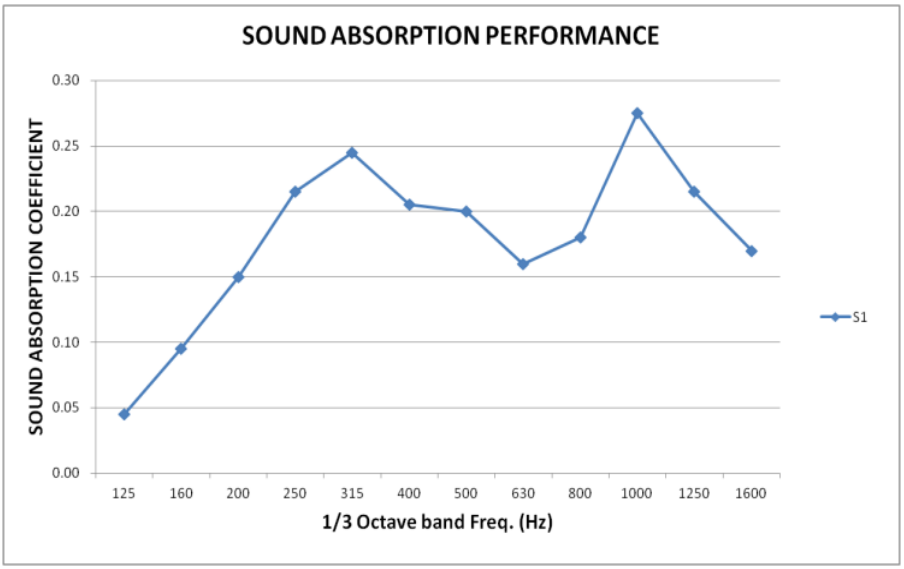

Fig. 5 Sound Absorption Performance (Low frequency tube)

2) Sound absorption coefficient (Vertical incidence, High frequency tube)

Table 3 Sound absorption coefficient (Vertical incidence, High frequency tube)

1/3 Octave Center Freq. [Hz]	S1
500	0.23
630	0.37
800	0.59
1000	0.78
1250	0.77
1600	0.61
2000	0.48
2500	0.46
3150	0.41
4000	0.38
5000	0.32
6300	0.30

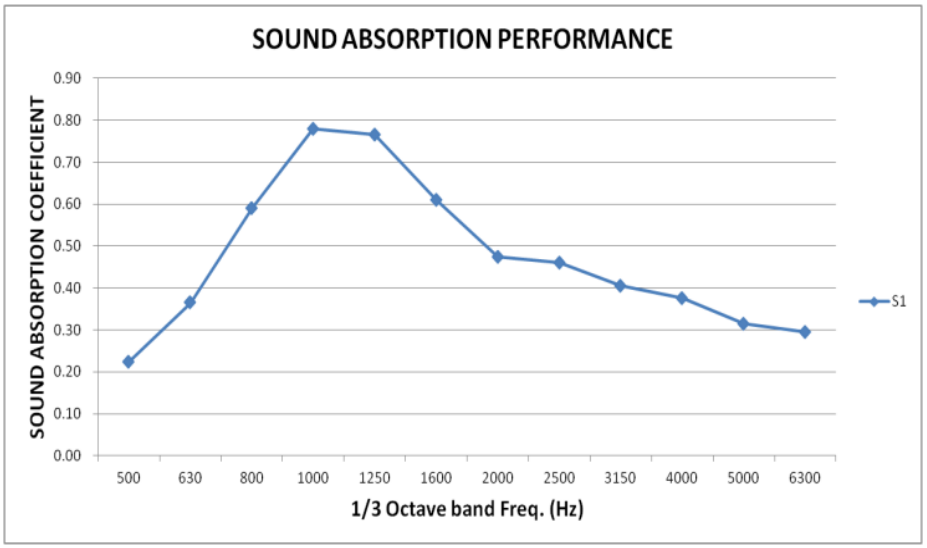

Fig. 6 Sound Absorption Performance (High frequency tube)

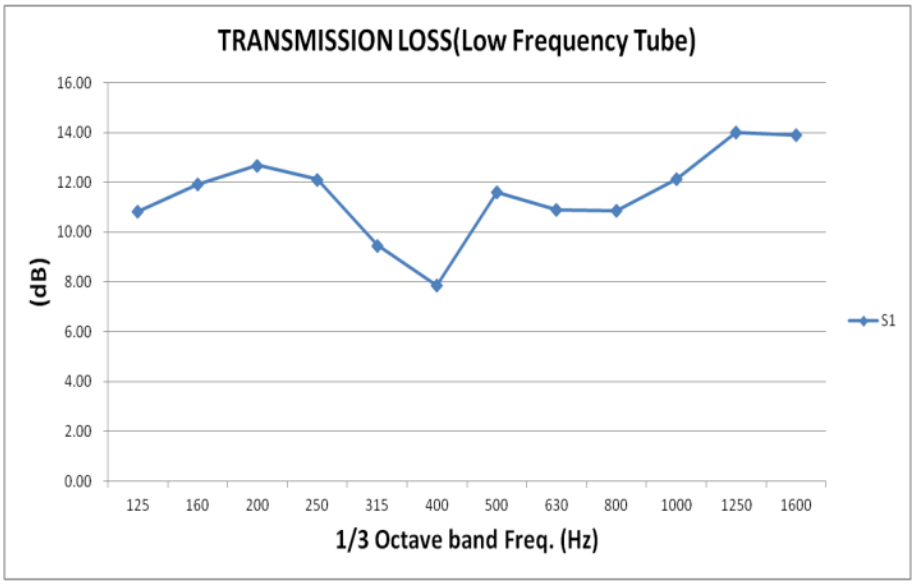

Fig. 7 Transmission Loss (Low Frequency tube)

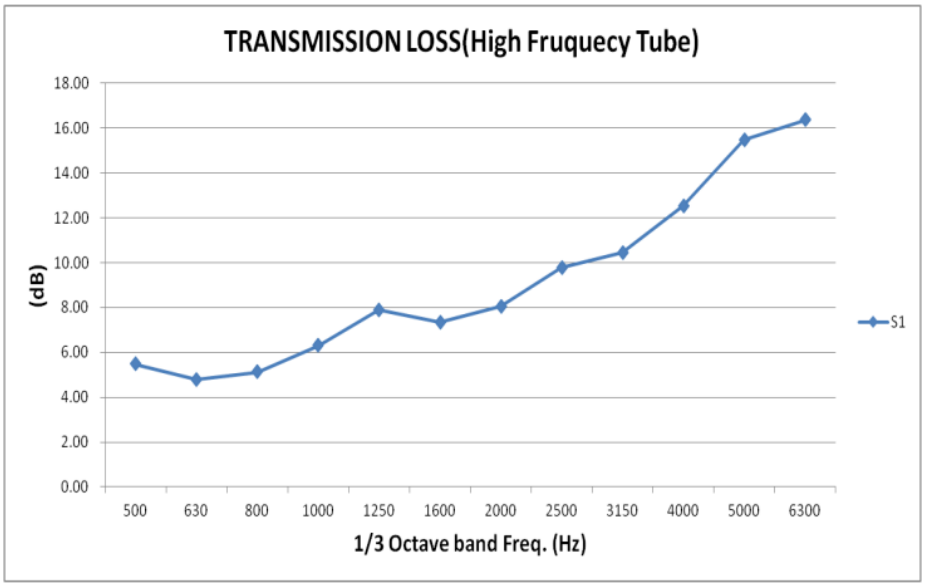

Fig. 8 Transmission Loss (High Frequency tube)

3) Transmission loss (Low frequency tube)

Table 4 Transmission loss (Low frequency tube)

1/3 Octave Center Freq. [Hz]	S1
125	10.08
160	11.92
200	12.68
250	12.12
315	9.47
400	7.87
500	11.60
630	10.90
800	10.86
1000	12.15
1250	14.01
1600	13.90

4) Transmission loss (High frequency tube)

Table 5 Transmission loss (High frequency tube)

1/3 Octave Center Freq. [Hz]	S1
500	5.48
630	4.78
800	5.13
1000	6.30
1250	7.88
1600	7.35
2000	8.04
2500	9.77
3150	10.43
4000	12.52
5000	15.49
6300	16.36

IV. CONCLUSION

Weight reduction can be realized while increasing the strength by applying the honeycomb structure for the first time to the material of automotive interior materials.

Therefore, in order to improve shape retention and impact resistance for weight reduction and environment-friendly application which is a problem of all current products, the weight has to be increased if the wall thickness is increased. However, the honeycomb structure could develop Insulator Covering Shelf Trim, which does not increase in weight even if it has a certain thickness but does not increase in weight and has high strength and impact resistance.

It is possible to develop interior materials that can reduce the interior noises of the vehicle by adding sound absorption and insulation performance. In addition, since it has a honeycomb structure, shock and twisting can be prevented. Finally, the weight of the entire Insulator Covering Shelf Trim product could be reduced by 30%.

ACKNOWLEDGMENT

This research was supported by the Ministry of Trade, Industry & Energy(MOTIE), Korea Institute for Advancement of Technology(KIAT) through the Encouragement Program for The Industries of Economic Cooperation Region

REFERENCES

[1] Y. Choi and D. Lim, “Light Weight Textile Materials for Automotive Industry”, Fiber Tech Ind, 2010, 14, 18-26.

[2] 小林稔, “自動車輕量化技術の開發動向“, 東レリサ一チセン タ一調查研究部, 東京, 2010, pp.1-11

[3] M. Matsudaira and Y. Kondo, “The Effect of a Grooved Hollow in a Fiber on Fabric Moisture and Heat Transport Properties”, J Text Inst, 1996, 87, 409-415.M. Young, *The Techincal Writers Handbook.* Mill Valley, CA: University Science, 1989.

[4] H. J. Shm, K. A. Hong, and H. S. Kim, “Comparison of Hand and Thermal Properties of Woven Fabrics Made from Hollow and Regular Fibers”, J Korean Fiber Soc, 2000, 37, 280-285.

[5] Y. Na and G. Cho, “Sound Absorption and Viscoelastic Property of Acoustical Automotive Nonwovens and Their Plasma Treatment”, Fiber Polym, 2010, 11, 782-789.

Numerical Experiments for the Purpose of Studying Space-Time Evolution of Various Forms of Pulse Signals in the Collisional Cold Plasma

N. Kh. Gomidze, I. N. Jabnidze, K. A. Makharadze

***Abstract*—**The influence of inhomogeneities of plasma and statistical characteristics on the propagation of signal is very actual in wireless communication systems. While propagating in the media, the deformation and evaluation of the signal in time and space take place and on the receiver we get a deformed signal. The present article is dedicated to studying the space-time evolution of rectangular, sinusoidal, exponential and bi-exponential impulses via numerical experiment in the collisional, cold plasma. The presented method is not based on the Fourier-presentation of the signal. Analytically, we have received the general image depicting the space-time evolution of the radio impulse amplitude that gives an opportunity to analyze the concrete results in the case of primary impulse.

***Keywords*—**Collisional, cold plasma, rectangular pulse signal, impulse envelope.

I. Introduction

THE study of the distortion of radio impulses in a dispersing plasma began a long time ago [1], [2], although the issue is still authentic due to its practical value. The objectives on the distribution of radio impulses through the ionosphere are also very important. In this direction, studies take into account the analysis of the frequency spectrum data of the scattered signal, which can be obtained through the analytical or numerical Fourier transformation [3]-[6]. In many of them, narrow band linear approximation of the signal is used, which greatly simplifies the analysis of distortion or Gaussian rectangular impulse analysis. Usually, there are many works that are devoted to the impulse propagation in non-collisional plasma, but in the communications, broadband linear impulses are mostly used during locating and sounding the surrounding environment, and therefore, the approximate assumptions made for the narrowband linear signals are unacceptable and unused. Fourier reversal transformation for wideband linear impulses can be done only with numerical methods. The results are partially presented in works [7]-[11].

II. Problem Statement: Receive a General Image for the Impulse Envelope

Let us say we have an impulse, the propagation of which is described as a wave equation [12]:

$$\frac{\partial^2 \vec{E}}{\partial z^2} = \frac{1}{c^2}\frac{\partial^2 \vec{E}}{\partial t^2} + \frac{4\pi}{c^2}\frac{\partial^2 \vec{P}}{\partial t^2} \tag{1}$$

where $\vec{E}$ is tension of electric field, c is the speed of light propagation in the media, z is the direction of the radio impulse propagation, t is the time of propagation, and $\vec{P}$ is the polarization of the unit volume in the media. Let us assume that media contains free charges, then the polarization vector $\vec{P}$ satisfies the equation [12]:

$$\frac{\partial^2 \vec{P}}{\partial t^2} + \nu\frac{\partial \vec{P}}{\partial t} = \frac{e^2 N}{m}\vec{E} \tag{2}$$

where e and n are the charge of the electron and mass, N is the electronic concentration, and ν is the effective frequency of collision, which envisages the loss of energy during the collision with the ions of electrons and neutral molecules.

On the boarder of $z \geq 0$ half-plane, on which an impulse is propagated, a field is created, the tension of which can be represented in the following way:

$$E(0,t) = A(0,t)\exp(i\omega t),\ t \geq 0 \tag{3}$$

where $\omega = 2\pi f$; f is a carrier signal of the impulse. $A(0;t)$ is an impulse envelope, when $z = 0$. It is obvious that the impulse is propagated by c speed, so it is advisable to look for the $E(z,t)$ field in the following form.

$$E(z,t) = \begin{cases} A(z,t')\exp[i(\omega t - kz)] & t' > 0 \\ 0 & t' \leq 0 \end{cases}. \tag{4}$$

Consider in (1) and (2) that:

$$z' = z \quad t' = t - \frac{z}{c} \tag{5}$$

Insert (4) in (1) and (2) and we receive:

$$\frac{\partial^2 A}{\partial z'^2} - \frac{2}{c}\frac{\partial^2 A}{\partial z' \partial t'} - 2ik\frac{\partial A}{\partial z'} = \frac{4\pi}{c^2}\frac{\partial^2 P}{\partial t'^2}\exp(-i\omega t') \tag{6}$$

N. Kh. Gomidze is with the Physics Department of Batumi Shota Rustaveli State University, Batumi, 6010 Georgia (corresponding author, phone: +995 77 17-97-27, e-mail: gomidze@ bsu.edu.ge).

I. N. Jabnidze and K. A. Makharadze are with the Physics Department of Batumi Shota Rustaveli State University, Batumi, 6010 Georgia (e-mail: izolda.jabnidze@bsu.edu.ge, k.makharadze.01@gmail.com).

$$\frac{\partial^2 P}{\partial t'^2}+\nu\frac{\partial P}{\partial t'}=\frac{e^2N}{m}A(z';t')\exp(i\omega t) \tag{7}$$

Let us say the duration of impulse t_i - satisfies the inequality:

$$ft_i >> 1 \tag{8}$$

and the impulse z' takes an interval on the axis:

$$L_i = ct_i >> \lambda \tag{9}$$

Therefore, the following condition is fulfilled:

$$\left|\frac{\partial^2 A}{\partial z'^2}\right| \approx \left|\frac{1}{L_i}\frac{\partial A}{\partial z'}\right| << \left|\frac{4\pi}{\lambda}\frac{\partial A}{\partial z'}\right| \tag{10}$$

The (10) condition allows to ignore the first member in the image (6). Since the location and speed of the electron cannot be changed immediately, at the time of transmitting impulse in the cold plasma, the following equation is fulfilled in the z' point:

$$P(z';0)=0\,,\ \left.\frac{\partial P}{\partial t'}\right|_{t'=0}=0 \tag{11}$$

By the strength of (11), the solution of (7) can be written as the following:

$$P(z';t')=\frac{e^2N}{m}\int_0^{t'}E(z';\tau)\frac{1-\exp[-\tau(t'-\tau)]}{\tau}\partial\tau \tag{12}$$

Insert the solution of (12) in (6) and take into consideration (10), then for the impulse envelope, the equation becomes:

$$\frac{\partial^2 A}{\partial z'\partial t'}+i\omega\frac{\partial A}{\partial z'}=-\frac{2\pi e^2N}{mc}A(z';t')+ \\ +\frac{2\pi e^2N}{mc}\nu\int_0^{t}A(z';\tau)\exp[-(\nu+i\omega)(t'-\tau)]\partial\tau \tag{13}$$

For (13), let us use the Laplace transformation towards the t' variable, we get [13]:

$$L(z';p)=L(p)\exp\left[-\frac{\eta z'}{p+\nu+i\omega}\right] \tag{14}$$

where the following indications are introduced:

$$L(z';p)=\int_0^{\infty}A(z't')\exp(-pt')dt'\,,\ L(p)=\int_0^{\infty}A(0,t')\exp(-pt')dt'$$

where, $\eta=\omega_p^2/(2c)$, $\omega_p^2=(4\pi e^2N)/m$ [5]; when $t=0$ impulse still is not in the media, and therefore $\partial A(z';0)/\partial z'=0$. Now, let us make Laplace's Reverse Transformation:

$$A(z';t')=A(0;t')-\int_0^{\infty}\frac{\sqrt{\eta}}{\sqrt{t'-\tau}}J_1\left(2\sqrt{\eta(t'-\tau)}\right)\cdot \\ \cdot\exp\left[-(\nu+i\omega t)(t'+i\omega t)\right]A(0;\tau)\,d\tau \tag{15}$$

where, $J_k(x)$ is Bessel function [13].

III. Spatial-Time and Spatial-Frequency Evolution for Bi-Exponential, Sinusoidal and Rectangular Pulse Signals in Dispersive Plasma

Let us write down the solution of (15) for the initial envelopes which have **bi-exponential** form:

$$A(0,t')=A_0\begin{cases}\exp\left(-\alpha\frac{t'}{t_i}\right)-\exp\left(-\beta\frac{t'}{t_i}\right), & t'\le t_i\\ 0, & t'>t_i\end{cases}, \tag{16}$$

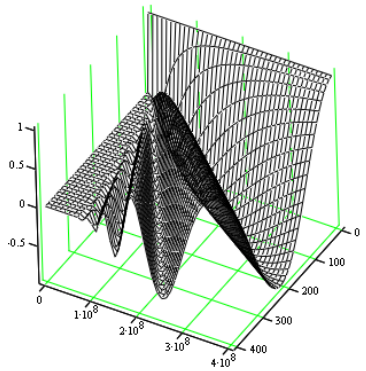

Fig. 1 The spatial-frequency evolution of the real and imaginary parts of the impulse envelope in collisional isotropic plasma when $\nu=10^7$ Hz, $0<z'\le 400$ m, $0<\omega\le 4\cdot10^8$ sec^{-1}

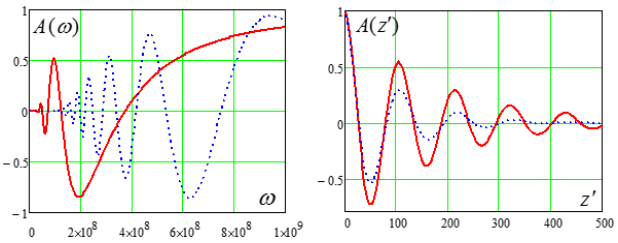

Fig. 2 (a) $A(\omega)$ attitude for different values of distance $z'=100$ m (red line) and $z'=1000$ m (dotted line), when $\nu=10^7$ Hz; (b) $A(z)$ attitude for different values of collision frequency $\nu=10^7$ Hz (red line) and $\nu=2\cdot10^7$ Hz (dotted line)

Here, A_0,α,β numbers determine the curvature of the front and rear fronts of the impulse. Let us introduce a new variable $x=\sqrt{\tau/t}$ and insert (16) in (15). We get:

$$A(z't') = A(z't';\alpha) - A(z't';\beta) \tag{17}$$

where:

$$A(z';t';\alpha) = A_0 \exp\left(-\alpha\frac{t'}{t_i}\right)\cdot \left[1-\int_0^1 J_1\left(2\chi\sqrt{\eta t'}\right)\exp\left[-\left(\nu-\frac{\alpha}{t_i}+i\omega\right)t'x^2\right]\right]\left(2\sqrt{\eta t'}\right)\partial x \tag{18}$$

$$A(z';t';\beta) = A_0 \exp\left(-\beta\frac{t'}{t_i}\right)\cdot \left[1-\int_0^1 J_1\left(2\chi\sqrt{\eta t'}\right)\exp\left[-\left(\nu-\frac{\beta}{t_i}+i\omega\right)t'x^2\right]\right]\left(2\sqrt{\eta t'}\right)\partial x \tag{19}$$

Consider the occasion when the initial impulse is of a **sinusoidal** form, then its initial envelope can be written down as following:

$$A(0,t) = \begin{cases} \sin\left(\dfrac{\pi t}{t_i}\right), & t \le t_i \\ 0, & t \ge t_i \end{cases} \tag{20}$$

Let us introduce (19) as follows:

$$A(0,t) = \begin{cases} g(0,t), & t \le t_i \\ g(0,t) + g(0,t-t_i), & t \ge t_i \end{cases} \tag{21}$$

where

$$g(0;t) = \frac{1}{2i}\left[\exp\left(i\pi\frac{t}{t_i}\right) - \exp\left(-i\pi\frac{t}{t_i}\right)\right].$$

Let us put (21) in (15) and do the same operations as above, then for the envelope of a deformed sinusoid impulse we get:

$$A(z',t') = \begin{cases} g(z',t'), & t \le t_i \\ g(z',t') + g(z,t'-t_i), & t \ge t_i \end{cases}, \tag{22}$$

where:

$$g(z';t') = \frac{1}{2i}\exp\left(i\pi\frac{t'}{t_i}\right)\left[1-\int_0^1 J_1\left(2x\sqrt{\eta t'}\right)\cdot \exp\left[-\left(\nu+\frac{i\pi}{t_i}+i\omega\right)t'x^2\left(2\sqrt{\eta t'}\right)\partial x\right] - \frac{\exp\left(-i\pi\dfrac{t'}{t_i}\right)}{2i}\right]\cdot \left[1-\int_0^1 J_1\left(2x\sqrt{\eta\cdot z\cdot t'}\right)\exp\left[\tau+\frac{i\pi}{t_i}+i\omega\right]t'x^2\right]\left(2\left(\sqrt{\eta\cdot z\cdot t'}\right)\partial x\right) \tag{23}$$

Now, go to the case of **rectangular** impulse envelope:

$$A(0;t) = \begin{cases} 1, & 0 < t \le t_i \\ 0, & t > t_i \end{cases} \tag{24}$$

After the distortion, such impulse can be described as:

$$A(z';t') = \begin{cases} g(z',t'), & 0 \le t' \le t_i \\ g(z',t') - g(z';t'-t_i), & t' > t_i \end{cases} \tag{25}$$

In the case of finding $g(z',t')$ function, we should pay attention to the fact that, at the same time, when $\alpha \to 0$ and $\beta \to \infty$, the bi-exponential impulse is transformed into a step-function signal with the height of A_0, at the same time $A = 0$, when $t = 0$. In (18) and (19) expressions after performing the corresponding transformations, when we get $t' > 0$, and we get the envelope of the step-function signal $(A_0 = 1)$:

$$g(z';t') = 1 - \int_0^1 \sqrt{\eta z'}\,J_1\left(2x\sqrt{\eta z'\tau}\right)\exp\left[-(\nu+i\omega)t'x^2\right]\partial x. \tag{26}$$

It should be noted that each of the above solutions can be presented as a combination of Lomel's function [14]. With t' growing, the task on the fall of the step-function signal on the semi-infinite boundary of homogeneous media is simplified and transfers onto the task of propagating the flat wave in a homogeneous media. Let us show that the obtained result satisfies this requirement. Apply (15) that takes the following image for the step-function signal:

$$A(z';t') = 1 - \int_0^{t'} \frac{\sqrt{\eta z'}}{\sqrt{\tau}} J_1\left(2\sqrt{\eta z'\tau}\right)\exp\left[-(\nu+i\omega)\tau\right]\partial\tau \tag{27}$$

It is easy to notice that in (26) and (27) the correlations are equal. In the last equation $t' \to \infty$; then the integral on the right side will be reduced to a tabular form. According to its calculations, we get:

$$A(z',\omega) = \exp\left[-\frac{\sigma(\omega)}{2\left(1+\dfrac{\nu^2}{\omega^2}\right)}\right]\exp\left[-i\frac{\chi(\omega)z'\omega}{2\left(1+\dfrac{\nu^2}{\omega^2}\right)\nu}\right] \tag{28}$$

where, $\chi(\omega) = \omega_p^2\nu/(\omega^2 c)$ - is plasma absorption coefficient and $\sigma(\omega)$ - is the optical depth on the z' distance the wave passes through.

In Fig. 1, the space-frequency evolution of the impulse envelope is represented as a three-dimensional schedule. The real part indicates at the change of impulse amplitude, and the imaginary - at the reduction, which is caused by relaxation processes. In this case, $0 < z' \le 400$ m, $0 < \omega \le 4\cdot 10^8$ sec^{-1}. For better observation on the picture, the value $\nu = 10^7$ Hz has been chosen for frequency of the collision. Fig. 2 shows $A(\omega)$ and $A(z')$ attitudes on the plane in the section. In Fig. 2 (a), it is possible to see the frequency dispersion effect, in particular, during value of $z' = 100$ m (unbroken line), the envelope aspires towards saturation along with the frequency increase

or when $\omega\to\infty$, then $A(\omega)\to 1$, and when $z'=1000$ m (dotted line), additional oscillations generate the amplitude of which increases slowly along with the frequency increase. From Fig. 2 (b) it is clear that the increase of the frequency of collisions causes the rapid reduction of oscillations of impulse; with the purpose of good visualization, we have brought here the values of the frequencies of $\nu=10^7$ Hz (dotted line) and $\nu=2\cdot10^7$ Hz (red line) collisions.

IV. Evaluation of the Impulse Propagation Rate in the Dispersive Plasma

Let us find the analytical expression for the speed of the radio impulse propagation. Let us use (26) and calculate the integral applying Bessel's well- known ratio:

$$\frac{\partial\left(x^{k+1}J_{k+1}(x)\right)}{\partial x}=x^{k+1}J_k(x) \tag{29}$$

As a result we receive:

$$g(z';t')=\exp\{-(\nu+i\omega)t'\}\sum\left\{(\nu+i\omega)\sqrt{\frac{t'}{\eta}}J_k\left(2\sqrt{\eta\cdot z'\cdot t'}\right)\right\} \tag{30}$$

The following equality will always be on the ionospheric track: $2\sqrt{\eta\cdot z'\cdot t'}>>1$.

Let us apply the asymptotic representation of the Bessel's function, for the greater value of the argument [14]:

$$J_k\left(2\sqrt{\eta\cdot z'\cdot t'}\right)\cong\frac{1}{\sqrt{\pi\sqrt{\eta\cdot z'\cdot t'}}}\cdot\cos\left(2\sqrt{\eta\cdot z'\cdot t'}-\frac{k\pi}{2}-\frac{\pi}{4}\right) \tag{31}$$

Insert (31) in (30), then for $A(z',t')$ to get the expression:

$$A(z',t')\cong\frac{1}{\sqrt{\pi}\sqrt{\eta\cdot z'\cdot t'}}\exp\left[-(\nu+i\omega)t'\right]\cdot \cdot\frac{\cos\left(2\sqrt{\eta\cdot z'\cdot t'}-arctg\left[(\nu+i\omega)\sqrt{\frac{t'}{\eta\cdot z'}}-\frac{\pi}{4}\right]\right)}{\sqrt{1+(\nu+i\omega)^2\left(\frac{t'}{\eta\cdot z'}\right)}}. \tag{32}$$

From (32), we can see that on z' axis, the impulse is concentrated near the point the coordinate of which satisfies the condition:

$$\left(\omega^2-\nu^2\right)\left(\frac{t'}{\eta\cdot z'}\right)=1 \tag{33}$$

From here, we receive that the front of the rectangular impulse propagates with the speed:

$$\mathrm{v}=\frac{c}{1+\frac{0.5\omega_p^2}{\omega^2-\nu^2}} \tag{34}$$

Equation (34) shows that the effects of collision effect on the speed of the impulse speed, when $\nu\to\omega$, i.e. while the impulse is strongly absorbed during propagation from the plasma media.

With the minimum losses for the impulse propagation, it is necessary to fulfill the following condition $\omega>>\nu$, therefore:

$$\mathrm{v}=\frac{c}{1+\frac{\omega_p^2}{2\omega^2}} \tag{35}$$

Equation (35) shows that the time required to overcome the distance by the impulse on a fixed length increases as a result of the frequency decrease and the increase of electronic concentration.

Fig. 3 shows the change of impulse speed in collisional plasma according to a frequency for different number of collisions. The wave propagates if the condition $f>>\nu$ is fulfilled, when $\nu\to f$ the speed of the signal propagation is minimal, as the absorption processes are important.

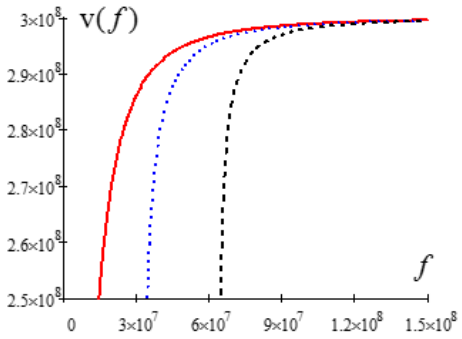

Fig. 3 Change of impulse speed according to a wave frequency during different frequencies of collisions $\nu=10^7$ Hz (red line); $\nu=2\cdot10^8$ Hz (blue dotted line); $\nu=4\cdot10^8$ Hz (black dotted line)

V. Outcomes of Numerical Experiment

Image (15) gives an opportunity to evaluate the change of the shape of the envelope of pulse signals of different shapes and durations in time at different altitudes from the Earth's surface. Numerical experiments are for the impulses of 10^{-4}, and 10^{-5} seconds when the frequency of the carrier signal $f=10$ MHz has been studied in [8]. The case of the numerical experiment when the frequency of the carrier signal is close to the plasma frequency, i.e. when: $f_0=2.84$ MHz ($f=3$ MHz) is represented [14], [15], it is obvious that the condition $f>f_0$ must be fulfilled, otherwise the impulse cannot be propagated in the plasma layer.

Suppose the impulse signal emits from the source of the Earth's surface. The objective of the current research is to determine the change of the impulse shape (distortion) in the

lower layers of the ionosphere at the altitude of $z = 100 - 1000$ km. Numerical calculations were carried out for the following parameters of the plasma media: Number of collisions $\nu = 10^3$, 10^4 sec^{-1}, concentration - $N = 10^5$.

We have studied the relationship of the radiation power $|A|^2$ on the time at different distances from the source, for different forms of impulse. It has been established that an increase in the number of collisions causes the distortion of the shape of the impulse, which is naturally explained by the emergence of dissipation processes.

Fig. 4 shows the change of the sinusoidal impulse envelope in the dispersive plasma layer at different altitudes. The impulse of $t_i = 10^{-3}$ sec of the duration at the altitude of $z = 200$ km still maintains the sinusoidal shape, and by the increase of the height ($z = 700$ km), the cyclical oscillations will be created in the impulse envelope. The back front of the impulse is basically distorted. And by shortening the impulse, on the contrary, the oscillations disappear and the displacement of the maximum can be noticed. Together with the rise of collisions, these oscillations disappear, but the impulse is sharply narrowed and the amplitude falls.

It should be noted that among the discussed impulses, the bi-exponential impulse can be distinguished by its steady shape, which is different from others with less oscillations than rectangular or sinusoidal impulses. In this case, the dissipative processes caused by the collisional effects are manifested primarily in a decrease in the intensity of the pulse signal.

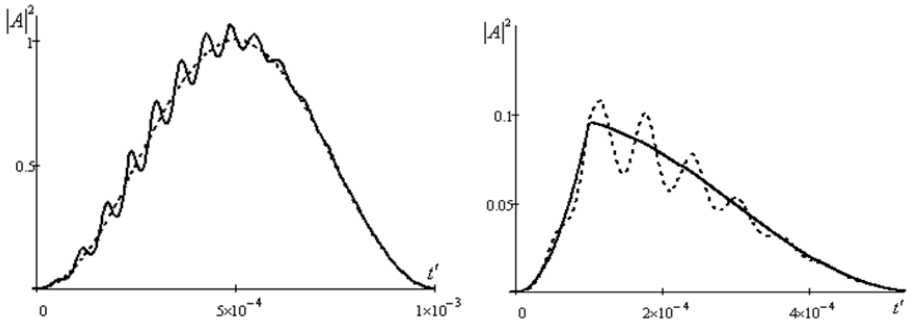

(a) (b)

Fig. 4 Evaluation of envelope of sinusoidal pulse signal in collisional, isotropic cold plasma at the altitude $z = 200$ km (dot line) and $z = 700$ km (solid line), when $\nu = 10^4$ sec^{-1}, $f = 10^7$ Hz, for impulse durations (a) $t_i = 10^{-3}$ sec and (b) $t_i = 10^{-4}$ sec

ACKNOWLEDGMENT

The work has been done within the framework of the following scientific projects:

1. "Radio Spectral Diagnostics of Media on the Basis Correlation between Signal and Dispersive Characteristics of Media" - RF/640/5-451 (№31/33. scientific supervisor Associated Prof. Izolda Jabnidze), financed by SRNSF (Shota Rustaveli National Scientific Found, Georgia).
2. "Quantitative analysis of fluorescence characteristics of optically solid, random phase screen and spectral analysis of the statistical moments of the correlation function of the intensity of scattered laser radiation" (FR/152/9-240/14 scientific supervisor Prof. Nugzar Gomidze), financed by SRNSF (Shota Rustaveli National Scientific Found, Georgia).

REFERENCES

[1] L. Brillouin. Apply Physics. 1914, v.44, p.203.
[2] N. Tessler, G. Eisenste. "Modelling carrier dynamics and small-signal modulation response in quantum-well lasers". Optical and Quantum Electronics, vol. 26, 1994. pp.767-787.
[3] L. A. Weinstein. "Propagation of pulses". UFN.1976, vol. 118, №2, pp. 339-367.
[4] B. N. Gershman, L. M. Yerukhimov, Yu. Ya. Yashin. "Wave phenomena in the ionosphere and cosmic plasma". M., 1984.
[5] V. L. Ginzburg. "The propagation of electromagnetic waves in a plasma". M: 1967.
[6] L. D. Landau, E. M. Lifshitz. "Theoretical physics. Electrodynamics of continuous media", vol. VIII, M.: "Nauka", 1982.
[7] N. Gomidze, O. Nakashidze, Z. Surmanidze. "Propagation of radio impulses in collisional isotropic plasma". Journal "Agmashenebeli", vol. 7, Tbilisi, 2009.
[8] N. Kh. Gomidze, M. R. Khajishvili, I. N. Jabnidze. "Changing form of the radio impulse in the dispersion media". Works of RSU, series: Natural Science and Medicine, vol. 15, Batumi, 2009, pp. 286-291 (in Georgian).
[9] N. Gomidze, M. Khajishvili, K. Makharadze, I. Jabnidze. "Some Features of Radio-Spectral Diagnostics of Random Media via PM and PRM Oscillations". Journal of Applied Mechanics and Materials, ISSN: 1660-9336, published by Trans Tech Publications inc. Switzerland, vol. 420 (2013), pp. 305-310.
[10] N. Kh. Gomidze, M. R. Khajishvili, I. N. Jabnidze, Z. J. Surmanidze. XXX URSI General Assembly, Istanbul, Turkey, August 13-20, 2011.
[11] D. V. Ivanov. Journal of communications technology & electronics. 2006, т. 51, №7, pp. 807-815.
[12] M. V. Vinogradova, O. V. Rudenko, A. P. Sukhorukov. "Theory of Waves". M: "Nauka", 1989.
[13] B. G. Korenev. "Introduction to the theory of Bessel functions". M: "Nauka", 1971.
[14] N. Kh. Gomidze, M. R. Khajishvi, I. N. Jabnidze. "About Change of Impulse Outskirts during Propagating in Dispersive Media". Journal of Physics Procedia, vol. 25, pp. 401-406, 2012.
[15] N. Kh. Gomidze, M. R, Khajishvili, K. A. Makharadze, I. N. Jabnidze Spatial-Frequency Evaluation of Radio Impulses on the Collisional Ionospheric Part. 2015 International Conference on Electromagnetics in Advanced Applications (ICEAA). Publisher IEEE, Torino, Italy, September 7-11, 2015, pp.486-489.

Nugzar Kh. Gomidze (22.09.1972) – Professor at the Batumi Shota Rustaveli State University, Batumi, Georgia. Doctor of Physical and Mathematical Sciences (1997). Scientific Interests: Radiophysics and research methods in radiophysics, remote sounding, spectroscopy and monitoring environment wave proceses in random media, physics of atmosphere.

Work experience: from 2013-until present - he works Quality Assurance Service of Faculty of Physics, Mathematics and Computer Sciences. 2006–2013 Head of Physics Department of Batumi Shota Rustaveli State University (BSU). 2008–2010 Scientific Secretary of Dissertation Council of Faculty of Natural Science and Medicine of BSU. 2006–2010 Member of Representative Council of BSU.

He is the author of about 40 scientific articles, 4 published books on general and applied physics (in Georgian). He developed scientific projects, which are funded by the Science Foundation of Georgia (FR/152/9-240/14, FR/640/6-110/12, SC/22/6-110/12, GNSF/ST08/5-451). Participated in about 20 scientific conferences. Under his guidance was created a laboratory for radiophysics and spectroscopy at BSU for the expressive and effective diagnostics of aqueous media based on spectrofluorescence.

Izolda N.Jabnidze (25.05.1973) –Associate Professor at the Batumi Shota Rustaveli State University, Batumi, Georgia. Doctor Physical and Mathematical Sciences (1999). Scientific Interests: Radiophysics and plasma Physics, research methods in radiophysics, remote sounding.

Work experience: from 2008-until present - she is Associate Professor of the Physics department at the BSU.

She is the author of some 20 scientific articles, and has published book on applied physics (in Georgian). She is scientific supervisor of one scientific project (GNSF/ST08/5-451) and the main personal in two scientific projects (FR/152/9-240/14, FR/640/6-110/12), which are funded by the Science Foundation of Georgia. She has participated in about 10 scientific conferences.

Flux-Gate vs. Anisotropic Magneto Resistance Magnetic Sensors Characteristics in Closed-Loop Operation

N. Hadjigeorgiou, S. Angelopoulos, E. Hristoforou, P. P. Sotiriadis

***Abstract*—**The increasing demand for accurate and reliable magnetic measurements over the past decades has paved the way for the development of different types of magnetic sensing systems as well as of more advanced measurement techniques. Anisotropic Magneto Resistance (AMR) sensors have emerged as a promising solution for applications requiring high resolution, providing an ideal balance between performance and cost. However, certain issues of AMR sensors such as non-linear response and measurement noise are rarely discussed in the relevant literature. In this work, an analog closed loop compensation system is proposed, developed and tested as a means to eliminate the non-linearity of AMR response, reduce the 1/f noise and enhance the sensitivity of magnetic sensor. Additional performance aspects, such as cross-axis and hysteresis effects are also examined. This system was analyzed using an analytical model and a P-Spice model, considering both the sensor itself as well as the accompanying electronic circuitry. In addition, a commercial closed loop architecture Flux-Gate sensor (calibrated and certified), has been used for comparison purposes. Three different experimental setups have been constructed for the purposes of this work, each one utilized for DC magnetic field measurements, AC magnetic field measurements and Noise density measurements respectively. The DC magnetic field measurements have been conducted in laboratory environment employing a cubic Helmholtz coil setup in order to calibrate and characterize the system under consideration. A high-accuracy DC power supply has been used for providing the operating current to the Helmholtz coils. The results were recorded by a multichannel voltmeter The AC magnetic field measurements have been conducted in laboratory environment employing a cubic Helmholtz coil setup in order to examine the effective bandwidth not only of the proposed system but also for the Flux-Gate sensor. A voltage controlled current source driven by a function generator has been utilized for the Helmholtz coil excitation. The result was observed by the oscilloscope. The third experimental apparatus incorporated an AC magnetic shielding construction composed of several layers of electric steel that had been demagnetized prior to the experimental process. Each sensor was place alone and the response was capture by the oscilloscope. The preliminary experimental results indicate that closed loop AMR response presented a maximum deviation of 0.36% with respect to the ideal linear response, while the corresponding values for the open loop AMR system and the Fluxgate sensor reached 2% and 0.01% respectively. Moreover, the noise density of the proposed close loop AMR sensor system remained almost as low as the noise density of the AMR sensor itself, yet considerably higher than that of the Flux-Gate sensor. All relevant numerical data are presented in the paper.

***Keywords*—**AMR sensor, chopper, closed loop, electronic noise, magnetic noise, Flux-Gate sensor, linearity improvement, sensitivity improvement.

N. Hadjigeorgiou is with the School of Electrical and Computer Engineering, National Technical University of Athens (NTUA), Athens, Greece (phone: +302107721482; e-mail: nhatzig@central.ntua.gr).

S. Angelopoulos is with the School of Electrical and Computer Engineering, National Technical University of Athens (NTUA), Athens, Greece (e-mail: spyrosag@gmail.com).

E. Hristoforou was with School of Mining and Metallurgical Engineering. Now he is with the School of Electrical and Computer Engineering, National Technical University of Athens (NTUA), Athens, Greece (e-mail: eh@mental.ntua.gr).

P. P. Sotiriadis is with the School of Electrical and Computer Engineering, National Technical University of Athens (NTUA), Athens, Greece (e-mail: pps@ieee.com).

Neoclis, G. Hadjigeorgiou is a PhD candidate at the School of Electrical and Computer Engineering, National Technical University of Athens (NTUA), Greece. He has had his Master Degree on the subject Automation Systems at the School of Mechanical Engineering, National Technical University of Athens. His Master thesis was "Detection of the position of sea vessel with magnetic techniques." in 2013. He has also had his Bachelor degree at the School of Electrical and Computer Engineering, of the National Technical University of Athens. He has his Bachelor thesis on "Acceleration of the search of the cyclic representation of posets with GPU" in 2011.

Spyridon Angelopoulos MSc. is PhD Candidate at the School of Electrical and Computer Engineering of the National Technical University of Athens (NTUA), Greece. In 2014, he received his MSc degree in Automation Engineering from the School of Mechanical Engineering of the NTUA, Greece. In 2012, he received his Bachelor Diploma on Applied Physics from the School of Applied Mathematical and Physical Sciences of the NTUA, Greece. The topic of his thesis is about the design and development of a magnetometer calibration device, based on magnetic effects. His research interests include the study, design and development of magnetic sensors and the design, simulation and development of electronic circuits.

Evangelos V. Hristoforou, D.Eng, Ph.D, C.Eng, is Professor of Electronic Materials at the School of Electrical and Computer Engineering, National Technical University of Athens (NTUA) and Director of the laboratory of Electronic Sensors. His group is performing research in the following fieldsclusters:

- Materials and Applications for Sensors and Transducers (MAST), with the most important product concerning a method and instrument to monitor the 3- d stess tensor distribution in steels
- Hybrid Electric Energy Integrated Cluster (HELENIC), with the most important advances referring to the sustainable and affordable production of hydrogen from water
- Magnetism for Biomedical Applications (MBA), a new-born activity, concerning driving and monitoring of magnetic nanoparticles

He is actively related to several industries in the field of sensors, energy and health, running industrial and research projects. He has published more than 150 papers in international journals (h-index=21) and he gave more than 30 invited talks in international conferences. He is the: Representative of Greece in the Universal Network of Magnetic NDE; Vice-Chair of the Hellenic NDT Association; Chair of the European Magnetic Sensor and Actuator (EMSA) Conference; Chair of the International Conference on Materials and Applications for Sensors and Transducers (IC-MAST); Editor-in-Chief in "Journal of Materials and Applications for Sensors and Transducers"; Regional Editor in "Recent Patents in Material Science"; Editorial Board in "Journal of Electrical Engineering", "Journal of Automation Mobile Robotics and Intelligent Systems" and "Measurement Automation Robotics".

Paul P. Sotiriadis (Senior IEEE member) received the Ph.D. degree in Electrical Engineering and Computer Science from the Massachusetts Institute of Technology, Cambridge USA, in 2002, the M.S. degree in Electrical Engineering from Stanford University, California USA in 1996 and the Diploma degree in Electrical and Computer Engineering from the National Technical University of Athens, Greece in 1994. In 2002, he joined the Johns Hopkins University as Assistant Professor of Electrical and Computer Engineering. In 2012, he joined the faculty of the Electrical and

Computer Engineering Department of the National Technical University of Athens, Greece.

He has authored and coauthored more than 95 technical papers in IEEE journals and conferences, holds one patent, has several patents pending, and has contributed chapters to technical books. His research interests include design, optimization, and mathematical modeling of analog and mixed-signal circuits, RF and microwave circuits, advanced frequency synthesis, biomedical instrumentation, and interconnect networks in deep-submicrometer technologies. He has led several projects in these fields funded by U.S. organizations and has collaborations with industry and national labs.

He has received several awards, including a Best Paper Award in the IEEE Int. Symp. on Circuits and Systems 2007, a Best Paper Award in the IEEE Int. Frequency Control Symp. 2012 and the 2012 Guillemin-Cauer Award from the IEEE Circuits and Systems Society. Dr. Sotiriadis is an Associate Editor of the IEEE Trans. on Circuits and Systems – I and the IEEE Sensors Journal, has served as an Associate Editor of the IEEE Trans. on Circuits and Systems – II from 2005 to 2010 and has been a member of technical committees of many conferences. He regularly reviews for many IEEE transactions and conferences and serves on proposal review panels.

Structural, Magnetic and Thermodynamic Investigation of Iridium Double Perovskites with Ir^{5+}

Mihai I. Sturza, Laura T. Corredor, Kaustuv Manna, Gizem Aslan Cansever, Tushar Dey, Andrey Maljuk, Olga Kataeva, Sabine Wurmehl, Anja Wolter, Bernd Buchner

***Abstract*—**Recently, the iridate double perovskite Sr_2YIrO_6 has attracted considerable attention due to the report of unexpected magnetism in this Ir^{5+} material, in which according to the J_{eff} model, a non-magnetic ground state is expected. Structural, magnetic and thermodynamic investigations of Sr_2YIrO_6 and Ba_2YIrO_6 single crystals, with emphasis on the temperature and magnetic field dependence of the specific heat will be presented. The single crystals were grown by using $SrCl_2$ and $BaCl_2$ as flux. Single-crystal X-ray diffraction measurements performed on several crystals from different preparation batches showed a high quality of the crystals, proven by the good internal consistency of the data collected using the full-sphere mode and an extremely low R factor. In agreement with the expected non-magnetic ground state of Ir^{5+} ($5d^4$) in these iridates, no magnetic transition is observed down to 430 mK. Moreover, our results suggest that the low temperature anomaly observed in the specific heat is not related to the onset of long-range magnetic order. Instead, it is identified as a Schottky anomaly caused by paramagnetic impurities present in the sample, of the order of $n \sim 0.5(2)$ %. These impurities lead to non-negligible spin correlations, which nonetheless, are not associated with long-range magnetic ordering.

***Keywords*—**Double perovskite, iridates, self-flux grown synthesis**,** spin-orbit coupling.

M. I. Sturza is with the Leibniz Institute for Solid State and Materials Research IFW, Institute for Solid State Research, 01069 Dresden, Germany (phone: +49-(0)351-4659759; e-mail: m.i.sturza@ifw-dresden.de).

L. T. Corredor, K. Manna, G. A. Cansever, T. Dey, A. Maljuk, S. Wurmehl, A. Wolter, B. Buchner is with the Leibniz Institute for Solid State and Materials Research IFW, Institute for Solid State Research, 01069 Dresden, Germany.

Olga Kataeva is with the A.E. Arbuzov Institute of Organic and Physical Chemistry, Russian Academy of Sciences, 420088 Kazan, Russia.

Investigation of Nd-Al-Fe Added Nd-Fe-B Alloy Produced by Arc Melting

Gülten Sadullahoğlu, Baki Altuncevahir

Abstract**—**The scope of this study, to investigate the magnetic properties and microstructure of $Nd_2Fe_{14}B_1$ by alloying with $Nd_{33.4}Fe_{62.6}Al_4$, and heat treating it at different temperatures. The stoichiometric $Nd_2Fe_{14}B$ hard magnetic alloy and $Nd_{33.4}Fe_{62.6}Al_4$ composition were produced by arc melting under argon atmosphere. The $Nd_{33.4}Fe_{62.6}Al_4$ alloy has added to the 2:14:1 hard magnetic alloy with 48% by weight, and melted again by arc melting. Then, it was heat treated at 600, 700 and 800˚C for 3h under vacuum. In AC magnetic susceptibility measurements, for the as-cast sample, the signals decreased sharply at 101 ˚C and 313˚C corresponding to the Curie temperatures of the two ferromagnetic phases in addition to Fe phase. For the sample annealed at 600 ˚C, two Curie points were observed at about 257˚C and at 313˚C. However, the phase corresponding to the Curie temperature of 101 ˚C was disappeared. According to the magnetization measurements, the saturation magnetization has the highest value of 99.8 emu/g for the sample annealed at 600 ˚C, and decreased to 57.66 and 28.6 emu/g for the samples annealed at 700˚ and 800 ˚C respectively. Heat treatment resulted in an evolution of the new phase that caused changes in magnetic properties of the alloys. In order to have clear picture, the identification of these phases are being under the investigation by XRD and SEM – EDX analysis.

Keywords**—**Arc melting, Bulk Magnetic Materials, Curie Temperature, NdFeB Hard Magnets, Heat treatment.

Gülten Sadullahoğlu is with Department of Metallurgical and Materials Engineering, Bulent Ecevit University, Zonguldak, Turkey (corresponding author, e-mail: gsadullahoglu@beun.edu.tr).

Baki Altuncevahir is with Department of Physics Engineering, Istanbul Technical University, Istanbul, Turkey.

Evaluation of the Heating Capability and *in vitro* Hemolysis of Nanosized $Mg_xMn_{1-x}Fe_2O_4$ (x = 0.3 and 0.4) Ferrites Prepared by Sol-gel Method

Laura Elena De León Prado, Dora Alicia Cortés Hernández, Javier Sánchez

***Abstract*—**Among the different cancer treatments that are currently used, hyperthermia has a promising potential due to the multiple benefits that are obtained by this technique. In general terms, hyperthermia is a method that takes advantage of the sensitivity of cancer cells to heat, in order to damage or destroy them. Within the different ways of supplying heat to cancer cells and achieve their destruction or damage, the use of magnetic nanoparticles has attracted attention due to the capability of these particles to generate heat under the influence of an external magnetic field. In addition, these nanoparticles have a high surface area and sizes similar or even lower than biological entities, which allow their approaching and interaction with a specific region of interest. The most used magnetic nanoparticles for hyperthermia treatment are those based on iron oxides, mainly magnetite and maghemite, due to their biocompatibility, good magnetic properties and chemical stability. However, in order to fulfill more efficiently the requirements that demand the treatment of magnetic hyperthermia, there have been investigations using ferrites that incorporate different metallic ions, such as Mg, Mn, Co, Ca, Ni, Cu, Li, Gd, etc., in their structure. This paper reports the synthesis of nanosized $Mg_xMn_{1-x}Fe_2O_4$ (x = 0.3 and 0.4) ferrites by sol-gel method and their evaluation in terms of heating capability and *in vitro* hemolysis to determine the potential use of these nanoparticles as thermoseeds for the treatment of cancer by magnetic hyperthermia. It was possible to obtain ferrites with nanometric sizes, a single crystalline phase with an inverse spinel structure and a behavior near to that of superparamagnetic materials. Additionally, at concentrations of 10 mg of magnetic material per mL of water, it was possible to reach a temperature of approximately 45°C, which is within the range of temperatures used for the treatment of hyperthermia. The results of the *in vitro* hemolysis assay showed that, at the concentrations tested, these nanoparticles are non-hemolytic, as their percentage of hemolysis is close to zero. Therefore, these materials can be used as thermoseeds for the treatment of cancer by magnetic hyperthermia.

***Keywords*—**Ferrites, heating capability, hemolysis, nanoparticles, sol-gel.

I. Introduction

THE search for a better quality of life has led to the development of more efficient treatments for diseases that affect a significant percentage of the population worldwide. In the specific case of cancer, one treatment that has attracted attention is hyperthermia, mainly due to the overcoming of some of the disadvantages that are present in the conventional approaches for treating this disease (surgery, radiation and chemotherapy). Generally, hyperthermia is a technique that utilizes heat to destroy or damage cancer cells. This procedure involves a moderate increase of temperature in the body or a specific region of it, above the normal value that is established by the thermoregulation system of an organism in a particular moment [1], [2]. The aim of increasing the temperature is achieving the eradication of cancer cells or provoke a higher sensitization of them to the effects of radiation and chemotherapy [1]–[3]. The range of temperatures used in this procedure varies between 41°C and 46°C, and these are maintained for periods of one hour or more for the majority of the tissues without causing damage to normal cells [1], [4], [5]. The increase of temperature in the tissues can be accomplished by several means, depending on the location, depth and staging of the tumor [1]. One approach that is being highly studied nowadays is the use of magnetic nanoparticles, mainly due to several attractive characteristics, which include dimensions smaller than or comparable to cells, viruses, proteins and gens, the possibility of coating them to interact with biological entities and the capability of these to produce heat under the action of an external magnetic field [6]. This technique is specifically termed magnetic hyperthermia and consists in the supply of the magnetic nanoparticles to a target tissue and then the application of an external magnetic field that results in the heating of the nanoparticles. Within the magnetic nanoparticles that are used for medical applications, the most used is magnetite [6]–[8]. However, recent research explores the possibility of incorporating different cations in the crystalline structure of ferrites [4], [9]; this is in order to improve either their magnetic properties or biocompatibility. The synthesis of mixed ferrites can be accomplished by several chemical methods, and among these sol-gel method offers the possibility of obtaining high purity and homogeneous nanoparticles [10], [11]. In this study, the synthesis of $Mg_xMn_{1-x}Fe_2O_4$ (x = 0.3 and 0.4) ferrites was carried out by sol-gel method, and then the obtained products were evaluated in terms of heating capability and *in vitro* hemolysis to determine their potential use as thermoseeds for the treatment of cancer by magnetic hyperthermia.

Laura Elena De León Prado, Dora Alicia Cortés Hernández, and Javier Sánchez are with the Centro de Investigación y de Estudios Avanzados del IPN, Unidad Saltillo, Ave. Industria Metalúrgica No. 1062, Parque Industrial Saltillo-Ramos Arizpe, Ramos Arizpe, Coah., México, CP 25900 (e-mail: laura.elena.prado@gmail.com, dora.cortes@cinvestav.edu.mx, h_javiersanchez@hotmail.com).

II. Materials and Methods

A. Materials

Nanosized $Mg_xMn_{1-x}Fe_2O_4$ (x = 0-1) particles were

synthesized by sol-gel method, using ferric nitrate ($Fe(NO_3)_3 \cdot 9H_2O$), magnesium nitrate ($Mg(NO_3)_2 \cdot 6H_2O$), manganese nitrate ($Mn(NO_3)_2 \cdot 4H_2O$) and ethylene glycol ($C_2H_6O_2$) as precursors.

B. Synthesis of the Magnetic Nanoparticles by Sol-Gel Method

Stoichiometric amounts of ferric nitrate, magnesium nitrate and manganese nitrate were dissolved into 5 mL of ethylene glycol in a 100 mL beaker. This solution was stirred for 2 h at 40 °C, and the obtained sol was then heated up to 80°C and kept at this temperature until a brown gel was formed. The gel was aged for 2 h at room temperature and then dried at 95°C for 72 h. Subsequently, the dry gel was heat treated at 50°C in air for 60 min. The obtained products were milled and washed several times with ethanol, in order to remove the ethylene glycol excess. Finally, the powders were dried at room temperature.

C. Sample Characterization

The characterization of the products was carried out by X-ray diffraction (XRD), vibrating sample magnetometry (VSM) and transmission electron microscopy (TEM). The phase structures of magnetic nanoparticles were characterized by XRD, using a X'Pert Philips diffractometer, with Cu Kα radiation (λ= 1.5418 Å) at a scanning rate of 0.02° s^{-1} (2θ scale) into the 20-80° interval. The magnetic properties were evaluated using a vibrating sample magnetometer PPMS (Physical Property Measurement System) of Quantum Design model 6000, with an option to measure the hysteresis loop in a measurement time of 60 min. TEM images were acquired using a Titan 80-300 microscope. For the evaluation of the heating capability of the nanoparticles an AMBRELL magnetic induction equipment model EasyHeat was used, with a power input of 200.2 A and a magnetic field of 10.2 KA/m with a frequency of operation of 354 KHz. The hemolysis assay was carried out according to the procedure described in the Standard Test Method for Analysis of Hemolytic Properties of Nanoparticles E2524 – 08.

III. Results and Discussion

A. XRD Analysis

Fig. 1 shows the XRD patterns of $Mg_xMn_{1-x}Fe_2O_4$ (x = 0, 0.3, 0.4 and 1) nanoparticles synthesized by sol-gel method and heat treated at 500°C for 1 h. In these, it can be observed for all the cases the presence of a single crystalline phase, which reflections correspond to a cubic inverse spinel structure and are similar to those of $MgFe_2O_4$ (JCPDS 88-1935).

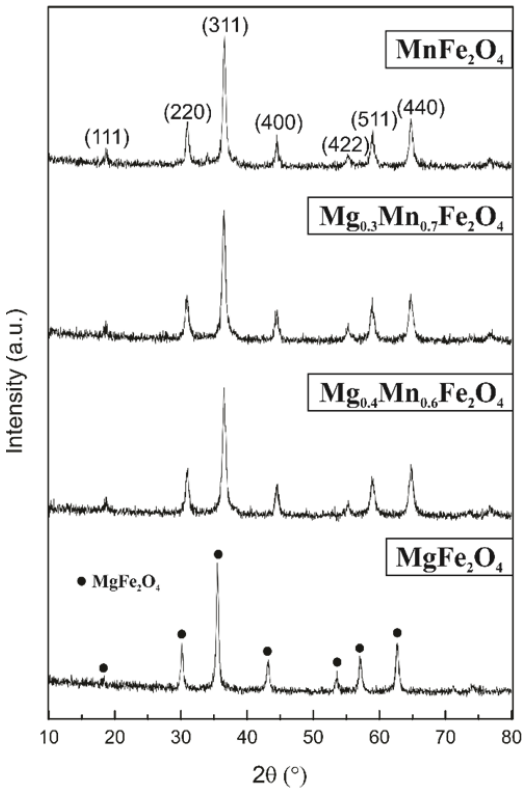

Fig. 1 XRD patterns of $Mg_xMn_{1-x}Fe_2O_4$ (x = 0, 0.3, 0.4 and 1) nanoparticles synthesized by sol-gel method and heat treated at 500°C for 60 minutes

B. VSM Analysis

Table I shows the magnetic properties and crystallite size (calculated by the Scherrer equation) of the $Mg_xMn_{1-x}Fe_2O_4$ (x = 0, 0.3, 0.4 and 1) nanoparticles. These results show that the manganese ferrite ($MnFe_2O_4$) and magnesium ferrite ($MgFe_2O_4$) show the highest and lowest values of saturation magnetization (M_s) respectively, and the mixed ferrites ($Mg_xMn_{1-x}Fe_2O_4$, x = 0.3 and 0.4) have values of M_s between these two. The value of M_s decreases when the content of Mn also decreases, this due to the fact that Mn has a higher magnetic moment (μ_B=5) than Mg (μ_B=0) [12], and their distribution in the interstitial sites of the spinel structure has a major influence on the values of this property [13]. In addition, in all cases the values of remanence (M_r) and coercivity (H_c) are close to zero, which results in a behavior near to the superparamagnetic regime. This can be observed also in Fig. 2, where the hysteresis loops of the ferrites show that these materials have a soft ferrimagnetic behavior that tends to the superparamagnetism, as the typical sigmoidal curve shape occurs.

TABLE I
MAGNETIC PROPERTIES (SATURATION, REMANENCE AND COERCIVITY) AND CRYSTALLITE SIZES (CALCULATED BY THE SCHERRER EQUATION) OF $Mg_xMn_{1-x}Fe_2O_4$ (X= 0, 0.3, 0.4 AND 1) NANOPARTICLES SYNTHESIZED BY SOL-GEL METHOD AND HEAT TREATED AT 500°C FOR 60 MINUTES.

$Mg_xMn_{1-x}Fe_2O_4$ (x = 0, 0.3, 0.4 and 1)	Saturation Ms (emu/g)	Remanence Mr (emu/g)	Coercivity Hc (Oe)	Crystallite Size Scherrer equation (nm)
$MnFe_2O_4$	49.7117	1.0156	10	18
$Mg_{0.3}Mn_{0.7}Fe_2O_4$	41.2598	0.7843	10	15
$Mg_{0.4}Mn_{0.6}Fe_2O_4$	38.6570	0	0	15
$MgFe_2O_4$	24.3022	0.5681	10	21

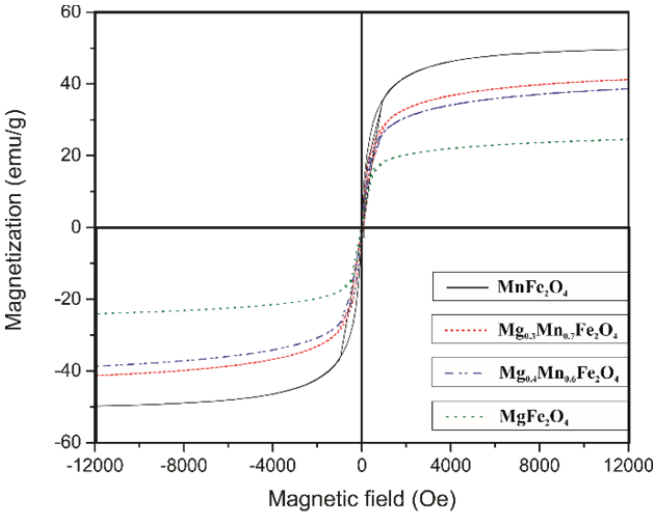

Fig. 2 Hysteresis loops of $Mg_xMn_{1-x}Fe_2O_4$ (x = 0, 0.3, 0.4 and 1) nanoparticles synthesized by sol-gel method and heat treated at 500°C for 60 minutes

C. TEM Analysis

Fig. 3 shows the TEM images of the $Mg_{0.3}Mn_{0.7}Fe_2O_4$ and $Mg_{0.4}Mn_{0.6}Fe_2O_4$ nanoparticles. It can be observed for both samples a spherical-like morphology and sizes in accordance to those calculated by the Scherrer equation. Furthermore, due to the soft ferrimagnetic behavior of the particles and their nanometric size, agglomerates can be observed. This also as a result of the permanent magnetic moments that experience small particles with single domains, which causes them to be permanently magnetized and agglomerate, as reported by Iftikhar et al. [14].

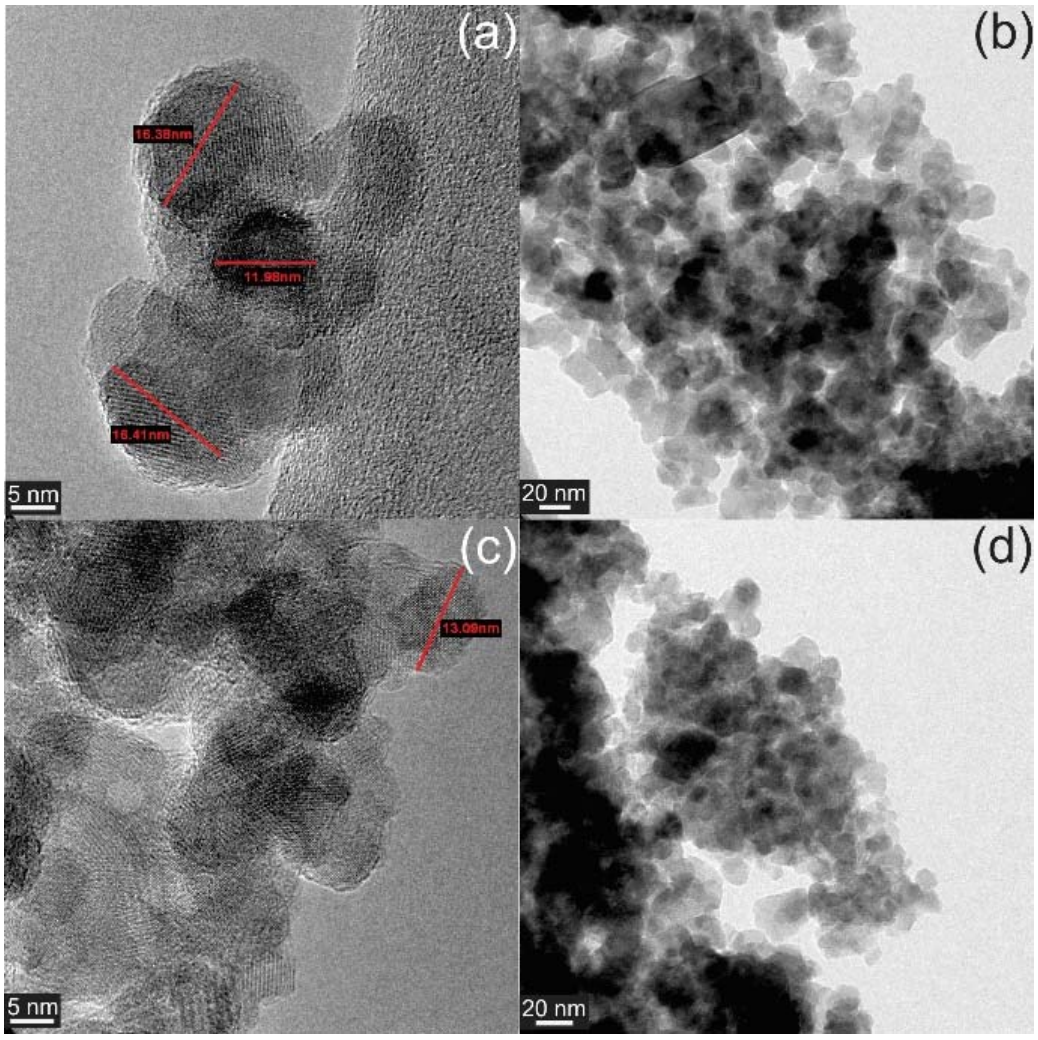

Fig. 3 TEM images of (a, b) $Mg_{0.3}Mn_{0.7}Fe_2O_4$ and (c, d) $Mg_{0.4}Mn_{0.6}Fe_2O_4$ nanoparticles synthesized by sol-gel method and heat treated at 500°C for 60 minutes

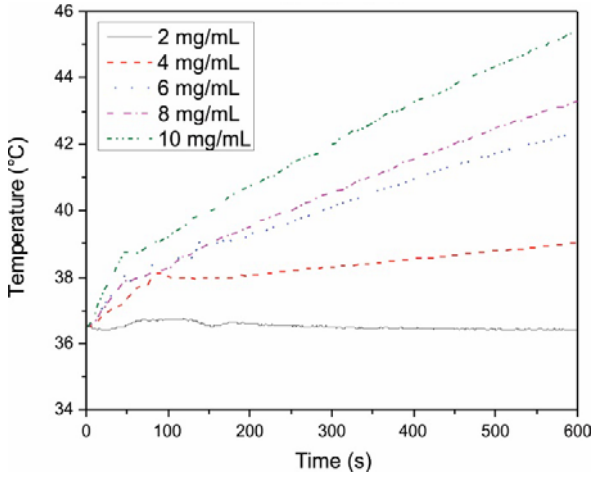

Fig. 4 Magnetic induction heating curves of the $Mg_{0.3}Mn_{0.7}Fe_2O_4$ nanoparticles dispersed in water at concentrations of 2,4,6,8 and 10 mg/mL

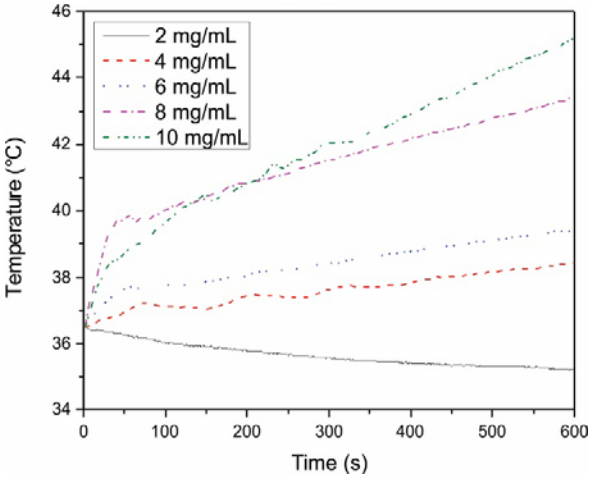

Fig. 5 Magnetic induction heating curves of the $Mg_{0.4}Mn_{0.6}Fe_2O_4$ nanoparticles dispersed in water at concentrations of 2,4,6,8 and 10 mg/mL

D. Heating Capability Test

Figs. 4 and 5 present the magnetic induction heating curves of the $Mg_{0.3}Mn_{0.7}Fe_2O_4$ and $Mg_{0.4}Mn_{0.6}Fe_2O_4$ nanoparticles dispersed in water at different concentrations (2, 4, 6, 8 and 10 mg/mL), respectively. For both samples, the initial temperature was established in 36.5°C and the evaluation of the heating capability was carried out for a time of 10 minutes. It can be observed that as the concentration of the particles increases, a higher temperature is reached. This corroborates the potential of the particles to generate heat under the action of an external magnetic field. Additionally, at the concentration of 10 mg/mL it was possible to accomplish, in both cases, a temperature of approximately 45 °C. In fact, at lower concentrations and times it was possible to obtain a temperature of 39 °C, which according to Bettaieb et al. [2], between temperature range 39 °C and 45 °C it is possible to cause damage or even the death of cancer cells without causing any significant damage to healthy tissues.

E. Hemolysis Assay

The toxicity *in vitro* generated by the materials when they are in contact with the erythrocytes (red blood cells) was measured according to the hemolysis assay described in the Standard Test Method for Analysis of Hemolytic Properties of Nanoparticles E2524 – 08. Generally, this procedure is based in the determination of the hemoglobin that is released when the erythrocytes are in contact with nanomaterials. Concentrations of 2 mg/mL, 4 mg/mL, 6 mg/mL, 8 mg/mL and 10 mg/mL were tested accordingly with what is reported for Pankhurst et al. [6], who found that concentrations between 5 mg and 10 mg per cm^3 of tumor tissue are adequate for magnetic hyperthermia in human patients. The results of this test showed that at all concentrations, for both samples, the degree of hemolysis is non-significant with values below 1%.

IV. Conclusion

Nanoparticles of $Mg_xMn_{1-x}Fe_2O_4$ (x = 0.3 and 0.4) with a single cubic spinel structure and a soft ferrimagnetic behavior near to the superparamagnetic regime were successfully synthesized by sol-gel method. In addition, these nanoparticles exhibited a spherical-like morphology and nanometric sizes (≈ 15 nm). Both samples, at concentrations of 10 mg of magnetic material per mL of water reached in 10 minutes a temperature of approximately 45 °C, which is within the range of temperatures used for the treatment of hyperthermia. Moreover, at the concentrations tested (2, 4, 6, 8 and 10 mg/mL), the materials show a non-significant hemolytic degree. Therefore, taking into account the obtained results, these nanoparticles have a promising potential to be used as thermoseeds in the treatment of cancer by magnetic hyperthermia.

Acknowledgment

The authors gratefully acknowledge CONACYT-Mexico for the scholarship of Laura Elena De León Prado.

References

[1] Chicheł, A., Skowronek, J., Kubaszewska, M. & Kanikowski, M. "Hyperthermia – Description of a method and a review of clinical applications." *Rep. Pract. Oncol. Radiother.* 12, 267–275 (2007).

[2] Bettaieb, A., Wrzal, P. K. & Averill-Bates, D. A., "Cancer Treatment - Conventional and Innovative Approaches" (ed. Rangel, L.) 257–283 (Intech, 2013).

[3] Johannsen, M., Thiesen, B., Wust, P. & Jordan, A. "Magnetic nanoparticle hyperthermia for prostate cancer." *Int. J. Hyperthermia* 26, 790–795 (2010).

[4] Kumar, C. S. S. R. & Mohammad, F. "Magnetic nanomaterials for hyperthermia-based therapy and controlled drug delivery." *Adv. Drug Deliv. Rev.* 63, 789–808 (2011).

[5] Jordan, A., Scholz, R., Wust, P., Fähling, H. & Felix, R. "Magnetic fluid hyperthermia (MFH): Cancer treatment with {AC} magnetic field induced excitation of biocompatible superparamagnetic nanoparticles." *J. Magn. Magn. Mater.* 201, 413–419 (1999).

[6] Pankhurst, Q. A., Connolly, J., Jones, S. K. & Dobson, J. "Applications of magnetic nanoparticles in biomedicine." *J. Phys. Appl. Phys.* 36, R167 (2003).

[7] Thiesen, B. & Jordan, A. "Clinical applications of magnetic nanoparticles for hyperthermia." *Int. J. Hyperthermia* 24, 467–474 (2008).
[8] Shubayev, V. I., II, T. R. P. & Jin, S. "Magnetic nanoparticles for theragnostics." *Adv. Drug Deliv. Rev.* 61, 467–477 (2009).
[9] Sharifi, I., Shokrollahi, H. & Amiri, S. "Ferrite-based magnetic nanofluids used in hyperthermia applications." *J. Magn. Magn. Mater.* 324, 903–915 (2012).
[10] Valenzuela, R. "Novel Applications of Ferrites." *Phys. Res. Int.* 2012, (2012).
[11] Escamilla-Pérez, A. M., Cortés-Hernández, D. A., Almanza-Robles, J. M., Mantovani, D. & Chevallier, P. "Crystal structure of superparamagnetic $Mg_{0.2}Ca_{0.8}Fe_2O_4$ nanoparticles synthesized by sol–gel method." *J. Magn. Magn. Mater.* 374, 474–478 (2015).
[12] Jeun, M., Park, S., Jang, G. H. & Lee, K. H. "Tailoring $Mg_xMn_{1-x}Fe_2O_4$ Superparamagnetic Nanoferrites for Magnetic Fluid Hyperthermia Applications." *ACS Appl. Mater. Interfaces* 6, 16487–16492 (2014).
[13] De-León-Prado, L. E. *et al.* "Synthesis and characterization of nanosized $Mg_xMn_{1-x}Fe_2O_4$ ferrites by both sol-gel and thermal decomposition methods." *J. Magn. Magn. Mater.* 427, 230–234 (2017).
[14] Iftikhar, A. *et al.* "Synthesis of super paramagnetic particles of $Mn_{1-x}Mg_xFe_2O_4$ ferrites for hyperthermia applications." *J. Alloys Compd.* 601, 116–119 (2014).

Magnetic Properties and Cytotoxicity of Ga-Mn Magnetic Ferrites Synthesized by the Citrate Sol-Gel Method

Javier Sánchez, Laura Elena De León Prado, Dora Alicia Cortés Hernández

***Abstract*—**Magnetic spinel ferrites are materials that possess size, magnetic properties and heating ability adequate for their potential use in biomedical applications. The $Mn_{0.5}Ga_{0.5}Fe_2O_4$ magnetic nanoparticles (MNPs) were synthesized by sol-gel method using citric acid as chelating agent of metallic precursors. The synthesized samples were identified by X-Ray Diffraction (XRD) as an inverse spinel structure with no secondary phases. Saturation magnetization (*Ms*) of crystalline powders was 45.9 emu/g, which was higher than those corresponding to $GaFe_2O_4$ (14.2 emu/g) and $MnFe_2O_4$ (40.2 emu/g) synthesized under similar conditions, while the coercivity field (*Hc*) was 27.9 Oe. The average particle size was 18 ± 7 nm. The heating ability of the MNPs was enough to increase the surrounding temperature up to 43.5 °C in 7 min when a quantity of 4.5 mg of MNPs per mL of liquid medium was tested. Cytotoxic effect (hemolysis assay) of MNPs was determined and the results showed hemolytic values below 1% in all tested cases. According to the results obtained, these synthesized nanoparticles can be potentially used as thermoseeds for hyperthermia therapy.

***Keywords*—**Cytotoxicity, heating ability, manganese-gallium ferrite, magnetic hyperthermia.

I. Introduction

MAGNETIC nanoferrites are materials that have been extensively studied for the last decade due to their potential as contrast agents for magnetic resonance imaging and thermoseeds for hyperthermia treatment [1]-[4]. A great quantity of synthesis routes, such as microwave [5]-[9], co-precipitation [10]-[17], thermal decomposition [18]-[22], mechano-chemical synthesis [23]-[26], among others [27]-[41], has been developed for obtaining MNPs with desirable magnetic properties for biomedical and technological applications. Among all these synthesis methods, sol-gel is one of the best ways to synthesize pure and mixed magnetic ferrites with appropriate crystalline structure and magnetic properties for their use in biomedical areas [42]-[48]. The sol-gel auto-combustion technique combines the gelification step and the combustion process to obtain crystalline, magnetic and nano-sized simple and mixed ferrites [49]-[61]. Citric acid is one of the three most popular fuels used for the synthesis of fine ceramics such as ferrites by combustion process. This chelating agent can initiate the combustion reaction due to its high negative combustion heat (-2.76 kcal g^{-1}), and at the same time prevents particle agglomeration and undesired spontaneous condensation reactions [62]. However, in this method, important reaction conditions may be considered, such as the type and quantity of organic fuel, pH, combustion source, auto-combustion temperature, etc., which may influence the crystalline structure and properties of synthesized samples [54].

This work reports the synthesis of $Mn_{0.5}Ga_{0.5}Fe_2O_4$ MNPs by the citrate sol-gel method, evaluating the magnetic properties and crystalline structure of the synthesized samples for their potential use on biomedical applications, without considering the auto-combustion step and the pre-heating of the powder precursor. The heating ability of samples and the hemolytic damage to red blood cells were also studied, taking into account the chemical composition of the magnetic core with the aim to determine the potential utilization of the synthesized particles as thermoseeds in hyperthermia treatment. Paramagnetic gallium was selected as part of magnetic core due to its biological properties and its antineoplastic effect on cancer cells [63]-[65]. In recent years, manganese has been extensively investigated as a component of magnetic ferrites [5], [10], [66]-[69] due to its contribution to the net magnetic moment and the heating capacity of samples. Manganese can also be used in ferrites for magnetic resonance imaging due to its higher relaxivity when it is part of paramagnetic organic molecules and MNPs [41], [70] containing paramagnetic cations such as gallium ions [71]. Gallium ferrites with orthorhombic structure have been extensively studied due to their magnetoelectric properties. However, for the spinel structure, which is necessary for biomedical applications, there is no much research performed.

II. Materials and Methods

MNPs of $Mn_{0.5}Ga_{0.5}Fe_2O_4$ were synthesized by the citrate sol-gel method using iron [$Fe(NO_3)_3 \cdot 9H_2O$], gallium [$Ga(NO_3)3 \cdot H_2O$] and manganese [$Mn(NO_3)_2 \cdot 4H_2O$] nitrates and citric acid ($C_6H_8O_7$) as raw materials. For comparison purposes, samples of $GaFe_2O_4$ and $MnFe_2O_4$ were also synthesized under similar conditions. Stoichiometric amounts of metallic nitrates and citric acid, in a molar ratio of 2:1 (Fe_2:Ga_1, Fe_2:$Ga_{0.5}$-$Mn_{0.5}$, Fe_2:Mn_1) and 3:1 ($C_6H_8O_7$:metals), were placed into a 250 mL glass beaker that already contained 20 mL of deionized water. The mixture was magnetically stirred for 2 h at room temperature until a homogenous solution was obtained. The temperature of the solution was

Javier Sánchez, Laura Elena De León Prado and Dora Alicia Cortés Hernández are with the Centro de Investigación y de Estudios Avanzados del IPN, Unidad Saltillo, Ave. Industria Metalúrgica No. 1062, Parque Industrial Saltillo-Ramos Arizpe, Ramos Arizpe, Coah., México, CP 25900. (e-mail: h_javiersanchez@hotmail.com, laura.elena.prado@gmail.com, dora.cortes@cinvestav.edu.mx).

slowly increased to promote the formation of a viscous gel and the elimination of both nitric acid and water molecules. The viscous gel was aged for 2 h at room temperature and dried at 95°C for 72 h in a stove obtaining a soluble and brittle gel that was used as magnetic precursor. In accordance to previous results [64], the precursor was heat treated for 1 h at 500°C in air and the powders obtained were characterized by XRD, Vibration Sample Magnetometry (VSM), Infrared Spectroscopy (FT-IR), Transmission Electronic Microscopy and Energy Dispersive Spectroscopy (TEM-EDS). This deep characterization was performed in the aim to identify the crystalline structure and determine the magnetic parameters (magnetization saturation, *Ms*; remanent magnetization, *Mr*; coercive field, *Hc*), the chemical composition and the average core size of synthesized powders. The evaluation of the magnetic properties was carried out at an applied field within a range of -12000 to 12000 Oe. The cell parameter (*a*) of the synthesized samples was calculated using (1), in which the interplanar distance (*d*) and *hkl* planes were acquired from the diffraction patterns. The crystallite size (*D*) and the magnetic moment per molecule (n_B) was also calculated from the most intense diffraction peak and (2), respectively.

$$a = d\sqrt{h^2 + k^2 + l^2} \quad (1)$$

$$n_B = \frac{M_{wt} \cdot Ms}{5585} \quad (2)$$

where M_{wt} is molecular weight, *Ms* is saturation magnetization and 5585 is a magnetic factor. Heating ability of magnetic suspensions (3.0 mg, 4.5 mg, 6.0 mg and 10.0 mg of MNPs per mL of water) was measured by solid state magnetic induction using a field of 10.2 kA/m and a frequency of 354 kHz to determine the potential application of synthesized powders as thermoseeds for hyperthermia treatment. These magnetic conditions are within the range specified for biomedical applications. From these heating curves, the specific absorption rate, SAR [72] (3) was calculated taking into account the mass of MNPs (m_{MNPs}) and carrier liquid (m_{LIQ}), the specific heat of carrier liquid (C_{LIQ}) and the initial slope of the time-dependent temperature curve ($\Delta T/\Delta t$) [73].

$$SAR = \frac{c_{LIQ} m_{LIQ}}{m_{MNPs}} \cdot \frac{\Delta T}{\Delta t} \quad (3)$$

The hemolytic degree of magnetic powders was measured following the experimental procedure described in ASTM E2524-08 (Standard Test Method for Analysis of Hemolytic Properties of Nanoparticles). For these tests, suspensions of 3.0 mg, 4.5 mg, 6.0 mg and 10.0 mg of material per mL of liquid medium and human whole blood were used. Six samples were tested for each suspension and the hemolytic degree was calculated by the quantitative determination of hemoglobin released due to the *in vitro* damage to red blood cells caused by their exposure to nanoparticles.

III. Results and Discussion

The XRD patterns of synthesized samples are presented in Fig. 1. All samples show the characteristic reflections of a cubic spinel structure and the XRD patterns were indexed using the JCPDS card 74-2228 ($Fe_{1.4}Ga_{1.4}O_4$) with good agreement for all *hkl* planes. A reflection displacement was observed in some *hkl* planes (220, 422, 511, 440) for both $Mn_{0.5}Ga_{0.5}Fe_2O_4$ and $MnFe_2O_4$ samples, in comparison to $GaFe_2O_4$, which indicates the correct substitution of Ga^{3+} (ionic radius of 0.62 Å) by Mn^{2+} cations that have a longer ionic radius (0.89 Å). The lattice parameters (*a*) of the samples are presented in Table I. This parameter increases as Mn^{2+} ions are introduced into the oxygen framework, which has high flexibility and tends to modify itself to accept cations with different ionic radii [74]. This may indicate the formation of the mixed ferrite. An increase from 5 nm to 20 nm in the crystallite size was also observed from the XRD diffraction patterns, as an effect of the lattice expansion and the crystallinity of the samples. Unlike both pure $GaFe_2O_4$ and $MnFe_2O_4$ samples synthesized under similar conditions, a cubic spinel phase and a high crystalline structure without secondary products was developed when the magnetic precursor of $Mn_{0.5}Ga_{0.5}Fe_2O_4$ was heat treated at 500°C for 1 h.

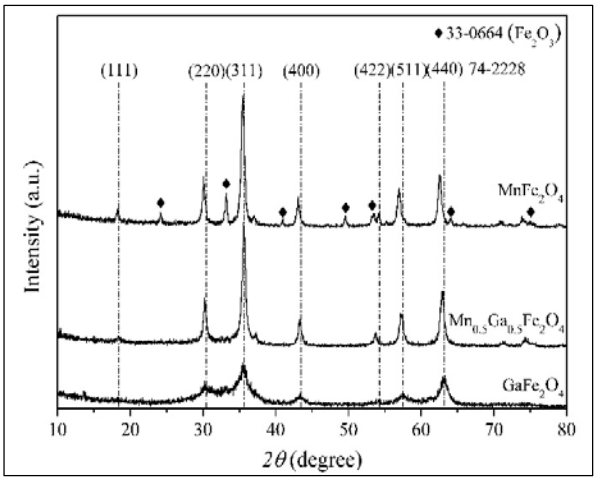

Fig. 1 XRD patterns of $GaFe_2O_4$, $Mn_{0.5}Ga_{0.5}Fe_2O_4$ and $MnFe_2O_4$ samples synthesized by the citrate sol-gel method

The identified crystalline powders showed an *Ms* value of 45.9 emu/g, which was higher than those corresponding to $GaFe_2O_4$ (14.2 emu/g) and $MnFe_2O_4$ (40.2 emu/g), while the *Mr* and *Hc* values were 2.0 emu/g and 27.9 Oe, respectively. This increase in *Ms* has been attributed to the formation of strong exchange interactions among Fe and Mn ions located into both tetrahedral (A) and octahedral (B) sites of the spinel structure [75]. The shape of the hysteresis loop (Fig. 2) indicate a ferrimagnetic behavior, thus the obtained powders can be classified as soft ferrites (high *Ms*, lower *Hc*) [76]. The magnetic moment per molecule increases and it is consistent with the increase of the magnetization values due to the element distribution into the structure, their preferential occupation site and the increase in the Fe-Mn sublattices exchange interactions [50].

TABLE I
MAGNETIC AND CRYSTALLOGRAPHIC PARAMETERS OF GA AND MN FERRITES SYNTHESIZED SAMPLES

Sample	$GaFe_2O_4$	$Mn_{0.5}Ga_{0.5}Fe_2O_4$	$MnFe_2O_4$
***Ms* (emu/g)**	14.2	45.9	40.2
***Mr* (emu/g)**	1.0	2.0	2.4
***Hc* (Oe)**	64.7	27.9	29.0
***D*, (nm)**	5.0	18.0	20.0
a, (Å)	8.3290	8.3602	8.3943
n_B **(μ_B)**	0.62	1.96	1.66

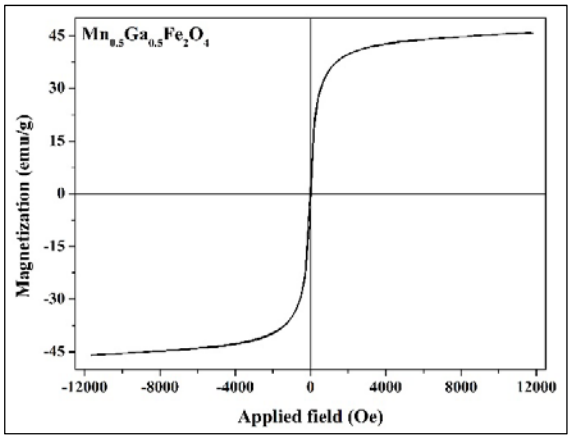

Fig. 2 Hysteresis loop of $Mn_{0.5}Ga_{0.5}Fe_2O_4$ sample at an applied field of 12 KOe

The FT-IR spectrum of synthesized powders is shown in Fig. 3. It was possible to identify the characteristic absorption band (≈550 cm^{-1}) of metal-oxygen bond (Fe-O, Ga-O and Mn-O) due to the intrinsic vibration stretch of A and B sites of the spinel structure. According to Briceño et al. [77], this absorption band indicates the correct formation of the magnetic oxide. Additional absorption bands corresponding to –OH groups (≈3300 cm^{-1}) and C-H bonds (≈2800 and ≈1500 cm^{-1}) were identified as part of the synthesized powders and correspond to water molecules and organic residues from citric acid, not completely burned during heat treatment, respectively. The CO_2 molecules (≈2350 cm^{-1}) may be attributed to the atmospheric conditions at which the analyses were performed.

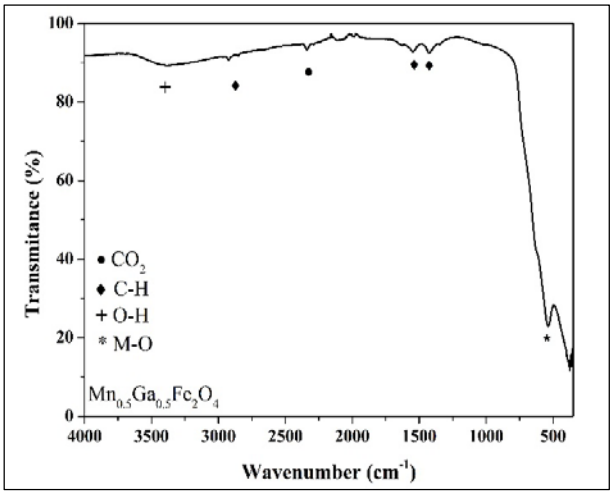

Fig. 3 FT-IR spectra of synthesized powders

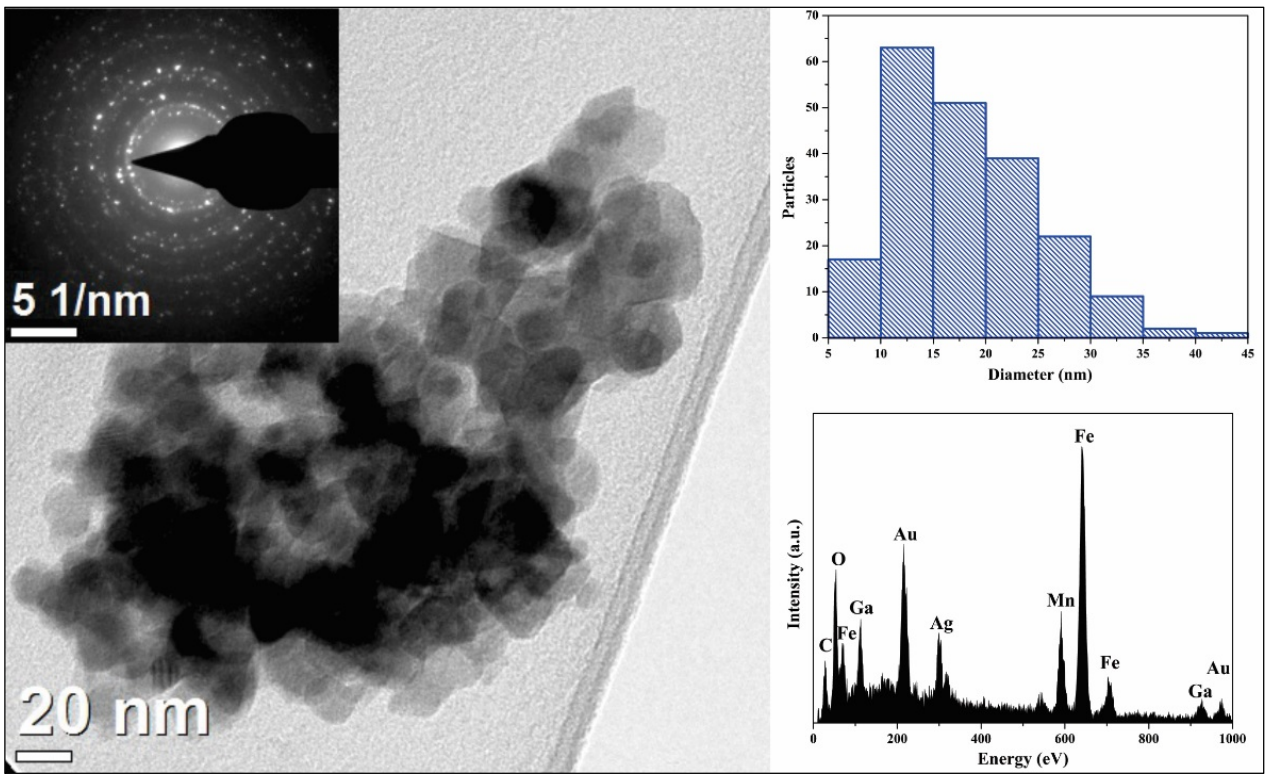

Fig. 4 TEM and SAED images, EDS spectrum and calculated size of $Mn_{0.5}Ga_{0.5}Fe_2O_4$ MNPs

The average size, morphology and the semi-quantitative chemical composition of particles were determined by TEM analysis (Fig. 4). The corresponding EDS spectrum, SAED and histogram are also shown in Fig. 4. Synthesized MNPs showed an average particle size of 18 ± 7 nm. The observed agglomeration is due to magnetic interactions among particles (Van der Waals forces and dipole-dipole interactions) [78]. According to the EDS spectrum, Ga, Fe, O and Mn were the only elements present in the powders, while Au and Ag elements correspond to the conductive metallic layer applied on the samples for their semi-quantitative characterization. NPMs have a non-spherical morphology as an effect of the reaction medium used (citric acid) and the heat treatment conditions, which was not observed for synthesized MNPs under different conditions [63]-[65].

The heating ability of $Mn_{0.5}Ga_{0.5}Fe_2O_4$ is shown in Fig. 5. As expected, temperature increases as the suspension concentration is increased. From these results, it is possible to demonstrate that, under these testing conditions (10.2 kA/m and 354 kHz), the suspensions of 4.5 mg, 6.0 mg and 10.0 mg of MNPs per mL of water are able to increase their medium temperature up to 43.5°C in less than 10 min.

The SAR values are shown in Table II; these are lower than those reported by other authors [10], [70], [79]. This difference is mainly due to the calculations, which involve only the overall weight fraction of magnetic elements (Fe, Mn) without considering the mass of oxygen and paramagnetic gallium present in the mixed ferrites.

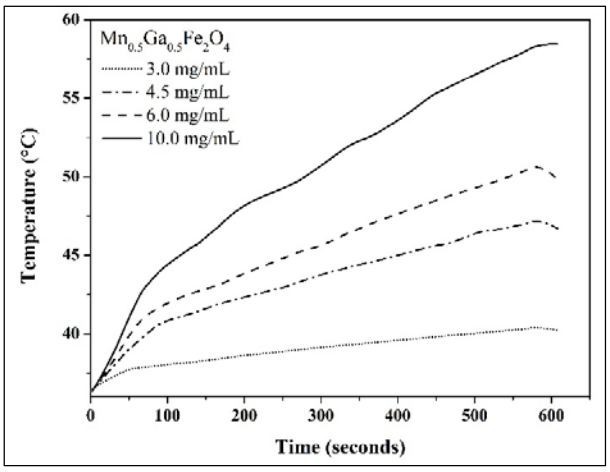

Fig. 5 Heating ability of $Mn_{0.5}Ga_{0.5}Fe_2O_4$ under an AC magnetic field of 10.2 kA/m and 354 kHz

TABLE II
HEMOLYTIC DEGREE AND SAR VALUES OF $MN_{0.5}GA_{0.5}FE_2O_4$ MNPS SYNTHESIZED BY THE CITRATE SOL-GEL METHOD

Sample	Quantity of MNPs (mg/mL)	Hemolytic value (%)	SAR Values (W/g)
1	3.0	0.01	7.5
2	4.5	0.27	14.3
3	6.0	0.10	14.4
4	10.0	0.66	13.8

The results of the red blood cells damage caused by MNPs are shown in Table II. In all cases, the hemolysis values were lower than 1% and according to ASTM E2524-08; the tested MNPs are nonhemolytic materials.

IV. CONCLUSION

MNPs of $Mn_{0.5}Ga_{0.5}Fe_2O_4$ were successfully synthesized by the citrate sol-gel method. Powders showed an inverse spinel crystalline structure with no other secondary phases. Saturation magnetization increases as gallium ions are replaced by manganese ions due to the net magnetic moment between A and B sublattices, while *Mr* and *Hc* values decrease as an effect of the super-exchange interactions among Mn cations. The synthesized MNPs showed an average size of 18 ± 7nm and a homogeneous chemical composition. A quantity of 4.5 mg of MNPs per mL of deionized water was enough to increase the medium temperature at the required range for hyperthermia treatment (43.5 °C) in less than 10 min. In all the cases, the hemolysis percentage was below 1%. According to the results obtained, $Mn_{0.5}Ga_{0.5}Fe_2O_4$ has adequate properties for its potential use in hyperthermia therapy.

ACKNOWLEDGMENT

The authors gratefully acknowledge CONACyT Mexico the PhD scholarship granted to Héctor Javier Sánchez Fuentes (347034) and the research grants 222755 and 230253.

REFERENCES

[1] Liu, X.L. & Fan, H.M., "Innovative magnetic nanoparticle platform for magnetic resonance imaging and magnetic fluid hyperthermia applications." *Current Opinion in Chemical Engineering*. 4, 38-46 (2014).

[2] Mornet, S., Vasseur, S., Grasset, F., Veverka, P., Goglio, G., Demourgues, A., Portier, J., Pollert, E. & Duguet, E., "Magnetic nanoparticle design for medical applications." *Progress in Solid State Chemistry*. 34, 237-247 (2006).

[3] Hergt, R., Dutz, S., Müller, R. & Zeisberger, M., "Magnetic particle hyperthermia: nanoparticle magnetism and materials development for cancer therapy." *J. Phys.: Condens. Matter.* 18, S2919-S2934 (2006).

[4] Lin, M., Huang, J. & Sha, M., "Recent advances in nanosized Mn–Zn ferrite magnetic fluid hyperthermia for cancer treatment." *J. Nanosci. Nanotechnol.* 14, 792-802 (2014).

[5] Makridis, A., Chatzitheodorou, I., Topouridou, K., Yavropoulou, M.P., Angelakeris, M. & Dendrinou-Samara, C. "A facile microwave synthetic route for ferrite nanoparticles with direct impact in magnetic particle hyperthermia." *Materials Science and Engineering:* C. 63, 663-670 (2016).

[6] Verma, S., Khollam, Y.B., Potdar, H.S. & Deshpande, S.B., "Synthesis of nanosized MgFe2O4 powders by microwave hydrothermal method." *Materials letters.* 58, 1092-1095 (2004).

[7] Kuznetsova, V., Almjasheva, O. & Gusarov, V., "Influence of microwave and ultrasonic treatment on the formation of CoFe2O4 under hydrothermal conditions." *Glass Physics and Chemistry.* 35, 205-209 (2009).

[8] Manikandan, A., Vijaya, J., Sundararajan, M., Meganathan, C., Kennedy, L. & Bououdina, M., "Optical and magnetic properties of Mg-doped ZnFe2O4 nanoparticles prepared by rapid microwave combustion method." *Superlattices and Microstructures.* 64, 118-131 (2013).

[9] Wang, Y.M., Cao, X., Liu, G.H., Hong, R.H., Chen, Y.M., & et al., "Synthesis of Fe3O4 magnetic fluid used for magnetic resonance imaging and hyperthermia." *Journal of Magnetism and Magnetic Materials.* 323, 2953-2959 (2011).

[10] Doaga, A., Cojocariu, A.M., Amin, W., Heib, F., Bender, P., Hempelmann, R. & Caltun, O.F., "Synthesis and characterizations of manganese ferrites for hyperthermia applications." *Materials Chemistry and Physics.* 143, 305-310 (2013).

[11] Mozaffari, M., B. Behdadfar, & J. Amighian, "Preparation and characterization of manganese ferrite nanoparticles via co-precipitation method for hyperthermia." *Iranian Journal of Pharmaceutical Sciences*. 4, 115-118 (2008).

[12] Iftikhar, A., Islam, M.U., Awan, M.S., Ahmad, M., Naseem, S. & Asif Iqbal, M., "Synthesis of super paramagnetic particles of Mn 1−xMgxFe2O4 ferrites for hyperthermia applications." *Journal of Alloys and Compounds.* 601, 116-119 (2014).

[13] Lungu, A., Malaescu, I., Marin, C.N., Vlazan, P., & Sfirloaga, P., "The electrical properties of manganese ferrite powders prepared by two different methods." *Physica B.* 462, 80-85 (2015).

[14] Sharifi, I. & Shokrollahi, H., "Structural, magnetic and Mössbauer evaluation of Mn substituted Co–Zn ferrite nanoparticles synthesized by co-precipitation." *Journal of Magnetism and Magnetic Materials*, 334, 36-40 (2013).

[15] Farooq, H., Ahmad, M.R., Jamil, Y., Hafeez, A., Mahmood, Z. & Mahmood, T., "Structural and Dielectric Properties of Manganese Ferrite Nanoparticles." *J. Basic Appl. Sci.* 8, 597-601 (2012).

[16] Aakash, Choubey, R., Das D., & Mukherjee, S., "Effect of doping of manganese ions on the structural and magnetic properties of nickel ferrite." *Journal of Alloys and Compounds*. 668, 33-39 (2016).

[17] Cao, X., Liu, G., Wang, Y., Li, J. & Hong, R., "Preparation of octahedral shaped Mn0.8Zn0.2Fe2O4 ferrites via co-precipitation." *Journal of Alloys and Compounds.* 497, L9-L12 (2010).

[18] Kang, E., Park, J., Hwang, Y., Kang, M., Park, J.G., & Hyeon, T., "Direct synthesis of highly crystalline and monodisperse manganese ferrite nanocrystals." *J. Phys. Chem. B.* 108, 13932-13935 (2004).

[19] Monfared, A.H., Zamanian, A., Beygzadeh, M., Sharif, I. & Mozafari, M., "A rapid and efficient thermal decomposition approach for the synthesis of manganese-zinc/oleylamine core/shell ferrite nanoparticles." *Journal of Alloys and Compounds.* 693, 1090-1095 2(017).

[20] Vamvakidis, K., Sakellari, D., Angelakeris, M. & Dendrinou-Samara, C., "Size and compositionally controlled manganese ferrite nanoparticles with enhanced magnetization." *J Nanopart Res.* 15, 1-11 (2013).

[21] Stoia, M., Barvinsch, P., Barbu, L., Barbu, M. & Stefanescu, M., "Synthesis of nanocrystalline nickel ferrite by thermal decomposition of organic precursors." *J Therm Anal Calorim.* 108, 1033-1039 (2011).

[22] Yang, H., Zhang, C., Shi, X., Hu, H., Du, X., et al. "Water-soluble superparamagnetic manganese ferrite nanoparticles for magnetic resonance imaging." *Biomaterials*. 31, 3667-3673 (2010).

[23] Bellusci, M., Aliotta, C., Fiorani, D., La Barbera, A., Padella, F., et al "Manganese iron oxide superparamagnetic powder by mechanochemical processing. Nanoparticles functionalization and dispersion in a nanofluid." *J Nanopart Res.* 14, 1-11 (2012).

[24] Arana, M., Bercoff, P., Jacobo, S., Mendoza, P. & Pasquevich, G., "Mechanochemical synthesis of MnZn ferrite nanoparticles suitable for biocompatible ferrofluids." *Ceramics International.* 42, 1545-1551 (2016).

[25] Iwasaki, T., Nakatsuka, R., Murase, K., Takata, H., Nakamura, H. & Watano, S., "Simple and rapid synthesis of magnetite/hydroxyapatite composites for hyperthermia treatments via a mechanochemical route." *Int. J. Mol. Sci.* 14, 9365-9378 (2013).

[26] Bėčytė, V., Mažeika, K., Rakickas, T. & Pakštas, V., "Study of magnetic and structural properties of cobalt-manganese ferrite nanoparticles obtained by mechanochemical synthesis." *Materials Chemistry and Physics.* 172, 6-10 (2016).

[27] Sasaki, T., Ohara, S., Naka, T., Vejpravova, J., Sechovsky, V., Umetsu, M., et al. "Continuous synthesis of fine MgFe2O4 nanoparticles by supercritical hydrothermal reaction." *J. of Supercritical Fluids.* 53, 92-94 (2010).

[28] Freire, R., Freitas, P., Ribeiro, T., Vasconcelos, I., Denardin, J. et al. "Effect of solvent composition on the structural and magnetic properties of MnZn ferrite nanoparticles obtained by hydrothermal synthesis." *Microfluidics and nanofluidics.* 17, 233-244 (2014).

[29] Zahraei, M., Monshi , A., del Puerto Morales, M., Shahbazi-Gahrouei, D., Amirnasr, M. & Behdadfar, B., "Hydrothermal synthesis of fine stabilized superparamagnetic nanoparticles of Zn2+ substituted manganese ferrite." *Journal of Magnetism and Magnetic Materials.* 393, 429-436 (2015).

[30] Szczygiel, I. & Winiarska, K., "Low-temperature synthesis and characterization of the Mn–Zn ferrite." *J Therm Anal Calorim*. 104, 577-583 (2010).

[31] Mazario, E., Menendez, N., Herrasti, P., Cañete, M. & Connord, V., Carrey, J., "Magnetic hyperthermia properties of electrosynthesized cobalt ferrite nanoparticles." *The Journal of Physical Chemistry* C. 117, 11405-11411 (2013).

[32] Phong, P., Nam, P., Manh, D. & Lee, I., "Mn0.5Zn0.5Fe2O4 nanoparticles with high intrinsic loss power for hyperthermia therapy." *Journal of Magnetism and Magnetic Materials.* 433, 76-83 (2017).

[33] Mosivand, S. & Kazeminezhad, I., "A novel synthesis method for manganese ferrite nanopowders: The effect of manganese salt as inorganic additive in electrosynthesis cell." *Ceramics International.* 41, 8637-8642 (2015).

[34] Pradhan, P., Giri, J., Banerjee, R., Bellare, J. & Bahadur, D., "Preparation and characterization of manganese ferrite-based magnetic liposomes for hyperthermia treatment of cancer." *Journal of Magnetism and Magnetic Materials.* 311, 208-215 (2007).

[35] Yang, C. & Jianbo, L., "Preparation and characterization of Mn–Zn ferrite/poly (N, N′-isopropyl acrylamide) core/shell nanocomposites via in-situ polymerization." *Materials Letters.* 64, 1570-1573 (2010).

[36] Kuruva, P., Matteppanavar, S., Srinath, S. & Thomas, T., "Size control and magnetic property trends in cobalt ferrite nanoparticles synthesized using an aqueous chemical route." *IEEE Transactions on Magnetics.* 50, 1-8 (2014).

[37] Goswami, P.P., Choudhury, H.A., Chakma, S. & MoholkarV.S., "Sonochemical synthesis of cobalt ferrite nanoparticles." *International Journal of Chemical Engineering.* 2013, 1-6 (2013).

[38] Gurumoorthy, M., Parasuraman, K., Anbarasu, M. & Balamurugan, K., "Synthesis and Characterization of MnFe2O4 Nanoparticles by Hydrothermal Method." *Nano Vision.* 5, 39-168 (2015).

[39] Peng, E., Guang, E.S., Chandrasekharan, P., Yang, C.T., Ding, J. et al., "Synthesis of manganese ferrite/graphene oxide nanocomposites for biomedical applications." *Small.* 8, 3620-3630 (2012).

[40] Pemartin, K., Solans, C., Alvarez, J. & Sanchez, M., "Synthesis of Mn–Zn ferrite nanoparticles by the oil-in-water microemulsion reaction method." *Colloids and Surfaces A: Physicochemical and Engineering Aspects.* 451, 161-171 (2014).

[41] Sahoo, B., Sanjana, K., Dutta, S., Maiti, T., Pramanik, P. & Dhara, D., "Biocompatible mesoporous silica-coated superparamagnetic manganese ferrite nanoparticles for targeted drug delivery and MR imaging applications." *Journal of colloid and Interface Science*. 431, 31-41 (2014).

[42] Sanpo, N., Wang, J. & Berndt, C.C., "Sol-gel synthesized copper-substituted cobalt ferrite nanoparticles for biomedical applications." *Journal of nano research*. 22, 95-106 (2013).

[43] Jasso-Terán, R.A., Cortés-Hernández, D.A., Sánchez-Fuentes, H.J., Reyes-Rodríguez, P.Y., de-León-Prado, L.E., Escobedo-Bocardo, J.C. & Almanza-Robles, J.M., "Synthesis, characterization and hemolysis studies of Zn(1−x)CaxFe2O4 ferrites synthesized by sol-gel for hyperthermia treatment applications." *Journal of Magnetism and Magnetic Materials.* 427, 241-244 (2017).

[44] Ali, M.B., Maalam, K.E., Moussaoui, H.E., Mounkachi, O., Hamedoun, M. et al. "Effect of zinc concentration on the structural and magnetic properties of mixed Co–Zn ferrites nanoparticles synthesized by sol/gel method." *Journal of Magnetism and Magnetic Materials.* 398, 20-25 (2016).

[45] Sulaiman, N.H., Ghazali, M.J., Majlis, B.Y., Yunas, J. & Razali, M., "Superparamagnetic calcium ferrite nanoparticles synthesized using a simple sol-gel method for targeted drug delivery." *Bio-Medical Materials and Engineering.* 26, S103-S110 (2015).

[46] Beji, Z., Hanini, A., Smiri, L.S., Gavard, J., Kacem, K. et al. "Magnetic properties of Zn-substituted MnFe2O4 nanoparticles synthesized in polyol as potential heating agents for hyperthermia. Evaluation of their toxicity on Endothelial cells." *Chem. Mater.* 22, 420-5429 (2010).

[47] Kanagesan, S., Aziz, S.B.A., Hashim, M., Ismail, I., Tamilselvan, S. et al. "Synthesis, Characterization and in vitro evaluation of manganese ferrite (MnFe2O4) nanoparticles for their biocompatibility with murine breast cancer cells (4T1)." *Molecules.* 21, 312 (2016).

[48] Jeun, M., Park, S., Jang, G. & Lee, K., "Tailoring MgxMn1–xFe2O4 Superparamagnetic Nanoferrites for Magnetic Fluid Hyperthermia Applications." *ACS Appl. Mater. Interfaces.* 6, 16487-16492 (2014).

[49] Md Gazzali, P., Kanimozhi, V., Priyadharsini, P. & Chandrasekaran, G., "Structural and Magnetic properties of Ultrafine Magnesium Ferrite Nanoparticles." *Advanced Materials Research.* 938, 128-133 (2014).

[50] Yadav, R.S., Havlica, J., Hnatko, M., Šajgalík, P., Alexander, C. et al. "Magnetic properties of Co1−xZnxFe2O4 spinel ferrite nanoparticles synthesized by starch-assisted sol–gel autocombustion method and its ball milling." *Journal of Magnetism and Magnetic Materials.* 378, 190-199 (2015).

[51] Bifa, J., Changan, T., Quanzheng, Z., Dongdong, J., Jie, Y. et al.

"Magnetic properties of samarium and gadolinium co-doping Mn-Zn ferrites obtained by sol-gel auto-combustion method." *Journal of Rare Earths.* 34, 1017-1023 (2016).

[52] Ebrahimi, S.S. & Masoudpanah, S.M,, "Effects of pH and citric acid content on the structure and magnetic properties of MnZn ferrite nanoparticles synthesized by a sol–gel autocombustion method." *Journal of Magnetism and Magnetic Materials.* 357, 77-81 (2014).

[53] Masoudpanah, S.M., Seyyed, S.A., Derakhshani, M. & Mirkazemi, S.M., "Structure and magnetic properties of La substituted ZnFe2O4 nanoparticles synthesized by sol–gel autocombustion method." *Journal of Magnetism and Magnetic Materials.* 370, 122-126 (2014).

[54] Deganello, F., Marcì, G. & Deganello, G., "Citrate–nitrate auto-combustion synthesis of perovskite-type nanopowders: a systematic approach." Journal of the European Ceramic Society. 29, 439-450 (2009).

[55] Mohseni, H., Shokrollahi, H., Sharif, I. & Gheisari, Kh., "Magnetic and structural studies of the Mn-doped Mg–Zn ferrite nanoparticles synthesized by the glycine nitrate process." *Journal of Magnetism and Magnetic Materials.* 324, 3741-3747 (2012).

[56] Winiarska, K., Szczygieł, I., & Klimkiewicz, R., "Manganese–zinc ferrite synthesis by the sol–gel autocombustion method. Effect of the precursor on the ferrite's catalytic properties." *Industrial & Engineering Chemistry Research*. 52, 353-361 (2012).

[57] Topkaya, R., Kurtan, U., Baykal, A. & Toprak, M.S., "Polyvinylpyrrolidone (PVP)/MnFe2O4 nanocomposite: sol–gel autocombustion synthesis and its magnetic characterization." *Ceramics International.* 39, 5651-5658 (2013).

[58] Murugesan, C., Sathyamoorthy, B. & Chandrasekaran, G., "Structural, dielectric and magnetic properties of Gd substituted manganese ferrite nanoparticles." *Phys. Scr.* 90, 085809 (2015).

[59] Azadmanjiri, J., "Preparation of Mn–Zn ferrite nanoparticles from chemical sol–gel combustion method and the magnetic properties after sintering." *Journal of Non-Crystalline Solids*. 353, 4170-4173 (2007).

[60] Ebrahimi, S.S., Masoudpanah, S.M., Amiri, H. & Yousefzadeh, M., "Magnetic properties of MnZn ferrite nanoparticles obtained by SHS and sol-gel autocombustion techniques." *Ceramics International*. 40, 6713-6718 (2014).

[61] Shirsath, S.E., Toksha, B.G., Kadam, R.H., Patange, S.M., Mane, D.R. et al. "Doping effect of Mn2+ on the magnetic behavior in Ni–Zn ferrite nanoparticles prepared by sol–gel auto-combustion." *Journal of Physics and Chemistry of Solids.* 71, 1669-1675 (2010).

[62] Sanpo, N., Berndt, C.C., Wen, C. & Wang, J., "New Approaches to the Study of Spinel Ferrite Nanoparticles for Biomedical Applications." Handbook of Nanoelectrochemistry: Electrochemical Synthesis Methods, *Properties, and Characterization Techniques.* 1417-1441 (2016).

[63] Sánchez, J., Cortés-Hernández, D.A., Escobedo-Bocardo, J.C., Jasso-Teràn, R.A. & Zugasti-Cruz, A., "Bioactive magnetic nanoparticles of Fe–Ga synthesized by sol–gel for their potential use in hyperthermia treatment." *J Mater Sci: Mater Med.* 25, 2237-2242 (2014).

[64] Sánchez, J., Cortés-Hernández, D.A., Escobedo-Bocardo, J.C., Almanza-Robles, J.M., Reyes-Rodríguez, P.Y. et al. "Sol-gel synthesis of MnxGa1−xFe2O4 nanoparticles as candidates for hyperthermia treatment." *Ceramics International.* 42, 13755-13760 (2016).

[65] Sánchez, J., Cortés-Hernández, D.A., Escobedo-Bocardo, J.C., Almanza-Robles, J.M., Reyes-Rodríguez, P.Y. et al. "Synthesis of MnxGa1−xFe2O4 magnetic nanoparticles by thermal decomposition method for medical diagnosis applications." *Journal of Magnetism and Magnetic Materials.* 427, 272-275 (2017).

[66] Vamvakidis, K., Sakellari, D., Angelakeris, M. & Dendrinou-Samara, C., "Size and compositionally controlled manganese ferrite nanoparticles with enhanced magnetization." *J Nanopart Res.* 15. 1743 (2013).

[67] Makridis, A., Topouridou, K., Tziomaki, M., Sakellari, D., Simeonidis, K. et al. "In vitro application of Mn-ferrite nanoparticles as novel magnetic hyperthermia agents." J. Mater. Chem. B. 2, 8390-8398 (2014).

[68] Zipare, K., Dhumal, J., Bandgar, S., Mathe, V. & Shahane, G., "Superparamagnetic manganese ferrite nanoparticles: synthesis and magnetic properties." *Journal of Nanoscience and Nanoengineering.* 1, 178-182 (2015).

[69] Rodrigues, A.R.O., Ramos, J.M.F., Gomes, I.T., Almeida, B.G., Araújo, J.P. et al. "Magnetoliposomes based on manganese ferrite nanoparticles as nanocarriers for antitumor drugs." *RSC Adv.*. 6, 17302-17313 (2016).

[70] Mazarío, E., Sánchez-Marcos, J., Menéndez, N., Cañete, M., Mayoral. A. et al. "High specific absorption rate and transverse relaxivity effects in manganese ferrite nanoparticles obtained by an electrochemical route." *J. Phys. Chem. C.* 119, 6828-6834 (2015).

[71] Huang, C.-C., Su, C.-H., Liao, M.-Y. & Yeh, C.-S., "Magneto-optical FeGa2O4 nanoparticles as dual-modality high contrast efficacy T2 imaging and cathodoluminescent agents." *Physical Chemistry Chemical Physics.* 11, 6331-6334 (2009).

[72] Laurent, S., Dutz, S., Häfeli, U.O. & Mahmoudi, M., "Magnetic fluid hyperthermia: focus on superparamagnetic iron oxide nanoparticles. *Advances in colloid and interface science.* 166, 8-23 (2011).

[73] Lima, E., Torres, T.E., Rossi, L.M., Rechenberg, H.R., Berquo, T.S. et al. "Size dependence of the magnetic relaxation and specific power absorption in iron oxide nanoparticles." *J Nanopart Res.* 15, 1654 (2013).

[74] Cornell, R.M. & Schwertmann, U., "The iron oxides: structure, properties, reactions, occurrences and uses." John Wiley & Sons. (2003)

[75] Li, J., Yuan, H., Li, G., Liu, Y. & Leng, J., "Cation distribution dependence of magnetic properties of sol–gel prepared MnFe2O4 spinel ferrite nanoparticles." *Journal of Magnetism and Magnetic Materials.* 322, 3396-3400 (2010).

[76] Carter, C.B. & Norton, M.G., "Ceramic materials: science and engineering." Springer Science & Business Media. (2007).

[77] Briceño, S., Bramer-Escamilla, W., Silva, P., Delgado, G.E., Plaza, E. et al. "Effects of synthesis variables on the magnetic properties of CoFe 2 O 4 nanoparticles." *Journal of Magnetism and Magnetic Materials.* 324, 2926-2931 (2012).

[78] Sheng-Nan, S., Chao, W., Zan-Zan, Z., Yang-Long, H., Venkatraman, S.S. & Zhi-Chuan, X., "Magnetic iron oxide nanoparticles: Synthesis and surface coating techniques for biomedical applications." *Chin. Phys. B.* 23, 037503 (2014).

[79] Peng, E., Ding, J. & Xue J.M., "Concentration-dependent magnetic hyperthermic response of manganese ferrite-loaded ultrasmall graphene oxide nanocomposites." *New J. Chem*. 38, 2312-2319 (2014).

Highly Linear and Low Noise AMR Sensor Using Closed Loop and Signal-Chopped Architecture

N. Hadjigeorgiou, A. C. Tsalikidou, E. Hristoforou, P. P. Sotiriadis

***Abstract*—**During the last few decades, the continuously increasing demand for accurate and reliable magnetic measurements has paved the way for the development of different types of magnetic sensing systems as well as different measurement techniques. Sensor sensitivity and linearity, signal-to-noise ratio, measurement range, cross-talk between sensors in multi-sensor applications are only some of the aspects that have been examined in the past. In this paper, a fully analog closed loop system in order to optimize the performance of AMR sensors has been developed. The operation of the proposed system has been tested using a Helmholtz coil calibration setup in order to control both the amplitude and direction of magnetic field in the vicinity of the AMR sensor. Experimental testing indicated that improved linearity of sensor response, as well as low noise levels can be achieved, when the system is employed.

***Keywords*—**AMR sensor, closed loop, memory effects, chopper, linearity improvement, sensitivity improvement, magnetic noise, electronic noise.

I. Introduction

MAGNETIC sensors are preferred types of sensors in industry for many applications. They can easily operate under severe environmental conditions, they are very reliable due to the absence of moving parts, they can be imbedded inside building materials, and they can operate at elevated temperatures.

Magnetic sensors are categorized primarily based on their sensing principle which impacts directly their operating characteristics like measurement range, obtained resolution, frequency response, working temperature, and manufacturing cost. For example, Hall effect and pick-up-coils based sensors have been proven to be quite practical and cost effective solutions in most common applications. Nevertheless, pick up coils are not appropriate for measuring low frequency magnetic fields, while Hall-effect devices cannot provide the resolution levels needed in demanding applications. On the other hand, Anisotropic Magnetoresistance (AMR), Giant Magnetoresistance (GMR), Giant Magneto-Impedance (GMI), Magnetostrictive and Flux-Gate sensors, although available at an increased cost, are frequently employed when higher resolution is required [1].

N. Hadjigeorgiou is with the School of Electrical and Computer Engineering, National Technical University of Athens (NTUA), Athens, Greece (phone: +302107721482, fax: +302107721484, e-mail: nhatzig@central.ntua.gr).

A. C. Tsalikidou and P. P. Sotiriadis are with the School of Electrical and Computer Engineering, NTUA, Athens, Greece (e-mail: anastasitsalik@gmail.com, pps@ieee.com).

E. Hristoforou, was with School of Mining and Metallurgical Engineering. Now he is with the School of Electrical and Computer Engineering, NTUA, Athens, Greece (e-mail: eh@mental.ntua.gr).

AMR sensors have emerged as a promising alternative, when higher resolution is required, providing an ideal balance between performance and cost. They offer considerably improved frequency response compared to more expensive solutions, like Flux-Gates, and have been used successfully in a wide variety of applications ranging from navigation, detection of ferromagnetic elements and monitoring purposes to EMF and sensitive current measurements [2]-[4].

AMR sensors are typically formed in a Wheatstone bridge structure with bridge elements commonly manufactured by thin-film permalloy materials of magnetoresistive nature. The size of the bridge is often in tens of μm allowing for higher spatial resolution compared to more traditional solutions. Despite their advantages, contemporary AMR sensors still have certain deficiencies like non-linear response, DC offset, magnetic hysteresis, cross-axis effects and they need periodic re-polarization of permalloy film magnetic domains, which gives room for considerable improvement [5].

Several techniques have been proposed to enhance the performance of AMR sensors, e.g. elimination of DC offset using digital feedback and/or implementation of a current pulsing circuit to accomplish the re-polarization of permalloy thin-film magnetic domains are some of the most common approaches that have been adopted [3]-[5]. Hysteresis issues can also be controlled with the current pulsing circuit architecture. In addition, different numerical as well as experimental techniques have been proposed as a means of reducing cross-axis measurement effects regarding the response of the Wheatstone bridge elements [6]-[8]. However, certain issues such as non-linear response and measurement noise of AMR sensors are rarely discussed in architectures proposed in the literature. Moreover, while in most cases open loop feedback architectures are employed to improve the sensitivity of the magnetic measurement, this can lead to an increase in the uncertainty of measurement due to the corresponding increase of magnetic noise. In addition, the digital closed loop compensation systems proposed up to date tend to reduce the bandwidth of the closed loop.

In this work, an analog closed loop compensation system is proposed, developed, and tested as a means to eliminate the non-linearity of AMR response, considerably reduce the 1/f noise, and enhance the sensitivity of magnetic measurement. The experimental results indicate that AMR response presented a maximum deviation of 0.36% with respect to the ideal linear response. Furthermore, the proposed closed loop system is able to maintain the measured noise density levels as low as the corresponding intrinsic noise density values of the AMR sensing element provided by the manufacturer [9].

II. Proposed Closed Loop Architecture

For the purposes of this work, the HMC-1001 and 1002 AMR sensor elements, manufactured by Honeywell Inc., have been used. The structure of the proposed closed loop system is illustrated in Fig. 1.

The system is composed of the AMR Wheatstone bridge sensor elements and the accompanying electronic circuitry, all of which are discussed in detail in the subsections "AMR Sensor Mathematical and SPICE Model".

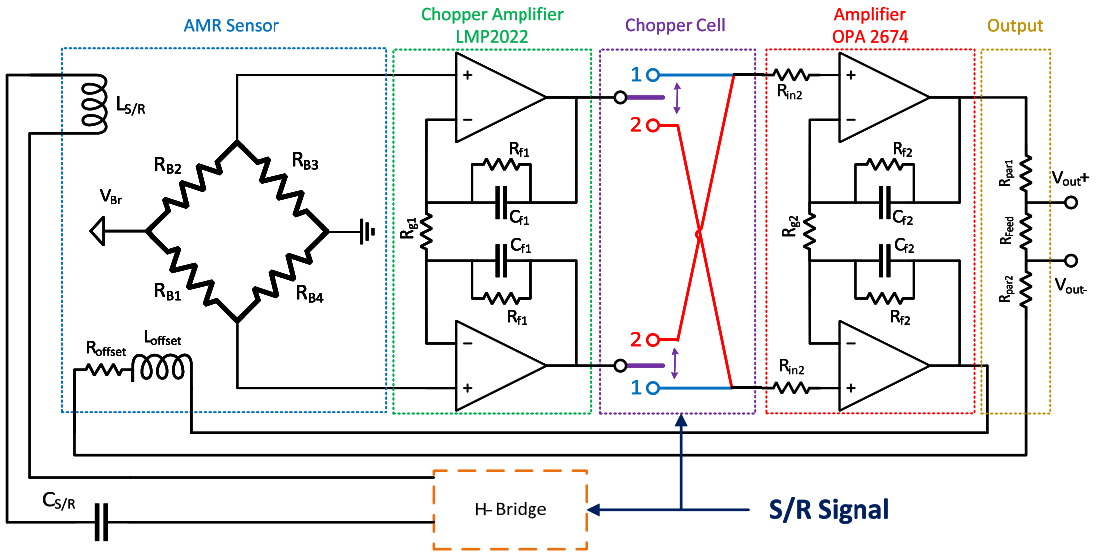

Fig. 1 The proposed closed loop architecture

There are two (integrated) coils in the AMR sensor. The bottom one, L_{offset} is used for feedback purposes to improve linearity and reduce memory effects. The top-left one, $L_{S/R}$, is the set-reset coil used for the re-polarization of permalloy thin-film magnetic domains with short but strong current pulses. Those pulses are generated by the H-Bridge switches using a capacitor in series. When a set pulse is given, the voltage output of the sensor is F(B) switching to -F(B) when a reset pulse is given. The chopper cell between the two amplifying stages reverses the polarity according to the set-reset pulses.

A. AMR Sensor Mathematical and SPICE Model

The simplified linear analytical model of the HMC-1001/2 sensor elements in Fig. 2 has been developed to obtain a first order approximation of sensors system frequency response and closed loop stability.

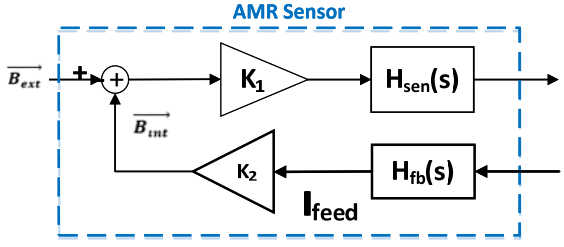

Fig. 2 Simplified analytic HMC-1001/2 sensor diagram

The model includes two paths: 1) The forward one, $H_{sen}(s)$, representing the transfer function of the conversion of the magnetic field intensity to voltage; it captures the inherent bandwidth of the sensing element using a simplified dominant-pole model, i.e. $H_{sen}(s) = \frac{2\pi f_{sen-3dB}}{s + 2\pi f_{sen-3dB}}$. 2) The feedback path $H_{fb}(s)$ capturing the voltage to magnetic field intensity conversion via the offset coil $H_{fb}(s) = 1/(s \cdot L_{offset} + R_{offset})$. Constants K_1 and K_2 stand for the conversion gain ratios.

The non-linear behavior (at high magnetic field) of the magnetoresistive Wheatstone bridge of both HMC-1001/2 sensor elements was taken into account using the detailed SPICE model in Fig. 3.

With the model in Fig. 3, the behavior of the complete system in terms of frequency response, non-linearity and closed loop stability can be captured. The Voltage-Controlled Voltage Sources (VCVS) E are used as ideal buffers. The VCVS E_{K1} and the Current Controlled Voltage Source (CCVS) H_{K2} are the conversion parameters of the forward and feedback paths respectively as provided by the manufacture of the sensor. The offset strap that creates the offset magnetic field was modeled by the inductor L_{offset} with a resistor R_{offset} in series. In order to create the non-linear behavior of the sensor, a careful selection of the Zener Z_D and the resistor R_Z has been done by simulation and curve fitting. The low pass filter R_{LP}-C_{LP} was used to simulate the bandwidth of the sensor. The DC bias and the output resistance of the sensor were simulated by using the voltage source V_B and the resistor R_{Br}, respectively. Finally, the manufacturer's operating parameters [9] have been taken into account in the linear (Fig. 2) and non-linear (Fig. 3) models.

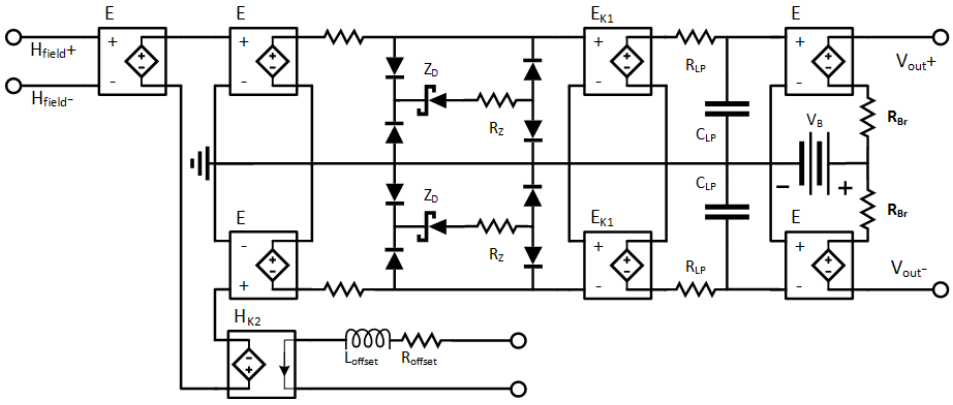

Fig. 3 Spice model for HMC-1001/2

B. System Model of the Closed Loop Architecture

The model of the additional circuitry, implementing the signal conditioning and closed loop operation, was developed. The circuit is divided into two stages: 1) The chopper voltage amplification (LMP2021 chopper opamp); in this stage the sensor's output voltage is amplified, while maintaining the 1/f noise level as low as possible. 2) High current output voltage amplification (OPA2674 opamp); this stage provides the high output current needed to drive the internal compensation coil L_{offset} of the sensor element and implement the closed loop architecture.

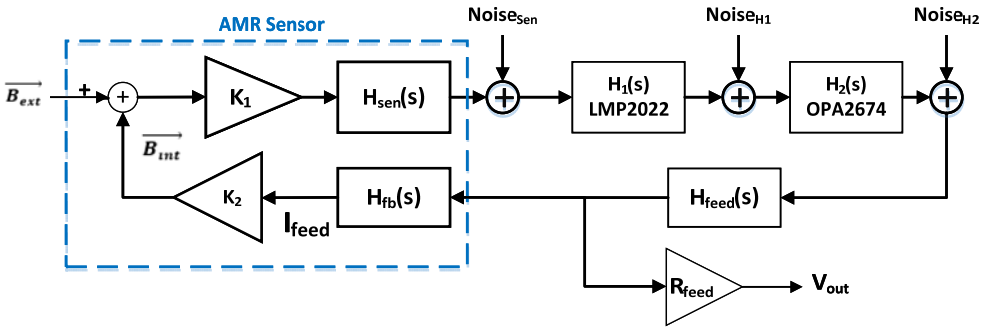

Fig. 4 Simplified analytic system diagram

Fig. 4 shows the complete system model of the sensor element and electronic circuit. The transfer function of the amplifying stages $H_i(s)$, $i = 1,2$ are given by

$$H_i(s) = \frac{A_i \cdot R_{g_i} \cdot (s \cdot R_{f_i} \cdot C_{f_i} + 1)}{(A_i \cdot R_{g_i} \cdot R_{f_i} \cdot C_{f_i}) \cdot s + A_i \cdot R_{g_i} + R_{f_i}} \quad (1)$$

and the remaining feedback loop behavior is captured by

$$H_{feed}(s) = \frac{R_{feed}}{R_{feed} + R_{par1} + R_{par2} + R_{offset} + s \cdot L_{offset}} \quad (2)$$

The output voltage noise power spectral density of $H_1(s)$ and $H_2(s)$ are $E_{H1} = 7{,}7\,\mu V/\sqrt{Hz}$ and $E_{H2} = 69\,nV/\sqrt{Hz}$ respectively. Finally, (3) gives the complete transfer function

$$H_T(s) = \frac{K_1 \cdot H_{sen} \cdot H_1 \cdot H_2 \cdot H_{feed} \cdot R_{feed}}{1 + K_1 \cdot K_2 \cdot H_{sen} \cdot H_1 \cdot H_2 \cdot H_{feed} \cdot H_{fb}} \approx \frac{15697.2 \cdot \pi \cdot 5.6K}{s + 2 \cdot \pi \cdot 5.6K} \left(\frac{Volt}{Tesla}\right) \quad (3)$$

and the close loop noise is

$$E_{Total} = 28.77\,\mu V/\sqrt{Hz} \text{ @ } 10\text{Hz} \quad (4)$$

Considering (4), it should be mentioned that, according to the theoretical analysis of (3), the total close loop noise density referred to the input is $1.9\,nT/\sqrt{Hz}$ @ 10Hz.

C. Measurement Setup

The experimental setup consists of two different setups which are presented in Fig. 5. DC magnetic field measurements have been conducted in laboratory environment employing a cubic Helmholtz coil setup (Fig. 5 (a)) in order to calibrate/characterize the system under consideration. The effective bandwidth of the system was identified by AC field measurements using the same setup. Finally, the setup used for magnetic noise characterization is displayed in Fig. 5 (b).

In the former case, a high accuracy DC power supply (Yokogawa 7651) has been used for providing the operating current to the Helmholtz coils. On the other hand, a voltage controlled current source driven by a function generator (Agilent 33220A) has been utilized for AC measurements. The results were recorded by a multichannel voltmeter (Keithley 2000) and by an oscilloscope (Agilent MSO9404A).

(a) (b)

Fig. 5 Experimental setup, (a) cubic Helmholtz Coils (b) Magnetic Shield

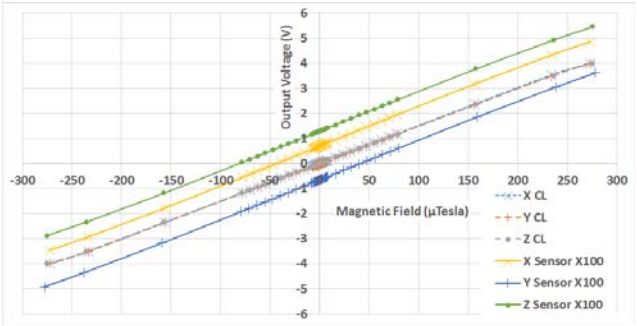

Fig. 6 DC measurements

III. Measurements and Discussion

Every sensor system needs to be calibrated and characterized. This process is presented in the next section. First the "DC Measurements and Calibration" presents the result for the identification of the sensor as well as relationship between the magnetic field and the voltage output. Consequently, it presents the deviation from linearity both for the system and the sensor. The bandwidth of the sensor is presented in the section "Frequency Response". Finally, the section "Magnetic Noise Characterization" corresponds to the noise level at each frequency. The latter is very important due to the fact that is the main reason which reduces the resolution capability of a sensor.

A. DC Measurements and Calibration

Using a high precision current source and the Helmholtz coils of Fig. 5 (a), a controlled linear magnetic field was generated. Both the proposed closed loop sensor system and the sensor alone were tested in this chamber.

Utilizing the method of the least squares, a first order correlation between the magnetic field and the voltage output of the closed loop system (V_{CL}) as well as the voltage output of the sensor (V_S) was obtained (Fig. 6 and Table I). It can be seen that the closed loop system demonstrates lower diversion in the slope and the constant coefficients than the sensor elements.

To observe the (DC) nonlinearity of the system and the sensor element, the linear components were subtracted from their curves, and the remaining nonlinear components were normalized. The results are shown in Fig 7.

The superiority of the proposed close loop sensor system can be clearly identified in Fig. 7. The experimental results indicate that this close loop AMR sensor has a maximum deviation of 0.36% with respect to the ideal linear response.

TABLE I
Equations Correlating the Measured Magnetic Field and the Voltage Output

Axis	Equation
X	$V_{CL_X} = 14{,}89\left(\frac{mV}{\mu T}\right)\cdot B + 12{,}4(mV)$
Y	$V_{CL_Y} = 14{,}86\left(\frac{mV}{\mu T}\right)\cdot B + 10{,}5(mV)$
Z	$V_{CL_Z} = 14{,}84\left(\frac{mV}{\mu T}\right)\cdot B + 7{,}6(mV)$
X	$V_{S_X} = 0{,}155\left(\frac{mV}{\mu T}\right)\cdot B + 7{,}04(mV)$
Y	$V_{S_Y} = 0{,}156\left(\frac{mV}{\mu T}\right)\cdot B - 6{,}5(mV)$
Z	$V_{S_Z} = 0{,}154\left(\frac{mV}{\mu T}\right)\cdot B + 13(mV)$

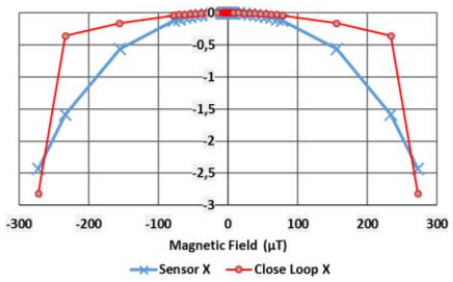

Fig. 7 Nonlinearity of the close loop system and the sensor element

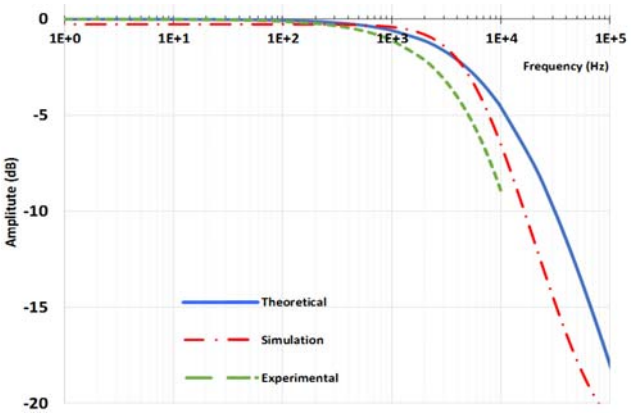

Fig. 8 AC bandwidth measurements

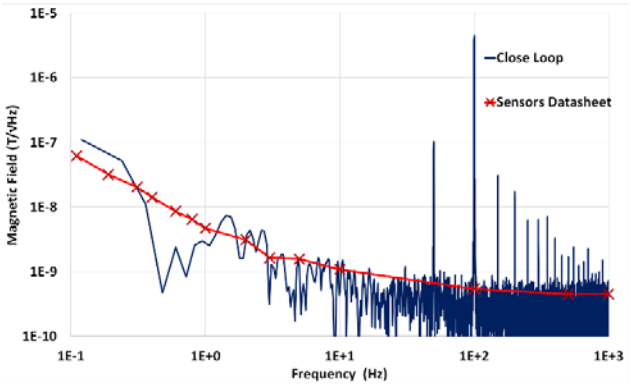

Fig. 9 Magnetic noise measurements

B. Frequency Response

The frequency response was derived by stimulating the Helmholtz coils with AC current. The provided current was generated by a (voltage-output) function generator driving a high precision voltage controlled current source (VCCS). Fig. 8 displays the frequency response of one axis (the response of the other two is similar). The experimental and the theoretical data are in good agreement.

C. Magnetic Noise Characterization

In order to obtain the noise figure, the closed loop system was placed inside the magnetic shield as shown in Fig. 5 (b). The experimental results with respect to the noise of the sensor and the closed loop system, stimulated by a 100-Hz magnetic field, are presented in Fig. 9. The theoretical data extracted through the datasheet of the sensor have also been included for comparison.

IV. Conclusion

The experimental and the theoretical results of the closed loop AMR sensor system indicate that the proposed architecture can provide an alternative and cost effective solution for high precision measurements compared to more expensive sensors types like Flux-Gate. The system demonstrated very good linearity, while maintaining the magnetic noise levels as low as possible. Moreover, the effective bandwidth of the close loop system is wider compared to the other closed loop architectures of other AMR sensor systems found in the literature.

References

[1] P. Ripka, Magnetic Sensors and Magnetometers. Artech House Publishers, 2001.

[2] F. Paixao, C. Quini, O. Baffa, J. Miranda, "A novel device with 36 channels for imaging and signal acquisition of the gastrointestinal tract based on AC biosusceptometry", 2010 Annual International Conference of the IEEE Engineering in Medicine and Biology, Buenos Aires, 2010, pp. 6457-6460.

[3] S. S. Ibanez et al., "A Front-End ASIC for a 3-D Magnetometer for Space Applications by Using Anisotropic Magnetoresistors", IEEE Transactions on Magnetics, vol. 51, pp. 1-4, January 2015.

[4] S. Leittner et al., "Design of the Magnetoresistive Magnetometer for ESA's SOSMAG Project", IEEE Transactions on Magnetics, vol. 51, pp. 1-4, January 2015.

[5] M. Janosek, J. Vyhnanek and P. Ripka, "CW Metal Detector Based on AMR Sensor Array", Sensors, 2011 IEEE, Limerick, 2011, pp. 1515-1517.

[6] J. Chen, L. Yu, C. Zuo, X. Chen, S. Wu, X. Yang, "Compensation Method of Cross-axis Effect for AMR Sensor", Electrical and Control Engineering (ICECE), 2010 International Conference on, Wuhan, 2010, pp. 603-606.

[7] K. Mohamadabadi, C. Coillot, M. Hillion, "New Compensation Method for Cross-Axis Effect for Three-Axis AMR Sensors", IEEE Sensors Journal, vol. 13, no. 4, pp. 1355-1362, April 2013.

[8] L. Yu et al., "Error Compensation and Implementation of Embedded High-Precision Magnetometer", Electrical and Control Engineering (ICECE), 2010 International Conference on, Wuhan, 2010, pp. 911-914.

[9] Datasheet 1- and 2-Axis Magnetic Sensors HMC 1001/1002/1021/1022, https://aerospace.honeywell.com/en/~/media/aerospace/files/datasheet/1and2axismagneticsensorshmc1001-1002-1021-1022_ds.pdf, April 2017.

Neoclis, G. Hadjigeorgiou is a PhD candidate at the School of Electrical and Computer Engineering, National Technical University of Athens (NTUA), Greece. He has had his Master Degree on the subject Automation Systems at the School of Mechanical Engineering, National Technical University of Athens. His Master thesis was "Detection of the position of sea vessel with magnetic techniques." in 2013. He has also had his Bachelor degree at the School of Electrical and Computer Engineering, of the National Technical University of Athens. He has his Bachelor thesis on "Acceleration of the search of the cyclic representation of posets with GPU" in 2011.

Anastasia C. Tsalikidou has also had his Bachelor degree at the School of Electrical and Computer Engineering, of the National Technical University of Athens. He has his Bachelor thesis on "Design and construction of closed-loop circuit for AMR sensor" in 2016.

Evangelos V. Hristoforou, D.Eng, Ph.D, C.Eng, is Professor of Electronic Materials at the School of Electrical and Computer Engineering, National Technical University of Athens (NTUA) and Director of the laboratory of Electronic Sensors. His group is performing research in the following fields-clusters:

- Materials and Applications for Sensors and Transducers (MAST), with the most important product concerning a method and instrument to monitor the 3-d stress tensor distribution in steels
- Hybrid Electric Energy Integrated Cluster (HELENIC), with the most important advances referring to the sustainable and affordable production of hydrogen from water
- Magnetism for Biomedical Applications (MBA), a new-born activity, concerning driving and monitoring of magnetic nanoparticles

He is actively related to several industries in the field of sensors, energy and health, running industrial and research projects. He has published more than 150 papers in international journals (h-index=21) and he gave more than 30 invited talks in international conferences. He is the: Representative of Greece in the Universal Network of Magnetic NDE; Vice-Chair of the Hellenic NDT Association; Chair of the European Magnetic Sensor and Actuator (EMSA) Conference; Chair of the International Conference on Materials and Applications for Sensors and Transducers (IC-MAST); Editor-in-Chief in "Journal of Materials and Applications for Sensors and Transducers"; Regional Editor in "Recent Patents in Material Science"; Editorial Board in "Journal of Electrical Engineering", "Journal of Automation Mobile Robotics and Intelligent Systems" and "Measurement Automation Robotics"

Paul P. Sotiriadis (Senior IEEE member) received the Ph.D. degree in Electrical Engineering and Computer Science from the Massachusetts Institute of Technology, Cambridge USA, in 2002, the M.S. degree in Electrical Engineering from Stanford University, California USA in 1996 and the Diploma degree in Electrical and Computer Engineering from the National Technical University of Athens, Greece in 1994. In 2002, he joined the Johns Hopkins University as Assistant Professor of Electrical and Computer Engineering. In 2012, he joined the faculty of the Electrical and Computer Engineering Department of the National Technical University of Athens, Greece.

He has authored and coauthored more than 95 technical papers in IEEE journals and conferences, holds one patent, has several patents pending, and has contributed chapters to technical books. His research interests include design, optimization, and mathematical modeling of analog and mixed-signal circuits, RF and microwave circuits, advanced frequency synthesis, biomedical instrumentation, and interconnect networks in deep-submicrometer technologies. He has led several projects in these fields funded by U.S. organizations and has collaborations with industry and national labs.

He has received several awards, including a Best Paper Award in the IEEE Int. Symp. on Circuits and Systems 2007, a Best Paper Award in the IEEE Int. Frequency Control Symp. 2012 and the 2012 Guillemin-Cauer Award from the IEEE Circuits and Systems Society. Dr. Sotiriadis is an Associate Editor of the IEEE Trans. on Circuits and Systems – I and the IEEE Sensors Journal, has served as an Associate Editor of the IEEE Trans. on Circuits and Systems – II from 2005 to 2010 and has been a member of technical committees of many conferences. He regularly reviews for many IEEE transactions and conferences and serves on proposal review panels.

Nonlinear Static Analysis of Laminated Composite Hollow Beams with Super-Elliptic Cross-Sections

G. Akgun, I. Algul, H. Kurtaran

Abstract**—**In this paper geometrically nonlinear static behavior of laminated composite hollow super-elliptic beams is investigated using generalized differential quadrature method. Super-elliptic beam can have both oval and elliptic cross-sections by adjusting parameters in super-ellipse formulation (also known as Lamé curves). Equilibrium equations of super-elliptic beam are obtained using the virtual work principle. Geometric nonlinearity is taken into account using von-Kármán nonlinear strain-displacement relations. Spatial derivatives in strains are expressed with the generalized differential quadrature method. Transverse shear effect is considered through the first-order shear deformation theory. Static equilibrium equations are solved using Newton-Raphson method. Several composite super-elliptic beam problems are solved with the proposed method. Effects of layer orientations of composite material, boundary conditions, ovality and ellipticity on bending behavior are investigated.

Keywords**—**Generalized differential quadrature, geometric nonlinearity, laminated composite, super-elliptic cross-section.

I. Introduction

COMPOSITE beams with various cross-sectional shapes such as circular, rectangular or elliptic in solid or hollow form are used in many engineering fields like civil engineering, aeronautics, military, automotive and marine industry as reinforcement elements or load carrying structures. Hence, understanding the mechanical behavior of these structures is very essential to enable safe and economical designs. Following studies from literature are related to the beams with various cross-sectional shapes such as circular, rectangular or elliptic in solid or hollow form. Guo et al. [1] conducted an experimental study on the bending behavior of thin-walled circular hollow section tube structures. Karagiozova et al. [2] ,[3] studied on the dynamic response of circular and square metallic hollow cross-section beams subjected to an impulsive loading in order to investigate the deformation and energy absorption characteristics of such structures. Zheng et al. [4] investigated the bending capacity of cold-formed stainless steel beams with rectangular and circular cross-section both experimentally and numerically. Li and Yang [5] studied on thermal post-buckling behavior of anisotropic laminated beams with tubular cross-sections resting on elastic foundation under a variety of temperature distributions through the thickness. Asadi and Aghdam [6] performed large amplitude free vibration and post-buckling analysis of laminated composite beam with non-uniform cross-section resting on a nonlinear elastic foundation using Euler–Bernoulli beam theory and GDQ method. Zhao et al. [7] used Chebyshev polynomials theory to investigate the free vibration behavior of functionally graded Euler–Bernoulli and Timoshenko beams with non-uniform cross-sections. Ghafari and Rezaeepazhand [8] employed dimensional reduction method in order to perform an isogeometric analysis on composite beams with arbitrary cross-section. Jiao et al. [9] conducted both theoretical and experimental studies on the buckling and post-buckling behavior of bilaterally constrained beams with non-uniform cross-sections. Law and Gardner [10] investigated the lateral instability of beams with elliptical hollow cross-section. Murin et al. [11] conducted experimental, numerical and semi-analytical studies on torsional warping free vibration behavior of rectangular hollow beams.

As it can be seen from the literature, there are studies about beams with various cross-sections. In this study circular, elliptical or oval cross-sections can be expressed through super-ellipse formulation. Thus, in this study, geometrically nonlinear static behavior of laminated composite hollow beams with super-elliptic cross sections is investigated using generalized differential quadrature (GDQ) method. Static equilibrium equations are obtained through virtual work principle and von-Kármán nonlinear strain-displacement relations are utilized to represent the geometric nonlinearity. Transverse shear effect is taken into account according to the first-order shear deformation theory. Newton-Raphson method is used to solve equilibrium equations. Several laminated composite super-elliptic beam problems are solved using GDQ method to investigate bending behavior under different boundary conditions considering different layer orientation angle, ovality and ellipticity values.

II. Statement of the Problem

Cross-section of a super-elliptical beam is formed with Lamé curves defined by

$$\left|\frac{y}{a}\right|^n + \left|\frac{z}{b}\right|^n = 1 \tag{1}$$

where a and b are the major and minor radius at a cross-section. a/b ratio defines the ellipticity of the cross-section. n is a positive number determining the ovality of the cross-section. The curve is called as ellipse for $n = 2$, hypo-ellipse for $n < 2$ and hyper-ellipse for $n > 2$. The ovality of the cross-

G. A. and İ. A. are with the Department of Mechanical Engineering, Gebze Technical University, Gebze – Kocaeli, Turkey (phone: +90 262 605 27 88; e-mail: agokce@gtu.edu.tr, ilkees@gtu.edu.tr).

H. K. is with the Department of Mechanical Engineering, Gebze Technical University, Gebze – Kocaeli, Turkey (phone: +90 262 605 27 78; e-mail: hasan@gtu.edu.tr).

section increases with increasing value of n as it is shown in Fig. 1. Dimensional properties of super-elliptic beam are shown in Fig. 2 where t is the wall thickness, h and L are the height and length of the beam, respectively.

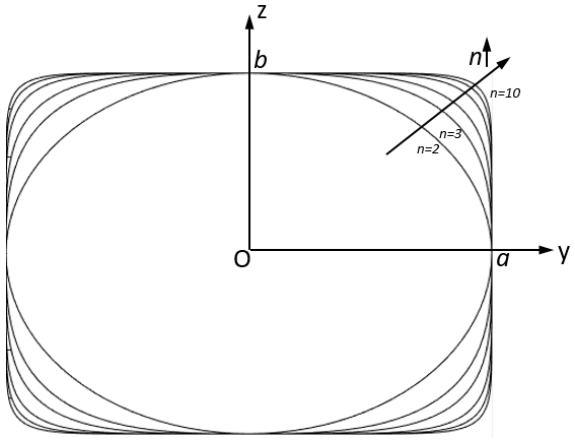

Fig. 1 Cross section of a beam with different Lamé curves

In a moderately thick beam, based on first-order shear deformation theory (FSDT) displacement field can be written in terms of mid-plane displacements and rotation as

$$u(x,z) = u_0(x) + z\theta_x(x)$$
$$w(x,z) = w_0(x) \tag{2}$$

where u_0, w_0 denote longitudinal and transverse displacements at reference mid-plane (x-y) and θ_x represents the rotation about y axis.

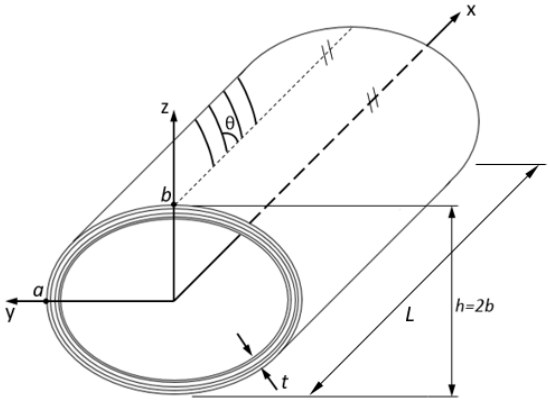

Fig. 2 Hollow cross section parameters and fiber orientation for laminated composite

Nonlinear strain components for moderately thick beam can be expressed as [12]

$$\varepsilon_x = \varepsilon_0 + z \cdot \varepsilon_1$$
$$\gamma_{zx} = \varepsilon_s \tag{3}$$

where

$$\varepsilon_0 = \frac{\partial u_0}{\partial x} + \frac{1}{2} \cdot \left(\frac{\partial w_0}{\partial x} \right)^2$$
$$\varepsilon_1 = \frac{\partial \theta_x}{\partial x} \tag{4}$$
$$\varepsilon_s = \theta_x + \frac{\partial w_0}{\partial x}$$

The constitutive equation for a laminated composite beam can be expressed in terms of in-plane force and moment resultants as

$$N = \begin{Bmatrix} N_1 \\ N_2 \end{Bmatrix} = \begin{bmatrix} A & B \\ B & D \end{bmatrix} \cdot \begin{Bmatrix} \varepsilon_0 \\ \varepsilon_1 \end{Bmatrix} = A_{mat} \cdot \varepsilon_b \tag{5}$$

Laminate constitutive equation for transverse shear in terms of shear force resultant can be stated as

$$Q = A_s \cdot \varepsilon_s \tag{6}$$

A, B, D, and A_s are laminate stiffness coefficients representing in-plane, bending-stretching coupling, bending and transverse shear stiffnesses respectively. They are obtained as:

$$\{A, B, D\} = \sum_{k=1}^{n} \int_A E_x^{(k)} \cdot \{1, z, z^2\} dA_c^{(k)}$$
$$A_s = \sum_{k=1}^{n} k_s \cdot \int_A \overline{Q}_{55}^{(k)} dA_c^{(k)} \tag{7}$$

where $k_s = 1/2$ is the shear correction factor for hollow circular cross-sections [13]. $E_x^{(k)}$ is the equivalent elastic modulus for composite layer and it is given as [14]

$$\frac{1}{E_x^{(k)}} = \frac{\cos^4(\theta_k)}{E_{11}} + \left(\frac{1}{G_{12}} - \frac{2\nu_{12}}{E_{11}}\right) \cdot \cos^2(\theta_k) \cdot \sin^2(\theta_k) + \frac{\sin^4(\theta_k)}{E_{22}} \tag{8}$$

$\overline{Q}_{55}^{(k)}$ is the shear modulus of composite layer calculation of which can be found in composite mechanics books.

Static equilibrium equations of a beam can be derived through the virtual work principle. In this context, virtual work principle can be stated as the virtual work of internal forces is equal to the virtual work of external forces.

For a beam in the absence of damping it can be written as

$$\int_0^L \int_A \left(\sigma_x^{(k)} \delta\varepsilon_x + k_s \tau_{zx}^{(k)} \delta\gamma_{zx} \right) dA_c^{(k)} dx = \int_0^L q\, \delta w_0 dx + \sum_{i=1} F_i \delta w_i \tag{9}$$

where $q(x)$ is the distributed load on the beam and F_i is the concentrated load on the corresponding node. In (9), the terms on the left-hand side denote the virtual work of internal forces due to stresses. First term on the right hand side denotes the virtual work of external forces due to distributed load and second term indicates the virtual work of concentrated forces.

Equation (9) can be written in terms of force and moment resultants as

$$\int_0^L \left[N_1\delta\varepsilon_0 + N_2\delta\varepsilon_1 + Q\delta\varepsilon_s\right]dx = \int_0^L q\,\delta w_0\,dx + \sum_{i=1} F_i\delta w_i \tag{10}$$

Using virtual work equation (10), equation of motion can be obtained in matrix form as:

$$\mathbf{P} = \mathbf{F} \tag{11}$$

where **P** and **F** denote internal force and external force vectors, respectively. Nonlinear static equation of equilibrium in (11) can be solved by using iterative Newton Raphson method. In the implicit solution procedure, equation of equilibrium is written in residual form where displacements are to be calculated as:

$$\mathbf{R} = \mathbf{P} - \mathbf{F} \tag{12}$$

Residual equation is linearized leading to the incremental equilibrium equation as

$$\mathbf{K}\Delta\mathbf{U} = -\mathbf{R} \tag{13}$$

Solution of (13) iteratively leads to displacement increments. Displacement increments are added to the previous values to yield final displacement values.

K matrix in (13) is often referred to as tangent stiffness matrix and for thick straight beam it is given as

$$K = \int_0^L \left[N_d^T N_P N_d + N_d^T B_b^T A_{mat} B_b N_d + N_d^T B_s^T A_s B_s N_d\right]dx \tag{14}$$

where B_b, B_s, N_p, N_d are given as

$$B_b = \begin{bmatrix} 0 & 0 & 0 & 1 & \dfrac{\partial w_0}{\partial x} & 0 \\ 0 & 0 & 0 & 0 & 0 & 1 \end{bmatrix} \tag{15}$$

$$B_s = \begin{bmatrix} 0 & 0 & 1 & 0 & 1 & 0 \end{bmatrix} \tag{16}$$

$$N_p = \begin{bmatrix} 0 & 0 & 0 & 0 & 0 & 0 \\ 0 & 0 & 0 & 0 & 0 & 0 \\ 0 & 0 & 0 & 0 & 0 & 0 \\ 0 & 0 & 0 & 0 & 0 & 0 \\ 0 & 0 & 0 & 0 & N_1 & 0 \\ 0 & 0 & 0 & 0 & 0 & 0 \end{bmatrix} \tag{17}$$

Tangent stiffness matrix is calculated using numerical integration. Nd matrix in the tangent stiffness matrix for the i-th integration point (N_d^i) is given as

$$\text{Columns: } 1 \quad 2 \quad 3 \qquad 3i-2 \quad 3i-1 \quad 3i \qquad 3n-2 \quad 3n-1 \quad 3n$$

$$N_d^i = \begin{bmatrix} 0 & 0 & 0 & \cdots & 1 & 0 & 0 & \cdots & 0 & 0 & 0 \\ 0 & 0 & 0 & \cdots & 0 & 1 & 0 & \cdots & 0 & 0 & 0 \\ 0 & 0 & 0 & \cdots & 0 & 0 & 1 & \cdots & 0 & 0 & 0 \\ C_{i1} & C_{i2} & C_{i3} & \cdots & C_{i(3i-2)} & C_{i(3i-1)} & C_{i(3i)} & \cdots & C_{i(3n-2)} & C_{i(3n-1)} & C_{i(3n)} \\ C_{i1} & C_{i2} & C_{i3} & \cdots & C_{i(3i-2)} & C_{i(3i-1)} & C_{i(3i)} & \cdots & C_{i(3n-2)} & C_{i(3n-1)} & C_{i(3n)} \\ C_{i1} & C_{i2} & C_{i3} & \cdots & C_{i(3i-2)} & C_{i(3i-1)} & C_{i(3i)} & \cdots & C_{i(3n-2)} & C_{i(3n-1)} & C_{i(3n)} \end{bmatrix} \tag{18}$$

where C_{ij} are weighting coefficients used in GDQ method.

III. Numerical Results

GDQ method is used in the solution of super-elliptic composite beam equilibrium equations in this study. In order to employ the GDQ method, a computer program was developed. GDQ code was validated with analysis results from the literature.

For validation, a circular hollow isotropic beam made of stainless steel (SUS304) from the literature is considered [15]. Material properties are: E=201.04 GPa, G=75.8 GPa and ν= 0.3262. Dimensional properties are: t=0.005 m, a=b=0.01 m, h=0.02 m, L=1 m. Both ends of the beam are clamped. Comparisons of load-displacement curves under uniformly distributed load with literature and GDQ method are shown in Fig. 3. Good agreement is obtained with the results of the given reference.

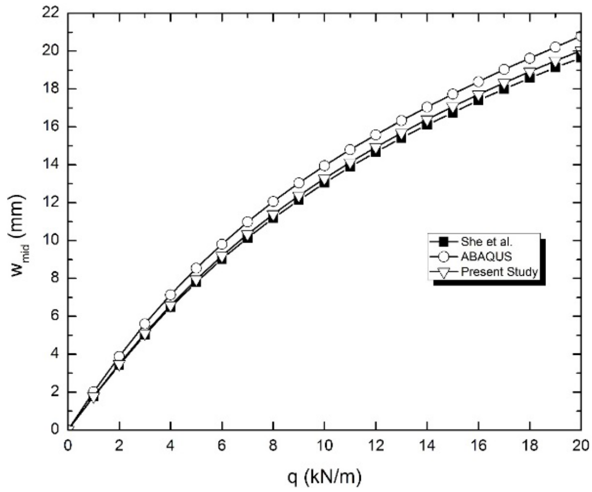

Fig. 3 Comparisons of load-displacement curves for SUS304 beam subjected to uniformly distributed load (q). (a/b=1, a/t=2, L/h=50)

In this study, several super-elliptic composite beam problems are solved with the GDQ method. In the solved examples, different ovality and ellipticity values, layer orientations and boundary conditions are used.

Composite material properties used are: E_{11}=525.38 GPa, E_{22}= E_{33}=21.015 GPa, G_{12}= G_{13}=G_{23}=10.508 GPa, ρ=775.523 kg/m^3 and ν_{12}=0.25. Two different composite layer angle orientations are used in the analyses: [0°/90°/0°/90°/0°] and [0°$_5$]. Wall thickness of the hollow cross-section (t) is taken as t=0.0025 m. Major radius (a) is taken as a=0.025 m. The length of the beam is L=1 m. a/t=10 and h/b=2 are utilized in analyses. In all cases, concentrated transverse force is applied (F=1 kN) on the free end of the beam for cantilever beam (CF)

and in the middle of the beam for both clamped (CC) and both simply supported (SS) boundary conditions as shown in Fig. 4. Analysis results are obtained using 11 grids with GDQ method.

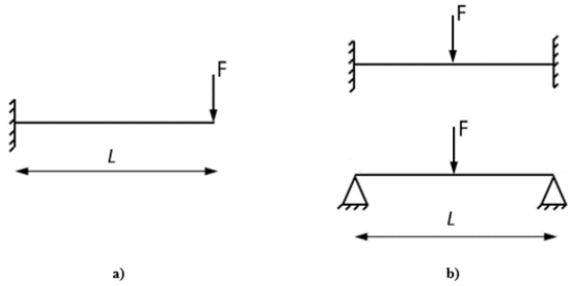

Fig. 4 Loading conditions for (a) cantilever beam (b) beam with CC and SS boundary condition

Transverse displacement values of laminated composite super-elliptic beam with different ovality values for [0°/90°/0°/90°/0°] composite layer orientation under CF, CC and SS boundary condition are given in Figs. 5-7, respectively (*a/b*=2). Transverse displacement values of laminated composite super-elliptic beam with different ovality values for [0°_5] composite layer orientation under CF, CC and SS boundary condition are given in Figs. 8-10, respectively (*a/b*=2). As seen in Figs. 5-10, transverse displacement values decrease with increasing ovality values under CF, CC and SS boundary conditions for [0°/90°/0°/90°/0°] and [0°_5] composite layer orientations. CF boundary condition has led higher displacement values than those for CC and SS boundary conditions. Bending stiffness of [0°_5] composite layer orientation is higher than [0°/90°/0°/90°/0°] layer orientation under CF, CC and SS boundary conditions.

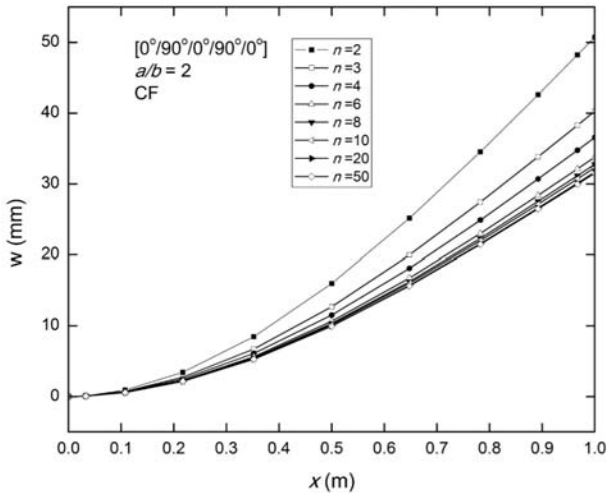

Fig. 5 Transverse displacement values of super-elliptic beam with different ovality values for CF boundary condition (a/b=2, [0°/90°/0°/90°/0°])

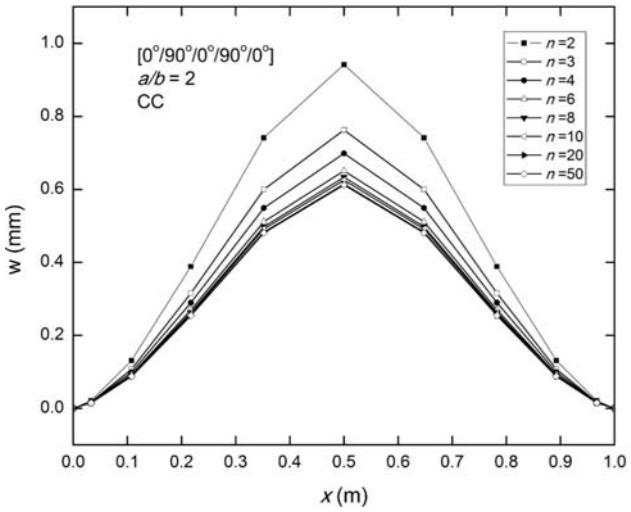

Fig. 6 Transverse displacement values of super-elliptic beam with different ovality values for CC boundary condition (a/b=2, [0°/90°/0°/90°/0°])

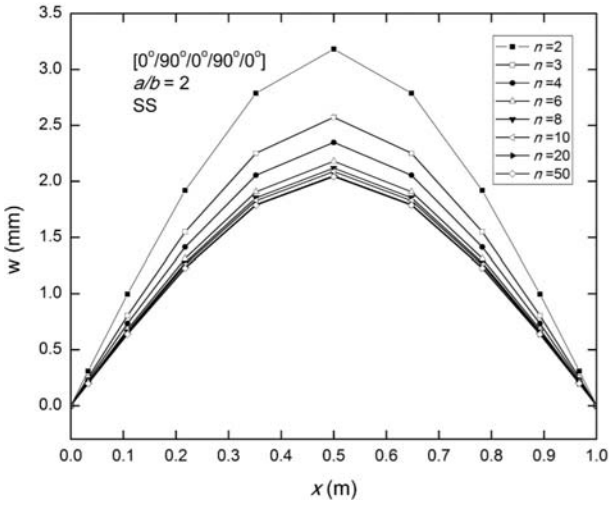

Fig. 7 Transverse displacement values of super-elliptic beam with different ovality values for SS boundary condition (a/b=2, [0°/90°/0°/90°/0°])

Maximum transverse displacement values of laminated composite super-elliptic beam with different ellipticity (*a/b*) and ovality values under CF, CC and SS boundary condition for [0°/90°/0°/90°/0°] layer orientation are shown in Figs. 11-13. As seen in Figs. 11-13, maximum transverse displacement values increase with increasing ellipticity values. However, increase in ovality decreases the displacement values for all ellipticity values ($0.5 \leq a/b \leq 2.5$) and boundary conditions (CF, CC and SS).

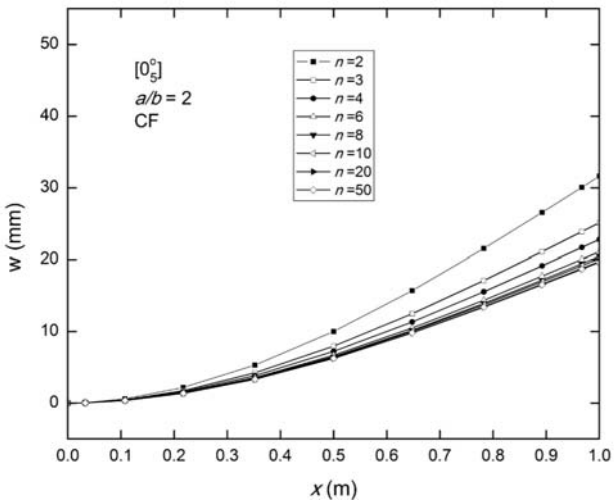

Fig. 8 Transverse displacement values of super-elliptic beam with different ovality values for CF boundary condition (a/b=2, [0^{o}_{5}])

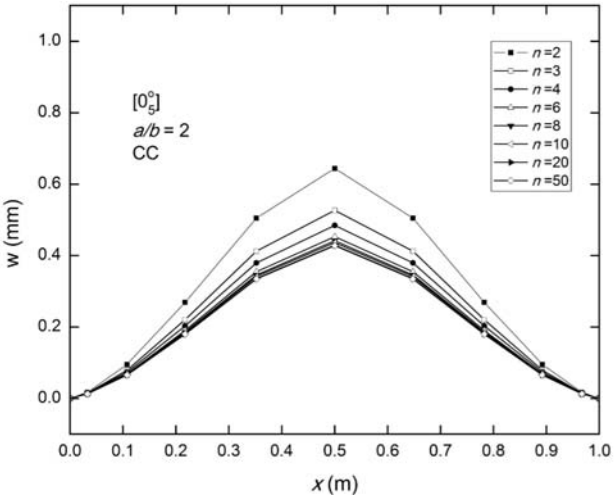

Fig. 9 Transverse displacement values of super-elliptic beam with different ovality values for CC boundary condition (a/b=2, [0^{o}_{5}])

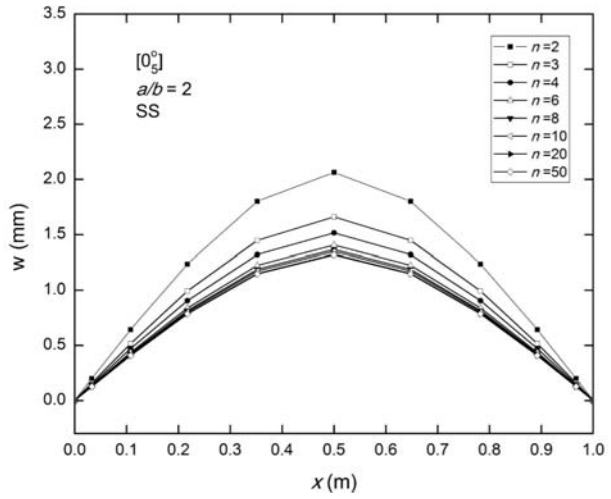

Fig. 10 Transverse displacement values of super-elliptic beam with different ovality values for SS boundary condition (a/b=2, [0^{o}_{5}])

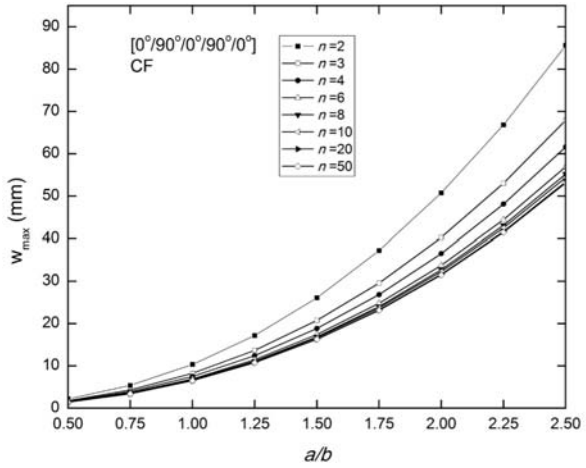

Fig. 11 Maximum transverse displacement values of super-elliptic beam with different ellipticity (*a/b*) and ovality values for CF boundary condition (For [0^{o}/90^{o}/0^{o}/90^{o}/0^{o}] layer orientation)

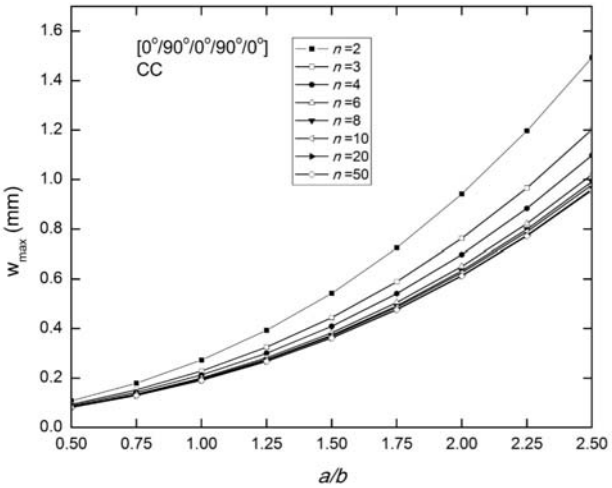

Fig. 12 Maximum transverse displacement values of super-elliptic beam with different ellipticity (*a/b*) and ovality values for CC boundary condition (For [0^{o}/90^{o}/0^{o}/90^{o}/0^{o}] layer orientation)

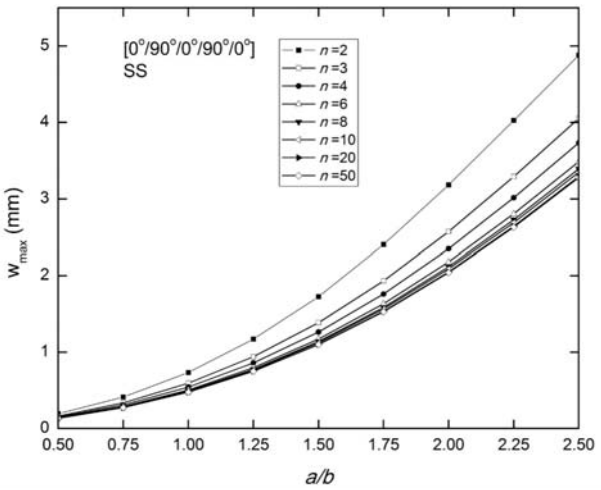

Fig. 13 Maximum transverse displacement values of super-elliptic beam with different ellipticity (*a/b*) and ovality values for SS boundary condition (For [0^{o}/90^{o}/0^{o}/90^{o}/0^{o}] layer orientation)

IV. Conclusions

In this study, geometrically nonlinear static behavior of laminated composite hollow super-elliptic beams is investigated using GDQ method. Super-ellipse formulation is used to represent the oval, elliptic and circular cross-sections. Virtual work principle is used to obtain equilibrium equations of super-elliptic beam and von-Kármán nonlinear strain-displacement relations are utilized. FSDT is considered to represent transverse shear effect. GDQ method is used to calculate the spatial derivatives in strains and Newton-Raphson method is utilized to solve static equilibrium equations.

Regarding the examples solved in this study, outlines of the study can be summarized as below:

- Transverse displacement values decrease with increasing ovality values under CF, CC and SS boundary conditions for $[0^o/90^o/0^o/90^o/0^o]$ and $[0^o_5]$ composite layer orientations.
- Bending stiffness of $[0^o_5]$ composite layer orientation is higher than $[0^o/90^o/0^o/90^o/0^o]$ layer orientation under CF, CC and SS boundary conditions.
- CF boundary condition has led higher displacement values than those for CC and SS boundary conditions.
- Maximum transverse displacement values increase with increasing ellipticity values for CF, CC and SS boundary conditions.
- GDQ method is an efficient and effective method to analyze such systems like in this study.

References

[1] L. Guo, S. Yang, H. Jiao, "Behavior of thin-walled circular hollow section tubes subjected to bending," Thin-Walled Structures, vol. 73, pp. 281-289, 2013.

[2] D. Karagiozova, T. X. Yu, G. Lu, X. Xiang, "Response of a circular metallic hollow beam to an impulsive loading," Thin-Walled Structures, vol. 80, pp. 80-90, 2014.

[3] D. Karagiozova, T. X. Yu, G. Lu, "Transverse blast loading of hollow beams with square cross-sections," Thin-Walled Structures, vol. 62, pp. 169-178, 2013.

[4] B. Zheng, G. Shu, L. Xin, R. Yang, Q. Jiang, "Study on the Bending Capacity of Cold-formed Stainless Steel Hollow Sections," Structures, vol. 8, pp. 63-74, 2016.

[5] Z. Li, D. Yang, "Thermal post buckling analysis of anisotropic laminated beams with tubular cross-section based on higher-order theory," Ocean Engineering, vol. 115, pp. 93-106, 2016.

[6] H. Asadi, M. M. Aghdam, "Large amplitude vibration and post-buckling analysis of variable cross-section composite beams on nonlinear elastic foundation," International Journal of Mechanical Sciences, vol. 79, pp. 47-55, 2014.

[7] Y. Zhao, Y. Huang, M. Guo, "A novel approach for free vibration of axially functionally graded beams with non-uniform cross-section based on Chebyshev polynomials theory" Composite Structures, vol. 168, pp. 277-284, 2017.

[8] E. Ghafari, J. Rezaeepazhand, "Isogeometric analysis of composite beams with arbitrary cross-section using dimensional reduction method" Computer Methods in Applied Mechanics and Engineering, vol. 318, pp. 594-618, 2017.

[9] P. Jiao, W. Borchani, H. Hasni, A. Alavi, N. Lajnef, "Post-buckling response of non-uniform cross-section bilaterally constrained beams" Mechanics Research Communications, vol. 78, pp. 42-50, 2016.

[10] K. H. Law, L. Gardner, "Lateral instability of elliptical hollow section beams" Engineering Structures, vol. 37, pp. 152-166, 2012.

[11] J. Murin, V. Goga, M. Aminbaghai, J. Hrabovsky, T. Sedlar, H. A. Mang, "Measurement and modelling of torsional warping free vibrations of beams with rectangular hollow cross-sections" Engineering Structures, vol. 136, pp. 68-76, 2017.

[12] J. N. Reddy, "Geometrically Nonlinear Transient Analysis of Laminated Composite Plates" AIAA Journal, vol. 21(4), pp. 621-628, 1983.

[13] G. R. Cowper, "The Shear Coefficient in Timoshenko's Beam Theory" Journal of Applied Mechanics, vol. 33(2), pp. 335-340, 1966.

[14] M, Hajianmaleki, M. S. Qatu. "Static and vibration analyses of thick, generally laminated deep curved beams with different boundary conditions" Composite Part B: Eng, vol. 43, pp. 1767–75, 2012.

[15] G. She, F. Yuan, Y. Ren, "Nonlinear analysis of bending, thermal buckling and post-buckling for functionally graded tubes by using a refined beam theory" Composite Structures, vol. 165, pp. 74-82, 2017.

The Influence of Characteristics of Waste Water on Properties of Sewage Sludge

Catalina Iticescu, Lucian P. Georgescu, Mihaela Timofti, Gabriel Murariu, Catalina Topa

***Abstract*—**In the field of environmental protection in the EU and also in Romania, strict and clear rules are imposed that are respected. Among those, mandatory municipal wastewater treatment is included. Our study involved Municipal Wastewater Treatment Plant (MWWTP) of Galati. MWWTP began its activity by the end of 2011 and technology is one of the most modern used in the EU. Moreover, to our knowledge, it is the first technology of this kind used in the region. Until commissioning, municipal wastewater was discharged directly into the Danube without any treatment. Besides the benefits of depollution, a new problem has arisen: the accumulation of increasingly large sewage sludge. Therefore, it is extremely important to find economically feasible and environmentally friendly solutions. One of the most feasible methods of disposing of sewage sludge is their use on agricultural land.

Sewage sludge can be used in agriculture if monitored in terms of physicochemical properties (pH, nutrients, heavy metals, etc.), in order not to contribute to pollution in soils and not to affect chemical and biological balances, which are relatively fragile. In this paper, 16 physico-chemical parameters were monitored. Experimental testings were realised on waste water samples, sewage sludge results and treated water samples. Testing was conducted with electrochemichal methods (pH, conductivity, TDS); parameters N-total (mg/L), P-total (mg/L), N-NH4 (mg/L), N-NO2 (mg/L), N-NO3 (mg/L), Fe-total (mg/L), Cr-total (mg/L), Cu (mg/L), Zn (mg/L), Cd (mg/L), Pb (mg/L), Ni (mg/L) were determined by spectrophotometric methods using a spectrophotometer NOVA 60 and specific kits.

Analyzing the results, we concluded that Sewage sludges, although containing heavy metals, are in small quantities and will not affect the land on which they will be deposited. Also, the amount of nutrients contained are appreciable. These features indicate that the sludge can be safely used in agriculture, with the advantage that they represent a cheap fertilizer.

***Keywords*—**Municipal wastwater, physico-chemical properties, sewage sludge, technology.

Catalina Iticescu is with the "Dunarea de Jos" University of Galati, European Center of Excellence for the Environment, Faculty of Sciences and Environment, 111 Domneasca Street, 800201, Galati, Romania (e-mail: catalina.iticescu@ugal.ro).

Lucian P. Georgescu is with the "Dunarea de Jos" University of Galati, European Center of Excellence for the Environment, Faculty of Sciences and Environment, 111 Domneasca Street, 800201, Galati, Romania (e-mail: lucian.georgescu@ugal.ro).

Mihaela Timofti is with the "Dunarea de Jos" University of Galati, European Center of Excellence for the Environment, Faculty of Sciences and Environment,, Faculty of Sciences and Environment, 111 Domneasca Street, 800201, Galati, Romania (e-mail: mihaela.timofti@ugal.ro).

Gabriel Murariu is with the "Dunarea de Jos" University of Galati, European Center of Excellence for the Environment, Faculty of Sciences and Environment, 111 Domneasca Street, 800201, Galati, Romania (e-mail: gabriel.murariu@ugal.ro).

Catalina Topa is with the "Dunarea de Jos" University of Galati, European Center of Excellence for the Environment, Faculty of Sciences and Environment, 111 Domneasca Street, 800201, Galati, Romania (e-mail: catalina.topa@ugal.ro).

Acknowledgement: This work was supported by a grant of the Romanian National Authority for Scientific Research and Innovation – UEFISCDI, PNCDI III project, 79BG/2017, Efficiency of the technological process for obtaining of sewage sludge usable in agriculture, Eficient.

Synergistic Sorption of Cr(VI) and Cu(II) onto Sweet Potato Vine from Binary Mixtures Cr(VI)-Cu(II)

C. Liu, N. Fiol, I. Villaescusa, J. Poch

***Abstract*—**Over the last decades, biosorption has been an alternative to costly wastewaters treatment for metal removal. Most of the literature on metal biosorption was devoted to studying of single metal ions but nowadays studies on multi-components biosorption are booming. Hexavalent chromium is usually found in mixtures with divalent metal ions in industries wastewaters. However, studies on the simultaneous removal of Cr(VI) and divalent metals are hardly found and the cooperative or competitive mechanism governing each metal ions sorption is still unclear. In this work, simultaneous sorption of Cr(VI) and Cu(II) from their binary mixtures by using sweet potato vine (SPV) was investigated. Sweet potato is one of the four major grain crops in China. Each year about 2000 tons of SPV are generated as by-products. SPV could be a low-cost biosorbent for metal ions due to its rich in cellulose and lignin. In this work, the sorption of Cr(VI) and Cu(II) from their binary mixtures solutions was studied by using SPV sorbent. Equilibrium studies were carried out in binary mixtures in which Cr(VI) and Cu(II) concentration was both varied between 0.1 mM and 0.3 mM, Cr(VI) and Cu(II) single solutions were also prepared as comparison. All the experiments were performed at pH 3±0.05 under 30±2ºC for 7 days to make sure sorption achieved equilibrium. Results showed that (i) chromium was partially (10.93%-42.04%) eliminated under studied conditions through reduction and sorption of hexavalent and trivalent forms. The presence of Cu(II) exerts a synergistic effect on the overall sorption process in all the cases of the 0.1-0.3 mM binary mixtures concentration range. (ii) Cr(VI) removal by SPV is favoured by the presence of Cu(II) in solution, because more protons needed for Cr(VI) reduction are available due to Cu(II)-proton competition; however sorption of the formed Cr(III) is unfavoured as a result of the competition between Cr(III) and Cu(II) for protons and sorbent active sites. (iii) Copper was partially (9.26%-13.91%) sorbed onto SPV under studied conditions. The presence of Cr(VI) in binary mixtures also exerts a synergistic effect on the Cu(II) removal in all the cases of the 0.1-0.3 mM binary mixtures concentration range. The results of the present work indicate that sweet potato vine can be successfully employed for the simultaneously removal of Cr(VI) and Cu(II) in binary mixtures, taking advantage of the synergistic effect provoked by one of the metal ion to each other, even though the acquisition of higher removal yields has to be further investigated.

***Keywords*—**Sweet potato vine, chromium reduction, divalent metal, synergistic sorption.

C. Liu is with the College of Environmental Science and Engineering, Anhui Normal University, Wuhu 241002, China (phone: +86 18155337070; e-mail: lc2014@ahnu.edu.cn).

N. Fiol is with the Chemical Engineering Department, University of Girona, Girona 17071, Spain (e-mail: nuria.fiol@udg.edu).

I. Villaescusa is with the Chemical Engineering Department, University of Girona, Girona 17071, Spain (e-mail: isabel.villaescusa@udg.edu).

J. Poch is with the Applied Mathematics Department, University of Girona, Girona 17071, Spain (e-mail: jordi.poch@udg.edu).

Acknowledgements—This work has been financially supported by Ministry of Human Resources and Social Security of PRC (Anhui15), Education Department of Anhui Province (KJ2016A270) and Anhui Normal University (2015rcpy33, 2014bsqdjj53).

Performance Analysis of Geophysical Database Referenced Navigation: The Combination of Gravity Gradient and Terrain Using Extended Kalman Filter

Jisun Lee, Jay Hyoun Kwon

***Abstract*—**As an alternative way to compensate the INS (inertial navigation system) error in non-GNSS (Global Navigation Satellite System) environment, geophysical database referenced navigation is being studied. In this study, both gravity gradient and terrain data were combined to complement the weakness of sole geophysical data as well as to improve the stability of the positioning. The main process to compensate the INS error using geophysical database was constructed on the basis of the EKF (extended Kalman filter). In detail, two type of combination method, centralized and decentralized filter, were applied to check the pros and cons of its algorithm and to find more robust results. The performance of each navigation algorithm was evaluated based on the simulation by supposing that the aircraft flies with precise geophysical DB and sensors above nine different trajectories. Especially, the results were compared to the ones from sole geophysical database referenced navigation to check the improvement due to a combination of the heterogeneous geophysical database. It was found that the overall navigation performance was improved but not all trajectories generated better navigation result by the combination of gravity gradient with terrain data. Also, it was found that the centralized filter generally showed more stable results. It is because that the way to allocate the weight for the decentralized filter could not be optimized due to the local inconsistency of geophysical data. In the future, switching of geophysical data or combining different navigation algorithm are necessary to obtain more robust navigation results.

***Keywords*—**Extended Kalman Filter, Geophysical Database Referenced Navigation, Gravity Gradient, Terrain.

Jisun Lee is with the University of Seoul, Seoul, 02504 Korea (phone: +82-2-6490-5665; e-mail: leejs@uos.ac.kr).

Jay Hyoun Kown is with the University of Seoul, Seoul, 02504 Korea (phone: +82-2-6490-2890; e-mail: jkwon@uos.ac.kr).

Study of Landslide Behavior with Topographic Monitoring and Numerical Modeling

ZerarkaHizia, Akchiche Mustapha, Prunier Florent

Abstract**—**Landslide of Ain El Hammam (AEH) has been an old slip since 1969; it was reactivated after an intense rainfall period in 2008 where it presents a complex shape and affects broad areas. The schist of AEH is more or less altered; the alteration is facilitated by the fracturing of the rock in its upper part, the presence of flowing water as well as physical and chemical mechanisms of desegregation in joint of altered schist. The factors following these instabilities are mostly related to the geological formation, the hydro-climatic conditions and the topography of the region. The city of AEH is located on the top of a steep slope at 50 km from the city of TiziOuzou (Algeria). AEH's topographic monitoring of unstable slope allows analyzing the structure and the different deformation mechanism and the gradual change in the geometry, the direction of change of slip. It also allows us to delimit the area affected by the movement. This work aims to study the behavior of AEH landslide with topographic monitoring and to validate the results with numerical modeling of the slip site, when the hydraulic factors are identified as the most important factors for the reactivation of this landslide. With the help of the numerical code PLAXIS 2D and PlaxFlow, the precipitations and the steady state flow are modeled. To identify the mechanism of deformation and to predict the spread of the AEH landslide numerically, we used the equivalent deviatory strain, and these results were visualized by MATLAB software.

Keywords**—**Equivalent deviatory strain, landslide, numerical modeling, topographic monitoring.

I. Introduction

THE AEH landslide movement is an interesting case study to model. As the slide's reactivation appears to have been triggered by local water conditions after a strong rainfall treated by [1], we modeled the problem with a hydro-mechanical finite element formulation.

The several reactivations compel us to look closely at its triggers in order to better understand the mechanisms of its evolution in mass. For that, we used two approaches: topographic surveying, and the equivalent deviatory strain, to predict and to identify the deep of slip surface and to understand the sliding direction and velocity. Furthermore, [2]-[4] demonstrate that topographic surveying allows us to discover and to predict the future evolution of the landslide for taking the safety measures.

II. Study Area

AEH is a mountainous town, situated at 1500 m altitude; the climate of the area is Mediterranean, continental, relatively cold, rainy in winter, hot and dry in summer. Temperatures vary from year to year, from -5 °C to 35 °C with occasional peaks of 40 °C in July and August; the rains are spread over a period of five to six months with heavy rain and snow between November and March. The geology of the study area is characterized essentially by dark gray satin schist's belonging to the metamorphic crystallophyllian base of the massif of the Great Kabylia. Satiny schist has a mean direction of schistosity oriented ENE-WSW with a dip that varies from 40 to 60° to the southeast [5].

The landslide of the city of AEH is important and old landslide in Algeria, which affected urbanized part of the AEH city (Fig. 1). The perpetual reactivation of AEH landslide after each rainfall, we require to research and predict its manifestation and its evolution in future.

Fig. 1 Satellite view of the location of AEH landslide

The alteration product is reddish clay silt which contains fragments of shale and makes up the layer of the embankment. The rate of schist alteration depends on the depth of the layer, exposure to climate hazards, and the circulation of groundwater.

The city of AEH is characterized by the existence of numerous water sources in the catchment leaking. This means that there is a substantial aquifer because the shale formations are a priori permeable in one direction of the cleavage.

From the geotechnical point of view, the presence of water in abundance in this region promotes a physical and chemical alteration of the rock (shale satin which is an indication of old compression clay). Schist of metamorphic origin presents multiple structures which have been exposed to the air. The rock has poor resistance to physical and chemical stresses, and easily deteriorates under the action of frost or rainwater [6].

The presence of water in the soil acts directly on its geotechnical characteristics [7]. It greatly reduces its strength when saturated and affects its stability with the fluctuation of

Hizia Zerarka is with the University of Sciences and Technology Houari Boumediene, Algeria (e-mail: zerarkahizia@yahoo.fr).

the groundwater. This could be a trigger factor of land movements.

III. Topographic Monitoring

The topographic monitoring followed by implantation of the target, is indicated on the map in Fig. 2. The target baseline measurement was conducted in October 2009. The surveys were then carried out on monthly basis. The last measurement was in May 2012 with six-month of interruption. The movements of the targets are plotted along the **Z** axis for each section in the graphs to better monitor and study the movements of the slope.

Measurements are carried out from the AEH area, and allow having indications of the existence of ground movement in the basement. The measurements which are based on measuring the relative position of the point in question by providing a stable reference point, displacement in time of the five cuts made in the field are given by Figs. 3-7.

Based on topographic monitoring, it is notable that the downstream ground movement is relatively more active than upstream. There are also significant peak values over all cuts during the months of April 2011, December2011, April 2012, and May 2012. Finally, it is assumed that heavy rainfall during the months of September 2011(45.3mm / day and 162.5 to 181.6 mm/day source [8]) has caused the notable shifts recorded.

By studying the different graphs, we see that the displacements are largest on-DT DT cuts and ET-ET. The vertical displacements Δz range from -0.5 to 0.5 m can also be seen and point downstream moves differently compared to the upstream side. This explains that the landslide will expand on the upstream side of the slope and also causes movement to the beat of the slope by generating sags and bulges at ground level.

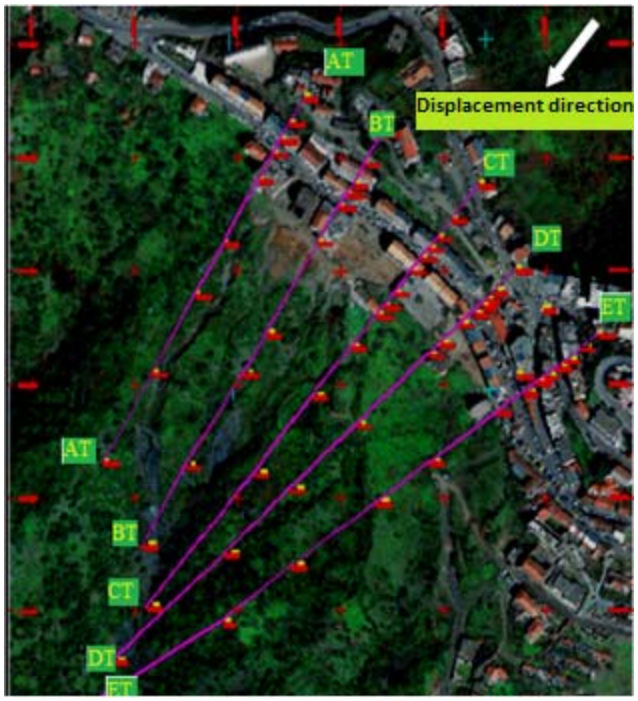

Fig. 2 Satellite photos with the topography monitoring sections

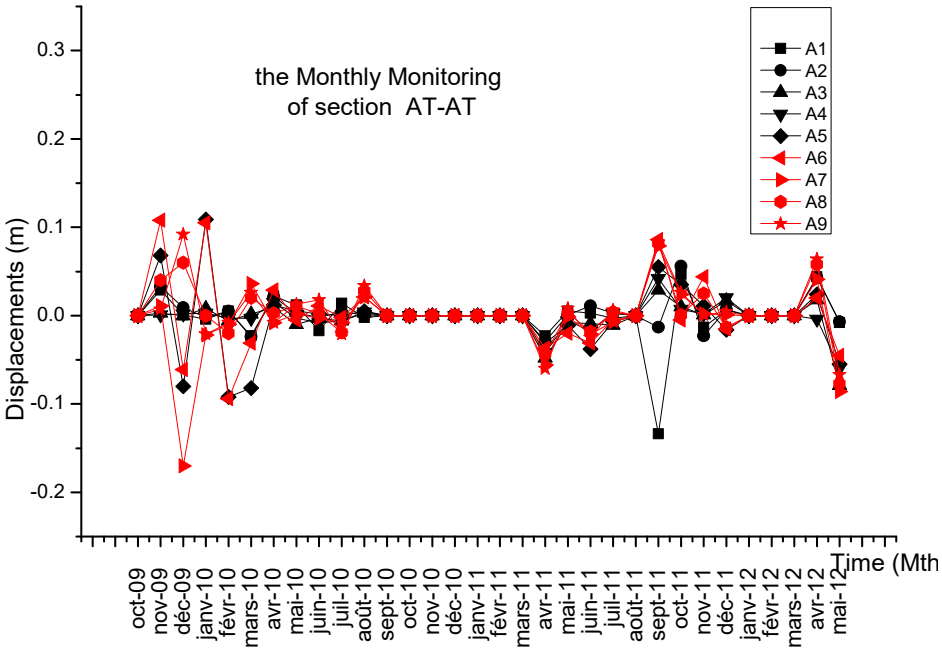

Fig. 3 Displacement of topographic point according to cut AT-AT

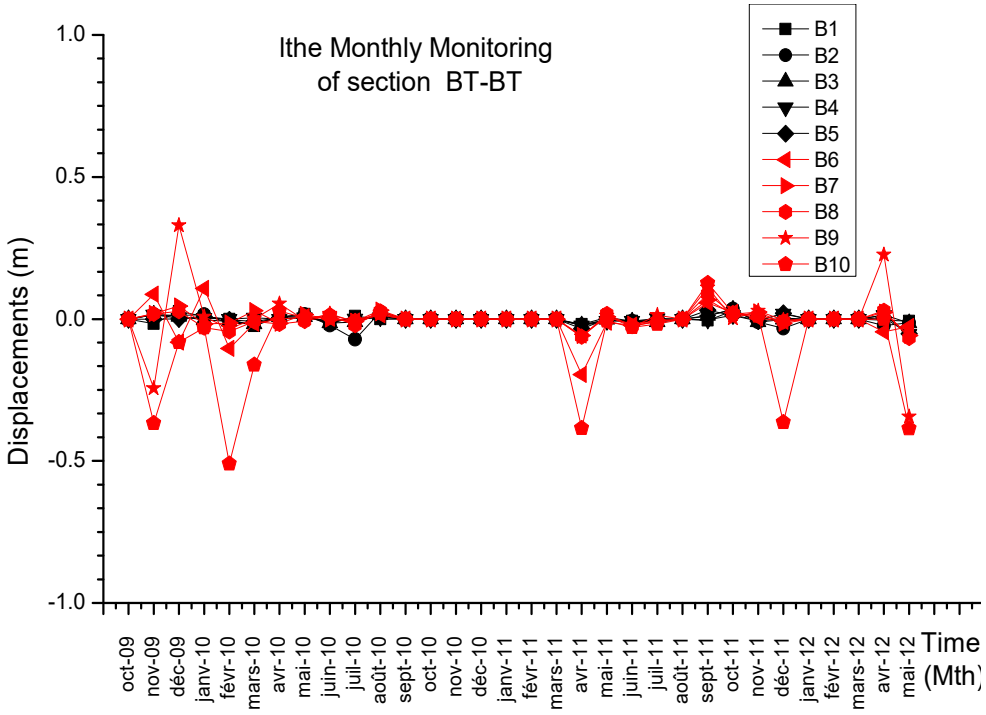

Fig. 4 Displacement of topographic point according to cut BT-BT

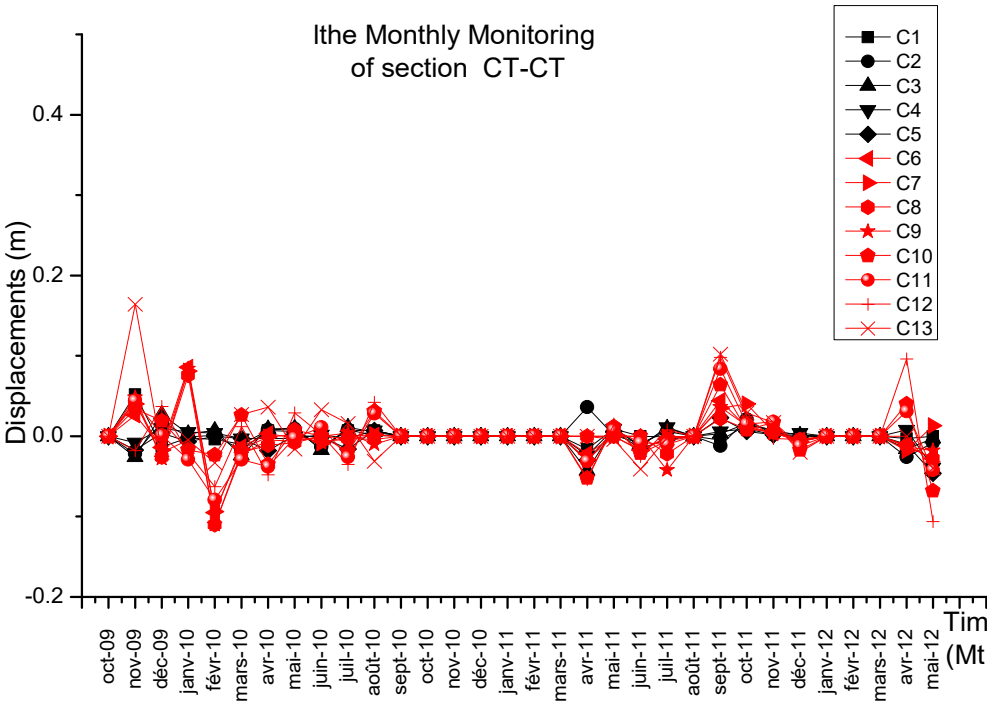

Fig. 5 Displacement of topographic point according to cut CT-CT

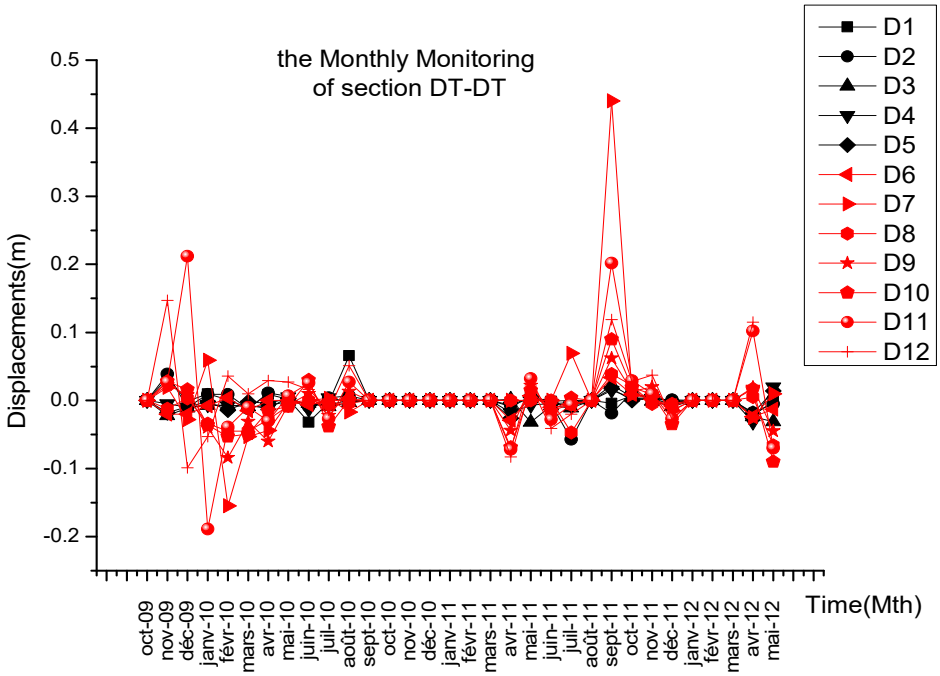

Fig. 6 Displacement of topographic point according to cut DT-DT

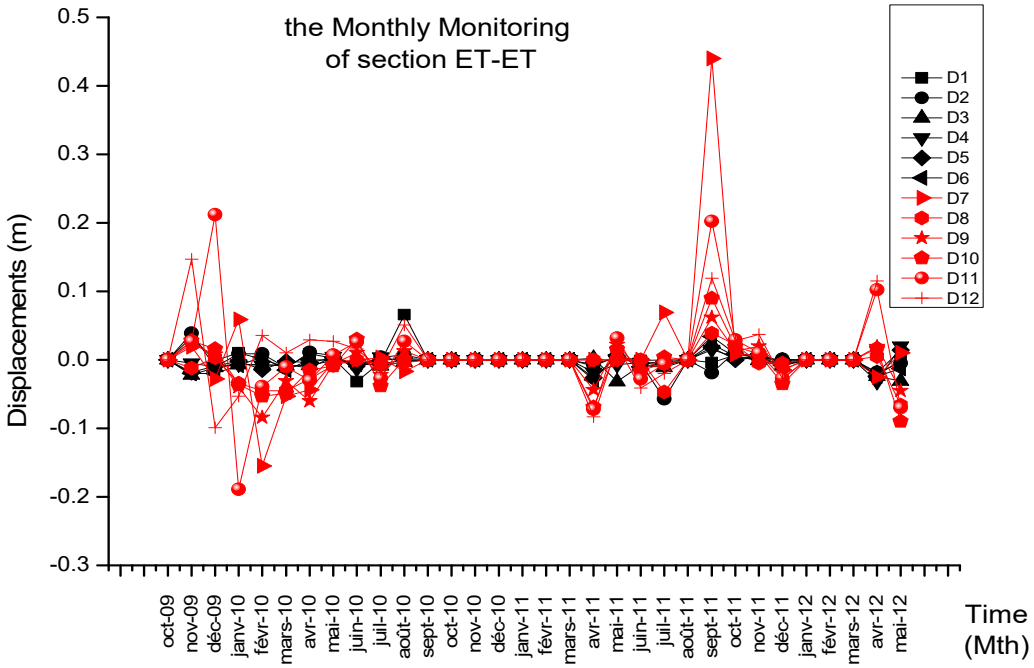

Fig. 7 Displacement of topographic point according to cut ET-ET

IV. Equivalent Plastic Deviatory Strain ε_{eq}^{p}

The purpose of the modeling is to determine the stress and strain fields through hydro-mechanical finite element coupled formulation.

The hydro-mechanical finite element coupled formulation takes into account with high precision the factors affecting this area: such as mechanical actions, climate, and water. For the adequate numerical modeling of the behavior of AEH slip, five cuts are made on the unstable zone, through the constructions presented at actual state.

The results of numerical modeling under the effect of hydro-mechanical conditions, introducing the fluctuation of the groundwater effect and a strong precipitation in the transitional flow regime, enabled to study of the evolution of the rupture slope of AEH. The morphology of the equivalent plastic deviatory deformation ε_{eq}^{p} obtained by modeling facilitates the determination of deformation mechanisms within the slope. The analysis shows the shape of the sliding

surface which are not similar in all the sections, in the sections AA and BB, we notice a linear sliding and deformation which reaches to the foot of the slope, explained by the strong urbanization along this section. However, the circular sliding surface for the sections C - C, D – D, and EE was observed, which is explained by the heterogeneous geology, and the horizontal permeability of altered schist layers, causing planes of weakness and voids filled with schist alteration product (clay silt of low geotechnical characteristics). ε_{eq}^{p} gives good representations of the state of deformation of the ground, and the results are given in Figs. 8-12. Based from these results, we can consider that the slip of AEH is complex and extended under the influence of the new surface evolution. The sliding surface found by modeling reaches the embankment layer; destructed schist on all the sections with a depth between 20 and 30 m, while on the CC and EE sections the sliding surface even reaches the layer of altered schist and its depth varies between 30 m and 50 m.

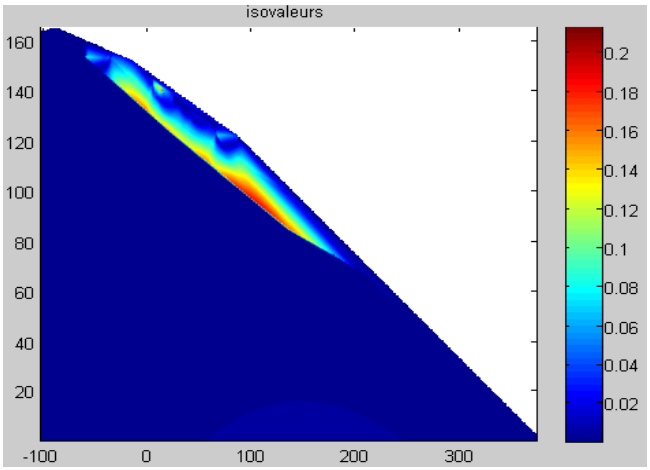

Fig. 8 Equivalent deviatory strain of the section A-A

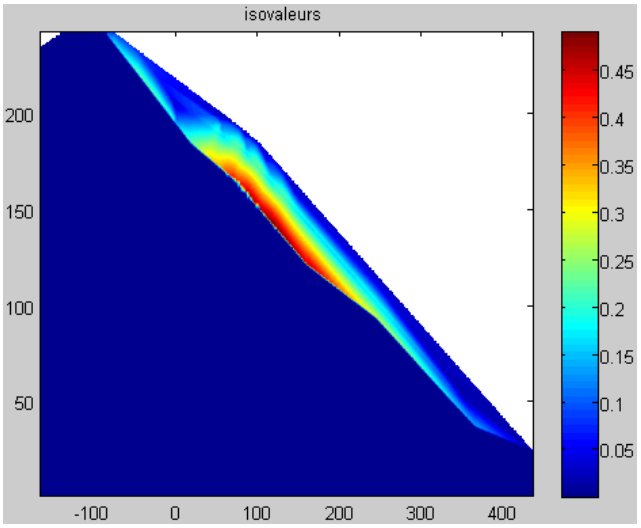

Fig. 9 Equivalent deviatory strain of the section B-B

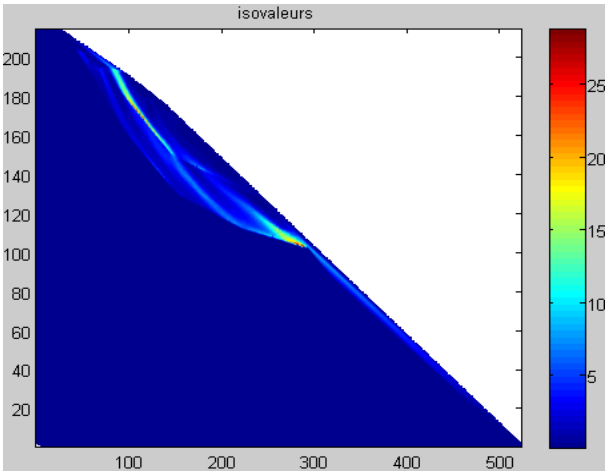

Fig. 10 Equivalent deviatory strain of the section C-C

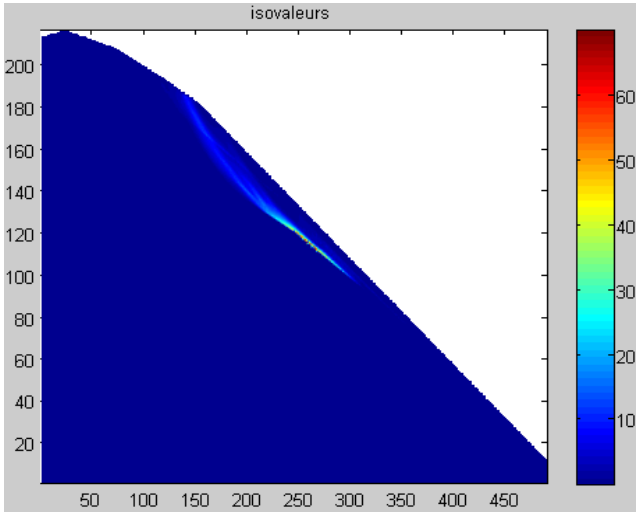

Fig. 11Equivalent deviatory strain of the section D-D

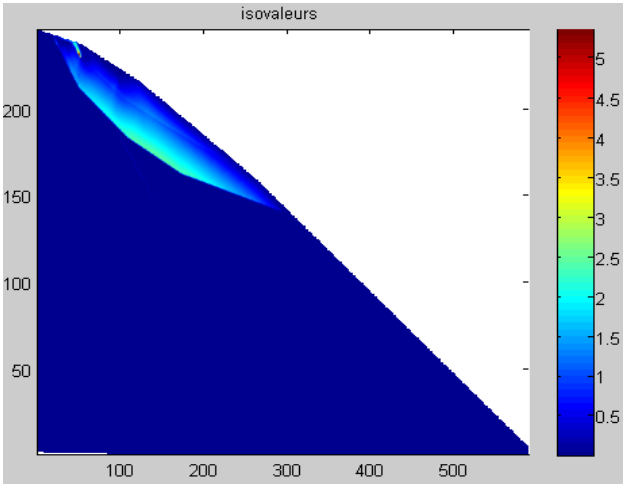

Fig. 12 Equivalent deviatory strain of the section E-E

V. Conclusion

The AEH landslide is still active and characterized by a complex structure. That is why we embarked on a numerical

modeling to refine the analysis of the behavior of the slope and its long-term response mode, using in one hand the equivalent deviatory strain and compared them with area measurements in the other hand. These results show that the slope is unstable and confirms the existing of a new slip surface in the southern part of the city. These results are also validated by the topographic monitoring which followed important cinematic on that part of the city. Given the site geology and numerical results, we can also confirm that the propagation direction of the slide is along the natural stratification of shale.

REFERENCES

[1] L. Djerbal ''Le glissement de terrain d'Ain El Hammam (Algérie) causes et évolution''. Bull EngGeol Environ 71:587–597. 2012. DOI 10.1007/s10064-012-0423-x.

[2] G. Bièvre, U. Kniess, D. Jongmans, E. Pathier, S. Schwartz, C. van Westen, T. Villemin, V. Zumbo,'' control of landslides in lacustrine deposits (Trièves plateau, French western Alps2011'', Geomorphology. 125:214–224. DOI: 10.1016/j.geomorph.2010.09.018.

[3] J. Travelletti, J. Malet, K. Samyn, G. Grandjean, M. Jaboyedoff''Control of landslide retrogression by discontinuities evidences by the integration of airbone- and ground-based geophysical information''.2013 Landslides 10:37–54. DOI: 10.1007/s10346-011-0310-8.

[4] L. Guerriero, J. Coe, P. Revellino, G. Grelle, F. Pinto, F. Guadagno''Influence of slip surface geometry on earth-flow deformation Montaguto earth flow, southern Italy'', 2014, Geomorphology 219:285–305.

[5] ANTEA 2011 Etude du glissement de terrain d'Ain El Hammam par le groupement Hydroenvironnement et TTI DOI: 10.1016/j.geomorph.2014.04.039.

[6] G. Guitard ''ROCHES (Classification) - Roches métamorphiques'' 2015. Encyclopædia Universalis (enligne), URL: http://www.universalis.fr/encyclopedie, accessed October 26, 2016.

[7] Z. Kechidi ''Application des études minéralogiques et géotechniques du schiste au glissement de terrain d'Ain El Hammam. Mémoire Master, université de Tizi-Ouzou, 2010 Algérie, 152 p.

[8] ANRH ''Données de l'Agencenationale de ressourceshydrauliques, Rapport interne''2014.